Tool Wear Monitoring in Machining of Stainless Steel

PB ODEDEYI

Tool Wear Monitoring in Machining of Stainless Steel

By

PETER BABATUNDE ODEDEYI

(STUDENT NUMBER: S215391292)

Supervisor: Prof. Khaled Abou El-Hossein

Submitted in fulfilment of the requirements for the Degree: Master of Engineering (Mechatronics)

April 2017

Author's Declaration

I, Odedeyi Peter Babatunde hereby declare that:

- The work contained in this thesis is my own original work;
- All sources used or referred to have been documented and recognized; and
- This thesis has not been in its entirety previously submitted in full or partial fulfilment of the requirements for an equivalent or higher qualification at any University for a degree.

Authors' Signature **Date: April 2017**

……

Abstract

Modern monitoring systems for automated machines must be capable of operating on-line and interpret the working condition of machining process at a given point in time because it is an automated and unmanned system. But this has posed a challenge that lead to this research study. Generally, optimization of machining process can be categorized as minimization of tool wear, minimization of operating cost, maximization of process output and optimization of machine parameter.

Tool wear is a complex phenomenon, capable of reducing surface quality, increases power consumption and increased reflection rate of machined parts. Tool wear has a direct effect on the quality of the surface finish for any given work-piece, dimensional precision and ultimately the cost of parts produced. Tool wear usually occur in combination with the principal wear mode which depends on cutting conditions, tool insert geometry, work piece and tool material. Therefore, there is a need to develop a continuous tool monitoring systems that would notify operator the state of tool to avoid tool failure or undesirable circumstances.

Tool wear monitoring system for macro-milling has been studied using design and analysis of experiment (DOE) approach. Regression analysis, analysis of variance (ANOVA), Box Behnken and Response Surface Methodology (RSM). These analysis tools were used to model the tool wear. Hence, further investigations were carried out on the data acquired using signal processing and Neural networks frame work to validate the model. The effects of cutting parameters are evaluated and the optimal cutting conditions are determined. The interaction of cutting parameters is established to illustrate the intrinsic relationship between cutting parameters, tool wear and material removal rate. It was observed that when working with stainless steel 316, a maximum tool wear value of 0.29mm was achieved through optimization at low values of feed about 0.06mm/rev, speed of 4050mm/min and depth of cut about 2mm.

ACKNOWLEDGEMENT

First, I would like to give thanks to God the almighty, in whom I live, move and have my being, the all great without whom I could not have completed this educational endeavor, I return all the glory back to HIM. I wish to express my sincere thanks to Nelson Mandela Metropolitan University, especially the Mechatronics Engineering Centre (MEC) for the use of their facilities to pursue this research. I would like to extend special thanks and unending gratitude to my supervisor Professor Khaled Abou-El-Hossein. Thanks for all the opportunities, inspiring and wonderful discussions, invaluable guidance, strong support, encouragement and patience he provided throughout my studies at Nelson Mandela Metropolitan University. Prof, I am ever grateful for this privilege.

In addition, I would like to express my gratitude to the entire eNtsa department especially Mr Andrew Young, I am deeply grateful to him for his invaluable guidance and strong support during Experiment. Also, grateful to Riaan Brown, Miss Amy van Grend and Stembiso Peter. I am highly indebted to Kyle Donaldson, I must appreciate his ever-ready helping attitude, which was a constant motivating factor for me during Machining.

However, the support provided by my Research group and colleagues Mr Liman Muktar, Mr. Abdulkadir Lukman, Jumare, Mr Noah, Kopi Fundiswa and Goodness Onwuka from the MEC is more than appreciated. I am also very grateful to all the members of the Metallurgy Centre for their friendship and help. Special thanks go to Mr Jenniker Kurtz, Mr Christian du Preez, and Mr Marlon Koopman for their sincere help and support.

I would like to give special appreciation to the staff of the Centre for Teaching Learning and Media/student academic development (CTLM), for providing open arms whenever I need them.

I would like to thank the Department of Science and Technology of South Africa and Research Capacity development of NMMU for the financial support provided for this research.

I would like also to acknowledge and thank my Brother Pastor Funsho Williams for his immense support through encouragement, understanding and prayers. Thank you my Mother Esther Odedeyi for your patience and perpetual prayers and my Late Father Augustine Odedeyi.

Finally, thanks should go to my beloved wife, Victoria Chidinma, for her warm comfort and great assistance and for her patience and understanding which has inspired my research work from the beginning to the end.

Table of Contents

List of Figures

List of Tables

Definition of terms

	Abbreviations	Full name
	TCM	Tool Condition Monitoring
	CNC	Computer Numerically Controlled
	BCC	Back Centre Cubic
	BUE	Built Up Edge
	FCC	Face Centre Cubic
	AISI	American Iron and Steel Institute
	MPa	Mega Pascal
	IC	Inscribed Circle
	CBN	Cubic Boron Nitride
	PCD	Polycrystalline Diamond
	DLC	Diamond-Like Carbon
	HSS	High Speed Steel
	CVD	Chemical Vapor Deposition
	PVD	Physical Vapor Deposition
	AE	Acoustic Emission
	ANN	Artificial Neural Network
	AI	Artificial Intelligent
	ACO	Ant Colony Optimization
	PSO	Particle Swarm Optimization
	CCD	Charge Couple Device
	RMS	Root Mean Square
	DSP	Digital Signal Processing
	DVD	Digital Video Disc
	CD	Compact Disc
	ADC	Analog to Digital Component
	DAC	Digital to Analog Component
	MA	Moving Average
	ARMA	Auto-Regression Moving Average
	CF	Crest Factor

	SNR	**Signal to Noise Ratio**
	DFT	**Discrete Fourier Transform**
	PSD	**Power Spectral Density**
	STFT	**Short Time Fourier Transform**
	FFT	**Fast Fourier Transform**
	DWT	**Discrete Wavelet Transform**
	CWT	**Continuous Wavelet Transform**
	WPD	**Wavelet Packet Decomposition**
	LMS	**Least Mean Square**
	LDF	**Linear Discriminator Function**
	BPNN	**Back Propagation Neural Network**
	DNN	**Deep Neural Network**
	RNN	**Recurrent Neural Network**
	SOM	**Self-Organizing Map**
	RBM	**Restricted Boltzmann Machine**
	CNN	**Convolution Neural Network**
	DOE	**Design of Experiment**
	MRR	**Material Removal Rate**
	BBD	**Box-Behnken Design**
	CCD	**Central Composite Design**
	RSM	**Rough Surface Modelling**
	NI	**National Instruments**
	CVI	**Computer Virtual Image**
	VI	**Virtual Image**
	DAQ	**Data Acquisition**
	ANOVA	**Analysis of Variance**

Chapter One

1 Introduction

1.1 Overview and background

It was during the industrial revolution that people began to recognize manufacturing as a modern way of engineering. This term is now associated with mass production with modern process on a large scale. This is far better than the traditional way in which one man handles one craft in a shop. This consumes a lot of time and energy coupled with low productivity.

In modern manufacturing industries, the use of automated processes has become the major way to create products rapidly and economically. Also, because of high demand for improved product quality, reliability and manufacturing efficiency degree, it has enforced inflexible requirements on automated product measurement and evaluation. These manufactured goods require high precision and accuracy. Interestingly, in recent years, elevated percentage of downtime has been attributed to tool failure in modern machining tools. Furthermore, manufacturing capability profiles require a healthy environment to meet market demand as well. Therefore, an automated monitoring process plays a vital role in ensuring products reliability, high quality product, machine efficiency and to avoid machine downtime that may occur because of excessive tool wear, tool breakage and chatter vibration.

In modern machining, great interest has indicated that Computer Numerically Controlled (CNC) machine have dominated and become the major driver of modern manufacturing processes. The advent of this innovation still has limitations on modern machining process due to the inability of this automated machining system to monitor some manufacturing capabilities such as quality of products during milling processes. This phenomenon of tool life truncation wear or early breakage of tool edge due to chipping, is indeed a priority in the literature.

However, modern monitoring systems for automated machines must be capable of operating on-line to interpret real data from diverse working conditions of machining processes at any given point in time because they are automated and diverse unmanned systems. However, this has posed a challenge that has led to this research. Generally, optimization of machining process can be categorized as minimization of tool wear, minimization of operating cost, maximization of process output and optimization of machine parameters.

Therefore, the awareness of tool condition monitoring has gained tremendous importance in the manufacturing industry and this can be attributed to the fact that modern machines are no longer operating manually but automatically through the operation of CNC machining.

All things being equal, tool wear is the most critical and influential feature to a successful maximization of manufacturing process in metal cutting processes. Characteristics of milling cutting operations such as cutting conditions, work-piece and tool materials must be considered for maximum output. Recently, interest has been placed on monitoring system in the manufacturing industry due to recent inclinations and advances in machining operations and technologies.

But the challenges are with reliability and applicability of sensor systems for tool condition monitoring. A high availability level of sophisticated manufacturing systems and high quality of manufactured parts can be achieved since the process will be unmanned. To achieve this, it is generally accepted that an intelligent sensor based manufacturing is highly required. Therefore, successful implementation of intelligent control system has become an area of interest in design of process control systems. Also, modern monitoring systems are required to operate on-line and must be capable of interpreting the working conditions of the process at any given point in time.

1.2 Problem statement

Tool wear is a complex phenomenon, generally, Tool wear reduces surface quality, increases power consumption, and causes rejection of machined parts. Tool wear has a direct effect on the quality of surface finish for any given work-piece, dimensional precision and ultimately the cost of the parts produced. Tool wear usually occur in combination with the principal wear mode which depends on cutting conditions, tool insert geometry, work piece and tool material. The challenges are with reliability and applicability of sensor systems for tool condition monitoring. When we combine work piece and cutting condition together, primarily for a milling process, the cutting speed of milling operation and chip dimension-thickness may be exclusively important together with other wear factors. Therefore, there is a need to develop a continuous tool monitoring system that would notify an operator about the state of a tool to avoid tool failure or undesirable circumstances.

1.3 Hypothesis

The on-line tool wear monitoring of stainless steel machining using selected cutting tool material will validate a reliable wear model from design of experiment for a capable automated tool change schedule.

1.4 Aim of the study

The aim and purpose of this research is to develop a tool wear monitoring systems for a selected milling operation on stainless steel using on-line acoustic emission systems to capture and predict the tool wear stages.

1.5 Objectives

In the course of the study, the following objectives are expected to be achieved:

i. To deploy in-process sensor successfully for tool condition monitoring during milling operations.
ii. To analyze data generated during milling operation and determine the effect, productivity and Optimization of parameters selected.
iii. To analyze and interpret data acquired during signal processing.
iv. To develop a valid model that can be used to predict tool condition during industrial machining processes of stainless steel.
v. To validate the model by using signal processing framework and Neural networks.

1.6 Scope of the research work:

The scope of this research work includes:

i. Literature studies on various techniques used in tool wear and how
ii. Data acquisition successfully during acoustic emission process
iii. Investigate flank wear using various electron microscopes to validate authors measurements
iv. To analyze data generated from the machining operations
v. To develop and validate model that is deployable for tool wear using design and analysis of experiment approach and signal process respectively.

1.7 Delimitations

The current research work is intended to provide a guide on how to use design of experiment to model a relevant tool wear while carrying out machining operation on stainless steel (Grade 316) using three machine parameters such as Feed, Speed and Depth of cut. Thereafter, signal processing and Artificial Neural networks will be employed to validate the flank wear generated during machining.

1.8 Rationale

Manufacturing is the wealth creating or wealth-producing sector in an economy, the economic values involved in automated manufacturing are very high. This is because of high investments in the manufacturing equipment. It would be in the interest of any manufacturing industry to benefit from the equipment in an optimal way especially with the use of unmanned automated production system with high availability. In Africa, South Africa has always been in the fore front of manufacturing such as automobile industry but still strife to be a major player globally. This means that South Africa could not meet global demand in terms of production, cost and time frame. Therefore, automated manufacturing with embedded tool condition monitoring can improve these short comings. Tool wear monitoring techniques can form a vital pivot to actualize tool condition monitoring in automated manufacturing in South Africa industries. Meanwhile, acoustic emission sensing parameters is far reaching to handle and generate adequate source of information that is required in tool wear monitoring.

1.9 Purpose of the study

The advantages of modern manufacturing process have confirmed the need for automated system over the traditional way of Manufacturing in terms of cost reduction, mass production, improved quality, increased competitive advantage, better management control and increased flexibility. On the other hands, if tool wear which mechanically leads to tool breakage or worn out is not properly addressed, then the listed above benefits will not be in view. Therefore, tool condition monitoring technique is employed.

South Africa is among the leader in manufacturing industries in Africa. This implies that to enhance manufacturing competitiveness in South Africa among developing nations there is a need to improve production time and reduce production costs. In order for time loss due to tool wear, breakage and tool change to be optimized to their advantage by implementing and embedding tool

wear monitoring system into the manufacturing process. The result of this research work is intended be used to develop a fundamental model that can predict tool failure during cutting operations when working on any stainless-steel materials.

1.10 Structure of the thesis

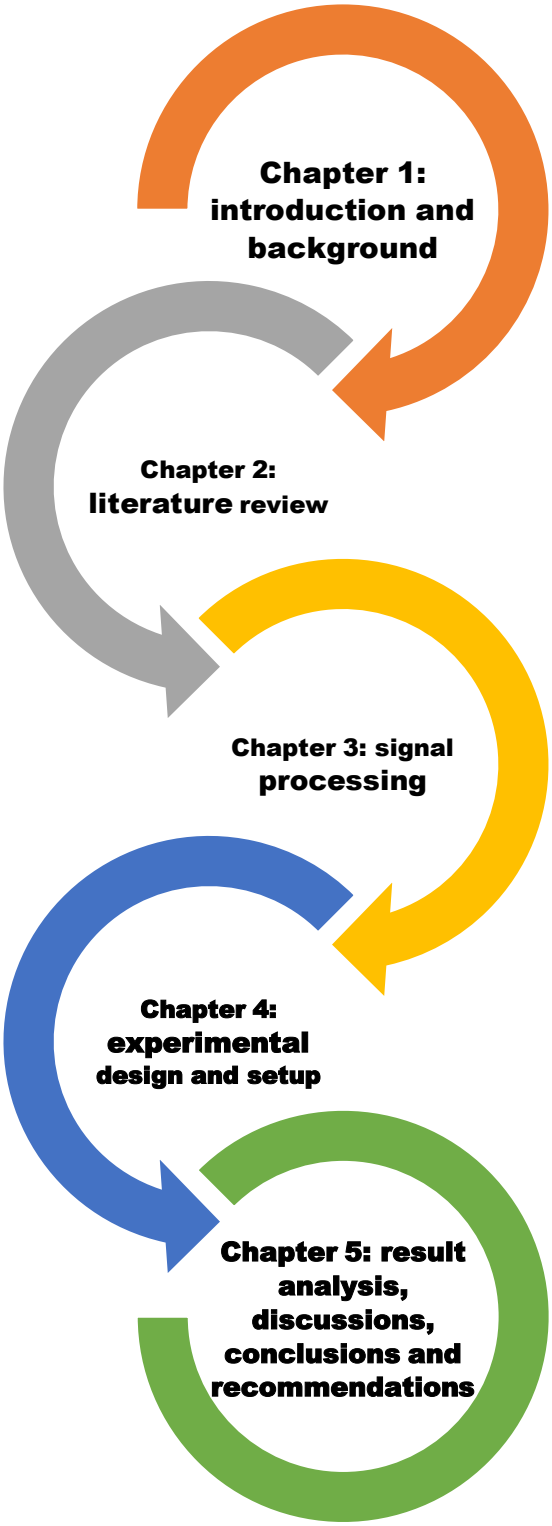

- Introduction
- Problem statement
- Aims and Objectives
- Scope and Purpose

- Literature review
  - ➢ Stainless steel
  - ➢ Tools and

- Signal Processing
- Design of Expert

- Experimental design
- Machine setup

- Analysis of Result
- Discussions,
- Conclusions and
- Recommendations

Figure 1-1: Research Approach

Chapter Two

2 Literature Review

2.1 Stainless Steel and Its Machinability Characteristics

2.1.1 Introduction

The purpose of this aspect is to lay some foundations for understanding about steel, stainless steel and its machinability characteristics. This aspect will highlight the characteristics of stainless steel, the wide use of stainless steel, the cutting behavior of stainless steel and the milling consideration of stainless steel.

2.1.2 Steel

In the world, we live today, there are two classes of metallic materials which are: ferrous and non-ferrous metals. Steel belongs to the class of ferrous materials, ferrous, which simply means comprising iron. The iron base in a steel is about 90% [1]

Although in some cases of some high alloy steel where alloy can form about 30-35% making the iron content to become 70-75% such as the popular 18cr-8Ni Austenitic stainless steel. Non-ferrous materials on the other hand, do not contain an appreciable amount of iron i.e. it is not iron based. Sometimes it can contain a very small amount as alloy just to improve some design property. Examples of Ferrous materials can be pure iron, cast iron, wrought iron and steel. Steel can be ordinary plain carbon steel or alloy steel which are all iron based but differ in terms of proportion, concentration, properties and applications.

In metallurgy, steel is a solid solution of iron and carbon where carbon atom is smaller compare to iron atoms that occupies the interstitial position in the iron crystal lattice. There are two crystal lattice structures Figure 2-1, in steel that describes their properties, the ferrite steel (α-steel) which has Body Centered Cubic (BCC) and Austenite steel (ϒ-steel) which has Face Centered Cubic (FCC) structured arrangement.

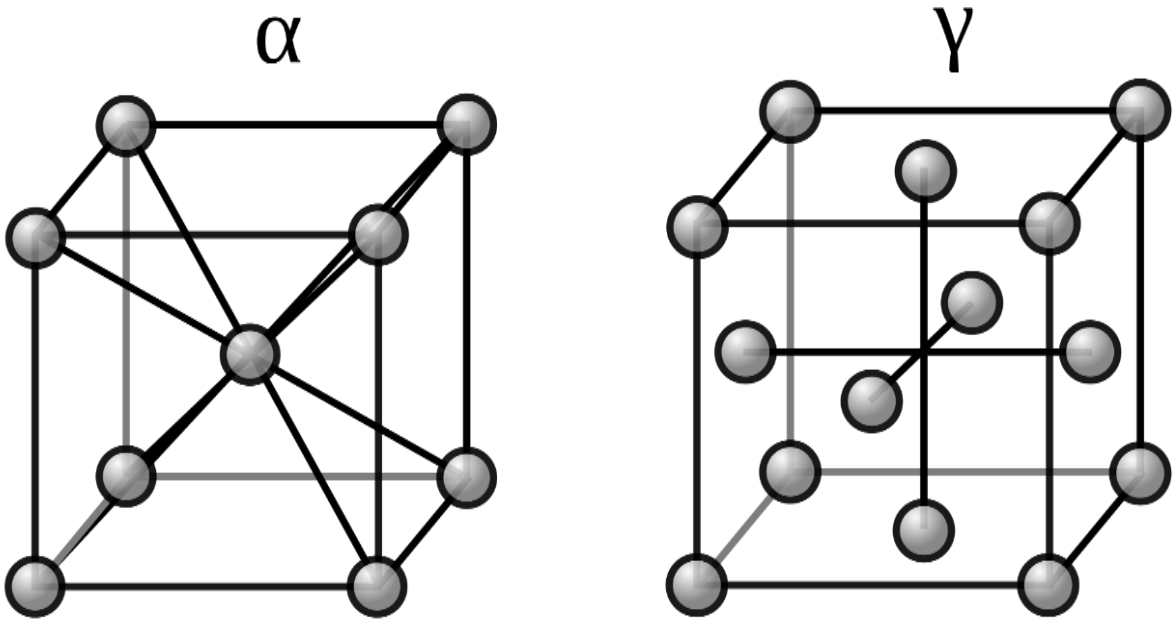

Figure 2-1: Atomic structure of Ferrite steel (α-steel) BCC and Austenite steel (ϒ-steel) FCC [2]

Furthermore, when other elements are added to steel, such as carbon or manganese, they occupy a position within the respective atomic crystal structure in relation to their atomic size thereby forming solid solution. The solid solution formed in steel causes decrease in plasticity of steel, increase in electrical resistivity and increase in mechanical strength of steel. Looking closely at the addition composition of steel, appropriate design for other mechanical properties such as machinability, gain in strength and other fabrication can be achieved. However, in Table 2-1, this further explained that the difference in microstructure of steel will lead to variation of strength in low and high carbon steel which suggests that all mechanical properties of steel such as machinability property are structure dependent [2]

Table 2-1: Influence of microstructural constituent on properties of steel [2]

Microstructural constituents	Srength Tensile	Strength Impact	Strength Fatigue	Ductility/ Toughness (D)	Ductility/ Toughness (T)	Cold Forming	Weldability	Machining	Corrosion
Austenite	↓	↑↑	↓	↑	↑	↑	↓	↓	↑
Ferrite	↓↓	↑	↓↓	↑	—	↑↑	↑↑	—	—
Pearlite	↑	↓	↑	↓	—	↓	↓	↑	—
Bainite	↑↑	↓	↑		↑	↓	↓	↓↓	—
Martensite*	↑↑↑	↑	↑↑		↑↑	↓	↓	†	—
Carbide	↑↑	↓↓	↓	↓↓	↓↓	↓↓	↓↓↓	↓↓↓	—
Grain size	↑	↑	↑	↑	↑	↑	↑	↓	↑
Inclusions		↓	↓↓	↓	↓	↓		↓	—

* Martensite referred here relates to tempered martensite

† On tempering

Note:

1. Note adverse effect of fine grain size on machining.
2. Toughness is not same as ductility. Toughness is indicated by the energy absorbed on fracture, whereas ductility is represented by % elongation of the steel at fracture. Toughness is generally referred with respect to heat treated steels where toughness is developed in the structure by appropriate tempering. Ductility is considered for cold forming operations.
3. Austenite as a phase in steel is predominant in stainless steel grades and in some high-alloy steels where austenite is stable at room temperature.

2.1.3 Tool steel:

The use of Tool steel for engineering purposes can be tailored into the following manufacturing operations: forming, Extruding, cutting, drawing, rolling, battening and shearing. So, that the combination of metallurgical characteristics such as hardness, wear resistance, toughness and a physical property are the requirements in Tool steel during these manufacturing operations to obtain an optimum performance. When tool is being selected, these considerations are very important.

According to SAE, Tool steel have been classified into six major groups which are: Water-hardening, Shock-resisting, cold-work, hot-work, high speed and special purpose tool steel. These groups are based on their applications, quenching methods, special characteristics and the use in specific industries.

2.1.4 Stainless steel

stainless steels are iron-based alloys that contain minimum of about 12% of chromium. This alloy is used for wide industrial, chemical, architectural and general consumer purposes for so many years. Stainless steel is also recognized by American Iron and Steel Institute (AISI) as a standard alloy. Chromium is the alloying element that imparts to stainless steels their corrosion resistance qualities and in addition, it has a wide range of excellent mechanical properties that are not offered by another metal alloy. Only few stainless steels contain more than 30% of Cr and less 50% of iron. These stainless characteristics are achieved through the formation of an invisible and adherent Chromium rich oxide film. Other elements can be added to improve a unique characteristic of the alloy, such elements are molybdenum, carbon, copper, aluminum, titanium, nickel, silicon, niobium, selenium, manganese and sulfur. The amount of carbon added can range from 0.03% to over 0.1% in certain ranges.

2.2 Metallurgical structure of stainless steels:

Stainless steels are categorized into five groups according to their metallurgical structures; these are; Austenitic, Martensitic, Ferritic, Duplex and Precipitation Hardening. These categories help us to have a better understanding of stainless steels usage and their machinability.

2.2.1 Austenitic stainless steels:

The most famous of all stainless steel is Austenitic alloy probably because of its ductility, ease to work on and corrosion resistance making up to 65-70% for the past years ([3] [4]. All Austenitic categories are derived from 18Cr-8Ni stainless steels but the most often used of this category is AISI 200 and 300 series. However, consumers have recorded a constant machinability difficulty with this category of grade. This can be explained due to the work hardening of the material during machining operation [4]. Austenitic stainless steel alloys are non-magnetic that can be strengthened by cold work but through traditional heat treatment, it can be hardened [5] [3]. Abou and Yahya further identified that during machining operation of austenitic stainless steel, a lot of Built up Edge (BUE) and irregular wear difficulty are found on the tool flank face and the crater

face making the surface integrity of the work and tool wear rate to be worsened by this BUE impact in the process [5].

2.2.2 Martensitic stainless steels:

These are stainless steels that are standard straight 400 series that contains 11-18% Cr, almost 1.2% Carbon, small amount of manganese and Nickel. This series can be hardened by heat treatment which can be heat treated up to a tensile strength of 1379MPa (200,000psi) (design and guidelines page 4). Excellent wear or abrasion resistance are typically exhibited by martensitic steels but this series have low corrosion resistance than austenitic.

2.2.3 Ferritic stainless steels:

Ferritic stainless steels, Figure 2.2a are alloy of chromium that can be recognized by 400 series range. This stainless steel can only be reasonably hardened by cold work not by heat treatment. These series of stainless steels have good ductility, magnetic, resistance to corrosion and oxidation which can be improved by addition of chromium and molybdenum contents. Also, reducing the carbon and nitrogen contents the weldability, ductility and toughness can be improved.

2.2.4 Duplex stainless steels:

Duplex stainless steels, Figure 2-2b are almost 50-50 balanced dual phase materials of ferrite and austenitic. Meaning it is a mixed microstructure of ferrite and austenitic which has been in existence nearly 80 years ago. Most of its grades contain Molybdenum, Nickel and Chromium alloys [6].

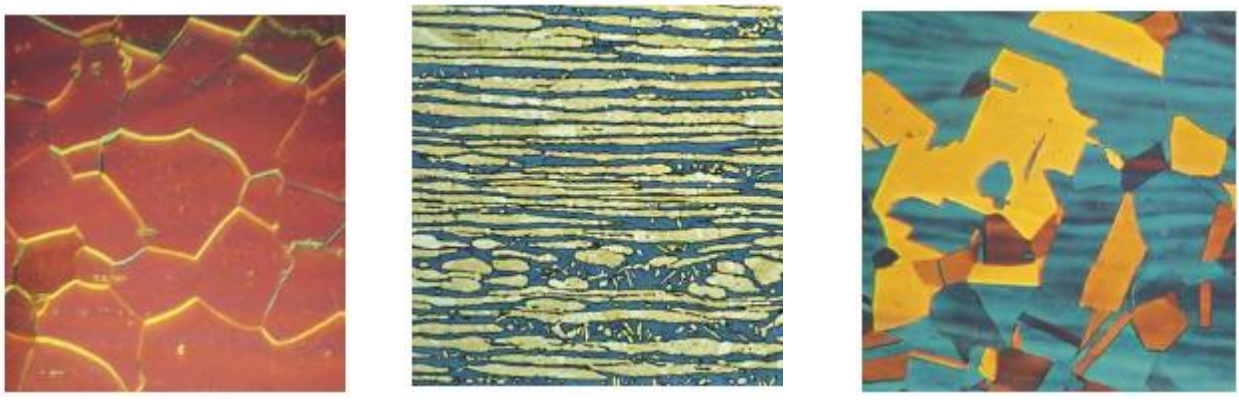

(a) Ferritic Structure (b) **Duplex Structure** (c) **Austenitic Structure**

Figure 2-2: The microstructure of stainless steels from ferritic to Duplex to Austenitic [6] [7]

According to IMO [6], the yield strength of a duplex stainless steel is as twice as that of non-nitrogen alloyed austenitic grades. For a higher alloyed grade, the chip morphology during machining of duplex stainless steel is strong and abrasive to tooling. Also, duplex stainless steels are produced with low Sulphur content which result in low chip breakage. This further defined the reason why duplex stainless steels are usually difficult to machine than the grade of 300 series-austenitic stainless steel Figure 2-2c [6] [8]. According to Hsien-Lung Tsai [9], duplex stainless steels are found useful mostly in oil and gas platforms, and unique application in wastewater, marine engineering and chemical industries.

2.2.5 Precipitation Hardness stainless steels:

Nickel-chromium are the major alloys and some alloys such as copper and aluminum are commonly found in S13800, S15500, S17700 and S17400 grades of Precipitation Hardness stainless steels Figure 2-3. These grades can be achieved by combining a low temperature (900^0F) aging treatment with cold working methods [8]. It was also discovered that prior to hardening of Precipitation hardness stainless steel, its machinability is slightly less or equal to type 304 annealing condition [8] [10].

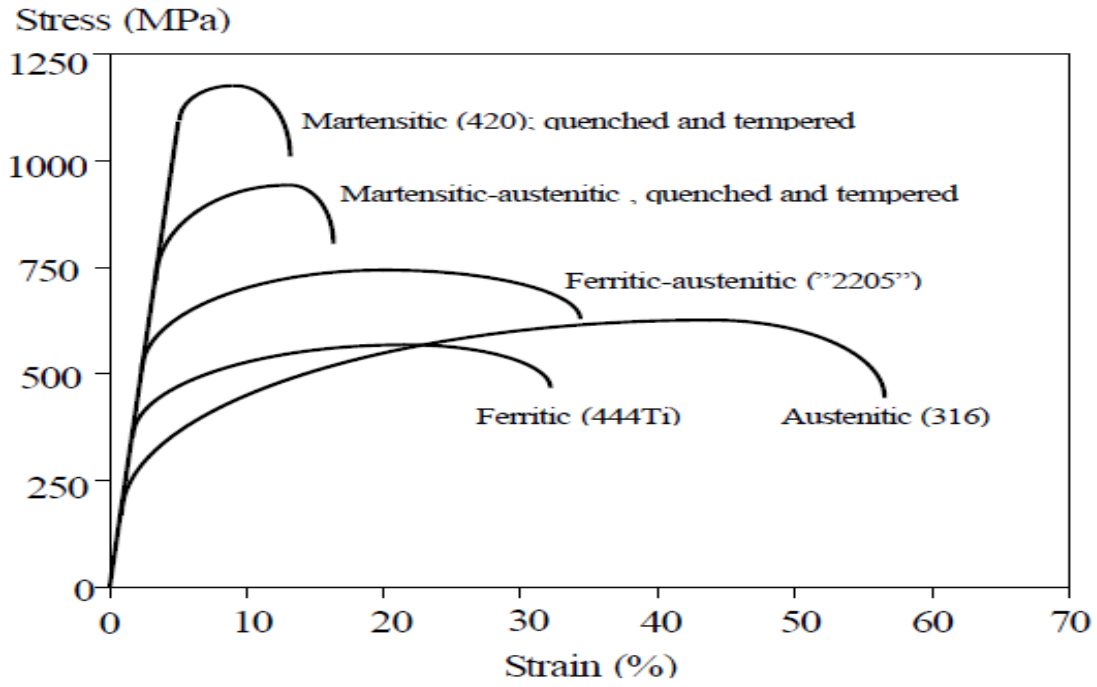

Figure 2-3: comparison of material stress – strain characteristics for different types of stainless steels [6]

2.3 Characteristics of stainless steel

Corrosion and Heat resistance: generally, depending on the alloy composition, stainless steels have good corrosion resistance to acid, moisture, atmospheric environment and other hostile environment at low and high temperatures. [8]

Strength: as it can be seen in Fig above (write the fig) parts that are made by stainless steels are often stronger than non-ferrous steels and mild steels regardless of the environment expose to [8]

Durability: due to enhanced manufactures reputations by products made from stainless steels, the combination of strength and corrosion resistance of this material has called for lifetime usage of products made from this material [8] [11]

Low maintenance: most of the home equipment, chemical industry and domestic tools are stainless steels which does not require protective coatings or special surface treatment that will depreciate leading to constant or periodic maintenance.

Fabrication flexibility: stainless steels can be welded, cold formed, forged, extruded and machined by different conventional fabrication techniques [8] [10]. Combining moderate and appropriate machining parameters, a desired part can be machined.

2.4 Stainless steel in Industry

According to Baddo [11], as at 2008, the annual consumption of stainless steels has gone up to 5% for two decades Figure 2-4. However, recent report by Engineering News [12], showed that stainless steel production has increase globally by 8.3% in 2015 [12]. It was estimated that in 2006, a total of about 4 million tons of stainless steels were used for construction purposes globally [11] [13]. This account for about 14% of total quantity used.

Duplex grades are found mostly in construction industries for Facades, structural design and roofing than Austenitic due to high strength and corrosion resistance [11]. Also, X5 CrMnN 18 - 18 Austenitic stainless steels have become valuable in the area of Fossil fuel power plants because of its creep rupture features and high oxidation [14]. In heat resistance, stainless steels, which contains of 3%Co-12%Cr composition makes it suitable for critical part in ultra-super critical power plant equipment [14]. Ferritic stainless steels are used for rail transport, vehicle Chassis and frame [15], Mining and power generation due to its better atmospheric corrosion resistance and mechanical properties [15].

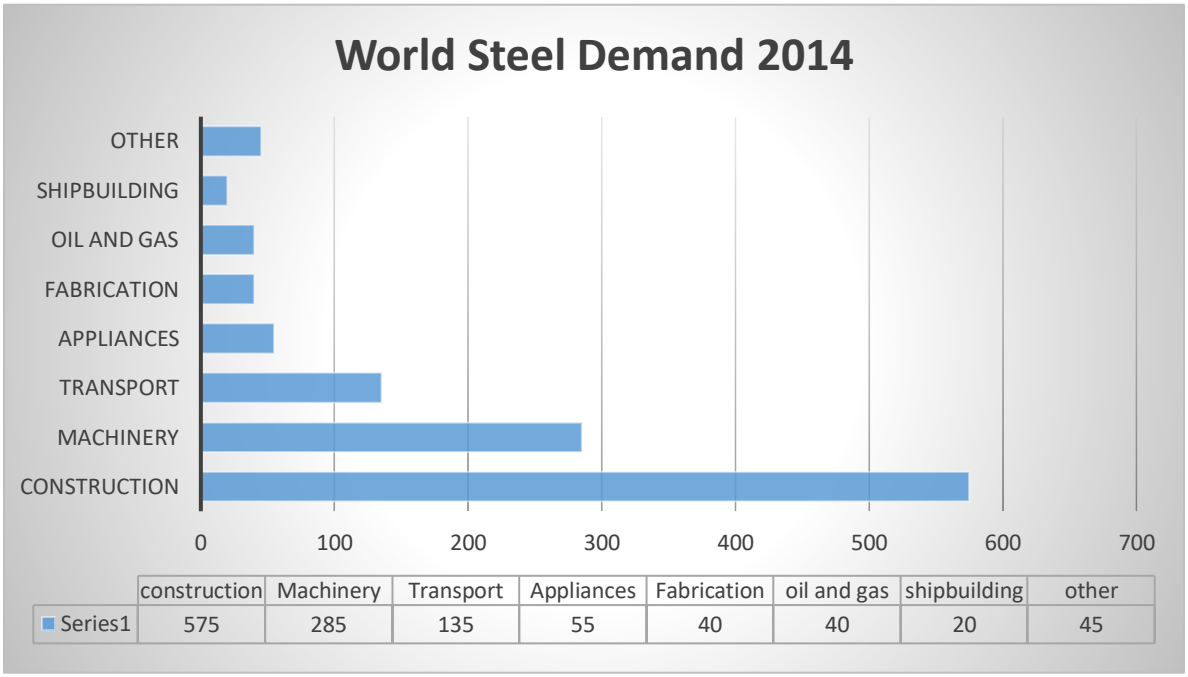

Figure 2-4: adapted from MCI [16]

2.5 Cutting behavior of stainless steel

2.5.1 Introduction

Generally, stainless steels are hard to cut with a very short tool life and poor surface finish [14]. Many research works have been carried out on cutting behavior of stainless steels using various combinations of feeds and speeds to overcome different cutting challenges. According to Lin [17], access problem in drilling stainless steel is unavoidable due to impossible prevention of burr formation. According to Ihsan [18], turning test were carried out on AISI 304 Austenite stainless steel to determine the optimum parameter for machining of this material and he found out that tool flank wear decrease with increase in cutting speed. He also noticed that on this material, surface roughness values were also found to be decreased with increase in cutting speed which could be due to the influence of built up edge (BUE) [18].

2.5.2 Physical and chemical properties

Physical properties: stainless steel has a wide range of physical properties. It must be noted that some of this wide range in properties are due to difference in Chromium percentage or content. Before I talk about some of stainless steel grades properties, I will highlight some general properties of stainless steels such as corrosion resistance which is usually between 13% - 26%

chromium depending on the environment. Work hardening comprises of cold wok and annealing which enhances its fabrication. Ductility in stainless steel helps to deform the material which can therefore be drawn into wire. Tensile Strength in stainless steel is considered to be very high compare to other mild steels. Other general properties include: acid resistance, base resistance, cryogenic resistance, hot strength, very poor heat and electricity conductivity [19].

2.5.3 Chemical contents and composition

Table 2-2: compositions of an ideal stainless steel

	Element	Effect on stainless steels
1	Chromium	Oxidation resistance
2	Nickel	Austenite former-increase resistance to mineral acids Produce tightly adhering high temperature oxides
3	Molybdenum	Increase resistance to chlorides
4	Copper	Provide resistance to sulfuric acids Precipitation hardener together with Titanium and Aluminum
5	Manganese	Austenite former- combine with sulfur Increases the solubility of Nitrogen
6	Sulfur	Austenite former- improves resistance to chlorides Improves weldability of certain austenitic stainless steels Improves the machinability of certain austenitic stainless steels
7	Titanium	Stabilizes carbides to prevent formation of chromium chloride Precipitation hardener
8	Niobium	Carbide stabilizer- Precipitation hardener
9	Aluminum	Deoxidizer-Precipitation hardener
10	carbon	Carbide former and strengthener

2.5.4 Chip formation

In 1940, Ernst and Marchant [20] [21] [22] came up with analytical model of chip formation that was based on assumptions of shear angle and chip formation [22] forgetting to take in consideration other features such as thermal softening, phase transformation, shear localization

band formation and serrated chip formation [22], although it was suggested that these short comings came as a result of inadequate experimental technical knowhow.

In drilling, cutting is considered to be a three-dimensional process involving complex mechanism due to complex edge geometrics [23]. This means that drilling will be made smooth and easy if it forms a well broken chip during this process but during drilling austenite stainless steels which are ductile materials, formation of a well broken chips was not experienced rather, continuous chip was formed [24].

Biermann and Steiner [25] discovered in their investigation that because of mechanical machining challenges the tools are exposed to during machining, austenite stainless steels featured a high ductility and toughness thus promotes burr formation. They further explained that the tools are also exposed to adhesive wear that lead to the formation of built up edge [25].

According to Denkana and Toenshoff [26], during cutting and abrasion processes, chip formation was described as a process whereby cutting edge penetrates the workpiece material which in turn deformed plastically and slides off along the rake faces of the cutting edge [26]. They further explained that this chip formation can be examined within orthogonal plane simply because important parts of the materials flow occurred along this plane.

However, in chip formation, depending on the workpiece material. There are different mechanisms of chip formation depending on the deformation behavior which can results in either continuous or discontinuous work flow. This work flow mechanism can further be classified as [27]:

- Discontinuous chip formation which is common in brittle materials at low cutting speed, high tool-chip friction, large feed and depth.
- Continuous chip which is common in ductile materials, small feed and depth of cut.
- Continuous chip with built up edge which can found in ductile material at low to medium speed.
- Serrated chip which is found in difficult to machine metal at high cutting speed. [27]

Generally during machining process, the cutter tooth shears from the surface of the work piece, giving it a define shape. This shear result is originated from friction of the chip hovering the surface

of the rake face Figure 2-5 (a and b) of the tool. Therefore, the built-up friction between the chip and the tool leads to the rake wear on the tool.

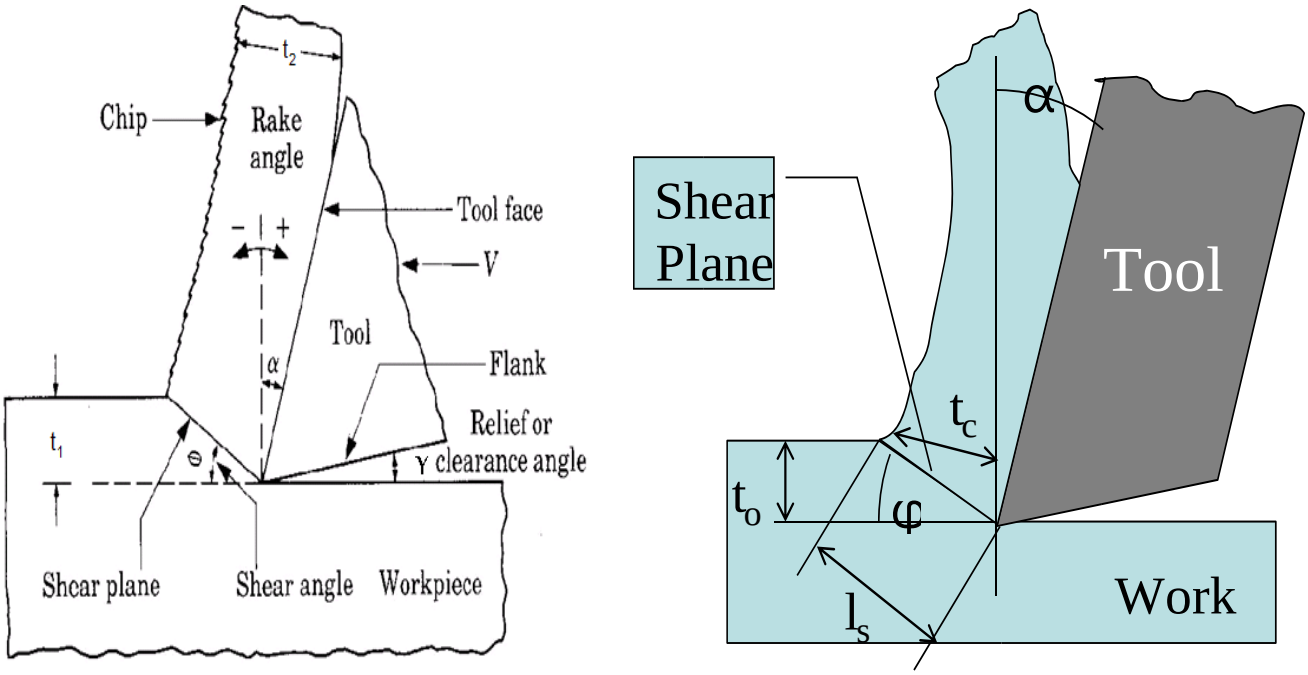

Figure 2-5: (a). Mechanics of orthogonal cutting (b). theory of chip formation [27] [28].

Rake angle: α Shear angle: ∅

$$r \equiv \frac{t_0}{t_C} = \frac{Is \sin \emptyset}{Is \cos[\phi - \alpha]} \quad \textbf{(2-1)}$$

$$\tan \phi = \frac{r\cos\alpha}{1 - r \sin \alpha} \quad \textbf{(2-2)}$$

Where r is always less than 1

According to [29], in their study during milling stainless steel 3Cr13Cu, they discovered that boundary wear and serrated chip of cemented tool are closely related to mechanical fatigue crack formation. Furthermore, these chips provide more understanding into the machining process and can be used as an analytical tool into cutting speed, temperature, speed, tool geometry, material type, tool wear and overall process effectiveness.

2.6 Milling consideration for stainless steel

2.6.1 Introduction:

One of the most significant manufacturing process is milling. This type of manufacturing process is classified by the fact that the interruption of cut is almost unavoidable. Typically, there are four types of manufacturing processes that are primarily different in operations namely:

- Material removal processing which includes: milling, drilling, grinding and turning,
- Deformation process such as forging, rolling, Extrusion
- Solidification process such as modelling and casting.
- Particulate processing such as sintering and pressing.

Material removal processing Table 2-7, which is the area of focus in this project for the author is further classified into three sub group namely:

- Convectional process
- Abrasive process
- Non-traditional machining

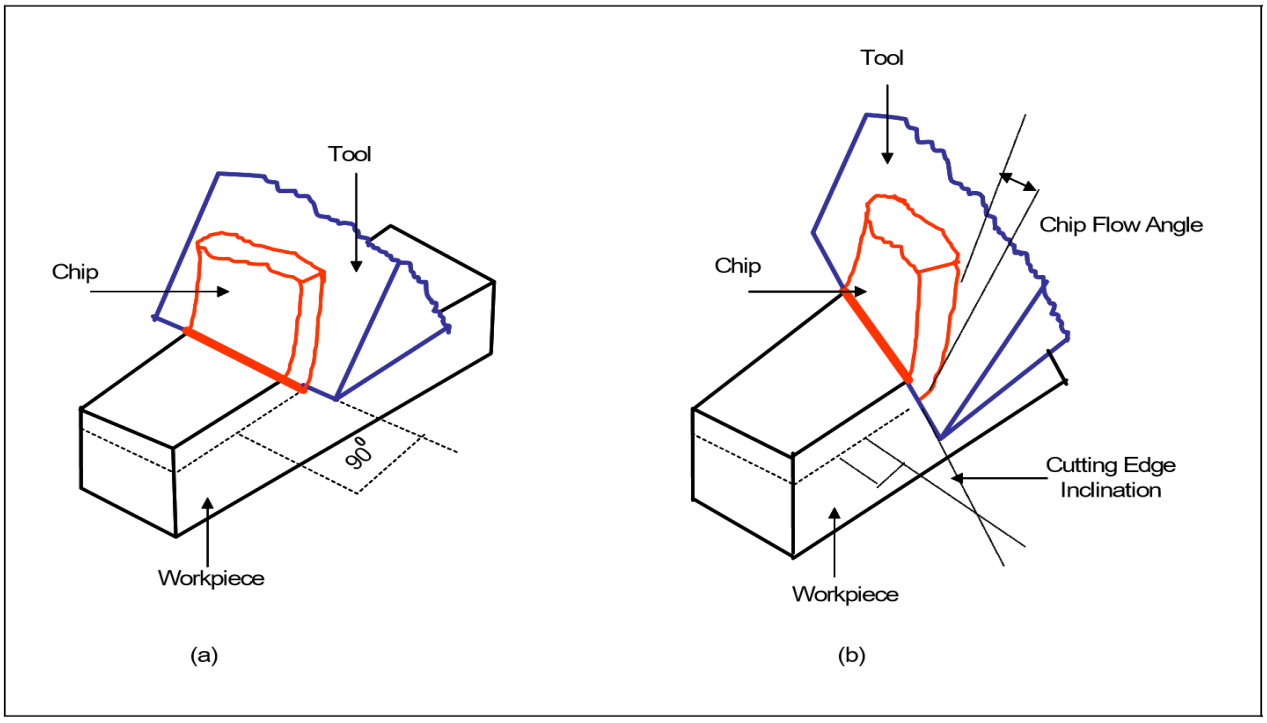

Figure 2-6: (a) orthogonal cutting (b) oblique cutting

The diagram below shows the trend for this project (highlighted in red)

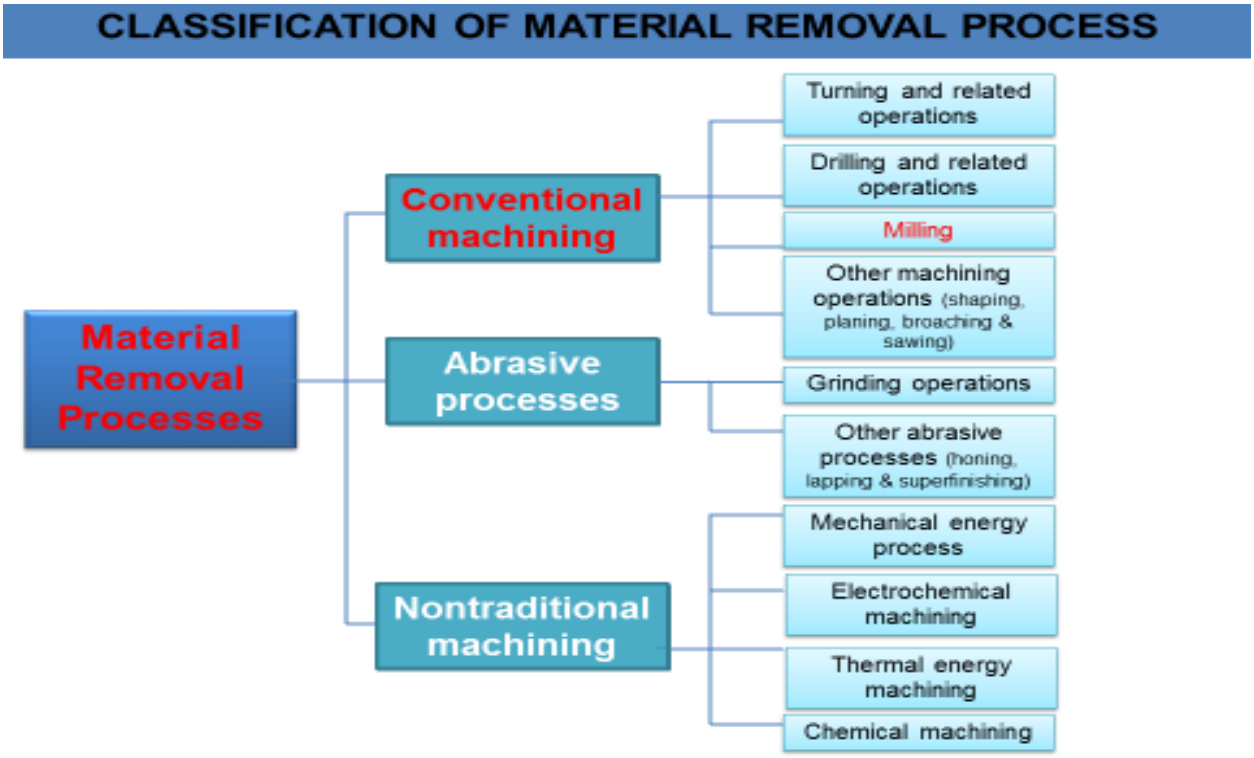

Figure 2-7: classification of material removal process

Milling can basically be grouped into two types of operations such as up milling (conventional milling) Figure 2-8 (b) and down milling Figure 2-8 (a) (climb milling) [30]. In climb milling figure A, the operation usually starts from the top of the workpiece and experience maximum chip width that latter reduces.

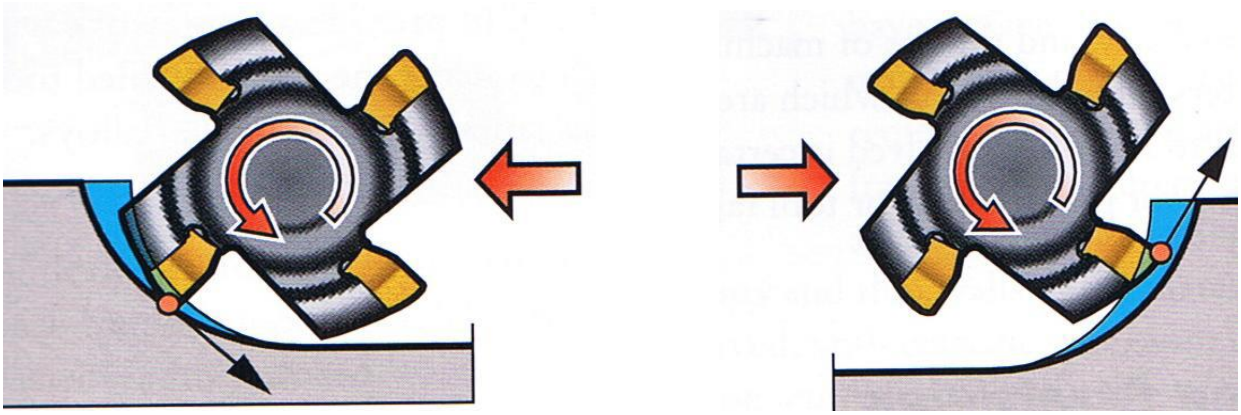

Figure 2-8: (a) Climbing milling (b) conventional milling [31] [32]

It was also noted that in climbing milling Figure 2-8 (a), less machine power is exerted as the force is acting downward on the workpiece in the direction of gravitational force thereby causing the operation to be cost effective and suitable to operate. [30] [31]. However, in conventional milling, the work piece and the tool meet at the bottom then figure 2-8 (b), up where the chip width starts from zero and then increases. In this type of milling, more power is needed to as a result of friction generated by the chip formation from small width size to big size. [31].

In the Figure 2-9, different forms of milling can be established as mechanical overload and thermal shock are the mechanism that can act in parallel while inserts will serve as the biggest component of mechanical load that will penetrate the cut and thermal shock will act as the inserts leaving the cut and go into the cutting fluid [31] [33].

In addition, looking at the Figure 2-9, the radial engagement will represent the time of contact with the thermal load and the cutting speed will serve as the magnitude of the same thermal load [31]. Critical analysis from this figure shows that increase in the breakage resistance of the inserts due to this mechanical impact can increase the tool life for milling operations [31] [33]

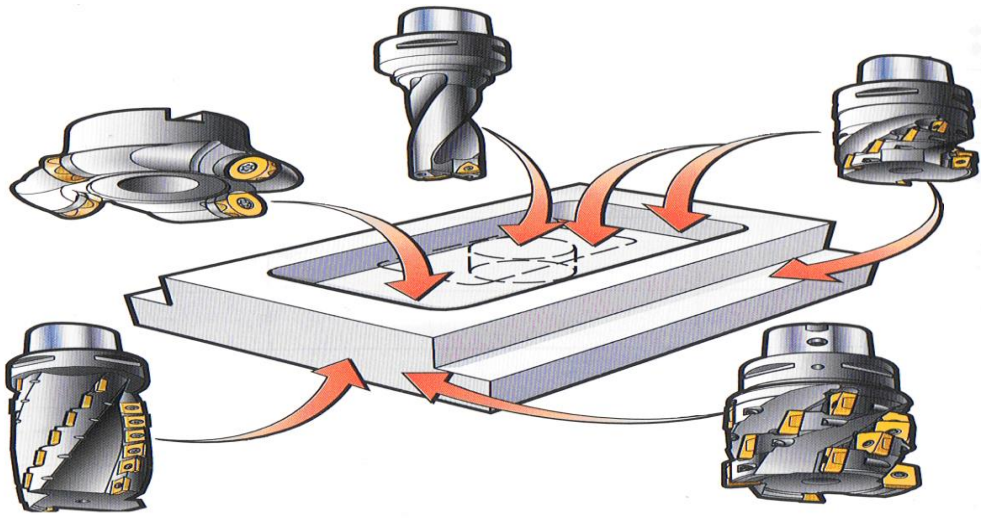

Figure 2-9: different milling operations [33]

2.7 Influence of different cutting parameters

Is well established that the variables that are easily changed by operator during machining or metal removal are feed rate, cutting speed, depth of cut- axial depth of cut and radial depth of cut. These parameters have direct impact on the surface roughness and the rate of metal removal. Several

Literatures have revealed that the two major variables among others that has most influence on tool life are cutting speed and feed rate commonly denoted by V_c and F_z respectively. Therefore, good understanding of these parameter in machining stainless steel is highly recommended.

2.7.1 Cutting speed (VC)

This can be defined as the largest of the relative velocity between the cutting tool and workpiece material [34]. According to Oosthuizen [31], cutting speed affects the tool tip temperature severely. He also added that a low speed can minimize tool edge temperature thereby increase tool life that are sensitive to high temperatures. In milling process, the cutter moves to generate cutting speed which is expressed in units of meter or feet per minute [34]. Equation 2 shows how to calculate cutting speed:

$$v = \frac{\pi . D . n *}{1000} \qquad \textbf{(2-3)}$$

where: V = Cutting speed (m/min)

D = Tool diameter (min)

n * = Spindle speed (rpm)

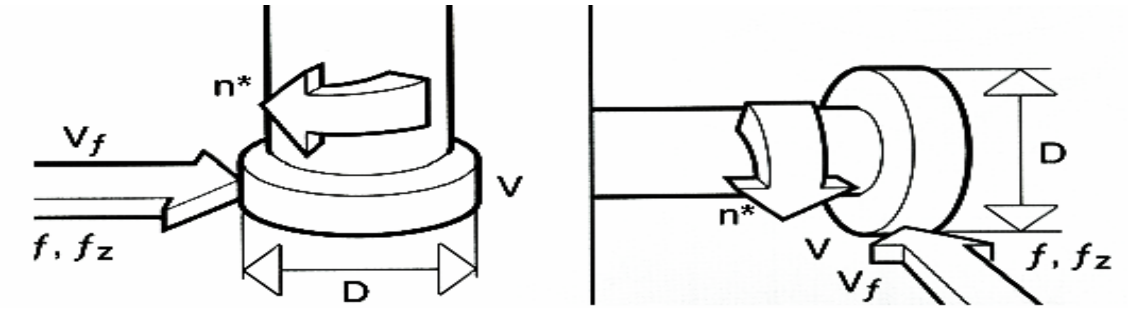

Figure 2-10: cutting speed and the parameters related to cutting process. [34]

(n*=spindle speed, V=cutting speed, fz=feed per tooth, D=tool diameter)

2.7.2 Feed per tooth (FZ)

During machining operation, the relative movement between the tool and the workpiece can be described as Feed Figure 2-10, [34]. This can be expressed in millimeters on inches per min, the author further said that Feed rate is less affected by temperature at the cutting edge. In machining, it is always advisable to use the highest feed rate because material removal rate is directly

proportional to the feed rate [31]. It also worth noted that in milling operation, the capability of each tooth defines the limits for the tool [34]. This relationship can be shown in the equation? below:

$$fz = \frac{Vf}{n *. z} \quad \textbf{(2-4)}$$

where:

Fz = feed per tooth(mm/rev*teeth), Vf = feed speed (mm/min), N* = spindle speed(rpm), Z = number of cutting teeth. The figure below shows the feed and the related parameters.

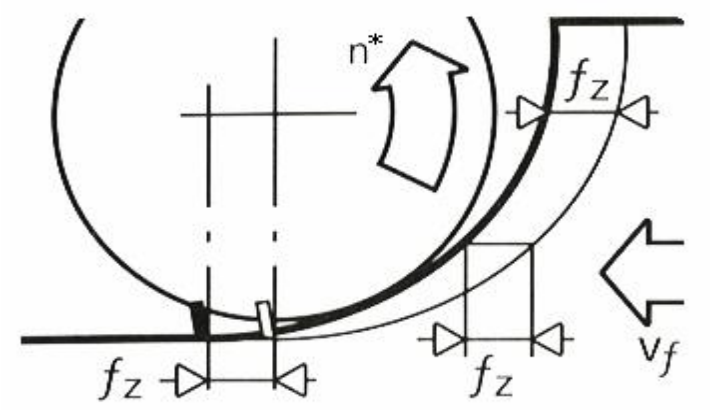

Figure 2-11: feed variable and the parameters [34]

2.7.3 Influence of axial depth of cut (ap)

This is depth the tool penetrates the workpiece usually measured along the axis [34] . According to machining guidelines [33], it was shown that a reduced tool life is faintly associated with an increase in axial engagement. Oosthuizen in his research said that therefore it is important that the depth of cut should be bigger than the work-hardened layer cut from the previous cut [31].

2.7.4 Influence of radial depth of cut (ae)

This is the distance by which the tool covers the workpiece surface measured along the cutting tool diameter [34]. The radial cut influence the tool life and the removal rate mostly when it is deeply plunged into workpiece which ultimately increases the removal rate. It is also recommended that for every new insert, the best balance for good removal rate and a lasting tool life must be established because the relationship between radial cut and depth of cut is crucial [31].

2.7.5 Coolant

The common term used in industry to describe coolants and lubrications used in machining is "Cutting fluids" this can be made up of dissolved chemicals (such as sulfur, chloride, or phosphorous) usually water based fluids [35]. The goal of machining industries is essentially for high removal rate of material and the quality of the product machined, but there are problems associated with this which are caused by high temperature developed during machining [36]. They further said that due to this effect, premature tool failure and dimensional deviation cutting tools are always the result in machining.

Currently what coolant does is to reduce these effects of heat generated at shear zone and friction zone which in turn elongate the tool life. Venugopal et al, investigated the tool wear and tool life of carbide inserts in turning of Ti- 6Al-4V alloy under dry, wet and cryogenic environments and came to conclusion that there were less tool wear parameters under the influence of cryogenic machining compare to dry machining [37].

According to Domenico [38], in his work to understand the effects of cryogenic coolant application and machining surface alteration during orthogonal machining of hardened AISI5200 bearing steel, he found out that the white layer is partially reduced or it can be totally removed under certain process parameters and cryogenic cooling condition [38].

2.7.6 Temperature

Cutting temperature is known to affect and influence the tool wear progressively both in cutting forces of milling operation and in the tool life [31]. According to Dar and Kamruzzaman [39], in their investigation on the role of cryogenic cooling by liquid nitrogen on cutting temperature shows that tool life improved substantially mainly by the reduction in cutting temperature. Childs et al [40] , estimated cutting edge temperatures in micro machining of Cu-Ni alloys with single crystal diamond tools and concluded that thermal activation depends on temperature with action energy 53 plus or minus 6 KJ/mol [40]. Oosthuizen [31] further added that a cutting material that has a relative high transverse rupture strength and thermal conductivity can generate aptitudes for high temperature together with increase mechanical shock resistance.

2.7.7 Cutting force

This is the force acting on tool during machining under specific condition [41]. Good machinability is defined as an optimal combination of factors such as low cutting force, good surface finish, low

tool temperature and low power consumption [41]. Jitendra Thakkar et al results indicated that feed rate and depth of cut both have significant influence on cutting force as well as surface roughness [42]. The cutting forces needed when machining stainless steels are slightly lower compare to the required cutting forces in Titanium [31].

2.8 Cutting materials and insert configuration

Recently with the new development in technologies, we have witnessed an increase in the quality of cutting tools which has led to global increase in production [31] [43]. Cutting tool inserts are disposable attachments used in cutting tools that usually contain the real cutting edge. Applications of Cutting tool inserts includes boring, construction, cutoff and parting, drilling, grooving, hobbing, milling, mining, sawing, shearing and cutting, tapping, threading, turning, and brake rotor turning [44].

2.8.1 Geometries and Uses of cutting tool inserts

Cutting tool inserts can have many different geometries. These geometries are based on dimensions and tolerance which can be denoted by ISO standards, ANSI (America) and JIS, CIS from Japan [31] . In Figure 2-12, Round or circular inserts are used in applications such as button mills or in radius groove turning. Some types are adjustable to employ unused edge portions once part of the edge is worn. A diamond insert is a four-sided insert with two acute angles used for material removal. Triangle inserts have a triangular shape; three equal sides and three tips with included angles of 60°.

A trigon insert is a three-edged insert like a triangle, but with a reformed triangular shape, such as bowed sides or intermediate angles on either side, just to allow for higher built-in angles at the tips [44]. Square cutting tips have four equal sides [45] [44]. Rectangular inserts have four sides, two of which are longer than the other two. These inserts are often used for grooving, etc., where the short sides contain the actual cutting edge. Rhombic or parallelogram inserts are four-sided, with an angle on the sides for cutting point clearance. A pentagon insert has five equal sides and angles. An octagonal insert has eight sides, typically Indexable in nature [44].

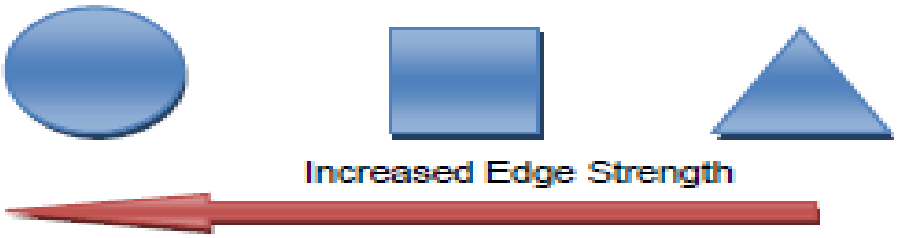

Figure 2-12: common insert geometry [31]

2.8.2 Types of inserts tips

In addition to inserts that are defined by their geometry, a few types are differentiated by their tip angles. A ball nose mill is an insert with a hemispheric "ball nose" whose radius is one half of the cutter diameter, useful for machining female semicircles, grooves or radii. A radius tip mill is a straight insert with ground radius on tips, typically for use on milling cutters. In a chamfer tip mill the insert side or ends contain an angled section on tip to produce an angled cut or a chamfered edge on the workpiece, typically attached to milling cutter holders. A dog bone is a two-edged insert with a narrow mounting center and, as the name implies, a broader cutting feature on both ends, often used for grooving. The following angles figure 2-13 can be found on the tips of an ordinary cutting tool inserts: 35°, 50°, 55°, 60°, 75°, 80°, 85°, 90°, 108°, 120°, and 135° [44].

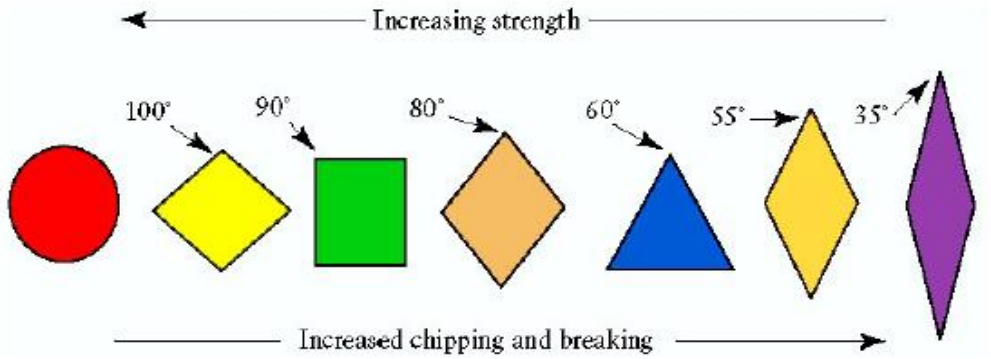

Figure 2-13: Typical insert shapes and Tip angles [44]

2.8.3 Key Specifications in cutting tool inserts

The diameter of the circle or The Inscribed Circle (I.C.), that fits completely within the insert geometry generally classifies insert size [45]. This is can be found mostly in Indexable inserts, except for rectangular and some parallelogram inserts, where length and width are commonly used. Important specifications for cutting tool inserts include thickness, radius if applicable, and chamfer angle if applicable. Common features for Cutting tool inserts include unground, Indexable, chip breaker, and dished [45]. Some common factors can also be considered when selecting tool inserts shapes Figure 2-3.

Table 2-3: factor affecting choice of insert shape [44]

Factors affecting choice of insert shape	R	90	80	80	60	55	35
Roughing (strength)	●	●	●	○	○		
Light roughing/Semi-finishing (No. of edges)		○	●	●	●	●	
Finishing (No. of edges)			○	○	●	●	●
Turning and Facing (feed directions)			●	○	○	●	●
Profiling (Accessability)			○	○	○	●	●
Operational versatility	○		●	○	○	●	○
Limited machine power			○	○	●	●	●
Vibration tendencies (reduction)				○	●	●	●
Hard material	●	●					
Intermittent Machining	●	●	○	○	○		
Large entering angle			●	●	●	●	●
Small entering angle	●	●		●	●		

● Most suitable ○ Suitable

2.9 Material for cutting tools

Generally, during machining process, different workpiece requires different cutting tool materials. But ideally a cutting tool material must have the following trade off characteristics [46]:

- High temperature stability
- Ability to resist wear and thermal shock to certain level
- Impact resistance
- Must be harder than the workpiece
- Chemically inert to the work material and cutting fluid or coolants

Inserts are usually made of carbide, micro grain carbide, CBN, ceramic, cermet, cobalt, diamond PCD, high-speed steel, and silicon nitride, Figure 2-14. Different coatings are used in cutting tool

inserts such as: titanium nitride, titanium carbo-nitride, titanium aluminum nitride, aluminum titanium nitride, aluminum oxide, chromium nitride, zirconium nitride, and diamond DLC.

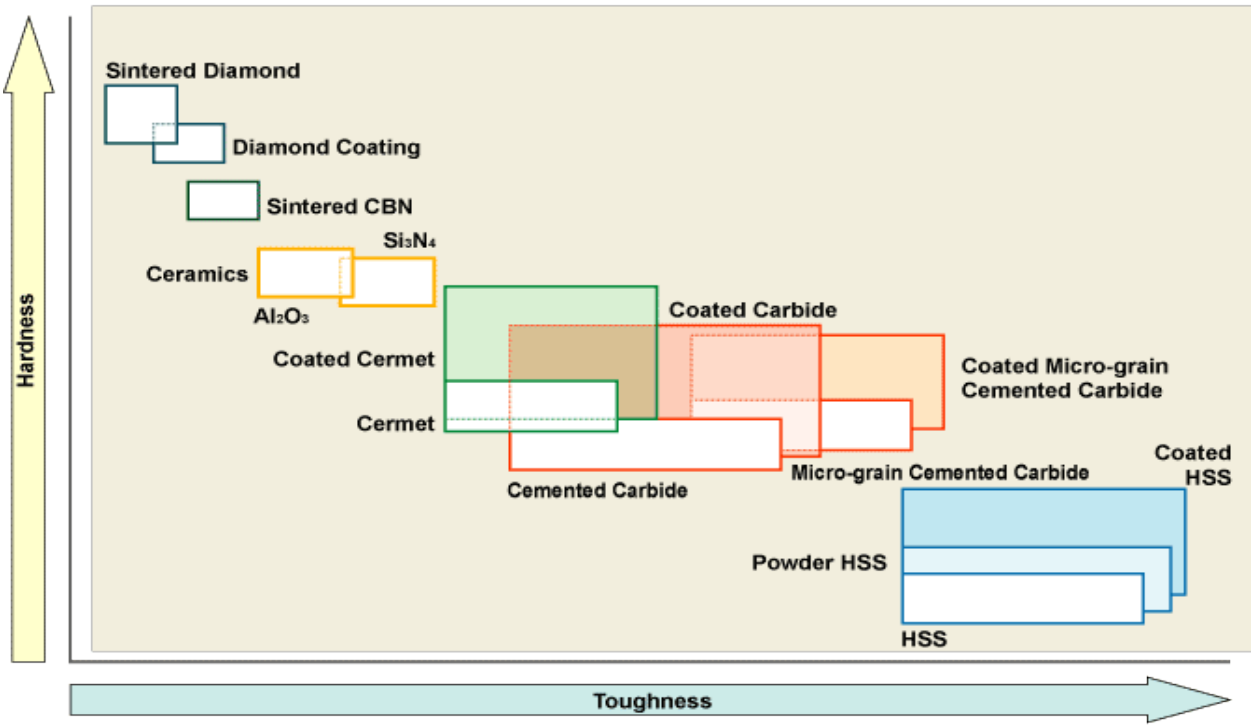

Figure 2-14: Cutting tool material chart [47] (source: Mitsubishi)

2.9.1 High Speed Steel

The High-Speed Steel (HSS) tools which form an important part category in metal cutting are so named because they were developed to cut at higher speeds. Developed around 1900 HSS are the most highly alloyed tool steels. The tungsten (T series) were developed first and typically contain 12 - 18% tungsten, plus about 4% chromium and 1 - 5% vanadium [48].

Most grades contain about 0.5% molybdenum and most grades contain 4 - 12% cobalt. HSS tools are tough and suitable for interrupted cutting and are used to manufacture tools of complex shape such as drills, reamers, taps, dies and gear cutters [48] [49]. Tools may also be coated to improve wear resistance. HSS accounts for the largest tonnage of tool materials currently used. Typical cutting speeds: 10 - 60 m/min.

2.9.2 Cast Cobalt Alloy

This material was made known to industries in early 1900s these alloys have compositions of about 40 - 55% cobalt, 30% chromium and 10 - 20% tungsten and are not heat treatable. Maximum

hardness values of 55 - 64 Rc. Cast cobalt Alloys have good wear resistance but are not as tough as HSS but can be used at somewhat higher speeds than HSS. Now only in limited use [48].

2.9.3 Carbon Steel

Since the 1880s, Carbon steels have been used for cutting tools. However, at 1800C temperature, carbon steels start to manifest a softness. This constraint means that such tools are hardly utilized for metal cutting operations. But the plain carbon steel tools, which contains about 0.9% carbon and about 1% manganese, hardened to about 62 Rc, are commonly used for woodworking and they can be used in a router to machine aluminum sheet up to about 3mm thick [31] [49].

2.9.4 Cemented Carbide or simply Carbide

There are two groups used for machining which are tungsten carbide and titanium carbide, both types may be coated or uncoated [48]. It has high hardness over a wide range of temperatures, high thermal conductivity, high Young's modulus making them effective tool and die materials for a range of applications [50]. Tungsten carbide particles (1 to 5 micro-m) are bonded together in a cobalt matrix using powder metallurgy.

The powder is pressed and sintered to the required insert shape. titanium and niobium carbides may also be included to impart special properties. A wide range of grades are available for different applications. Sintered carbide tips are the dominant type of material used in metal cutting [48].

The proportion of cobalt (the usual matrix material) present has a significant effect on the properties of carbide tools. 3 - 6% matrix of cobalt gives greater hardness while 6 - 15% matrix of cobalt gives a greater toughness while decreasing the hardness, wear resistance and strength. Tungsten carbide tools are commonly used for machining steels, cast irons and abrasive non-ferrous materials [46] [48].

Titanium carbide has a higher wear resistance than tungsten but is not as tough. With a nickel-molybdenum alloy as the matrix, TiC is suitable for machining at higher speeds than those which can be used for tungsten carbide. Typical cutting speeds are: 30 - 150 m/min or 100 - 250 when coated [46].

2.9.5 Coating

Often times carbide tool tips are coated to improve tool life or to enable higher cutting speeds. Coated tips Figures 2-15, typically have lives 10 times greater than uncoated tips. Common coating

materials include titanium nitride, titanium carbide and aluminum oxide, usually 2 - 15 micro-m thick. Often several different layers may be applied, one on top of another, depending upon the intended application of the tip. The techniques used for applying coatings include chemical vapor deposition (CVD) plasma assisted CVD and physical vapor deposition (PVD). Diamond coatings are in high demand for metal cutting use and further development are still ongoing [50] [46] [32] [48]. Various methods of attaching carbide inserts to tool holder is shown in Figure 2-16.

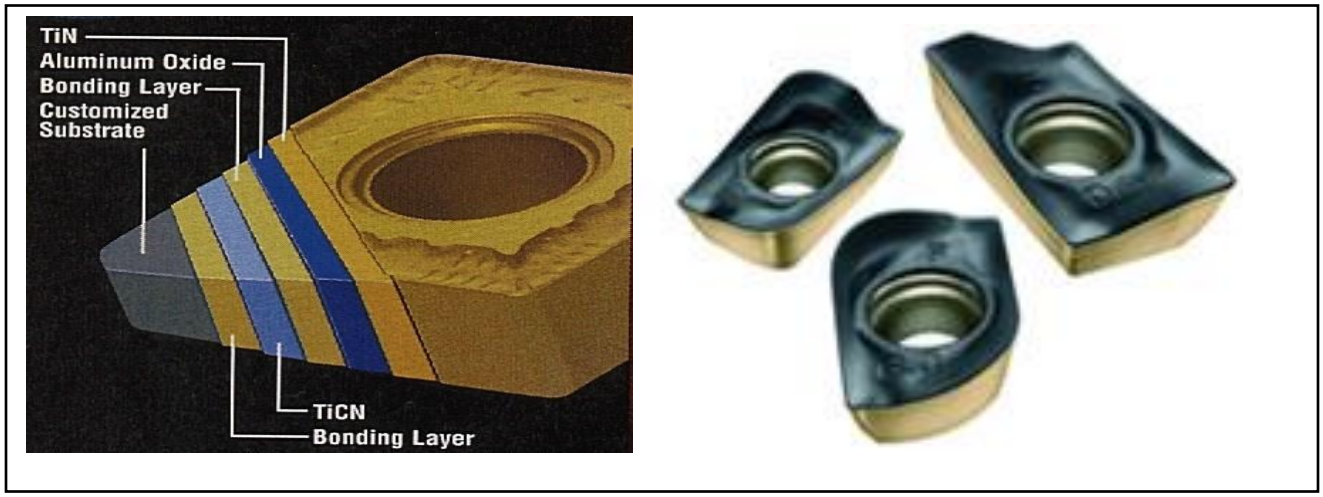

Figure 2-15: surface of a multi-layer coated carbide insert (b) different shapes of inserts [49]

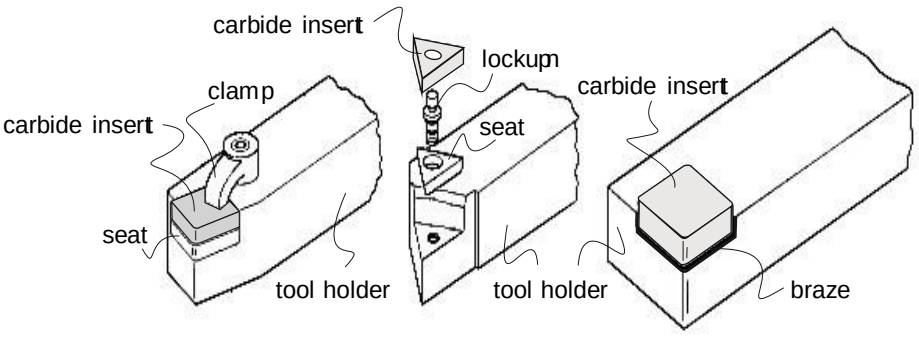

Methods of attaching carbide inserts to tool holder:
(a) clamping; (b) wing lock pins; and (c) brazing

Figure 2-16: method of attaching carbide inserts to tool holder [49]

2.10 Machining performance assessment

2.10.1 Tool life

Generally, Tool wear can be regarded as a gradual failure of a tool due to constant operation as usage. While Tool life can be defined as the length of cutting time a tool can be used until the tool

reaches catastrophic failure. According to [50] and [51], Tool life is usually defined by Flank wear because of its major influence this factor has on surface finish and dimensional accuracy of the part that is being machined. It is also noted that as the flank wear increases, surface roughness also increases. Therefore, a common way of quantifying the end of a tool life is by putting a limit to the maximum acceptable flank wear denoted as V_B. See Table 2-4 below:

Table 2-4: Typical V_B [52]

HSS tools, roughing	1.5 mm
HSS tools, finishing	0.75 mm
Carbide tools	0.7 mm
Ceramic tools	0.6 mm

However, process reliability can be greatly influenced by crater wear as this factor leads to immediate breakage because of tool chipping [31]. A failed cutting tool mostly causes problem with surface quality of workpiece and it has been suggested and estimated according to literatures that a flank wear scar band width should be as high as 0.3mm for experimental purposes [31].

In the figure below, a typical wear growth curve can be grouped into three sections, the break-in-section usually at the early stage of the tool usage which shows the sharp cutting edge wears quickly. Steady-state region is the second section with a relative uniform wear.

According to the Figure 2-17, the part which indicates the first slope is highly dependent on the work material and cutting conditions. This simply means that the harder the workpiece the steeper the slope which eventually the beginning of the accelerated failure sections [31] [53].

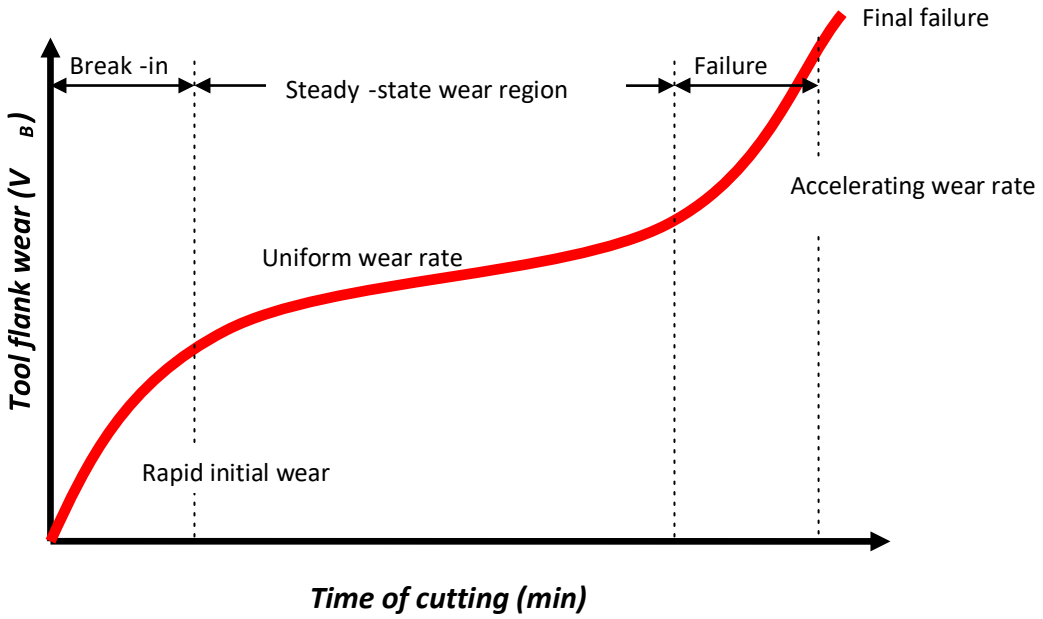

Figure 2-17**:** Tool life [53]

A widely known equation called Taylor equation has been established to determine tool life as a function of cutting speed. This can be expressed as:

$$VT^n = C$$

Where:

Table 2-5: Definition of Taylor's equation [50] [53]

v_c	cutting speed
T	tool life
n and C	constants

The constant c and n can be found for a tool material and specific workpiece while feed is extracted from experiment or from published data [48] [50]

2.11 Factors affecting tool life

There is a strong relationship between the rate of wear and the life span of a tool [54] [55]. This relationship can be largely affected by some influencing factors that are listed below;

- Types of surface on the metal (scaly or smoothness)
- Profile of the cutting tool

- Speed, feed and depth of cut (axial or radial)
- Material of cutting tool
- Microstructure of the material
- Type of material used
- Hardness of the material
- Type of machining operation being performed [54] [55].

According to Dimla and Lister work, they were able to established that irrespective of all these parameters the cutting speed still contribute the highest influence on tool wear [56].

2.12 Tool condition monitoring principles

In modern manufacturing, tool condition is critically needed in manufacturing process for the following reasons:

- Tool wear considerably affects production operation and thus should be carefully monitored to secure consistence product quality
- The advantage of economically utilizing tool life cannot be achieved without a means for tool wear monitoring as a result of variations in tool life.
- An automated high volume production cannot be sustained without an effective means for tool wear monitoring and tool breakage detection [57].

There are three major monitoring principles which are;

- Direct and indirect monitoring
- On-line and off-line monitoring
- Contact and non-contact monitoring

Direct and indirect monitoring: indirect monitoring method operates by measuring process variables such as vibration or acoustic emission from the process. Direct monitoring on the other hand measures physical geometry of the tool [50]. According to Shao et al [58], the direct method is the most accurate because the actual wear easily be measured while indirect method involves processing the signal and clear interpretation which may require an expert experience. Indirect method can also be referred to as in-process or on-line monitoring.

On-line and off-line monitoring: on-line as the name implies continuously measures and interpret incoming signal [50]. This helps to detect any signs the represent gradual wear [50]. As for the off-line method, this is suitable when sensors are used to measure cutting edge geometry.

Contact and non-contact method: contact method is a system when the workpiece or the critical part in the system has a physical contact with measurement instrument. Non-contact does not have to be in touch with the critical part in machinery an example can be measurement of surface roughness using Electron microscopes.

2.13 Tool condition monitoring system

Condition monitoring can be defined as the process of monitoring physical parameters, associated with machinery operation, for the purpose of determining machinery integrity [59]. Literatures have revealed to us that a lot of researchers have published so many systems that has been established in the process of monitoring tool these are listed below:

- Vibration monitoring system
- Mathematical modelling – analytical and empirical system
- Forced based monitoring system
- Acoustic emission monitoring system
- Sensor fusion and multiple sensors monitoring system
- Motor current measurement
- Vision (optical) measurement system
- Ultrasonic system
- Surface texture
- Laser scatter method
- Stereo imaging

But for the purpose of this research work, the author will focus on few monitoring systems that are of concern:

2.13.1 Surface texture

This method uses the surface roughness (Ra) of the work piece as the benchmark for tool wear. This system of measurement has been carried out both as an on-line and off-line system [50]. Dang and Wang concluded that the increase in Ra is caused as a result of waveform being copied by the

shape of the tool tip [60]. During experiment, surface roughness is commonly measured mechanically by using stylus device. In this process, the most widely used descriptor in engineering practice is Ra (average surface roughness) [50].

2.13.2 Vibration

Vibration measurement is well known and a widely-used technique for condition monitoring. In Dan and Mathew review, they came to conclusion that vibration signals are vary with tool failure in some frequencies this described the relationship between changes in vibration and progressive tool wear [61]. Scheffer in his work said that piezoelectric accelerometers can be used to measure any vibration generated by oscillation of cutting force and that these accelerometers met the ambient requirements for tool wear monitoring because they generally develop resistance to the hostile media that exists in machining operation [62]. However, Scheffer identified a challenge that can be encounter while using vibration. He said that the main worries of monitoring tool life through vibration system is to detect the frequency range that is influencing the tool life because most machining process consist of many factors that generates vibration that are not relevant to tool wear [62].

2.13.3 Forced based monitoring system

It is a well-known fact that an increase in cutting force components of a vibration is caused by worn tools [63] [64]. Therefore, to develop a monitoring system that will take care of different directions for a number of processes, a forced based system is used. Examples of force based monitoring tool are: direct measurement dynamometers, piles and rings, pins extension sensors, measure of displacement, force measure bearings, force and torque at spindles [62].

Sikdar and Chen described cutting forces as one of the most reliable methods used to monitor tool wear. The further explained into details that flank wear has been identified to increase the cutting forces in all the three components: radial, feed and tangential directions [65]. They concluded that all the three forces increase suddenly as soon as the tool begins to fail but Cakir and Isik added that only tangential force decreases consistently when the tool finally breaks [66].

2.13.4 Acoustic Emission:

Acoustic emission can be described as an elastic transient wave generated as a result of energy that is released from a localized source within a material [67]. According to Li review work, he highlighted some basic sources of acoustic emission during tool monitoring as listed below [68]:

- Fractional contact between the tool flank face and the work piece which eventually leads to flank wear;
- Plastic deformation during the cutting process in the work piece;
- Plastic deformation in the chip;
- fractional contact between the tool rack face and the chip which result in crater wear;
- tool fracture;
- chip breakage;
- collision between chip and tool;

Dan and Mathew [1990] came to conclusion in their review that the AE sensing technique appears to be more sensitive to tool fracture than cutting force and tool vibration measurements. This agrees with Dornfeld [1994] who indicated that the frequency-range experience during operation for the AE signal is far higher than the ambient noise and machine vibrations [61].

In Kannatey-Asibu and Dornfeld work, they used statistical analysis this revealed a clear sensitivity to tool wear when using AE signals [69]. Dimla Snr [70] highlighted that AE is less dependent on the cutting tool than on the cutting material, with its signal showing the all the activities of the response right from the machine tool set-up. Dimla further highlighted that AE may not be an appropriate wear indicator in monitoring applications but could be used to detect tool-tip breakage in machining operations [70].

Liang and Dornfeld presented a signal-processing system, which uses an autoregressive time-series to model the acoustic emission generated during cutting. This technique encodes the acoustic emission signal features into a time-varying model parameter vector [71]. Li [68], carried out a review and he came to conclusion that AE signals depend heavily on process parameters and sees the key issues as being how to reduce these effects in intelligent tool wear and fracture monitoring using AE signals in his work, he used an acoustic emission for cutting processes in turning which includes signal classification and correction; which are processing methodologies, such as time

series analysis wavelets and FFT, and finally pattern classification using a fuzzy classifier, a neural network and sensor and data fusion [68].

Dornfeld et al. [72] argue the accuracy of AE and concluded that AE has been introduced in the field of sources so far. Diei and Dornfeld [73] and Hutton and Hu [74] used the RMS signals, (Root Mean Square), and concluded that the signal is a periodic signal which can be regarded as a periodic random signal. They used TDA (Time- Domain-Averaging) to decompose the signal into a periodic component and concluded that the TDA deviation can be used as a feature for the AE RMS signal to detect tool wear because the mean of TDA describes the dynamic component in AE RMS therefore this can be linked to tool wear [74].

2.14 Tool wear

Tool wear can be described as the gradual failure of cutting tools due to regular operation. It is a term frequently associated with tipped tools, tool bits, or drill bits that are used with machine tools. This segment briefly describes mode of failures and types of tool wears.

2.14.1 Failure mode

Fracture: this is a mode of failure that are characterized by breakaway of material on the tool edge Figure 2-18. Fracture occur mostly when the feed rate is very high. Fracture can also be experienced when a very low fracture length is used as mechanical loading exceeds the fracture strength of the insert [62]. Temperature failure: this type of failure is encountered when the temperature of the tool tip reaches a certain value and plastic deformation is set in. this can also be explained that when the tool yield strength is lowered below the existed normal stress [62]. Ultimately Temperature failure is recognized by its thermal cracks that occur on the cutting edge [31] [53].

Gradual wear: this mode of wear manifest on top of rake face and flank. Gradual wear leads to reduction in cutting efficiency eventually loss of tool geometry. As the gradual wear scratch increases, as so also the tool becomes heavily worn-out [31].

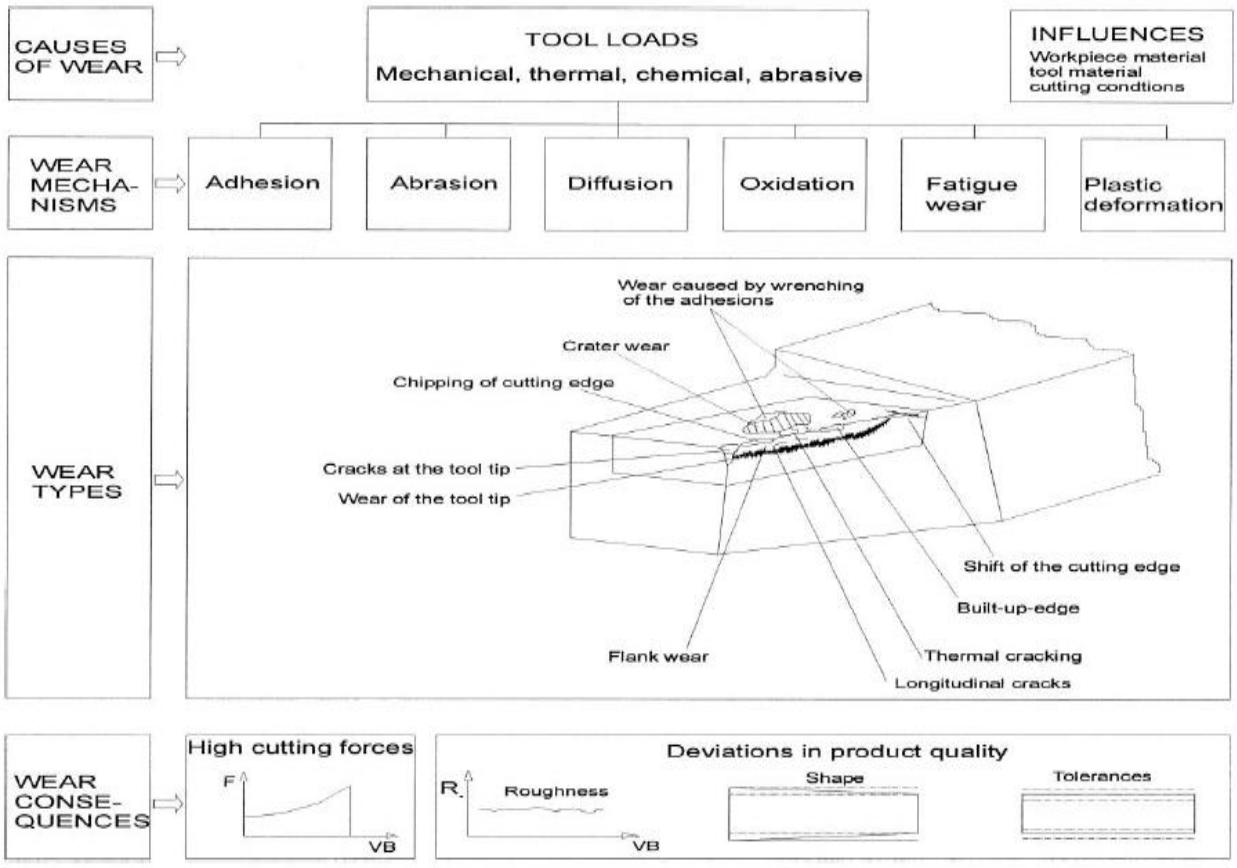

Figure 2-18: Causes, mechanism, types and consequences of tool wear [75]

2.15 Types of tool wear

2.15.1 Crater wear

As stated in the ISO (1993) that crater wear occurs on the rake face and does not usually limit tool life although excessive crater wear reduces the cutting edge thereby leading to deformation [76]. Oosthuizen Figure 2-19, explained that this type of wear is made because of chips rubbing against the surface [31]. Scheffer also stated that the tool-chip interface temperature dominates this type of tool failure which serve because of feed rate and speed [62].

2.15.2 Flank wear

The rubbing of the wear land against the machined surface causes damage to the surface, flank wear Figure 2-19, occurs on the relief face which results in the formation of the wear land [76]. Flank wear can also be a volumetric loss at the top of the tool tip edge that are mainly cause by abrasion, it also manifests at a very low operating speed [31].

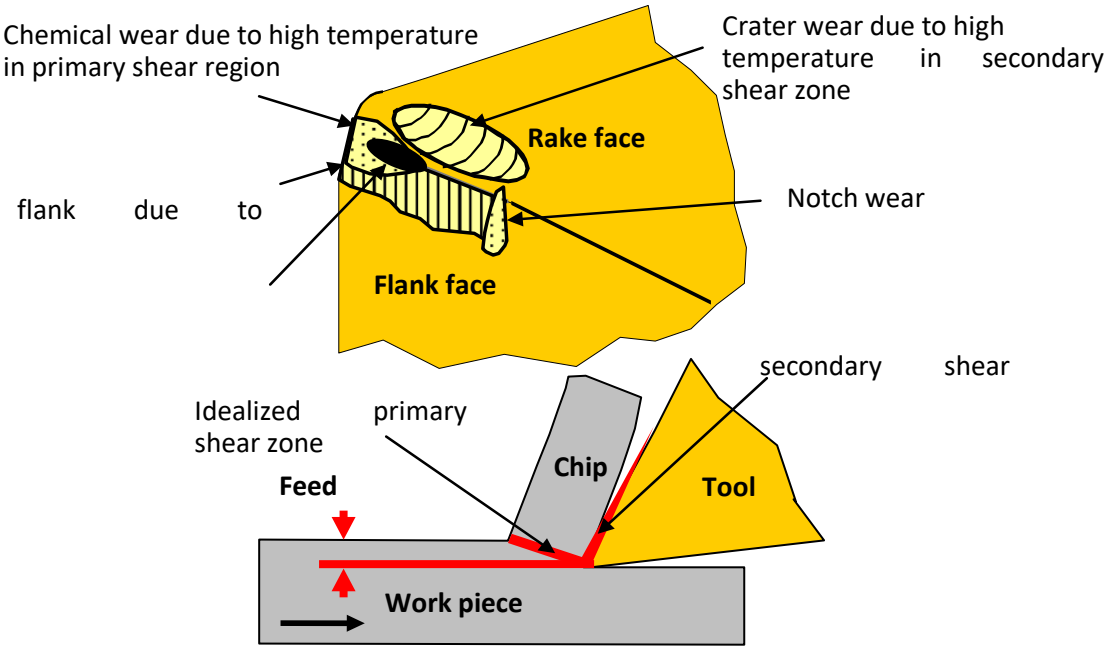

Figure 2-19: Types of tool wear [31]

2.15.3 Notch wear

An extreme case of flank wear can be term as Notch wear consequently reflect at the cutting edge. It was also found out that if the original surface is harder or more abrasive in nature than the internal material, notch can be experienced [31] [76].

2.15.4 Nose radius wear

This type of wear seems to resemble a combination of Notch wear and flank wear; it generally occurs on the nose radius of the tool that is on the trailing edge close to the end of the relief face [76]. At a high cutting speed, an entire nose may be lost due to the cutting edge deform plastically. The wear formed on the nose affects the quality of surface finish [77] [78].

2.16 Mechanism of tool wear

In everyday life, wear of material is constantly experienced as a result of gradual removal of materials that are relatively in contact due to sliding motion. It has also been universally established that wear and friction has close link. Consequently, friction results in important energy losses, while wear is accompanied with increased maintenance costs and costly machine operation downtime [79]. He further said that wear, frictional heat, fracture and fatigue are the main factors which governs machine tool life time.

Since wear cannot be completely eliminated, but reduced, there are methods used to accomplish this such as Lubrication, formation of sufficiently smooth surface, correct assembly and exploitation of fitted component part and modification of near-surface materials of frictional components [79]. However, different wear mechanisms have been identified in engineering practice according to their relative importance in order of wear types as follows: Abrasion, Adhesive, Diffusion, chemical reaction and Plastic deformation.

2.16.1 Abrasion Wear

Abrasion wear occurs when the softer metal may consist a substantial concentration of hard particles therefore, the friction that is created between the flank and the workpiece because of sliding chips in the shear leads to what is called abrasion [76] [31]. According to Silva [80], abrasion leads to loss of material by the activity of hard constituents as they are swept over the tool surface. This wear mechanism occurs progressively on the flank surface which enables us to measure and estimate the tool life. Crater wear can be accelerated by diffusion when the crater is weakened by diffusion [31].

2.16.2 Adhesion (Attrition)

This can be described as when two materials are forced into contact under high pressure and temperatures until they are bonded together [31]. According to [76], at low temperature range and relatively low cutting speed, adhesion is the major factor that controls tool wear going through a maximum value of wear rate of about 600^0C. He further highlighted that asides adhesion activity between the tool and the workpiece, resistance to micro-contact damage due to the periodic effect of local adhesion forces are the main characteristics determining the life of a tool material in this type of wear mechanism [76].

2.16.3 Diffusion

According to Hoglund, when a metallic material glides over another metal causing the temperature at their point of contact high, the condition becomes favorable for atoms from the harder metal to diffuse into the softer metal therefore increase the hardness of the latter and its abrasiveness and vice versa to the extent that particles on both metals are dislodged, torn, or cut off, finally swept away by the flowing medium [76] [81].

According to Hastings, Diffusion mechanism becomes a significant factor in tool life at a cutting temperature of about 800^0C [82]. Loladaze suggests that “high temperature, large rate of

deformation and continuous contact at the interface zone facilitate the initiation of intermetallic diffusion between the tool and the work piece [83].

2.16.4 Chemical reaction

The thermal activation process (oxidation) due to a chemical reaction between the tool or insert and the workpiece can be regarded as chemical wear [31]. The rate of this wear mechanism is directly proportional to the temperature of the cutting process.

2.16.5 Plastic deformation

The forces acting at the edge of cutting process at a very high temperature normally results to deformation plastically hence make it susceptible to abrasion [31]. This is being associated with the removal of shared layers resulting from excessive plastic deformation.

2.17 Process monitoring

2.17.1 Process monitoring with the use of sensors

Currently different Sensors are widely used for process monitoring in the industries. Some common examples of sensors that are found in the industry are basically force based, power based and acoustic emission sensors. However, other sensors Table 2-6, that can be seen around are:

Table 2-6: Types of sensors [62]

Smoke sensor	Image sensor	Flame sensor
Sound sensor	Tool wear sensor	Temperature sensor
Accelerometer or Vibration sensor	Seismic sensor	Tool damage sensor
Current sensor	Lubrication oil detector sensor	Touch sensor
Limit sensor	Edge sensor	Speed sensor
Clamping Force Sensor	Torque sensor	Acoustic emission sensor
pH sensor	Machined surface roughness sensors	Level meter
Coolant temperature sensor	Thermal deformation sensor	Chip monitoring sensor
Temperature distributor sensor	Dust sensor	Humidity sensor
CO2 gas sensor	Pressure sensor	

2.17.2 Areas of applications

Modern manufacturing industries have made us to know that there is a wide range of tool wear and surface monitoring systems applications. One of the notable application is On-line monitoring of tool wear which permits timely tool replacement with minimum down time [62]. Examples of these areas are:

- Manufacturing of machine components
- Mass production of household items
- The automobile industries
- Electrical and Mechanical product manufacture
- Computerized Numerical Control (CNC) machining optimization

2.18 Artificial/Intelligent monitoring systems

According to [84], a system can be defined as "Automated/Intelligent monitoring system if it has capability of sensing, analyzing, knowledge learning, and error correction features, essential to machining tool condition when incorporated". They further said that this AI system should be able to imitate humane capabilities as much as possible their operators. Therefore, for this to be carried out, the four components listed below must be included:

2.18.1 Sensing Techniques

This simply means indirect sensing techniques such as cutting forces, vibrations, and acoustic emission must be used. Although different types of sensors and sensory data from different areas are employed to yield optimum and valuable information [84]

2.18.2 Feature Extraction systems

Normally, signal from sensors contain the necessary information that are needed to separate between different process and tool conditions. Because the raw signals usually contain noise as such need further filtering and processing.

2.18.3 Decision making systems

Decision making strategies deal with processing of incoming signal features and perform a pattern association assignment, structure the features to proper classification of tool condition which depends on the target of the investigator.

2.18.4 Knowledge learning systems

"In order to make a correct decision, learning algorithms have to be provided. Such algorithms tune system parameters by observing the sample features corresponding to different tool conditions. Like human operators, automated monitoring systems should have the ability to learn from their experiences (past work) as well as from the new information generated from the machining process" [84].

2.19 Tool wear monitoring Techniques

2.19.1 Direct and indirect monitoring technique

There are two approaches that have been traditionally categorized as measuring techniques for the monitoring of machining operation; these are direct and indirect [85]. During direct approach, the

actual quantity of the variable such as tool wear is measured. According to Schaeffer, this deal with a measurement of volumetric loss at the tool tip [62].

Examples of direct measurement are found in the use of radioactive isotope, laser beams, electrical resistance, cameras for visual inspection. It was also revealed by [85] direct technique is suitable for laboratory research work due to its high degree of accuracy and practical limitations caused by accessing problem during machining and the use of cutting fluid.

However, indirect methods are less accurate than direct techniques but has its advantages over direct by having less complex process, cost effective and more suitable for practical applications in industries [62]. Indirect methods make use of a pattern in sensor data from process to detect failure mode therefore [62], both direct and Indirect method is greatly employed in this research work see Table 2-7.

Table 2-7: Examples for direct and indirect tool wear sensing methods [86]

Wear or process parameters	Examples for measurement procedures and transducers
	Direct methods
Shape or position of the cutting edge or the wear area	Measurement with optical methods (e.g. CCD camera or fiber optic sensor) or integration of thin film sensors into the coating of a cutting tool
Volumetric overall loss of the tool	Measurement of size and concentration of wear particles in the coolant (and electrochemical analysis) or measurement of radioactivity (for specifically, prepared tools)
Changes of the electrical resistance at the junction of tool and workpiece	Voltage measurement at a specific, conductive tool coating
Changes of workpiece dimensions	Dimension measurement by means or micrometers or optical, pneumatic, ultrasonic, or electromagnetic transducers
Change of distance between tool (or tool holder) and workpiece	Distance measurement by means of micrometers, pneumatic gauges, displacement transducers (e.g. inductive or capacitive), or ultrasonic sensors **Indirect methods**
Cutting forces	Force measurement with strain gauges or piezoelectric sensors at the tool or at (or in) the tool holder, piezoelectric force measuring plates or rings at the turret, force-measuring bearings, torque measurement at the main spindle
Vibration of tool or tool holder	Vibration measurement with accelerometers
Substrate-borne or airborne sound	Acoustic emission (AE) measurement by means of transducers integrated in the tool holder or coupled via the coolant; measurement of acoustic (audible) signals with microphones
Electrical current, power, or energy	Measurement of current or power consumption of spindle or feed motors (e.g. ampere meter or dynamometer)
Cutting temperature	Temperature measurement by means of thermocouples or pyrometers, reflectance of chip surface or chip color
Roughness of the machined surface	Measurement with a mechanical stylus or optical methods (e.g. CCD camera or fibre optic sensor)

2.19.2 Continuous and intermittent monitoring technique

In continuous monitoring technique, the variables that are measured are available during the course of the machining process which assist in the online classification of the process and make sure that any unexpected changes can be responded to in time [62]. For intermittent monitoring methods,

the variables can only be recorded during intervals in the machining process. Clearly there are shortcoming attached to this starting from loss of time and high cost. A good example of this practice can be found in the application of an intermittent system to detect wear measurement on a periodical set of tools while machine is engaged with a different tool [62].

2.19.3 The use of sensors for tool wear monitoring

The use of sensors for tool wear monitoring usually takes place in an uncomfortable environment this can be a harsh weather, cryogenic environment, superheat environment or in the sea. Sensors that are used for tool wear monitoring should therefore be simple, flexible to operate and robust. Often times the use of multiple sensors is required to improve the performance of tool wear monitoring system because each sensor is independently connected to the tool wear.

2.20 Acoustic emission and sensors in tool wear monitoring

2.20.1 Acoustic emission and tool wear monitoring

Acoustic emission (AE) can be commonly defined as transient elastic waves that are released within a material caused by the discharge of localized stress energy. During metal cutting, the workpiece undergoes substantial plastic deformation associated with the generation of Acoustic emission. During chip formation AE is linked to the plastic deformation process because of interaction between the workpiece and cutting tool [87]. According to Blum et al, AE is normal discovered to be more sensitive to tool wear than cutting forces [88].

Chao et al, developed a real- time tool breakage detection system for turning by the sensor fusion of an acoustic emission sensor and a built-in-force sensor. They used an inbuilt piezoelectric force sensor was used to measure the cutting force without altering the characteristics of the machine tool dynamics. The experiment was carried out using carbide inserts that has two tips. They concluded that whenever a tool breakage is experienced a noticeable drop in AE burst was used to detect cutting force change [89] .

Jemielniak and Otman used a statistical signal-processing algorithm to detect the root mean square, Kurtosis and skewness of the acquired AE signal in the detection of catastrophic tool failure [90]. In Lee research work [91], he cited that “Kakade et al applied AE analysis on the effect of tool wear and corresponding change in chip-form in face milling by selecting AE parameters namely ring-down count. Rise time was recorded simultaneously with the corresponding flank wear land

length measured at fixed intervals. The results concluded that AE may be readily used for in-process monitoring of chip status and consequently tool monitoring" [91] [92].

Blum and Iwasaki carried out investigations to determine the influence of cutting conditions on the generation of AE signals during machining S45C steel. The AE signals and tool dynamometer signals provided extensive theoretical and data relationships between the energy packet of the AE and the deformation both in primary and secondary zone during cutting process [88].

2.21 Acoustic Emission wave parameters

The AE burst shown in Figure 2-20 can explained the parameters commonly found in in a typical AE signal. They are as follows: event, ring down count, event energy, duration, rise time, and event energy.

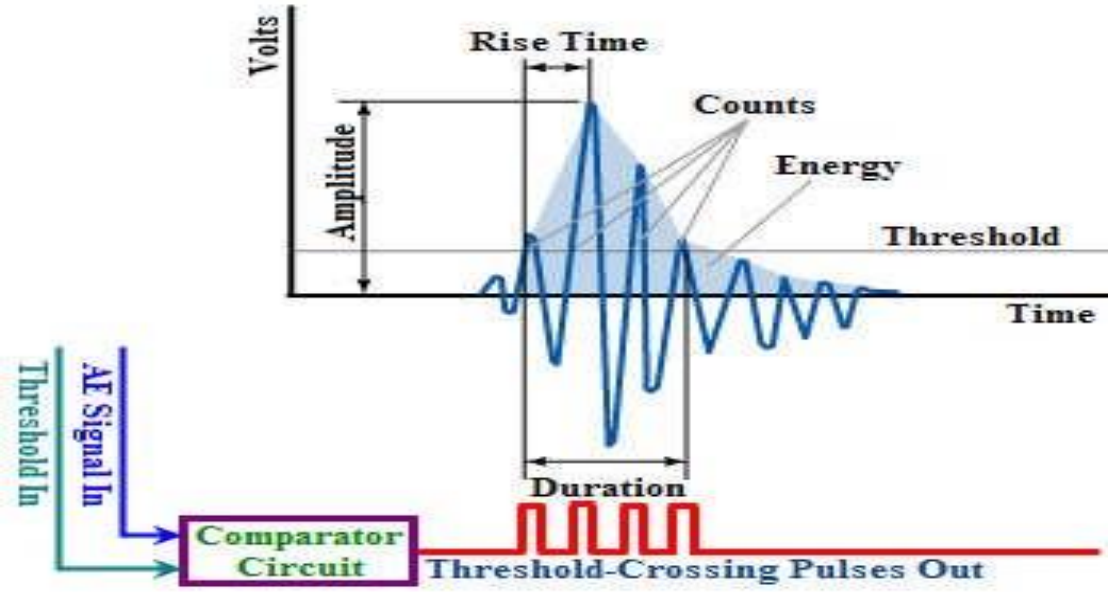

Figure 2-20: definition of common AE waveform parameters [93] [94] [95]

Ring down count: this is the number of times a signal exceeds a pre-set threshold. This is a measure of signal size therefore; a large signal will automatically present more count.

AE RMS: Root Mean Square is a value of input signal and the energy content of the acoustic emission signals that are related to energy release as mention earlier that it is the attributed to the transient release of energy in a material [96]. It can simply be termed as a measure of signal intensity.

Signal amplitude: an important parameter that defines the detect ability of the event is signal amplitude. Therefore, the maximum value of amplitude of the received signal is called signal amplitude [96]. It is also the suitable variable to be used for attenuation dimension.

Duration: the time between the point at which the event goes below the threshold and above the first threshold is called duration. This factor is closely correlated to the ring down count but most utilized for discrimination than measurement of emission variables. According to [96] signal from electromagnetic interference typically have very short durations, therefore, the duration is parameter can be used to filter them out.

Rise time: Rise time can be described as the point at which the event first goes above the threshold level and the point at which the amplitude reaches peak value [96]. This parameter has similar features as Duration.

Energy: this can be defined as the integral of the squared amplitude over time of signal duration.

2.22 Acoustic emission and sensor in tool wear monitoring

Acoustic emission technology has been discovered to be among the most suitable method to detect the rates of a very small energy release [70] [59]. AE has a very high sensitivity in detecting the loss of mechanical reliability when compare to the well-known vibration monitoring methods thus making it to have an edge over vibration techniques for tool wear monitoring [97] [98]. Because AE can provide effectiveness and superiority of a detectable indication from a minor defect, it has capability of giving early warning of emerging problems in other for proactive maintenance to be conveniently scheduled and carried out [59].

During acoustic emission process, the emissions generated on the surface of the material is presented as Rayleigh waves and as such can be measured with an AE sensor [59]. Other types of waves that can be found associated with this propagation are: Longitudinal, Lamb and shear waves [98].

There are two types of AE signals, transient(burst) and continuous signal. In AE burst signal, signal diverge completely from the background noise while in continuous AE signals, clear distinctions of amplitude and frequency can be seen and there is no ending for the signals [59]. The idea of AE technology is based on processing and detecting of these high frequencies elastic waves into electrical signals which can be applied by connecting sensitive AE sensors on the surface structure

[59] under test and applying an external inducement. Further processing can be done by amplifying sensor outputs using low-noise preamplifier then carry out filtering possible unwanted noise.

2.22.1 AE Sensors in tool wear monitoring

One of the fundamental success in tool wear monitoring process is the right choice of sensors. To carry out a successful and healthy machine monitoring, a wide range of sensors are used. These sensors are attached to the surface of the object or workpiece to detect dynamic motion generated as a result of acoustic emission activities thereby transforming this detected dynamic motion into voltage-time signal see Figure 2-21 for basic set of an AE sensor. This signal can be subsequently used in acoustic emission measurements for further processing. Further explanation will be carried out under signal processing.

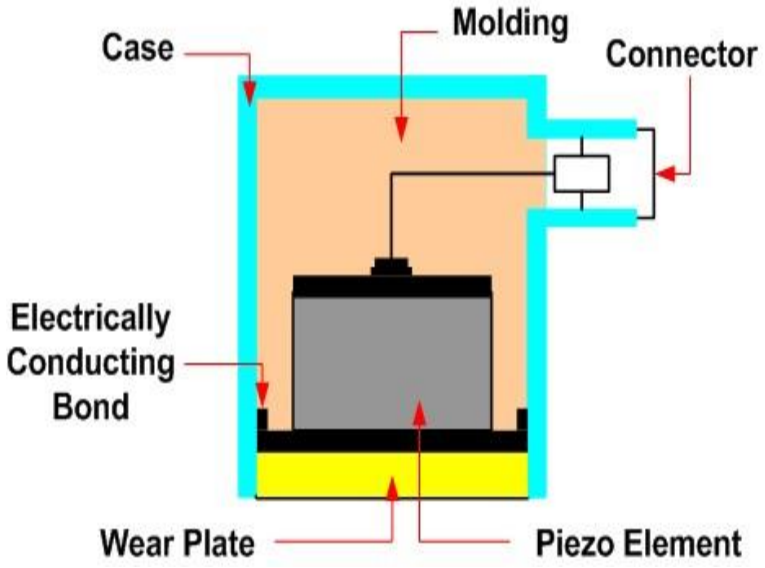

Figure 2-21: Basic set of an AE sensor [93]

2.23 Surface roughness

The surface nature and the features of a metal can be revealed in a circular, radial lays or straight patterns once the surface of a workpiece is newly machined Figure 2-22. According to [34], engineered components must fulfill surface texture requirements such as: roughness and waviness, which is the major method to access quality. Therefore, using surface integrity (SI) to describe the quality and the condition of the surface area of a component will be a great idea. "The SI did not just describe the geometric features of surfaces and their physical and chemical properties but their

mechanical and metallurgical and characteristics also" [34]. In addition, the defect generated form machining processes may practically affect the efficiency of the final component.

According to Edwards and Endean, the texture of the surface of a component is shown because of how component was processed [99]. The measurable geometric quantities for surface texture are: flaw or defect, Waviness, Roughness, Lay or directionality.

Flaws or defects: are irregularities, such as cracks, scratches, hole, depression, inclusions, seams and tears [100].

Waviness: this is a form of regular deviation from flat surface. This may be caused by deflections of tools, dies or work-piece [99].

Roughness: this consists of close spaced, irregular deviation on a small scale than waviness [100].

Lay or directionality: it is described as the predominant surface pattern which can be seen with naked eye [100].

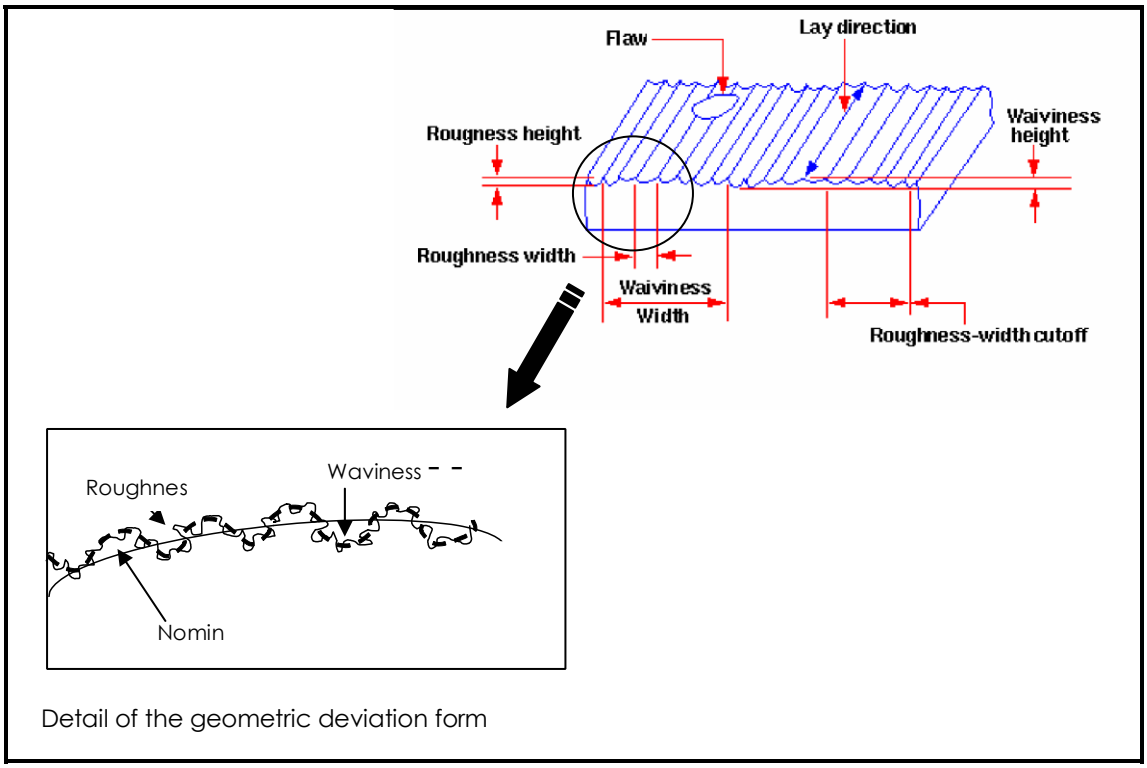

Figure 2-22: Details of workpiece surface texture [100]

According to Boothroyd [101], surface roughness can be defined as results from irregularities in the cutting operations such vibration, machining movement, cutting parameters etc which is often described by two parameters namely: arithmetic mean value (Ra) and root-mean-square average (RMS) Figure 2-23 below.

Arithmetic mean: is the value obtained by measuring the mean deviation of the peaks from the Centre-line of a trace. The Centre-line is the line in-between two lines of one above and the other below that has equal area between them. According to Shaw [102],

$$Ra = \frac{Y_1 + Y_2 + Y_3 + ... + Y_n}{n} \qquad \textbf{(2-5)}$$

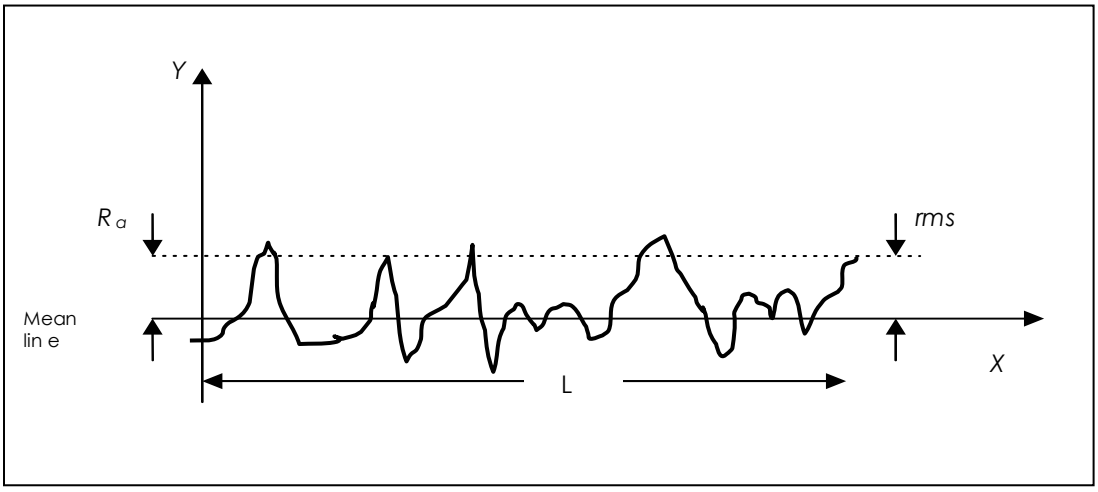

Figure 2-23: Arithmetic surface roughness average, Ra and geometric root mean square (RMS) [34]

Root mean square: Lindberg described RMS as being sensitive to occasional highs and lows making it more reasonable to complement Ra [103]:

$$rms = \sqrt{\frac{Y_1^{\,2} + Y_2^{\,2} ... + Y_n^{\,2}}{n}} \qquad \textbf{(2-6)}$$

Factors affecting surface roughness: the parameters such as the shape, arrangement, height and direction of all surface irregularities on the workpiece depend on the following factors [34]:

- The tool geometry such as rake angle, nose radius and cutting edge
- The quality and the type of machine tool
- The combination tool material and workpiece
- The machine variables such as Cutting speed, feed, and the depth of cut.

2.24 Surface roughness in milling operation

Many researchers have carried out studies to establish the relationship between surface roughness and cutting parameters. Although in reality other influences which may have an effect on surface roughness are not limited to vibration and inaccuracies in the machine tool, irregularities in feed mechanism, workpiece structure imperfection, surface damage caused by chip morphology [101].

2.24.1 Categories of surface roughness

surface roughness measurements are divided into two categories namely direct and indirect measurement.

Direct measurement- this involves directly the use of light scattering, ring field capacitance or Ultrasonic sensing, stylus type gauge are the most popular types of direct surface roughness measurement.

Indirect surface measurement- this method makes use of parameters of machining process such as acceleration, voltage, temperature, pressure. This type of measurement is common in in-process measurement. The data capture can be modelled and predicted to correlate with the expected surface roughness. Furthermore, to monitor surface roughness it is widely convenient using manual inspection of workpiece otherwise because of accuracy indirect measurement require and expert still [1, 16].

2.25 Relationship between Surface roughness and wear

In Wilkinson et al study, they argued that the key indicators of tool wear are the precision and surface shape of the machined profile of the machined surface [104]. Matsunmura et al, have suggested that when considering tool wear and surface roughness at the same time, to minimize cost, machining operations are improved by predicting flank wear using analytical method on metal cutting theory and using predicting surface roughness with the use of a neural network [105].

With this approach, flank wear will consider the initial wear and using surface roughness, tool wear can be modeled through adaptive prediction.

Goller et al, established that the surface roughness produced during turning operation, is influenced by a number of factors and it is therefore a challenge to predict in reality [106]. They further stated that the progressive dynamism that was experienced on the tool peripheral surface can be largely attributed to the roughness of the machine surfaces which in turn depends on the wear resistance of the tool materials. However, Komaraiah et al discovered that the harder the tool material, The lower the surface roughness [107]. On the contrary, Wada et al, suggested that the finished surface roughness of the workpiece may be affected if the wear occurs on the cutting edge [108] [76] . But Yang et al, state that the change seen in surface roughness is essentially caused by cutting flank wear [109].

According to [110] emphasis was placed on the surface roughness and profile in high-speed end milling, they presented a method using simulation of machine surface where accelerated signal was used rather than cutting force. They provided an argument that the vibration encountered by high speed of the spindle suddenly depreciates the geometric accuracy of the machined surface. In the end, they concluded that the generated surface data, surface roughness could be calculated and profile be plotted.

Ehmann et al, in their study introduced a method to represent the surface generation process, they called it “surface-shaping” the method comprises of two parts, the first part modelled the machine tool kinematics and the second part modelled the cutting tool geometry. The latter descried the intersection of the tools face and the flank surface along with the respective angles. [111]

Chapter Three

3 Review of Signal Processing and Design of Experiment

3.1 Review of Signal processing

3.1.1 Signal Processing

Signals are measurable quantities used to transfer data about time-changing physical phenomena. Basic examples of signs are human speech, temperature, pressure, electrical signals and stock price. Electrical signals, ordinarily transferred in the form of voltage or current waveforms, are some of the most direct signals that can be generated and further processed. Scientifically, signals are modeled as function of one or more autonomous variables. Example of independent variables used to express to signals are time, frequency or spatial directions.

Digital signal processing (DSP) innovation and its improvements have histrionically affected our cutting-edge society all over the place. Without DSP, we would not have digital/Internet sound or video; advanced recording; CD, DVD, and MP3 players; digital cameras; advanced mobile and cell phones; advanced satellite and TV; or wire and remote systems [112]. Medical instruments would be less efficient or not able to give valuable data to precisely analyze if there were no digital electrocardiography (ECG) analyzers or digitized x-beams and therapeutic image frameworks. We would likewise live in numerous less productive routes, since we would not be equipped with voice recognition systems, speech synthesis systems, and image and video editing systems [112].

Without DSP, scientists, engineers, and technologists would have no powerful tools to analyze and visualize data and perform their design, and so on. The concept of DSP is illustrated by the simplified block diagram in Figure 3.1, which consists of an analog filter, an analog-to-digital conversion (ADC) unit, a digital signal (DS) processor, a digital-to-analog conversion (DAC) unit, and a reconstruction (anti-image) filter. Usually a transducer (sensor) is used to convert the nonelectrical signal to the analog electrical signal (voltage).

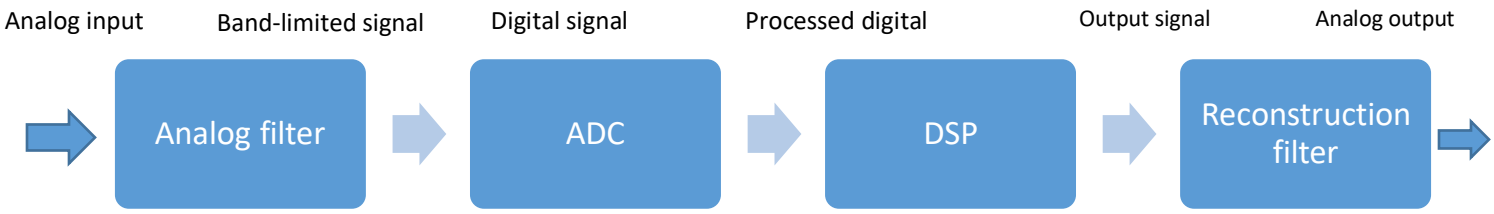

Figure 3-1: Analog to Digital signal processing schemes [112]

This analog signal is channel to an analog filter, which is used to limit the frequency range of analog signals before it gets to the sampling process. The reason behind filtering is to significantly attenuate aliasing bias, the band-limited signal which is set at the output of the analog filter is then sampled and converted passing through the ADC unit into the digital signal, which is discrete both in amplitude and in time [112]. The Digital signal processor then receives the digital signal and processes the digital data using DSP procedures such as low pass, high pass, and bandpass digital filtering, or different algorithms for different purposes. DSP rules can be implemented using software in general. With the Digital Signal processor and conforming software, a processed digital output signal is produced.

Furthermore, as shown in Figure 3.1, DSP structures still require minimum analog processing such as the anti-aliasing and reconstruction filters, which are musts for converting real-world information into digital form and digital form back into real-world information [112].

3.1.2 Feature model

To understand the monitoring strategies proposed in this study, it is very important to understand the signal processing techniques and methods used to carry out the tool wear monitoring system. This study focused on the normal trend in Digital signal processing to acquire raw data that are later processed using another software Figure 3-2.

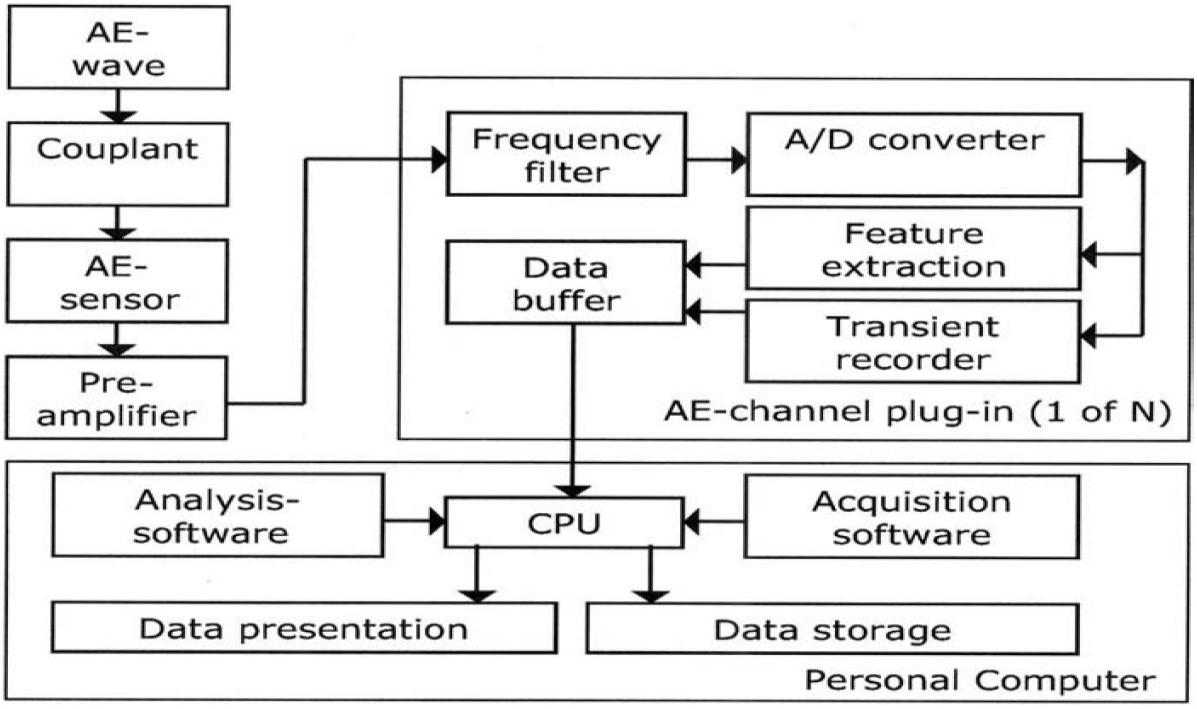

Figure 3-2: AE measurement chain; courtesy of Vallen-systeme, GmBH [113]

3.1.3 Signal Features

It is important to know that because signal features provide important information in the signal, therefore a good understanding of the process is required. This can be carried out by some characteristics of various model parameters in terms of data evaluation figure 3-3. The values of these parameters during analysis, has influence on the time of process, performance and the efficiency of the feature extraction process. Also, the choice of our parameters that will be used during selection will depend on the procedure employed. In figure 00, the procedure that will be followed to extract features is as follows:

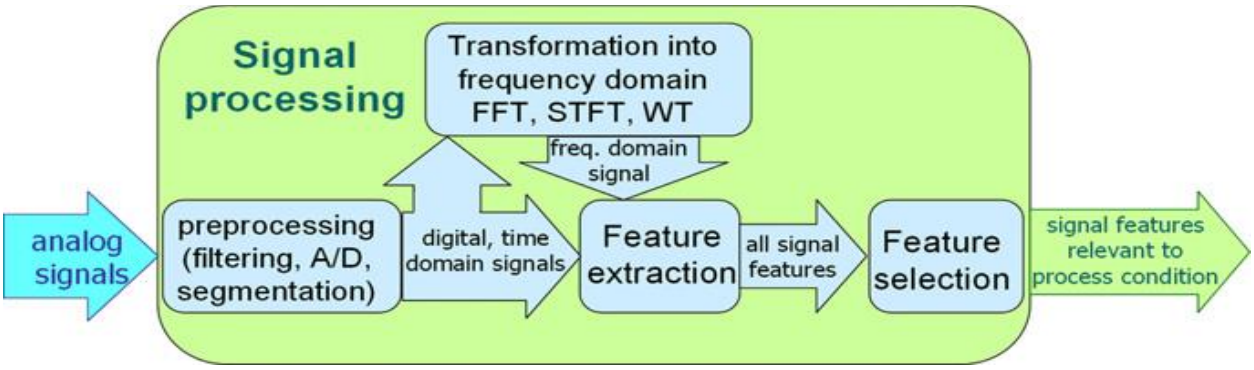

Figure 3-3: Signal Processing Features logical pattern [114]

3.1.4 Feature extractions

Feature extraction begins from an initial set of measured data and builds derived values which are features proposed to be revealing and non-redundant, smoothing the successive learning and generalization steps, sometimes leading to better human interpretations. Feature extraction is associated with dimensionality reduction. It involves reducing the amount of resources required to describe a large set of data.

3.1.4.1 Feature Domain

According to Pentaris, it is important to identify the appropriate domain of a feature before it can be extracted [115]. Therefore, digital signal processing is determined by the domain where the measurements are performed and explored. Domain can be either based on time, which simply means signal measurements are presented based on the time in time series. Domain can also be based on the frequency (frequency domain commonly called spectral). This present frequency measurement as spectral based on the frequency that takes place in each measurement analyzed. Another domain representation is wavelet; this is where signal measurements are presented in three-dimensional form such as in time, the frequency spectral content and the Power density also called the strength of each measurement. The last domain is Z-domain, where measurements are represented in Z-plan and S-plane and presented as an argument of base (e) and (ln e). Z-transform is useful in the analysis of discrete time signals [116] [112] [117]. For the purpose of this research, the author will shed light briefly on Time-domain, frequency-domain and Wavelet-domain as follows:

3.1.4.2 Time domain

The method used to process raw signal directly from acquired (stored) or online data without being transformed is called time domain analysis. To view raw signals, time domain is the traditional way of detecting them. The time domain is a record of what has happened to a parameter of the system against time lapses. Time domain features are extracted directly from the calibrated time domain signals as recorded by the sensors and analyzers. The features from time domain can be calculated easily and fast which can therefore be used in an online monitoring system [118]. The following are the features that can be extracted from time domain: mean, RMS, crest factor, variance, skewness, kurtosis, Power, standard deviation, range, the burst rate, maximum and minimum [77, 118, 62, 119]. However, time series features base on models can also be used as a

tool to monitor a process while the model coefficients are used as features. These model coefficients represent the behavior of the signal in time series. Common time based models are: Auto regression (AR)model, Moving Average (MA) model and the Auto Regression Moving Average (ARMA) model [62]. A brief discussion shall be made to all the features and time series models based as follows:

Arithmetic mean (μ): this is the mean of amplitude values of raw data signal. The mean of N amplitude values of a signal [x_1, x_2, x_3.... x_n] is

$$\mu = \frac{1}{n}\sum_{k=0}^{n}(x_i) \qquad \textbf{(3-1)}$$

Standard deviation (σ): this measure the variation of the data from the average. It can be expressed as:

$$\sigma = \sqrt{\frac{\sum_{k=1}^{N}(x_k - \mu)^2}{N-1}} \qquad \textbf{(3-2)}$$

Skewness (skew): this is the 3rd central moment and is a measure of the asymmetry of the probability distribution (Peak) of the raw data in the signal. Defined as:

$$Sk = \frac{1}{n}\sum_{i=1}^{n}\frac{(x_i - \mu)^3}{\sigma^4} \qquad \textbf{(3-3)}$$

Kurtosis (Ku): this is the 4rd central moment and is a measure of the asymmetry of the probability distribution (Peak) of the raw data in the signal. Defined as:

$$Ku = \frac{1}{n}\sum_{i=1}^{n}\frac{(x_i - \mu)^4}{\sigma^4} \qquad \textbf{(3-4)}$$

Root Mean Square (RMS): This is the collection of n-values in the raw data. Is defined as:

$$RMS = \sqrt{\frac{1}{n}\sum_{i=1}^{n}{x_i}^2} \qquad \textbf{(3-5)}$$

Crest factor (CF): The crest factor of any wave form can be defined as the ratio of the peak amplitude level to the RMS value. This value gives us an idea of the degree on how impacted a waveform is. It can be expressed as:

$$\mathbf{CF} = \frac{\mathbf{Peak\ level}}{\mathbf{RMS\ value}} \quad \textbf{(3-6)}$$

Power (P): the power of a signal can be described as the measured area under the corrected signal envelope. The signal amplitude can also be measured power although it is very sensitive to amplitude as well as duration and the operating frequency of the signal does not depend on it. Mathematically defined as:

$$P = \frac{1}{n}\sum_{i=1}^{N} {x_i}^2 \quad \textbf{(3-7)}$$

Variance (σ): the variability of the raw data can be regarded as variance. Which can be defined as:

$$\sigma^2 = \frac{1}{n}\frac{\sum_{i=1}^{n}(x_i - \mu)^2}{n-1} \quad \textbf{(3-8)}$$

The burst rate (Br): although burst rate is only applicable to AE and vibration. the burst rate which can also be called pulse rate is the number of times the signal exceeds the pre- set threshold per second.

Signal to noise ratio (SNR): this simply can be expressed as the value of the mean divided by standard deviation.

3.1.5 Time series model based features

These are: Moving average, Auto Regression and Auto Regression Moving Average. According to Olufayo, models are different in their number of orders which means the higher the order of a model the more features can be extracted and the higher the model splits the signal into more distinct bands where embedded noise can be highly distinguished [77].

- **Moving Average (MA):** In a q-th order of Moving Average, the current measurement is defined as a linear combination of q pervious values from a sequence of independent identically distributed random variables with a certain probability density function.

$$x(n) = b_1u(n-1) + b_2u(n-2) + \cdots . + b_qu(n-q) \quad \textbf{(3-9)}$$

where x(n)is the MA predicted value u(n), n=1,2, 3…. N is the time series (acoustic emission), q is the MA order, b_1, $b_2 \ldots b_p$ are MA coefficient parameters and the residual components is R(n) = U (n + q) – x (n + q), the first coefficient can be chosen as feature.

- **Auto Regression (AR):** In a f-th order for a time series x(n), where n is the discrete time index, the value of the measurement is expressed as a linear combination of f previous values:

$$x(n) = a_1x(n-1) + a_2x(n-2) + \cdots . + a_fx(n-f) \quad \textbf{(3-9)}$$

the first AR coefficient can be chosen as feature.

- **Auto Regression Moving Average (ARMA**): this can be defined as the combination of AR and MA Models.

$$x(n) = -\sum_{k=1}^{p} a_k\big(x(n-k)\big) + \sum_{k=1}^{q} b_k\big(u(n-k)\big) \quad \textbf{(3-10)}$$

The first two coefficients from this model ca be chosen as features [62, 77].

3.1.6 Frequency domain

Frequency domain analysis is used to extract relevant information that is hidden in time domain analysis therefore, in order for the frequency contents coming directly from the Time domain to be certain and regularly cleared, the analog signal has to be discretized into spectrum which provides additional information about time series data. According to [120], the parameters generated from frequency analysis are more reliable in damage detection than time domain analysis parameters. Theoretically, these signals can be represented as:

$$X_{(w)} = \int_{-\infty}^{\infty} x(t)e^{-jwt}\,dt \quad \textbf{(3-11)}$$

$$x(t) = \frac{1}{2\pi}\int_{-\infty}^{\infty} X(w)e^{-jwt}\,dw \quad \textbf{(3-12)}$$

Where: $x(t)$ is raw signal, $X_{(w)}$ is the transformed signal, w is the radian frequency and t is the time. To regenerate the time domain signal x(t) from the frequency domain signal X(w), an inverse Fourier transform must be computed equation (2).

However, because signals are usually acquired and stored digitally as just mention above as a set of data point in most application, it is necessary to discretize the Fourier transform. Therefore, a method called the Discrete Fourier Transform (DFT) algorithm is applied to discretized and exchange a digital Signal from time domain into a signal in frequency domain. This can be mathematically expressed as:

$$X[k] = \frac{1}{N}\sum_{n=0}^{N-1} x[n]e^{-jk\left(\frac{2\pi}{N}\right)n} \quad \textbf{(3-13)}$$

Where X[k] and x[n] represent discrete frequency and time signal respectively, k an n represents frequency and time indices and N represents the number of points that equally spaced in interval of 0 to 2π.

Spectral energy is normally obtained by computing Power Spectral Density (PSD) of the signal PSD provides good information on the nature of machining process i.e. increase or decrease based on the level of tool wear [77]. This is carried out by an intensive computational algorithm that contains large number of mathematical operations. Due to the length of the signals, whenever the signal power is in the order of two, a Fast Fourier Transformation (FFT) technique can be applied to reduce the large computational rigors and primarily to speed up the operation of the DFT [120] [121]. The PSD can be experienced as a result of two scenarios. First, high PSD due to excessive vibration of the machine resulted from tool breakage from new to worn. A sharp spike is experienced in amplitude as a result of this effect which can be true for flank wear. Secondly, if there is a system shifts in the natural frequency of the tool holder and the tool resulting in a decrease in Spectral energy Figure 3-4. The normal failure mode is crater wear [62]**.**

The Fast Fourier Transformation (FFT) algorithm that is used for analyzing the spectral content of a stationary signal and transitory signals due to its constant time and frequency resolution can be defined mathematically as:

$$X[k] = \sum_{n}^{N-1} x[n]\, W_N^{nk} \quad \textbf{(3-14)}$$

Where:

For k = 0,1, 2, ……, N-1

$$W_N = e^{\frac{-j2\pi}{N}} \quad \textbf{(3-15)}$$

3.1.7 Time-Frequency domain

The unique features of Time-Frequency analysis techniques Figure 3-4, means that it is capable for non-stationary signals as well. The following time-frequency domain techniques are explained briefly:

3.1.7.1 Short Time Frequency Transform (STFT)

Furthermore, if the signal consists of non-stationary characteristics in frequency domain, the drawback of Fourier analysis about the missing time information may be overcome by using Short-Time Fourier Transform (STFT). Meanwhile, this technique is still not flexible and is also limited in precision because this method is based on windowing the signal and later analyze each Short Time window independently from which the signal can be plotted on 2-dimensional display of frequency and time [62, 122]. According to [120] , though STFT provides both frequency and time evolution of the signal but it has a limitation which is a fixed resolution with respect to the time window size at all frequencies. This simply means that during FFT, only the frequency resolution (high) can be seen but no time resolution because window has covered the entire time interval from negative infinity $(-\infty)$ to positive infinity $(+\infty)$. On the contrary, when STFT is used, the frequency becomes very poor because the window has a finite length at this moment therefore only a small segment of the signal will be covered. However, to increase the frequency resolution, the window function must be wider or expanded. Again, if the frequency resolution is improved this will lead to missing time information which is contrary to the stationary assumption that requires small window. Therefore, to stay out of this trade off relationship between high frequency resolution with a wide window and poor time resolution in STFT. A technique called Discrete Wavelet Transform (DWT) Figure 3-5 was introduced to solve the resolution limitations.

3.1.7.2 Wavelet

During transformation process a short coming was established during Fourier Transformation from time domain to frequency domain, it was discovered that the time information part of the process was not revealed. This also explained why the exact time of an event that takes place in Frequency Spectrum was not feasible. It was this question that brought Wavelet onboard.

Wavelet helps break the signal down into sub-signals or levels of different frequencies which clearly carries the time information require in further analysis. It has been applied successfully in some applications such as: image analysis, transient analysis, communication system and other monitoring of machining processes applications [77, 62, 118]. Wavelet has the capability of revealing that part of a data other signal methods cannot unfold such as breakdown points, discontinuities in higher derivatives, trend and self-similarity [122].

Scaling and shift of Wavelet: scaling a wavelet means stretching or compressing the signal. It can be represented by a scale factor a. the smaller the scale factors the more compressed the wavelet. This shows that the frequency of a signal has relationship with scale factor. Also, in wavelet analysis, the Low and High frequency contents of the signal are referred to as Approximation (A) and Detail (D) respectively. Shifting in wavelet can be regarded as delaying or speeding up its commencement. In summary, High scale or stretched wavelet or low frequency give Approximation (A) and Low scale or compressed wavelet or High frequency will give Detail (D) see Figure 3-5. mathematically it can be expressed as:

$$y_{high}[k] = \sum_n x[n]n * g[2k - n] \quad \textbf{(3-16)}$$

$$y_{low}[k] = \sum_n x[n]n * h[2k - n] \quad \textbf{(3-17)}$$

Where $x[n]$ is original signal, $g[n]$ is high pass filter, $h[n]$ is low pass filter, $y_{high}[k]$ and $y_{low}[k]$ are the output of the high and low pass filter respectively.

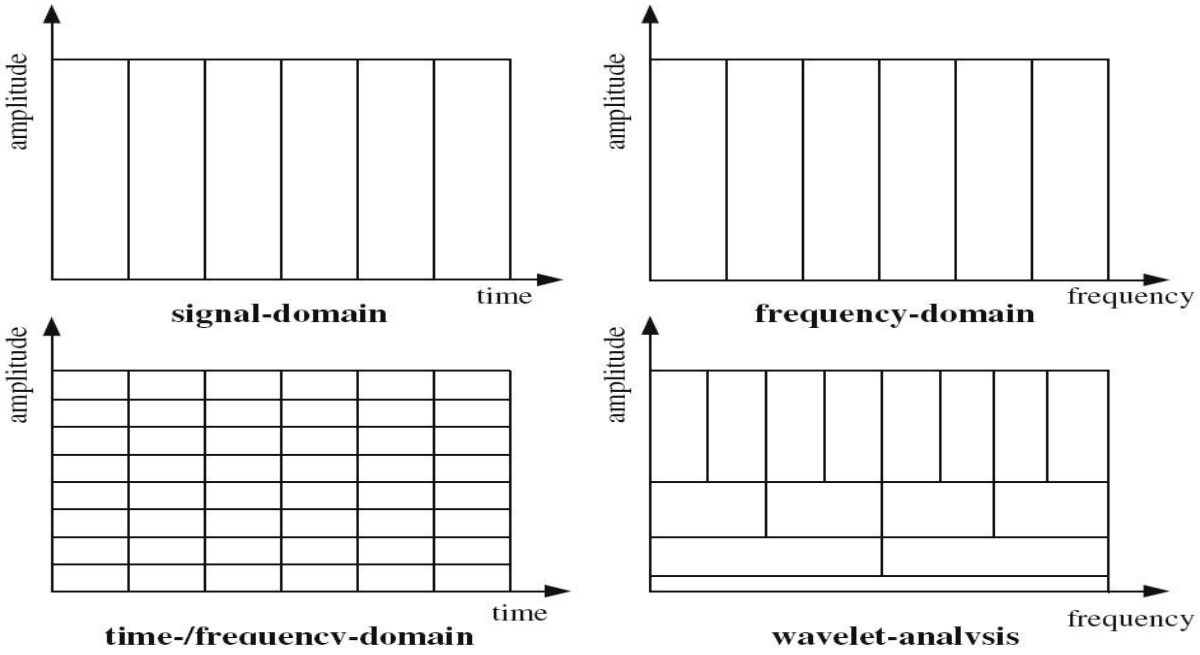

Figure 3-4: wavelet signal division graphical representations [77]

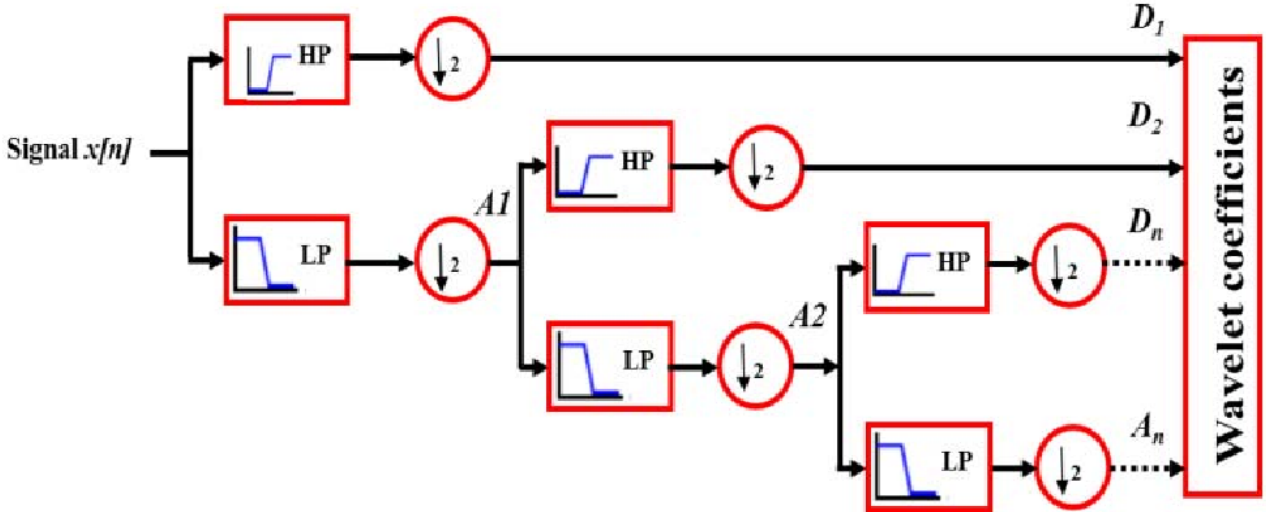

Figure 3-5: signal decomposition using discrete wavelet transform [120]

3.1.7.3 Discrete Wavelet Transform (DWT)

According to [123] the major difference between STFT and Wavelet transforms is that the latter has varying window length and represents the signal as a sum of wavelets at different scales.

3.1.7.4 Continuous Wavelet Transform (CWT)

The continuous Wavelet Transform can be defined as the sum of overall time of the signal multiplied by scaled and shifted versions of the wavelet function.

$$C(\text{Scale}, \text{Position}) = \int_{-\infty}^{\infty} f(t)\varphi(\text{scale}, \text{position}, t)dt \quad \textbf{(3-18)}$$

C is the coefficients of the wavelet which are functions of scale and position.

3.1.8 Decomposition and Reconstruction

Wavelet decomposition is a process whereby the successive approximations are being decomposed in turn, so that signal is broken down into many lower-resolution components. This wavelet decomposition tree can now be used to reconstruct the original which is called Inverse Wavelet Transform [62].

3.1.9 Wavelet Packet Analysis

Wavelet packet decomposition (WPD) based technique has been widely used for transient and non-stationary signal analysis [124]. with normal wavelet analysis, only approximations are fragmented in every step also in wavelet packet decomposition tree, the signal can be reconstructed using any number and combination of packets on the wavelet packet decomposition tree [62].

3.2 Signal feature selections

Feature selection is the process of selecting important features, or an applicant subset of features. To get the optimum feature subset, the evaluation criteria are used. In high-dimensional data (number of samples is usually less than number of features), finding the optimal feature subset is a demanding task. To use machine learning methods successfully, pre-processing of the data is crucial. Feature selection is one of the most common and important techniques in data pre-processing, and has become a key component of the machine learning process. It is the process of detecting relevant features and removing irrelevant, redundant, or noisy data [125]. Feature selection methods can be look at from three different perspectives: (a) which search method is employed; (b) what evaluation criteria are used; (c) and which real-world applications are the feature selection exercised with [126]. To get the optimum feature subset, the evaluation criteria are used.

a) **Search methods** – Subject to what type of search method is used, generally, feature selection methods can be classified into (i) optimal search (exhaustive search and branch & bound algorithms), (ii) heuristic search (sequential selection, floating selection, and decision tree methods, (iii) random search (genetic algorithms, simulated annealing, and Bayesian network algorithm), (iv) and weight based search (fuzzy set theory, fuzzy feature selection, neural networks, neuro-fuzzy approach, and relief). Compared to random search and weight based search, optimal search is more computationally expensive and therefore sometimes not feasible [126, 127].

b) **Evaluation criteria** - Each search method of feature selection has to use evaluation criteria to measure the "goodness" of a particular subset of features which helps in the selection process. Widely used evaluation criteria include (a) distance based measures, such as Mahalanobis distance, Hausdorff distance, and metric approach; (b) entropy measures; (c) statistical measures; (d) correlation based heuristic measures; e) accuracy measures; and (f) relevance measures. With regard to how to implement the evaluation criteria, filter and wrapper are the two well-known approaches [126, 128, 129].

c) **Real-world applications** - Feature selection is a crucial element for applications in areas such as statistics, pattern recognition, machine learning, and data mining. Of particular interest to us are machine-tool condition monitoring and tool wear diagnosis [126, 130].

3.3 Strategies used in feature selection systems

Two basic strategies are common to feature selection. One is the sequential selection method that chooses one feature at a time [126]. The underlying assumption for this approach is that the features and their diagnostic power are independent. The second strategy makes use of the combinations which addressed the shortcomings of feature selection [126]. However, the following scheme are commonly found during feature selection: scatter matrix, Decision Tree, Cross correlation, Parallel Adaptive Neuro-Fuzzy System (ANFIS) and Sequential ANFIS [126] .

3.4 General methodology for feature selection

There are three general approaches for feature selection that are being used in condition monitoring system. First, is the filter approach which exploits the general characteristics of training data with independence of the mining algorithm. The second is the wrapper approach which explores the relationship between relevance and optimal feature subset selection. It searches for an optimal

feature subset adapted to the specific mining algorithm. While the third, is the embedded approach carried out with a specific learning algorithm that performs feature selection in the process of training [125, 126]. Other recent feature selection and classification techniques algorithm are Particle Swarm Optimization (PSO) and Ant Colony optimization (ACO).

3.5 Decision making

In tool condition monitoring, several artificial Intelligent (AI) methods have been adapted to make decisions. Pattern recognition techniques are significant part of intelligent systems and these techniques are used for both data pre-processing and decision making. According to Schalkoff, Pattern recognition is the science that is concerned with the description or classification (recognition) of measurements [131].

Pattern recognition method has been applied to recognize the tool cutting states and to monitor the tool conditions in machining for years. The simplest and common algorithm is linear classifiers. The features for classifying the cutting states included cutting speed, feed and the power spectrum in different frequency bands. Also, the features used for the tool condition monitoring are usually feed rate, depth of cut, cutting force, cutting torque, sums of the magnitudes of spectral components at certain frequencies, and other signal features.

During Pattern classification, an approach using linear discriminator function (LDF), was used by Emel and Kannatey-Asibu Jr. The LDF is a separation technique that was used to distinguish between clusters of feature data. Using AE spectral signals, the feature selection techniques considered three classification criteria which are: the class-mean scatter criterion, the class variance criterion and the Fisher weight criterion. These are also referred to as interclass distance measures. Two classifier designs were discussed, the minimum error and the minimum cost. Experiments revealed that the minimum cost design had the highest success rate for detecting a worn tool [132].

All through literatures it has been revealed that the number of features and the different combinations of features had great effects on the correct classification rates. A range of AI techniques that are commonly used in modelling environment and in condition monitoring system are: case-based reasoning, rule-based systems, artificial neural networks, genetic algorithms, cellular automata, fuzzy models, multi-agent systems, swarm intelligence, reinforcement learning

and hybrid systems [133]. But for the purpose of this research work the most common in tool condition monitoring will be briefly discussed: Artificial Neural Network (ANN), Fuzzy decision and the Hybrid (Neuro-Fuzzy).

3.6 Artificial Neural Network (ANN)

Artificial Neural Networks are effort to imitate the computational architecture of the human brain Figure 3-6, in electrical hardware. It consists of an interconnected group of artificial neurons and processes information using a connectionist approach to computation. In most cases an ANN is an adaptive system that changes its structure based on external or internal information that flows through the network during the learning phase.

Figure 3-6: Typical Biological Neurons

An ANN usually organizes its units into several layers. The first layer or input layer, the intermediate layers or hidden layers, which are not always present because they are sometimes not needed, and the last or output layer. The information to be analyzed is presented (or fed) to the neurons of the first layer and then propagated to the neurons of the second layer for further processing. There are different configurations for ANN, but as discussed above, the most common of all is the three-layered Feed Forward Perceptron Neural Network trained by Back Propagation normally commonly called Feed Forward Perceptron Back Propagation Neural network (FFPBPNN). [134]

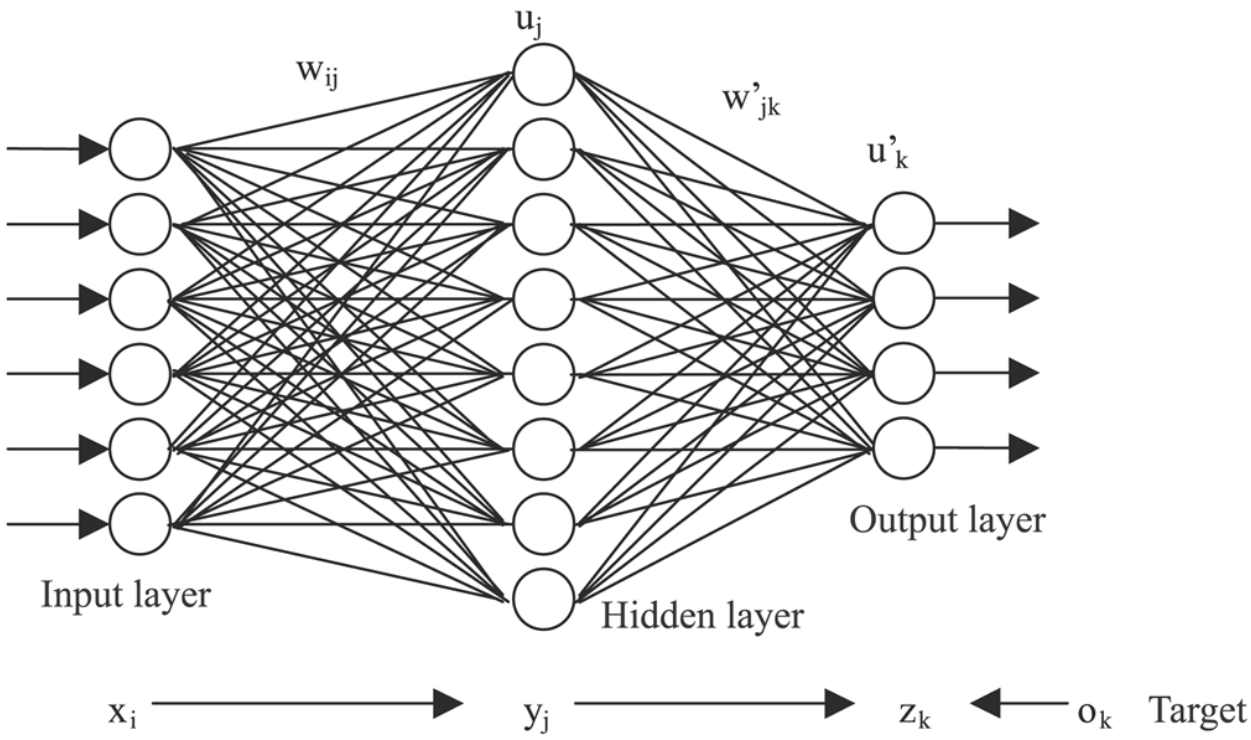

Figure 3-7: A three-layer Feed Forward Artificial Neural Network [134]

Where**:**

$\mathbf{W_{ij}}$ and $\mathbf{W'_{jk}}$ are weights and $\mathbf{U}_j$ and $\mathbf{U'_k}$ are biases respectively;

These results are propagated through each layer, converting the information into the network output in the final layer. The goal of an ANN is to discover some association between input and output patterns. Many different neural network structures have been developed to achieve different learning and processing speed capabilities.

The input of a neuron includes its bias and the sum of its weighted inputs as shown in Figure 3-7. The output of a neuron depends on its transfer function. Many transfer functions can be used and the three most commonly used functions are Hard Limit (Step function), Linear and Log-Sigmoid Figure 3-8.

The option of a transfer function with or without bias can be chosen. A bias can be a constant or allowed to change like the weights with an appropriate learning rule. The backpropagation learning rule is used to train non-linear, multilayered networks to perform function approximation, pattern association, and pattern classification. It can be used to adjust the weights and biases of the

networks to minimize the sum of squared error of the network [96]. The sum of squared error is defined as:

$$E = \frac{1}{2}\sum_{P=0}^{n}\sum_{i=1}^{m}\left(T_{pi} - O_{pi}\right)^2 \qquad \textbf{(3-19)}$$

Where:

m = the number of output in the output layers

n = the number of patterns

T_{pi} = the **ith** component of the desired output vector

$\mathbf{O_{pi}}$ = the calculated output of the **ith** neuron

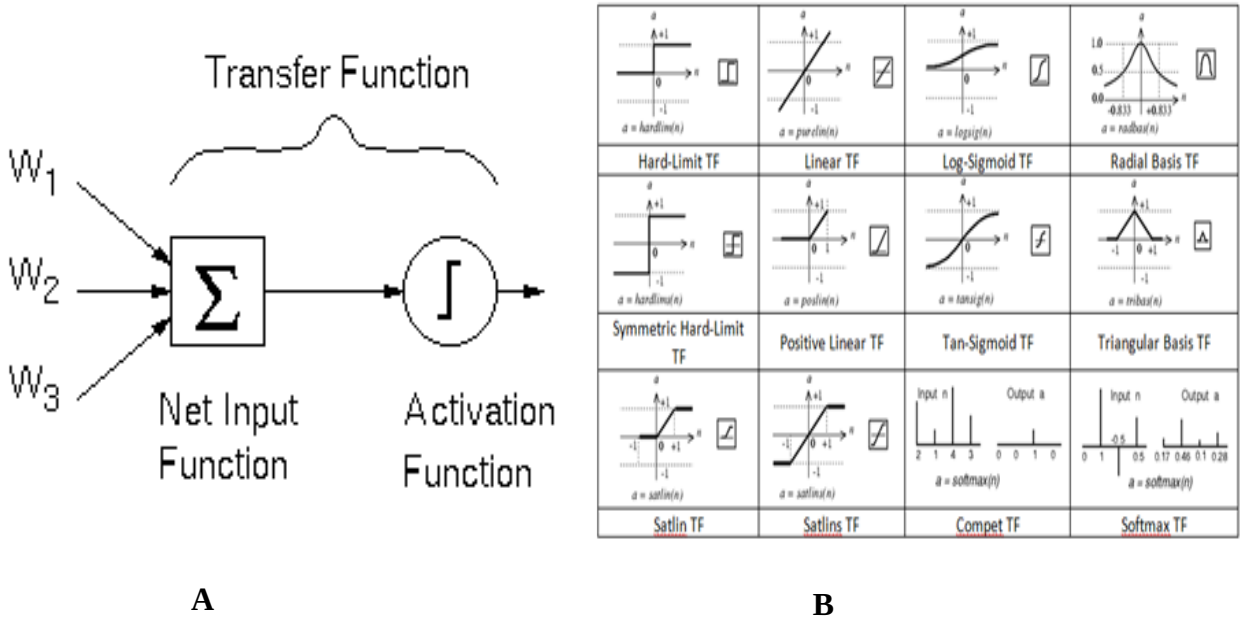

Figure 3-8: A: Neural Network Transfer function, B: Activation functions

3.7 Learning in Neural Networks — Back-Propagation

The idea of a neural network is acquired from learning processes. Learning means that the processing element somehow changes its input and output characteristics in response to the surroundings. Based on experience, Learning provides a vital organism with the means to adapt to

and survive in a changing environment. For pattern classifiers, the learning produces reliable, enhanced and flexible performances.

3.7.1 Types of Learning

Learning in neural networks can be supervised or unsupervised

- **Supervised learning:** this means that the network has some dependable inputs presented during training to instruct it what the correct output should be. The network then has a means to decide whether or not its output is wrong or correct and knows how to apply its particular learning rules to adjust its weights.

- **Unsupervised learning**: this simply means that the network has no such pre-knowledge of the desired output hence, cannot know exactly what the correct response should be before the incoming. However, Supervised classification has been commonly applied to the tool condition monitoring in machining.

A specific learning rule which is the most frequently used learning algorithm is the Delta rule or Least Mean Squared (LMS) training law. In learning, the rules provide guide on how to change the weights is subject to whether the output of classification was right or wrong. Firstly, the processing element must be modified so that it can monitor its own output, Then, it is enabled to compare its output to the desired output signal. Lastly, the researcher would calculate how to change the weights by using the Delta rule [135].

Delta rule is a gradient-descent learning rule. The learning constant is a measure of the speed of convergence of the weight vector to the minimum error position. The back-propagation algorithm uses a gradient search technique to minimize a cost function equal to the mean square difference between the desired and the actual output. A backpropagation neural network is developed based on processing elements by using the Delta rule.

The neural network is trained by first selecting smaller arbitrary weights and internal thresholds, and then presenting all training data recurrently. Weights are in sync after every trial using side information to state the correct class until weights converge and the cost function is reduced to a satisfactory level [135]. An important part of the algorithm is the iterative error method that propagates the error terms required to adapt weights back from the neurons in the output layer to neurons in a lower layer [136].

The ability of ANN to learn in noisy environment is a key tool in TCM, therefore, the author engaged with a feed forward BPNN with one (two) hidden layer using on tests results. By using this network design, lower mean square error was achieved. BPNN may not need further optimization algorithms such as genetic algorithm and particle swarm optimization due to the reverse process of computation and makes it quick and easy to use.

Furthermore, ANN offers some benefits over other classification techniques. Some of these benefits can be noticed from their capability to classify data without former knowledge. Fuzzy logic models do not possess huge learning capabilities. The combination of these models in the neuro-fuzzy approach is confronted with the number of learning parameters employed in the classification. Though there are other techniques such as statistical, Bayesian models or ACO. Other Artificial Neural Networks that cannot be explained in this research work but do exists are: Auto-encoder, Deep Neural Network (DNN) also called Deep Learning, Recurrent Neural Network (RNN), Restricted Boltzmann Machine (RBM), Self-Organizing Map (SOM) and Convolutional Neural Network (CNN).

3.8 Design of Experiment

Design of experiment (DOE) is a structured and organized method Figure 3-9, that is used to define the correlation between the different factors or parameter or variables affecting a process and the output of that process [137]. This method was first developed in the 1920s and 1930s by Ronald A. Fisher.

The objectives of any experiment are to:

- find the factor settings that optimize the response (max./min. problem, or hitting a specific target) for example Rough Surface Modelling (RSM), Tool wear (TW), and Metal Removal Rate (MRR).
- improve a process, in order to understand how certain factors (RSM, TW, MRR), influence the response.
- find out what tradeoffs can be made in factor settings, while staying near the optimal response.
- finding a model that describes the relationship between the vital factors and the response.

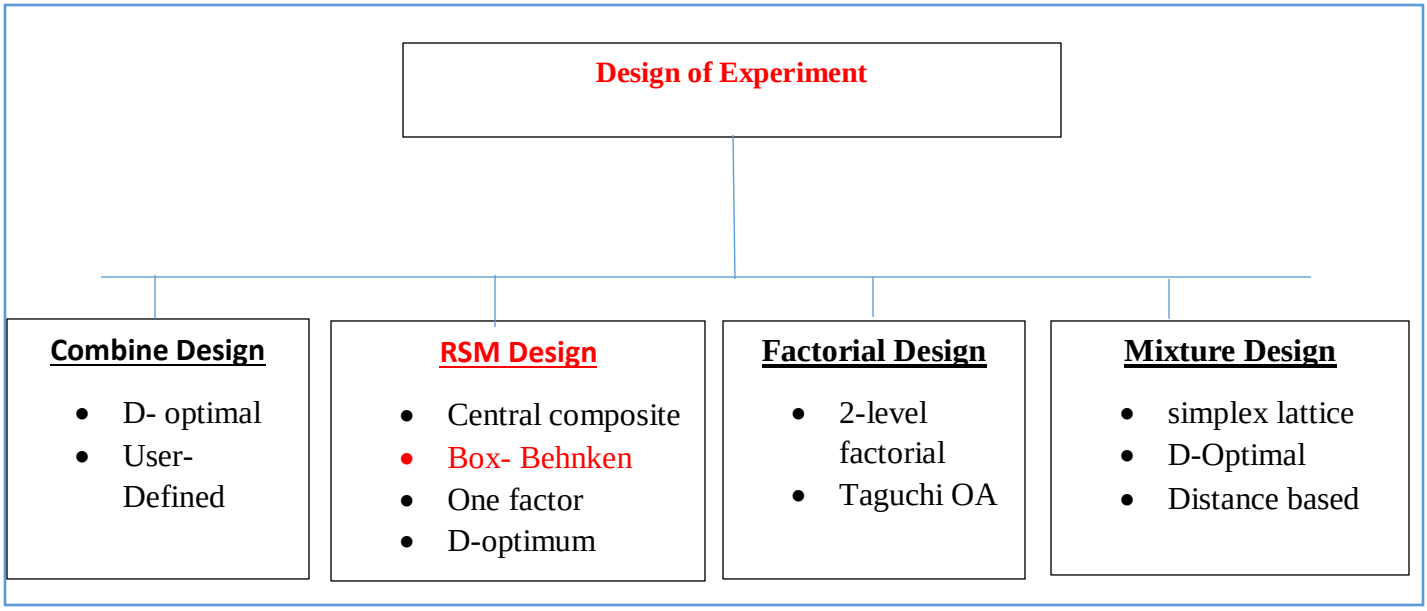

Figure 3-9: Design of Experiment framework [138]

3.8.1 Common Design Techniques

There are various DoE techniques that have been used for different experiment purposes Figure 3-9. The following list gives the commonly used design types [138]

1. For comparison:
    - One factor design
2. For variable screening:
    - 2 level factorial design
    - Taguchi orthogonal array
    - Plackett-Burman design
3. For transfer function identification and optimization:
    - Central composite design
    - Box-Behnken design
4. For system robustness:
    - Taguchi robust design

On the other hand, the designs used for transfer function identification and optimization are called Response Surface Method (RSM) designs. Therefore, Box-Behnken design (BBD) will be used in the experiment. Box–Behnken design, is frequently chosen, since interaction parameter estimates are not completely confused and in many cases, these designs are considerably smaller than 3^{p-s} fractional factorial designs [139]. A BBD also requires only three-levels and is a more efficient alternative to the full three-level factorial.

3.8.1.1 Rough Surface Modelling (RSM)

Response Surface Approach is one of the useful tools in statistical analysis used to examine the relationship between one or more response variables and a set of quantitative experimental variables. It is common in industries when the data may not be manageable and un-structure leads to an impact in waste of energy and accuracy of components. RSM is a method of identifying the controllable and uncontrollable to find the optimum performance to optimize the response. In order to observe the relationship between the surface machine, tool wear and material removal rate towards process parameters, In this study, Optimization and parameter control will be analyzed from the relationship of response which will be taken for further analysis.

3.8.1.2 Box-Behnken Design

Box and Behnken recommended three level designs for fitting response surfaces. coded as -1, 0, and +1. Box-Behnken designs are available for 3 to 10 factors. These designs are formed by combining 2^k factorials with incomplete block designs. Figure 3-10 (a) and (b) illustrates the three variable Box – Behnken design. It can be noticed that the Box-Behnken design is a spherical design with all points lying on a sphere of radius. Also, the Box – Behnken design does not contain any point at the vertices of the cubic region created by the upper and lower limits for each variable. 2.

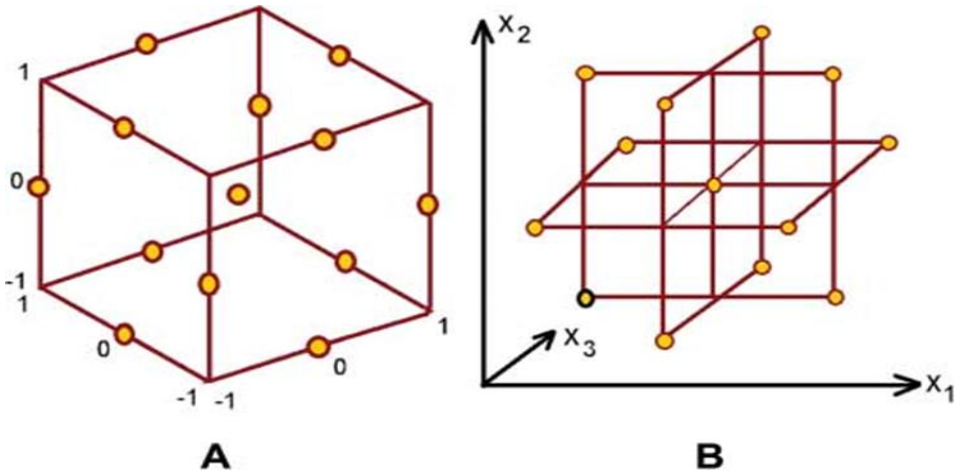

Figure 3-10: Box- Behnken design

This could be advantageous when the points on the corners of the cube represent factor level combinations that are impossible to test due to physical process constraints or prohibitively expensive. Its "missing corners" may be useful when the researcher should avoid combined factor extremes. This property prevents a potential loss of data in those cases. Box-Behnken designs require fewer treatment combinations than a CCD, in problems involving 3 or 4 factors. The Box-Behnken design is rotatable (or nearly so) but it contains regions of poor prediction quality like the CCD Table 3-1, [139].

Table 3-1: Comparison of the primary RSM [140]

	Central Composite Design	Box-Behnken Design	D-optimal Design
1	Created from a 2-level factorial design, augmented with center points and axial points	Has specific positioning of design points	Position of design points chosen mathematically according to the number of factors and the desired model, therefore the points are not at any specific positions - they are simply spread out in the design space to meet the D-optimality criteria (see below)
2	Regular central composite designs have 5 levels for each factor, although this can be modified by choosing alpha=1.0, a	Always has 3 levels for each factor	D-optimality mathematically chooses points to minimize the integrated variation of the coefficients for the model -

	face-centered CCD. The face-centered design has only three levels for each factor.		you get the most precise coefficients
3	Created for estimating a quadratic model.	Created for estimating a quadratic model	Can be used to create a good design for fitting a linear, quadratic or cubic model. You can also change the user preferences to get up to a 6th order model.
4	Rather insensitive to missing data	Provides strong coefficient estimates near the center of the design space (where the presumed optimum is), but weaker at the corners of the cube (where there weren't any design points)	If you have subject matter knowledge, you can edit the desired model by removing terms that you know aren't significant or can't exist. This will decrease the required number of runs.
5	Replicated center point provides excellent prediction capability near the center of the design space (where the presumed optimum is.)	If you end up missing any runs, the accuracy of the remaining runs becomes critical to the dependability of the model. We do not recommend Box-Behnken if it is common to have a bad run or have missing data. The central composite designs have more runs initially and this makes them more robust to problems.	Generally, the D-optimal design has 1-2 more runs than a Box-Behnken, so this provides a little more protection for the model coefficients if you end up losing some data.
6			Can add constraints to your design space, for instance to exclude a particular area that you can't get responses.
7			For a quadratic model, factors may have either 3 or 4 levels

Chapter Four

4 Experimental design and Machine set-up

4.1 Introduction

This chapter presents the experimental set-up and procedures, the stages and components of the implemented condition monitoring system in this research are covered in this Chapter. It further provides details regarding the machine tool, workpiece, cutting tool, sensors used, Data acquisition card and Data Card software. It also presents the surface roughness measuring device and the condition monitoring system set-up including the placement of sensors, the data acquisition system and programmed software. A brief description of sensors, signal processing methods and pattern recognition systems utilized for developing the proposed model is presented.

4.2 Experiment Equipment

4.2.1 Machine tool

The research work was carried out on an industrial five axis Deckel Maho DMU 40 CNC machine. As shown in Figure 4.1 The DMU 40 CNC machine belongs to the set of innovative mono BLOCK series of CNC machining centers produced by Deckel Maho. This machine set presents improved performance in terms of dynamics, high precision, higher machined surface, enjoys quality and lower space requirements. The DMU 40 possesses a motor spindle with a speed up to 12000 rpm. Its extensive large range of expansion options, advanced CNC control and numerous software features makes this machine ideal for conducting machining tests.

Figure 4-1: CNC 5-axis Deckel Maho Milling machine [141]

The innovative mono-block design has numerous benefits such as greater sturdiness, better dynamics, more precision, high surface quality and lower space requirements. The table traverses only in the vertical direction and when combined with the large linear guide ways, leads to better sturdiness in order to produce superb surface quality, regardless of the application height. Some highlights of this machine are: optimal access and greater visibility into the work area, a 19" CNC screen, Machine foot print of 4.2 m^2, accelerate up to 0.8g and a rapid travers of 30m/min, scraper-belt chip conveyor, 250-l coolant or lubrication tank, geometric temperature compensation, fully enclosed safety cabin, energy supply integrated into the milling head and a trailing cable installation in the base, has a maximum load up to 1100kg with a fixed table up to 800g Figure4-2a, with the NC rotary table, chain magazine with 60 tool pockets as an option, HSC motor spindle ranges from 12,000(optional), 24000 – 42000 rpm Figure 4-2b, for production package with 600-l coolant tank. These features make this machine suitable for the research work experiment.

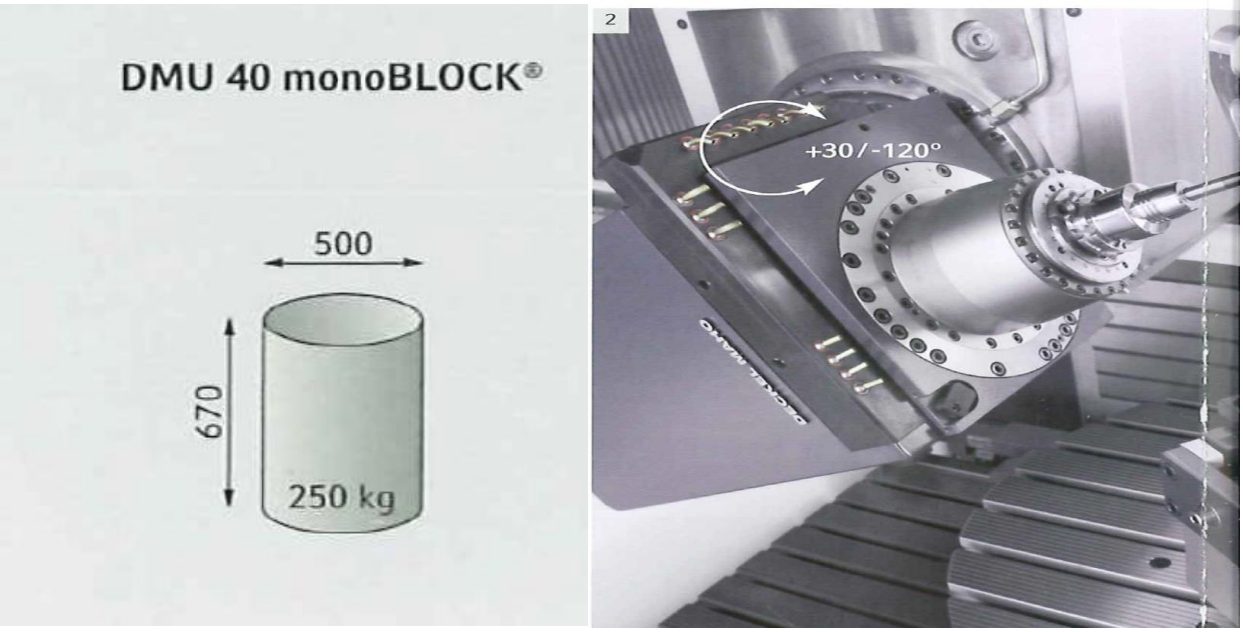

A B

Figure 4-2: A: maximum workpiece dimension/ weight (HSK-A63), B: machining of a long landing gear support beam with a b-axis and negative angles

4.2.2 Work piece

The workpiece that was used in this experiment is stainless steel 316 grade. This type of stainless steel belongs to the family of austenitic stainless steel 300-series which are generally difficult to machine. It is an austenitic chromium nickel stainless steel containing molybdenum. The steel Table 4-1, contains high percentage of Nickel than 304 stainless steel. The resultant composition of this material gives these steels much improved corrosion resistance in many aggressive environments. The molybdenum addition ensures more resistance to pitting and cavies' corrosion in chloride-containing media, sea water and chemical environments such as sulfuric acid compounds, phosphoric and acetic acids. 316 stainless steel offers good strength and creep resistance and possess excellent mechanical and corrosion-resistant properties at sub-zero temperatures. 316L is a low carbon modification of 316. When machining 316 stainless steel, unlike other austenitic steels, it alloys group machines with a rough and stringy swarf., rigidly supported tools with as heavy a cut as possible is used to prevent glazing. Typical applications of 316 SS includes exhaust manifolds, furnace parts, heat exchangers, jet engine parts, pharmaceutical and photographic equipment, valve and pump trim, chemical equipment, digesters,

tanks, evaporators, pulp, paper and textile processing equipment, parts exposed to marine architecture and tubing. Due to the above physical, chemical and commercial characteristics and features of 316 SS Table 4-1, it draws attention for the workpiece selection in this experiment.

Table 4-1: General Chemical properties of 316 Stainless steel (%):

	C	Mn	P	S	Si	Cr	Ni	N	Mo
316	0.08max	2max	0.045max	0.03max	0.75max	16-18	10-14	0.1max	2-3

Table 4-2: General Physical properties of Stainless steel

	Tensile strength (min)	Yield strength (min)	Elongation (min)	Hardness (max)
316	75ksi	30ksi	40%	95 HRB

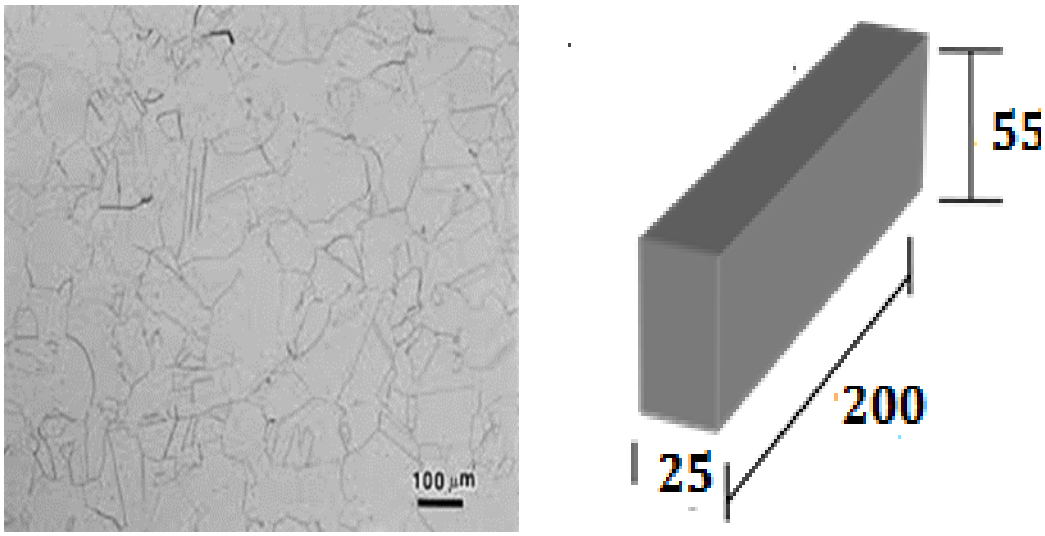

A **B**

Figure 4-3: A: microstructure of 316 SS; B: The dimension of the work piece is (200 x 55 x 25) mm

4.2.3 Cutting tool

End milling cutting experiments were performed in this study. The cutting tests were conducted on using a 16mm diameter Indexable end-mill with two cutting edges. Figure 4.4 shows a sample picture of the tool from Kennametal (Table 4.1). KC725M Grade Inserts Figure 4-4, utilized are composed of carbide grade with a TiAIN coating. A high-performance TiAlN-PVD-coated carbide grade for milling steel, stainless steel and ductile cast iron. KC725M Inserts can be identified with their shapes as highlighted in Table 4-3. The good thermal shock resistance of the substrate makes this grade ideal for both wet and dry machining. KC725M is primarily for use in general and heavy machining.

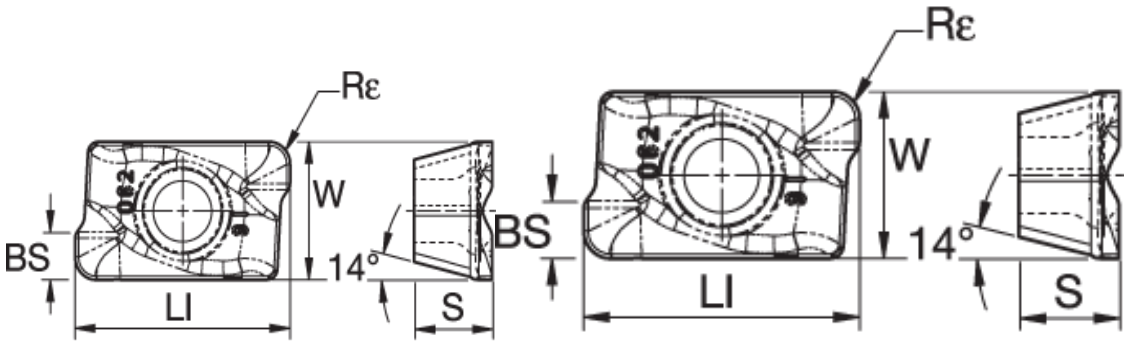

Li=12.06, S=3.7, W=6.74, Bs=1.3, Re=1.19, hm=0.082

Figure 4-4: Indexable tool inserts from Kennametal

Table 4-3: Brief insert Identification

	INSERTS CAT NO	Insert shapes	Clearance Angle	Size	Insert hand	Rake angle
1	ADPT150516ERHD	Parallelogram	7 °	06	R	7 °
2	ADPT150516ERGD	Parallelogram	15°	15	R	15°

Tool holders such as in figure 4-5 and 4-6, is manufactured from premium materials and meets or exceeds the latest ANSI B5.50 and ISO-1947 taper accuracy of AT3 specification standards Table 4-4 and 4-5. The CV 40 tools are either pre-balanced to a high specification or balanced-by-design. For high speed applications Kennametal recommends that the complete toolholder assembly (toolholder, retention knobs, collets, hardware, and cutting tools) be balanced as one entity. Exact

RPM limits can only be determined by considering machine and spindle configurations in conjunction with tooling design and safety limits factored as a complete system Figure 4-6. With the Taper Face System, toolholders are axially supported on the taper and flange face, which brings about higher rigidity and precision than a conventional 7/24 toolholder.

The system utilizes elastic deformation of the machine spindle to achieve simultaneous fitting of both the taper and flange face. Although the tapers are fit prior to clamping the mechanism, the faces are not yet secured because of a small amount of clearance between them. When the toolholder is pulled in by the drawbar mechanism, the machine spindle expands by elastic deformation and the faces are fit, completing the simultaneous fit between both taper and face. This synchronized fit prevents additional axial displacement of the taper providing high accuracy and superior surface finish in operations such as face milling, compared to the industry standard 7/24 V-flange.

Taper face tool's axial position is maintained even at high rotational speed. This specification supports both the CAT (CV) ANSI B5.50 and BT JIS B6339 versions in 40 and 50 taper sizes: for two surface contact. higher static and dynamic stiffness. higher axial and radial accuracy and rigid system.

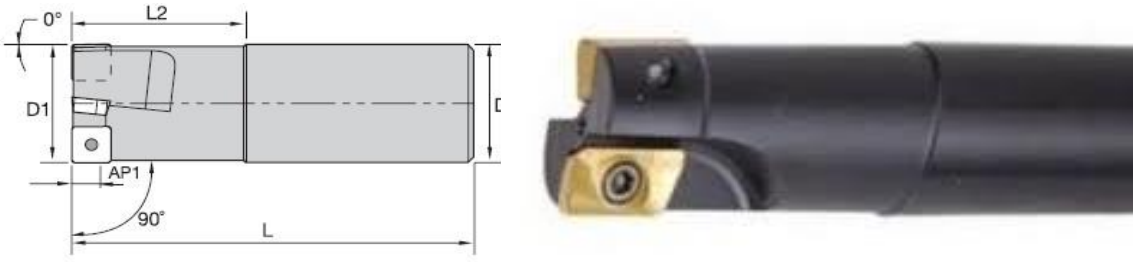

D1=16, D=16, L=74, L2= 25, Ap1 max= 10.06,

Figure 4-5: Tool Holder from Kennametal

Table 4-4*:* Kennametal tool showing manufacturer designation

Tool	End Mills —Weldon Shank from Kennametal	
16 mm diameter	16A02R025B16ED10	Tool manufacturers designation

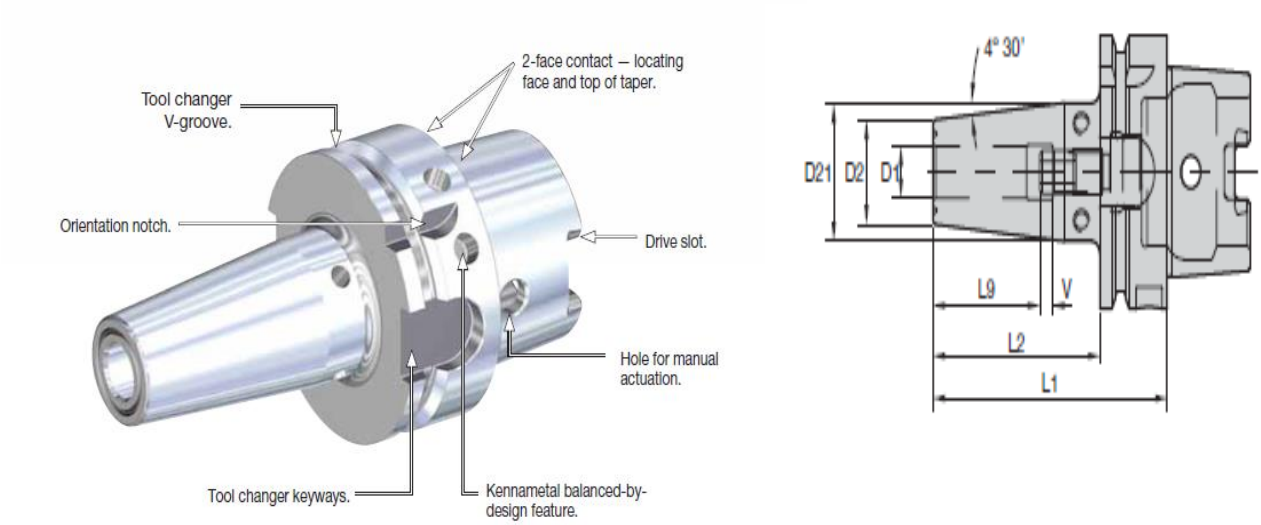

Figure 4-6*:* End Mill Adaptor from Kennametal

Table 4-5: Kennametal adaptor tool showing manufacturer designation

Tool	End Mills — Adaptor Weldon EM BT3016 from Kennametal	
16 mm diameter	BT30EM16060M	Tool manufacturers designation

4.2.4 Acoustic Emission Sensor and coupler

In recent years, AE instruments have been adopted for use in structure integrity valuation, non-destructive testing, and quality testing for advanced material industries. In this experiment, the acoustic emission signals are acquired and monitored using an AE-Piezotron Sensor (Kistler 8152B) which is mounted on the tool holder and is connected to AE Piezotron Coupler (Kistler 5125B) which gives the AE signals and the RMS of the AE signals. The continuous and burst type AE signals are acquired by Kistler 8152B AE piezotron sensors (Figure 4.8b). The coupler (Figure 4.8a) is used for signal preprocessing and conditioning, the input of the power supply was set at 220V Figure 4-8c, with the output voltage stepped down to 24V which was grounded this was used to power and regulate the amount of current that goes into the energizer of the sensor. Figure 4.7 shows the experimental workflow of the research.

Figure 4-8d is BNC-2110 is an ideal simplifying connector or interface between raw data measurement apparatus and DAQ device during experiments. The BNC-2110 has the following

features (Figure 8-4d) 15 BNC connectors for analog input, analog output, trigger/counter functions, and user-defined signals, a spring terminal block with 30 pins for digital and timing I/O signal connections, a 68-pin I/O connector that connects to multifunction DAQ devices and can be used on a desktop or mounted on a DIN rail.

An AE sensor basically consists of a sensor case, a piezoelectric measuring element and an integral impedance converter. In AE sensors, the diameter of the piezoelectric element is the main factor which defines the properties of that sensor. This piezoelectric measuring element is mounted onto a thin film steel diaphragm which is sensitive to elastic stress waves emitted during machining. It is however isolated from the metal case and other AE interference by design. Kistler AE sensors have a high sensitivity to surface and longitudinal waves over a wide frequency range. The type 8152B (Figure 4.8B) covers the range of 50 KHz to 900 KHz and outputs a low impedance voltage. acquired signals from the sensors are then relayed for pre-processing to a Kistler piezotron coupler type 5125B for amplification, filtration and RMS conversion. Kistler coupler is equipped with a jumper connection for adjustment of the gain from X10 to X100 indicating a 20dB or 40dB amplification factor. A high pass filter with frequency range from 50 kHz to 700 kHz and low pass filter of frequency range from 100 kHz to 1 MHZ are configurable to remove noise embedded within the signal.

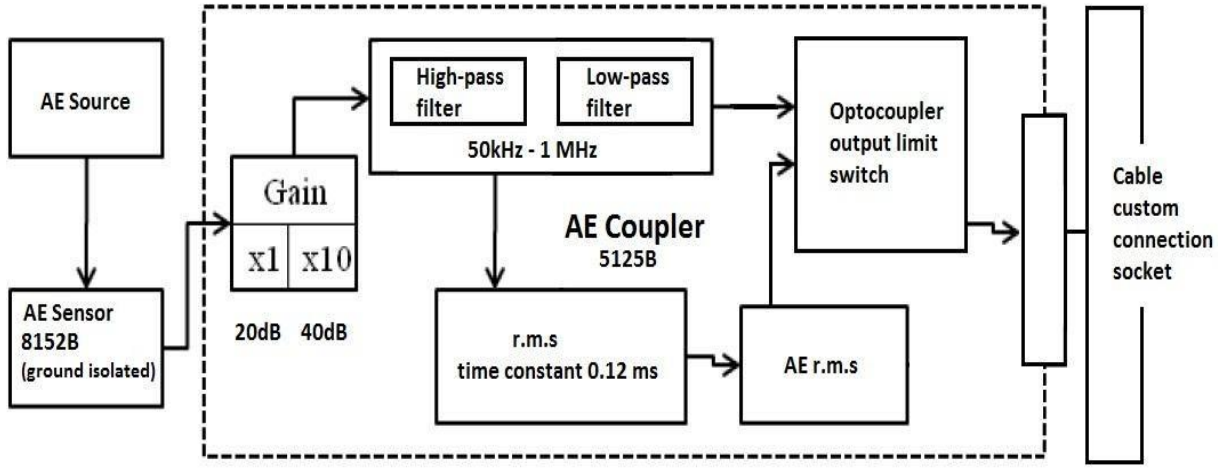

Figure 4-7*:* AE coupler circuit framework

The output signal of the filter can then be digitized via an inbuilt RMS compartment over a range of 0.12ms to 120ms time-constant. Figure 4.7 displays the operational workflow of the coupler.

The signals are then relayed to a data acquisition card via a NI BNC connection block and custom cable design. Finally, the signals are monitored using data acquisition card NI PCI-6071E from National Instruments using special data acquisition software written using the National Instrument CVI programming package and a computer. Matlab software is used for the complete analysis of this research.

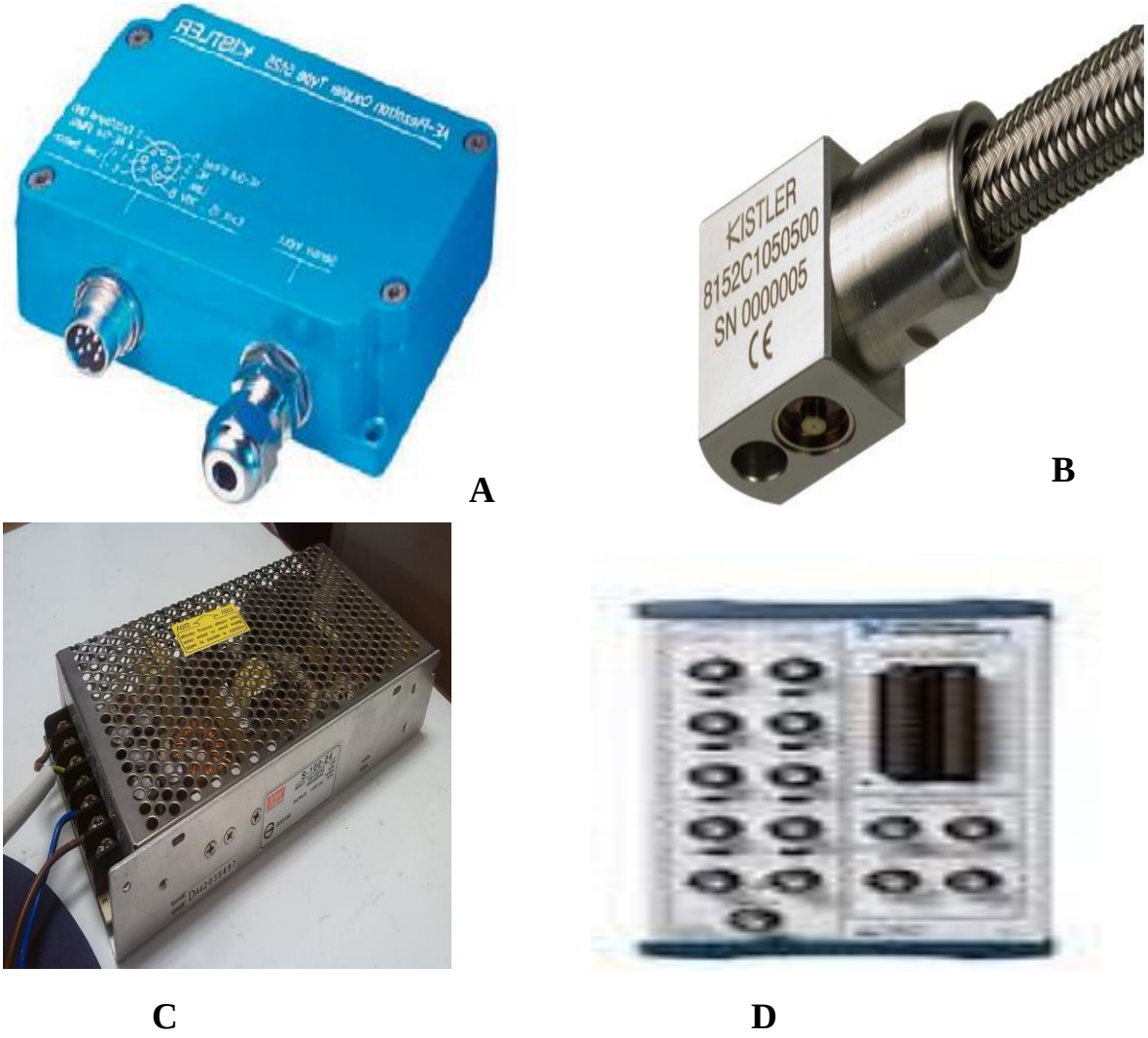

A **B**

C **D**

Figure 4-8: (A) AE coupler (Kistler 5125B); (B) AE Sensor (Kistler 8125B); (C) Power source; (D) BNC 2110

4.2.5 Optical microscopic (Non-contact Image analyzer)

4.2.5.1 Zeiss Stereo Microscope

The ZEISS stereo Microscope version 20 provides observation with a magnification as high as 150X. It possesses three focal lenses with motorized zoom expansion and resolution adjustment. The panel combines buttons, joystick and touch screen in a compact design, allowing intelligent control of all microscope functions with real time display of main microscope parameters. In order to determine the inserts, wear state, the optical microscope and analysis software Figure 4.9 was utilized.

Figure 4-9: ZEISS light microscope with image analyzer

4.2.5.2 Olympus DSX510 Digital Microscope

To ensure accuracy during wear measurements, the author also used another digital microscope and image analyzer to validate the wear progress during machining. Olympus microscopy with the DSX 510 was used. A digital microscope system that has unique combination of time-tested and optics digital imaging technology, the Olympus DSX510 (Fig 4.10) digital microscopes allow even first-time users to immediately produce superior images and highly reliable results with the following features:

- Efficient Observation: higher-quality optics and more advanced digital technology, the DSX510 delivers efficient observation, intuitive magnifying operation, a variety of observation methods, and reproducibility.
- Easy Image Capturing: Various image capturing methods provide easy, intuitive operation. Options include EFI and 3D imaging, wide area image capturing, movie capturing, and programmed image capturing
- Accurate Measurement: Live, 2D, and 3D measurement options are backed by guaranteed accuracy and repeatability, automatic calibration, and reproducibility self-check. Measurement can also be automated with a simple wizard function.
- High-Resolution 18MP Images Reproduced with High-Performance CCD
- Two lenses can be mounted at once for an even greater magnification range (70X to 9000X maximum range).
- the DSX510 offers optical zoom of up to 13X and digital zoom of up to 30X.
- Ideal for any industrial and experimental microscopic observation method, the DSX510 offers a variety of observation modes that deliver the high-resolution images users expect from high-end optics.

In Figure 4-11, it shows typical non-contact image analysis when using Olympus Digital Microscope to measure tool wear.

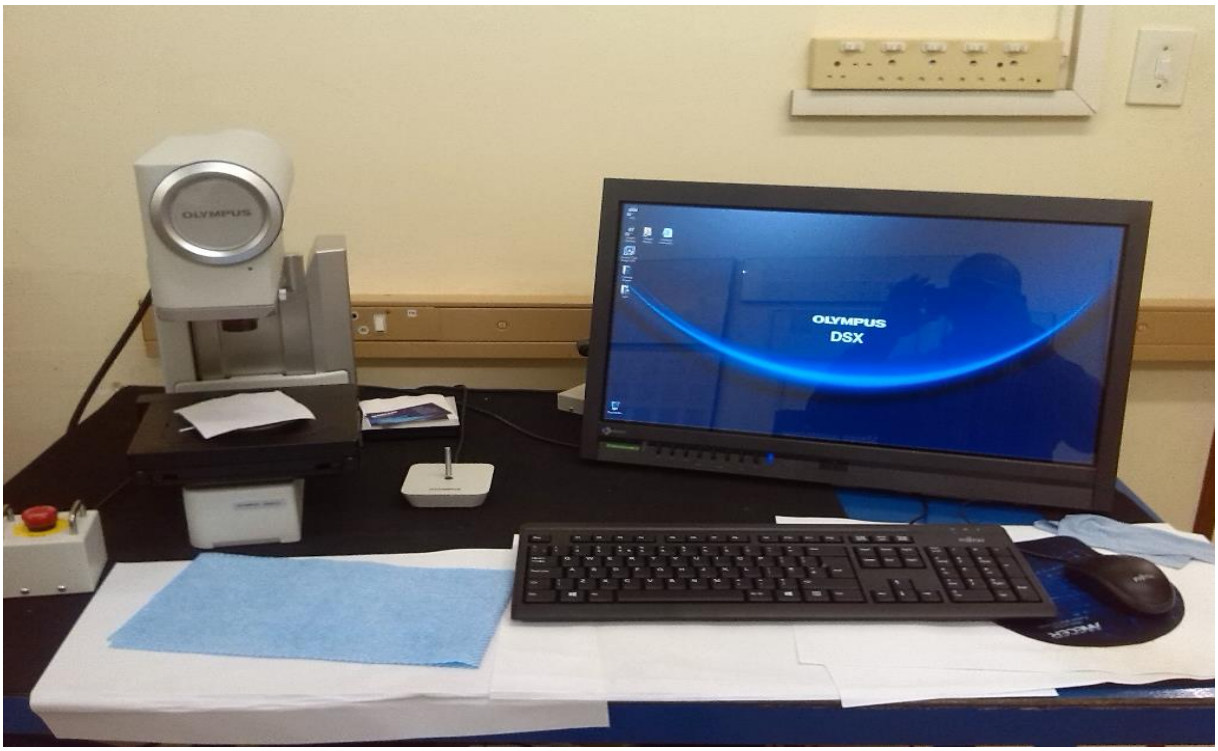

Figure 4-10: Olympus Digital Microscope (D S X 5 1 0)

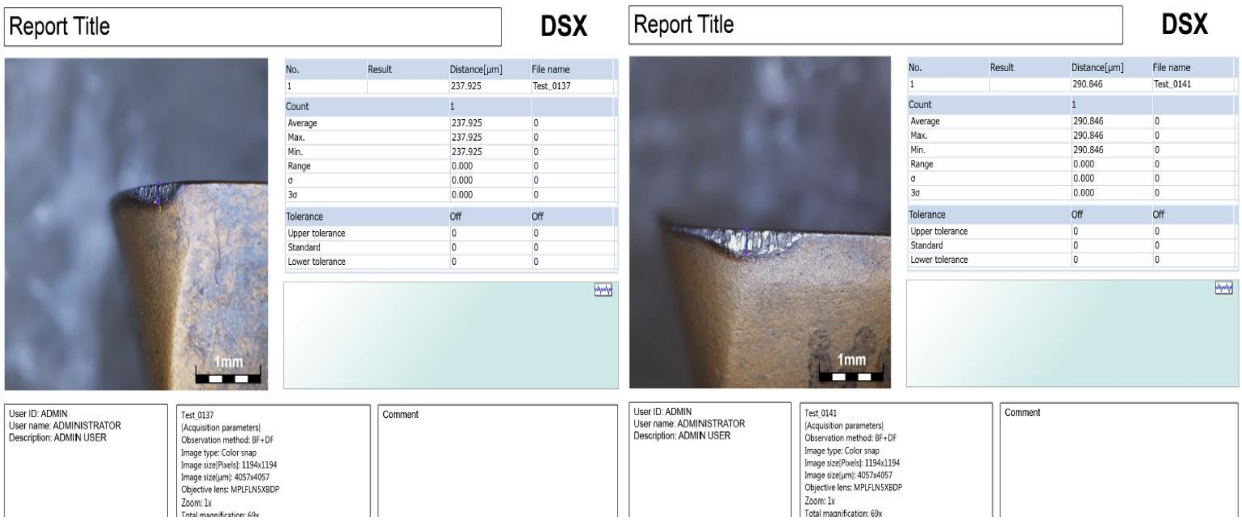

Figure 4-11: images of wear measurement from Olympus DSX510 (Experiment round 4 Run 9 and 11)

4.2.6 Data Acquisition Card

The data acquisition card used in this study (Figure 4-12) is the NI PCI-6110E from National Instruments, a multifunction analogue, digital, and timing I/O boards for PC AT. The card has 12-bits ADCs with 64 analogue input single ended or 32 differentials with a guaranteed sampling rate up to 5MS/s Per channel. The analogue input used was configured as differential inputs because of the low voltage levels involved, the noisy environment, and long wires used in connecting the signals to the data acquisition card. The analogue channel is used to acquire the machining data using a sampling rate of 1M – 5M samples per channel. The card is used in a bipolar mode of +10V or -10V with a board gain of 0.5. Hence, for 12-bit data samples the resolution is up to 9.76 mV.

This PCI from National Instruments (PCI-6110E) has further capabilities such as 4-Channel, Simultaneous-Sampling Multifunction DAQ with Extended Input Ranges up to ±42 V, 4 Simultaneously Sampled Analog Inputs, two 16-Bit Analog Outputs, 4 MS/s Single Channel, 2.5 MS/s Dual Channel, 8 Digital I/O Lines; Two 24-Bit Counters; Analog and Digital Triggering. The DAQ card in the experiment is used to interface the voltage and frequency controller from the output of the amplifier to a personal computer. The interfacing is done by using LabVIEW graphical data logging software.

Figure 4-12: DAQ card from the National Instrument

4.2.7 Data Acquisition software and programme

The data acquisition card is programmed using LabWindows from National Instruments, a developed software package for data acquisition and monitoring. The data acquisition software is flexible multipurpose data acquisition software using the LabWindows package from National Instruments. The software also has simple GUI panels which give the user a friendly and fast

interaction. The software loads the 119-acquired data to the computer memory first, draws it on the screen and then gives the user the option to save the data. Consequently, it gives the user more flexibility for data analysis, but at the same time, it limits the maximum number of samples which can be acquired. The Configuration Panel is used to choose the channels to monitor their color, save the configuration to a file and load any configuration file to the program. Figure 4-13 shows the Configuration Panel. Put live front panel

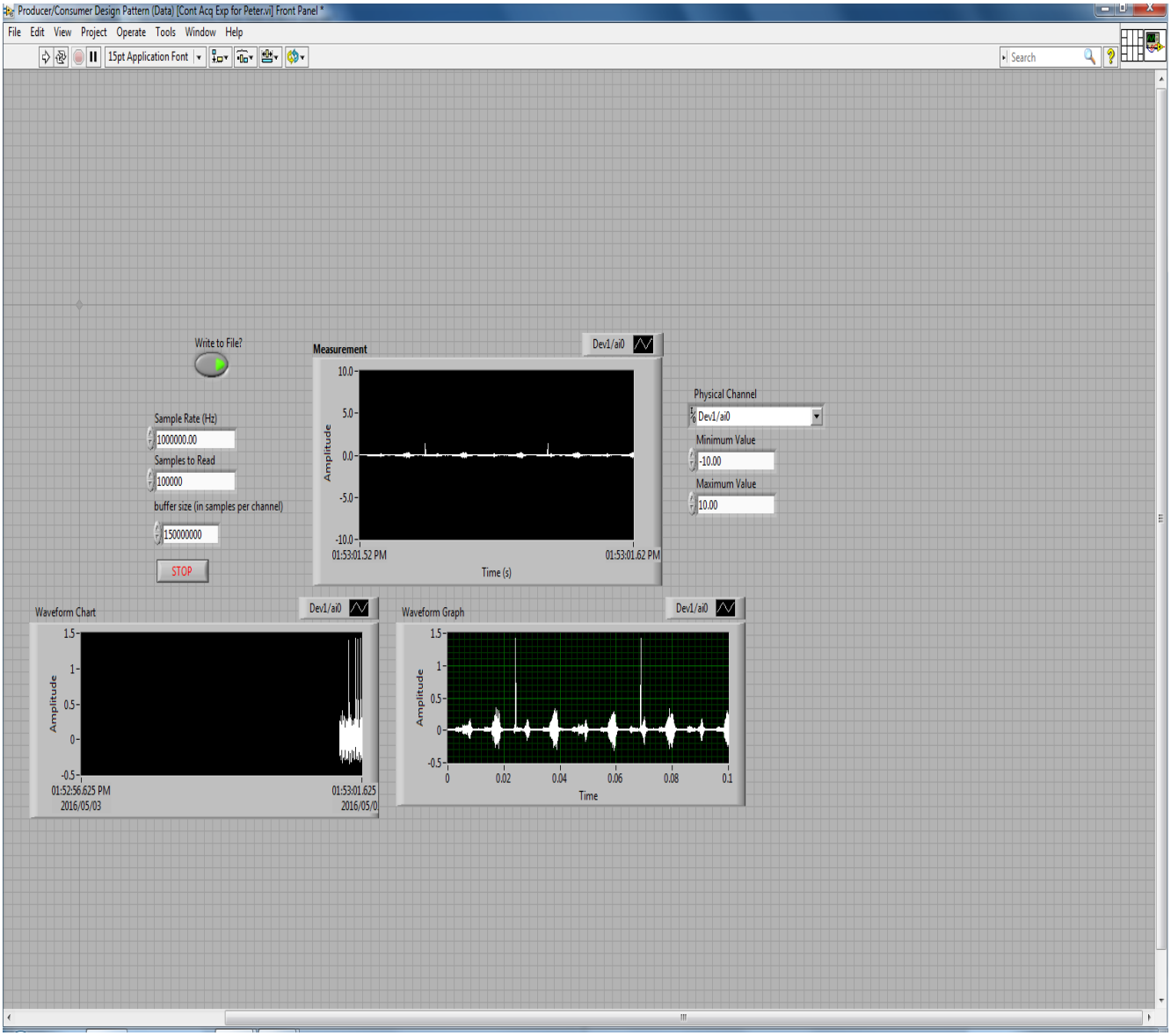

Figure 4-13: Live LabVIEW® data acquisition instrument for acoustic emission measurement

4.3 Experimental Set Up and Procedure

In this chapter, the experimental work is conducted to examine the behavior of the signals, material and monitor tools status (fresh and worn), and then to find the most sensitive sensory characteristic features to tool failures. Machining tests were conducted with coolant (soluble castor oil) machining conditions on the Deckel Maho 5-axis CNC machine. The acoustic sensor was mounted on the workpiece holder placed on the machine table via the use of the magnetic clamp. Figure 4-14 describes experimental setup used to perform cutting tests on stainless steel 316 grade and the sensor position. The milling process was carried out at the conditions using the machine parameters as shown in the Table 4-6, castor oil mixed with water was also used as coolant as wet milling was adopted for this experiment.

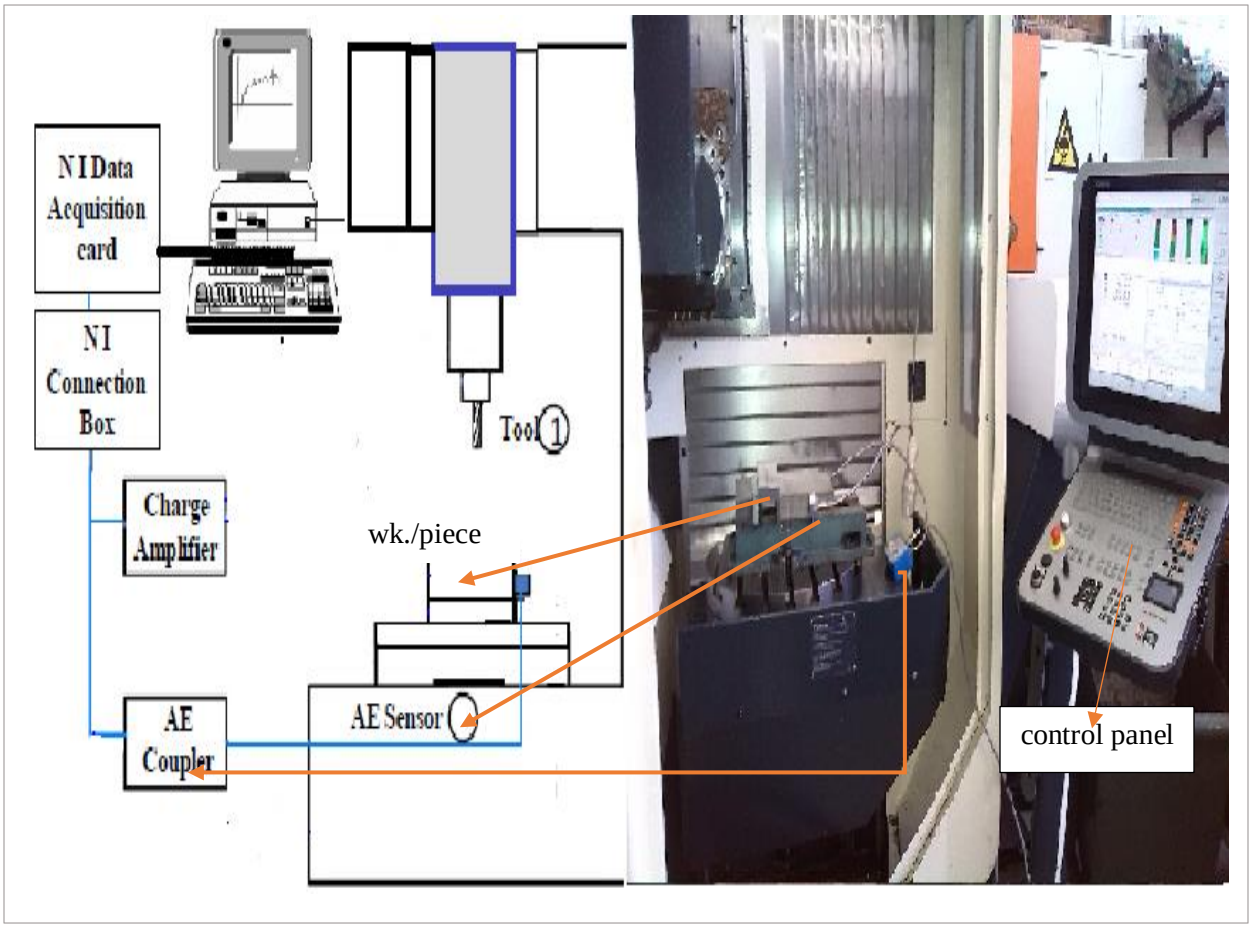

Figure 4-14: Schematic diagram of experimental setup for the monitoring system.

4.3.1 Machining Set Up and Procedure:

The common procedure of machining for tool condition monitoring was employed for the acquisition of data during the different machining phases. Enumerated below are the stages engaged to maintain reliability of data:

- With the help of a magnetic clamp and M6 bolt, the AE sensor was fastened to the spindle mount at a distance of 4cm from the workpiece (Figure 4-14). The distance is close enough to detect surface and Rayleigh acoustic waves from the workpiece.
- The AE coupler was attached directly above the set up to give room for the free rotation of the spindle on the B-axis and its travel on the x-axes without interference with the set up (Figure 4.14). This was also necessary to maintain the pre-processing unit as close to the acquisition point as possible and eliminate the effect of workpiece changing distance.
- The use of gauge indicator was used to ensure that the edge of the workpiece is parallel to the axis of the machine.
- The CNC G- codes were written for the parameters that will be used in the experimental work.
- Pre-processed signals were channeled to the BNC board and to the NI data card for further processing and storage.
- For clear results and consistent tests, the workpiece face was first cleaned and squared before conducting the primary tests with rough cutting inserts.
- Before machining tests at each layer depth, a shoulder of at least 25 mm in radial direction was cut to allow the whole tool to be within the workpiece before experiments commenced in order to prevent the acquisition of high amplitude data from collision entry.
- Machining tests were conducted with vertical and radial depth of 2mm.
- Each experiment was represented with specific cutting inserts which were stopped every certain number of passes to examine the wear progression on the microscope.
- Each machining test cutting pass were conducted along the length of the workpiece and the AE data of each pass was recorded.
- Prior to every cutting phase, the tool wear formed was observed in the laboratory with the microscopes.

- Each cutting phase consists of various cutting passes based on the observed wear progression observed from the microscope.
- AE raw data only was recorded over a time frame of 30 seconds over each cutting pass.

4.3.2 Machine Parameters of the milling Process

Table 4-6*:* Machine parameters

Machine conditions	Specifications		
	low	medium	high
Feed rate (mm/min)	58	243	520
Cutting speed (rpm)	2900	4050	5200
Depth of Cut (mm)	1	2	3
Coolant type	Castor oil		
Diameter of tool	16mm		
Material of tool (Inserts)	Indexable Solid Carbide (End mill Solid multi layered coated Carbide).		
Type of Tool	End mill Tool (2 Flutes, uncoated)		

Chapter Five

5 Analysis of experiment, results, Conclusions and Recommendations

5.1 Introduction

This chapter of the research work is categorized into three major parts, the first section explains the Process optimization control that details the application of regression analysis to develop a response surface model for predicting the surface roughness values, Tool wear, Productivity, the volume of material removed and the investigation of the interactive terms of the model and its validation. The second section highlights the signal processing of acoustic emission data acquired during the research experiment. The researcher engaged the use of Bolls spectral subtraction technique, feature extraction and selection of relevant features in the time, frequency and time-frequency domains, wavelet decomposition using relevant software listed below.

Finally, details of the training and testing of supervised back propagation neural network using the selected features as inputs to predict targeted tool wear values are discussed. The analysis in this chapter was made possible using Excel, Minitab, Statistical, LabVIEW, Design Expert and Matlab software. The third section of this chapter focus on the concluding remarks and recommendation for future work on this research work.

5.2 Process Optimization and Control

The optimization of cutting parameters is the key component in the planning of machining processes. However, deep analysis of cutting involves certain costs, particularly in the case of small series. In the case of individual machining, it is particularly necessary to shorten as much as possible the procedure for determination of the optimum cutting parameters, otherwise the cost of analysis might exceed the economic efficiency which could be reached if working with optimum conditions.

Optimum selection of cutting conditions importantly contributes to the increase of productivity and the reduction of costs, therefore utmost attention was paid to this problem as a contribution [142]. This section investigates the prediction of machinability of the process model and determines the optimal values of process parameters. The tools used are ANOVA, Box-Behnken

method and the Response surface methodology. This subject area is highly interesting for researchers and manufacturing engineers to control the production in a scientific manner.

5.3 Design of Experiment (DoE)

The Design of experiment (DOE) is a planned and organized method that is used to determine the relationship among the different factors or variables (Xs) affecting a process and the output of that process (Y) [143]. This method was first developed in the 1920s and 1930s by Ronald A. Fisher. DOE needed designing a set of multiple experiments where all the relevant factors (X‟s) are varied systematically. Through this process, it will be possible to analyze and identify optimal conditions, the factors that most influence the results, and those that do not, as well as details, for example the existence of interaction and synergies between factors.

In this work, the researcher used experimental design in process development or process troubleshooting to improve process performance and to obtain a process that is robust or insensitive to external sources of variability. It also can be good as a guideline in establishing statistical control of a process and be used to identify all the process influence variables. This is a critical engineering tool required to improve manufacturing process. It also has extensive application in the development of these techniques early in process development, which can result in Improved yield, reduced variability and closer conformance, reduced development time and reduced overall cost.

In this research work, a total of 17 machining trials were carried out to evaluate and validate the modelling approach and study the influences of linear and nonlinear factors under different operational conditions. There are three machining parameters that have been considered, which are Speed (rpm), feed rate (mm/min) and depth of cut (mm) The output is tool wear (mm) as shown in Table 5-2. There are three factors for the experiment and three levels for factors. These are divided under machining parameter (Table 5-1) into 3 levels which are level 1 (L1), level 2 (L2) and level 3 (L3) shown in under machining parameter Table 5-1. The speed for the three levels are L1= 2900rpm, L2 = 4050rpm and L3 = 5200rpm. The depths of cut are: 1mm, 2mm and 3mm. while the feed rates for the three level are also 0.02mm/min, 0.06mm/min and 0.1mm/min L1, L2 L3 respectively. Design of Experiments (DOE) for machine parameters were designed using Designed expert software.

Table 5-1*:* Machining Parameters used in the study

Machining variables	Levels		
	L1 (Low)	L2 (Medium)	L3 (High)
Speed (rpm)	2900	4050	5200
Feed (mm/min)	0.02	0.06	0.1
Depth of Cut (mm)	1	2	3

Table 5-2: Experimental Design of the experiment and results (using Box-Behnken Design)

Insert Types	Run	Spindle Speed (rpm)	Feed (mm/rev)	Feed rate (mm/min	Depth of cut (mm)	Tool wear (mm)
RGD	1	2900	0.02	58	2	0.43
RGD	2	5200	0.1	520	2	0.29
RGD	3	2900	0.1	290	2	0.18
RGD	4	4050	0.1	405	1	0.17
RGD	5	5200	0.02	104	2	0.29
RGD	6	5200	0.06	312	3	0.32
RGD	7	5200	0.06	312	1	0.20
RGD	8	2900	0.06	174	1	0.10
RGD	9	4050	0.02	81	1	0.33
RGD	10	4050	0.1	405	3	0.23
RHD	11	4050	0.06	243	2	0.30
RHD	12	2900	0.06	174	3	0.29
RHD	13	4050	0.06	243	2	0.26
RHD	14	4050	0.02	81	3	0.29
RHD	15	4050	0.06	243	2	0.36

RHD	**16**	**4050**	**0.06**	**243**	**2**	**0.30**
RHD	**17**	**4050**	**0.06**	**243**	**2**	**0.28**

5.4 ANOVA and Regression Analysis

ANOVA is a statistical method used to identify the differences between two or more independent groups (speed, feed and depth of cut) of data collected as seen in Figure 5.2. Source of variation are explained in their degree of freedom (DF), total sum of square (SS), and the mean square (MS). The analysis will calculate the F-statistic and p-values which are to determine whether the predictor of factors is significant/dominant related to the response**.** In Figure 5-1 and Figure 5-3, predicted wear was plotted against experimental wear and data validation of the research was confirmed with a scattered plot around the curve fittings.

Tool wear model

Using design expert software, the design of experiment of a **3x3** Box Behnken design with 3 center points will reflect 10 coefficients in a quadratic and 2FI model as follows:

$$TW = A_0 + A_1D + A_2F + A_3S + A_4D^2 + A_5F^2 + A_6S^2 + A_7\dot{D}F + A_8\dot{D}S + A_9\dot{F}S \ldots\ldots \quad \textbf{(5.1)}$$

Where:

$TW = Tool\ Wear$

$A_0 = Intercept$

$D = Depth\ of\ cut$

$F = Feed$

$S = Speed$

$= Feed$

$A_1 - A_3 = Coeefficient\ of\ first\ order\ terms\ in\ the\ model$

$A_4 - A_6 = Coeefficient\ of\ second\ order\ terms\ in\ the\ model$

$A_7 - A_9 = Coeefficient\ of\ \ cross\ terms\ in\ the\ model$

Predicted model:

Tool Wear =

+ 0.40 – 0.00007 * speed – 0.70 * feed + 0.27 * depth + 0.0014 * speed * feed - 0.057 * depth^2 **(5.2)**

In Figure 5-8, Regression Summary for Tool wear as dependent variable was carried out using traditional approach from excel software. R is 0.8635, R2 is 0.745 this accounts for 75% of the experimental model, Adjusted R2 is 0.62938 and standard error of estimate was recorded as 0.05.

Table 5-3: Regression table

Regression Summary for Dependent Variable: TW R= .86325112, R^2= .74520250, Adjusted R^2= .62938545 F (5,11) = 6.4343 p<.00496, Std. Error of estimate: .04736				
N = 17	**b**	**Std. Err.**	**T (11)**	**p-value**
Intercept	0.36010	0.166165	2.16712	0.053042
Speed	-0.00007	0.000034	-2.06891	0.062891
Feed	-6.97147	2.126639	-3.27816	0.007358
Depth of Cut	0.27181	0.093569	2.90487	0.014320
Depth squared	-0.05764	0.023015	-2.50445	0.029274
Speed * Depth of Cut	0.00136	0.000515	2.63916	0.023028

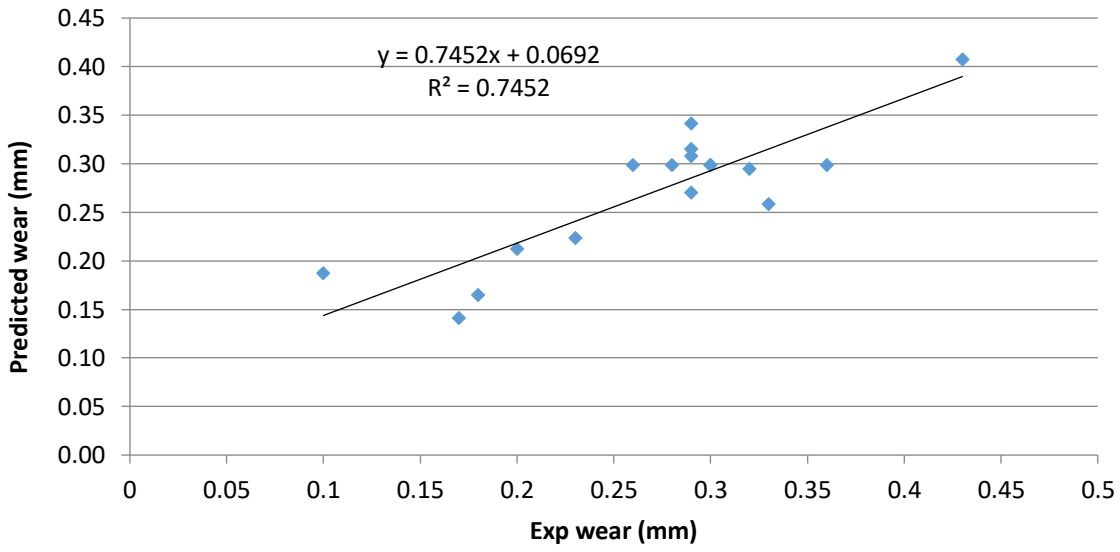

Figure 5-1: Data validation

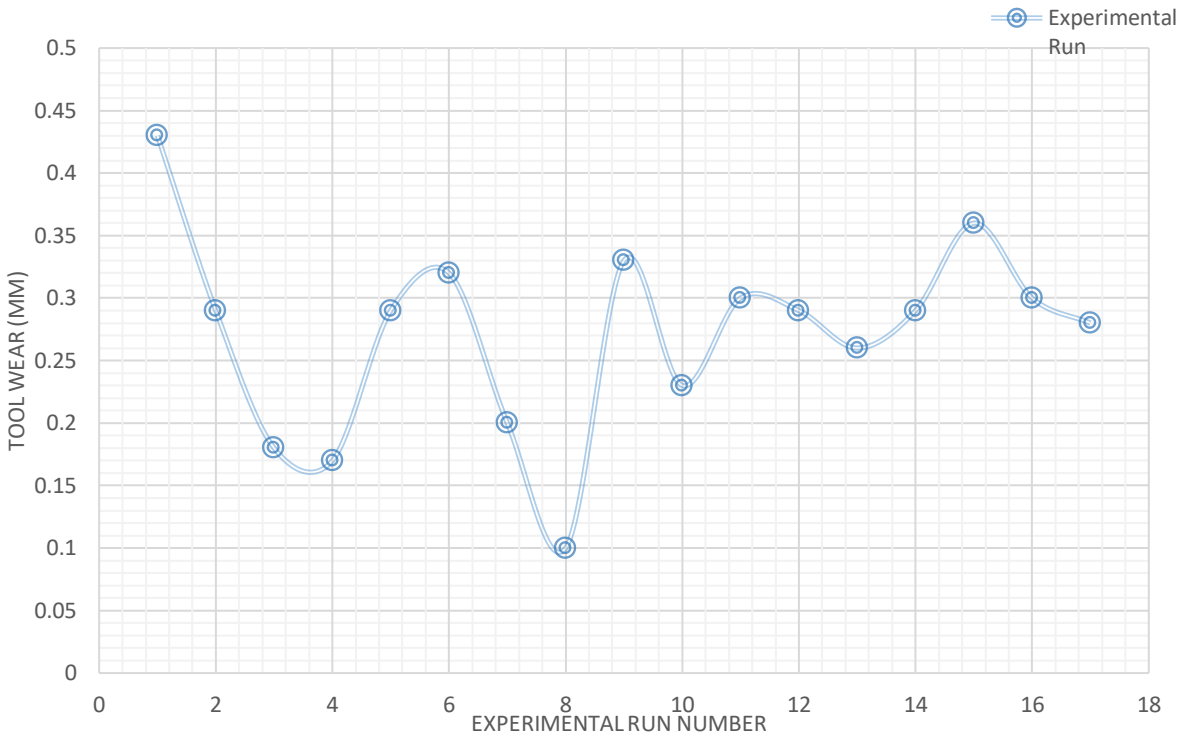

Figure 5-2*:* Graphical representation of Experimental wear versus Number of runs

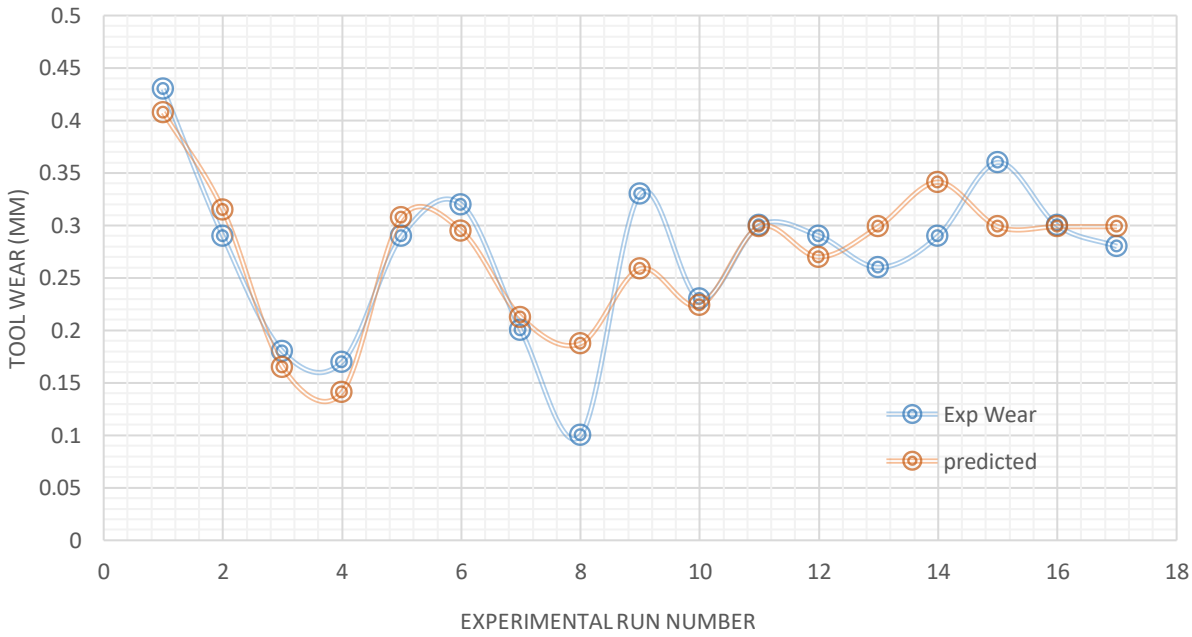

Figure 5-3*:* Plot for Experimental wear versus Predicted

In Figure 5-4, an error of high percentage was experienced during the machining at speed of 2900rpm, feed of 0.06 and depth of 1mm in run number 8. This could be as a result of machining parameter introduced in run number 8 as shown in Table 5-2, although runs number 8 and 12 are quite similar but looking at the depth of cut in 8, which was smaller could have accounted for low wear output.

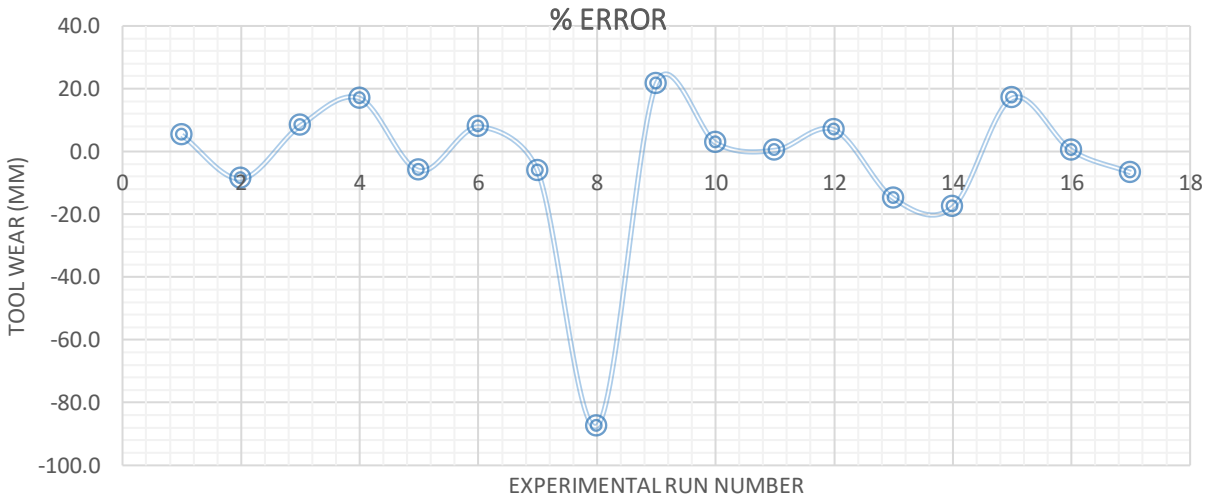

Figure 5-4: Plot of %error.

a) Design evaluation results

To ensure a valid test of Fit, further analysis was carried out using design expert software, a recommendation of a minimum of 3 lack of fit degree of freedom (dof) and 4 dof for pure error is always encouraged, because fewer dof will lead to a test that may not detect lack of fit. But in this research work, the following results were obtained Table 5-3:

Table 5-4: Degrees of Freedom for Evaluation

Model	**5**
Residuals	11
Lack of Fit	7
Pure Error	4
Corr Total	16

To evaluate the variance inflation factor (VIF) Table5-4, which measures how much the variance of the model is inflated by lack of orthogonality in the design, this needed to verify if the factor is orthogonal to all the other factors in the model, by confirming that VIF is 1.0. Therefore, from the design, Table 5-4, below confirms VIF is 1.0. Furthermore, a VIF that exceeds 10 may not be appropriate hence indicating that there is excessive correlation between the regression coefficients.

Table 5-5: Variance inflation factor (VIF)

Source	Std. Dev.	R-Squared	Adjusted R-Squared	Predicted R-Squared	PRESS	
Linear	0.065	0.4386	0.3090	-0.0797	0.10	Suggested
2FI	0.059	0.6384	0.4214	-0.4611	0.14	
Quadratic	0.053	0.7994	0.5415	-1.3744	0.23	

b) Analysis

Table 5-6: Fit summary

Terms	Std Err**	VIF	Ri-Squared	0.5 Std. Dev.	1 Std. Dev.	2 Std. Dev.
A	0.35	1.00	0.0000	9.9 %	25.3 %	73.1 %
B	0.35	1.00	0.0000	9.9 %	25.3 %	73.1 %
C	0.35	1.00	0.0000	9.9 %	25.3 %	73.1 %
AB	0.50	1.00	0.0000	7.4 %	15.0 %	44.6 %
C^2	0.49	1.00	0.0000	15.6 %	46.7 %	96.2 %

From observations in Table 5-7, which clearly explained why our model was chosen to be Quadratic. In Sequential Model Sum of Squares Table 5-7, P-value for quadratic is 0.2223 which

is the highest. This is the probability associated with adding these additional terms to the model. Lack of Fit Tests is the probability associated with the Lack of Fit calculation for this model. This confirm quadratic with 0.1399 being the highest as an insignificant probability value of P>0.10. For Model Summary Statistics, this represents the amount of variation in new data explained by the model. A negative value of -1.3744 (Table 5- 4) Predicted R-Squared means that the overall mean is a better predictor model. Therefore, the model for this research work shall be quadratic.

c) Model Summary Statistics

The "Lack of Fit F-value" of 1.95 in Figure 5-9, implies the Lack of Fit is not significant relative to the pure error. There is a 27.11% chance that a "Lack of Fit F-value" this large could occur due to noise. Non-significant lack of fit is good so the researcher can model to fit.

Table 5-7: Lack of fit

Lack of Fit Tests

Source	Sum of Squares	dof	Mean Square	F Value	P-Value Prob > F	
Linear	0.049	9	5.42E-03	3.87	0.1026	Suggested
2FI	0.029	6	4.90E-03	3.5	0.1227	
Quadratic	0.014	3	4.61E-03	3.29	0.1399	
Cubic	0	0				Aliased
Quartic	0	0				Aliased
Fifth	0	0				Aliased
Sixth	0	0				Aliased
Pure Error	5.60E-03	4	1.40E-03			

Table 5-8: Sequential Model Sum of Squares

Source	Sum of Squares	dof	Mean Square	F Value	p-value Prob > F	
Mean vs Total	**1.26**	**1**	1.26			Suggested
Linear vs Mean	**0.042**	**3**	0.014	3.39	0.0510	Suggested
2FI vs Linear	**0.019**	**3**	6.450E-003	1.84	0.2034	
Quadratic vs 2F	**0.016**	**3**	5.199E-003	1.87	0.2223	

Table 5-9: Analysis of variance table [Partial sum of squares - Type III]

Source	Sum of Squares	df	Mean Square	F Value	p-value Prob > F	
Model	0.072	5	0.014	6.43	0.0050	significant
A-speed	1.250E-003	1	1.250E-003	0.56	0.4710	
B-feed	0.028	1	0.028	12.31	0.0049	
C-depth	0.014	1	0.014	6.07	0.0315	
AB	0.016	1	0.016	6.97	0.0230	
C^2	0.014	1	0.014	6.27	0.0293	
Residual	0.025	11	2.243E-003			
Lack of Fit	0.019	7	2.725E-003	1.95	0.2711	not significant
Pure Error	5.600E-003	4	1.400E-003			
Cor Total	0.097	16				

Table 5-10: ANOVA summary

Std. Dev.	0.047	R-Squared	0.7452
Mean	0.27	Adj R-Squared	**0.6294**
C.V. %	17.43	Pred R-Squared	**0.353**
PRESS	0.063	Adeq Precision	**9.467**

In conclusion, the model explains 75% of the variation in the tool wear and the predicted effect of speed on the tool wear, is enhanced by increasing Feed. However, in Table 5-10, Pred R-Squared of 0.3530 is not as close to the Adj R-Squared of 0.6294 as one might normally expect. This indicates a large block effect due to model reduction and removal of outliers. Adeq Precision measures the signal to noise ratio in which according to leterature, a ratio greater than value of 4 is desirable. In this research work, a ratio of 9.467 indicates an adequate signal therefore, this model can be used to navigate the design space.

Model Diagnostic Plots:

Proceeding to Diagnostic Plots having ensure that the following are put into cosideration, Most of the plots display residuals, which shows how well the model satisfies the assumptions of the analysis of variance. Design experts' software was used and showed the studentized form of residuals. A breakdown of all the model diagnostic plots are given below:

- Normal probability plot of the studentized residuals to check for normality of residuals.

The normal probability plot Figure 5-5, indicates whether the residuals follow a normal distribution, in which in this case the points will follow a straight line as expected some moderate scatter even with normal data.

- Externally Studentized Residuals to look for outliers, i.e., influential values.
- Box-Cox plot for power transformations.
- Studentized residuals versus predicted values to check for constant error.

i. Diagnostic

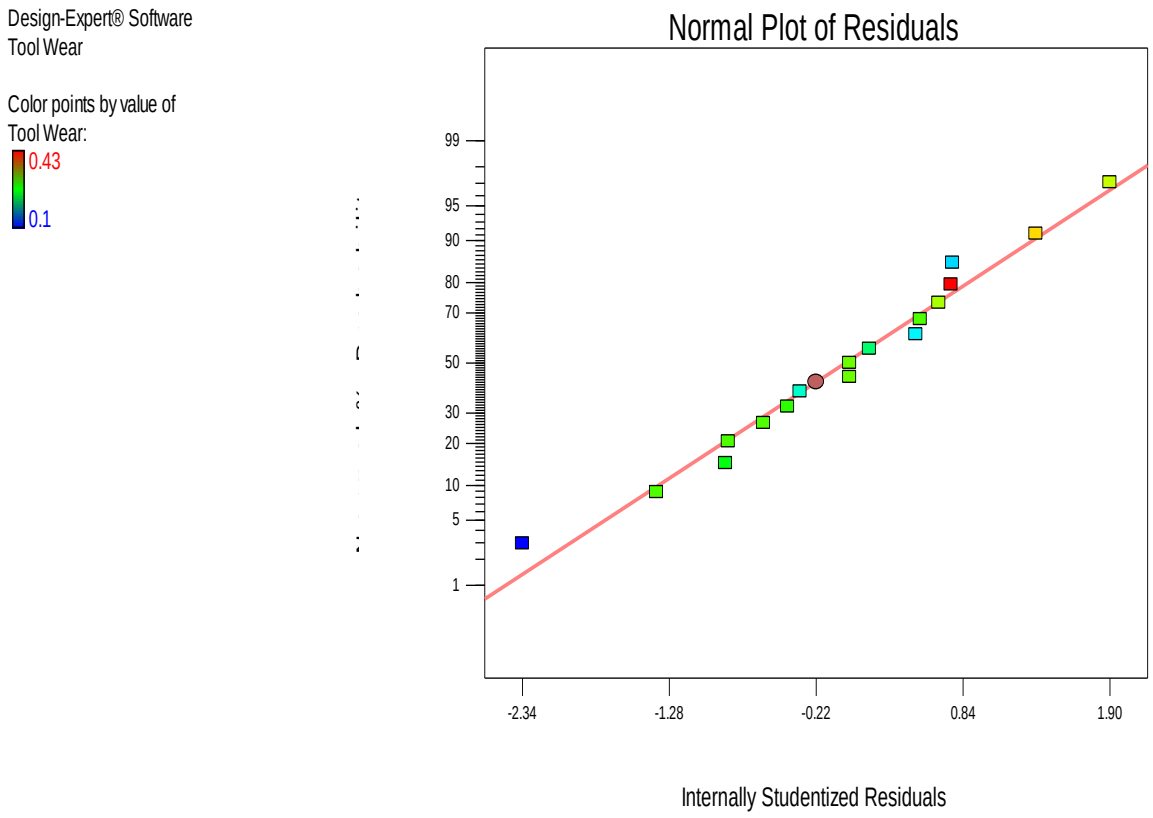

Figure 5-5: Normal plot of residual

Residuals vs Predicted: Figure 5- 6 is a plot of the residuals versus the ascending predicted response values. It tests the assumption of constant variance. Normally the plot should be a random scatter to satisfy good model that needs no transformation. From Figure 5-6, a constant range of residuals across the graph was satisfied.

Actual vs Predicted: Figure 5-7 is a graph of the actual response values versus the predicted response values. It helps to detect a value, or group of values, that are not easily predicted by the this model. Figure 5-7, confirmed our data validation carried out with raw data in Figure 5-1.

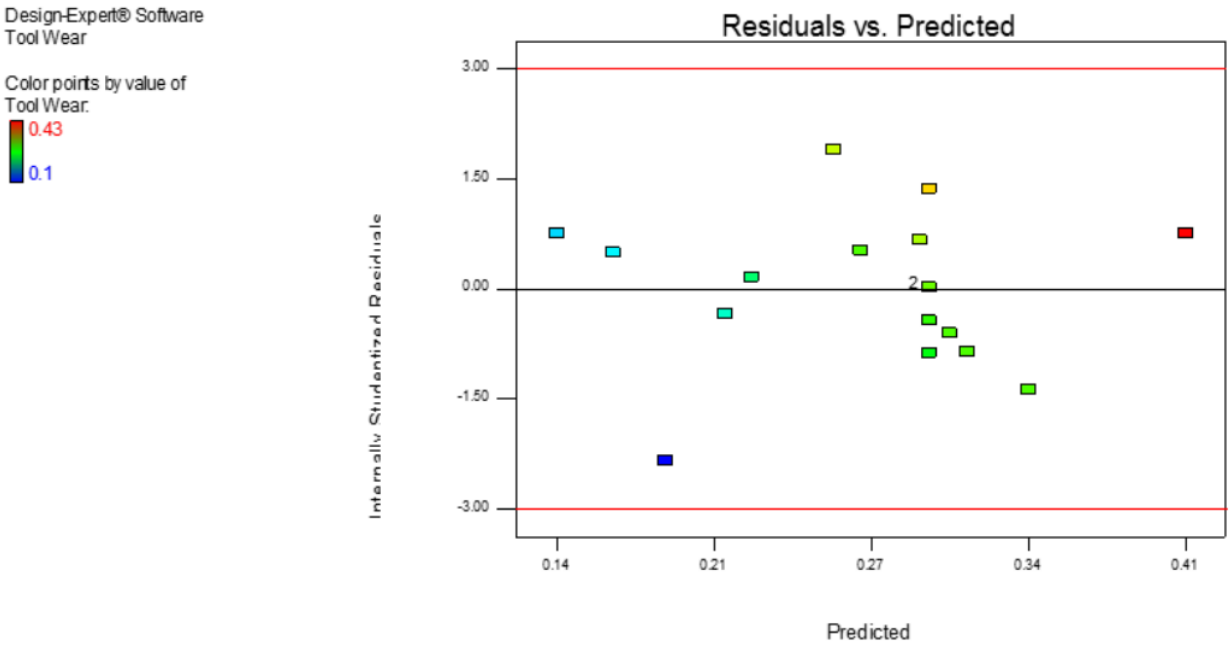

Figure 5-6: Residual versus predicted

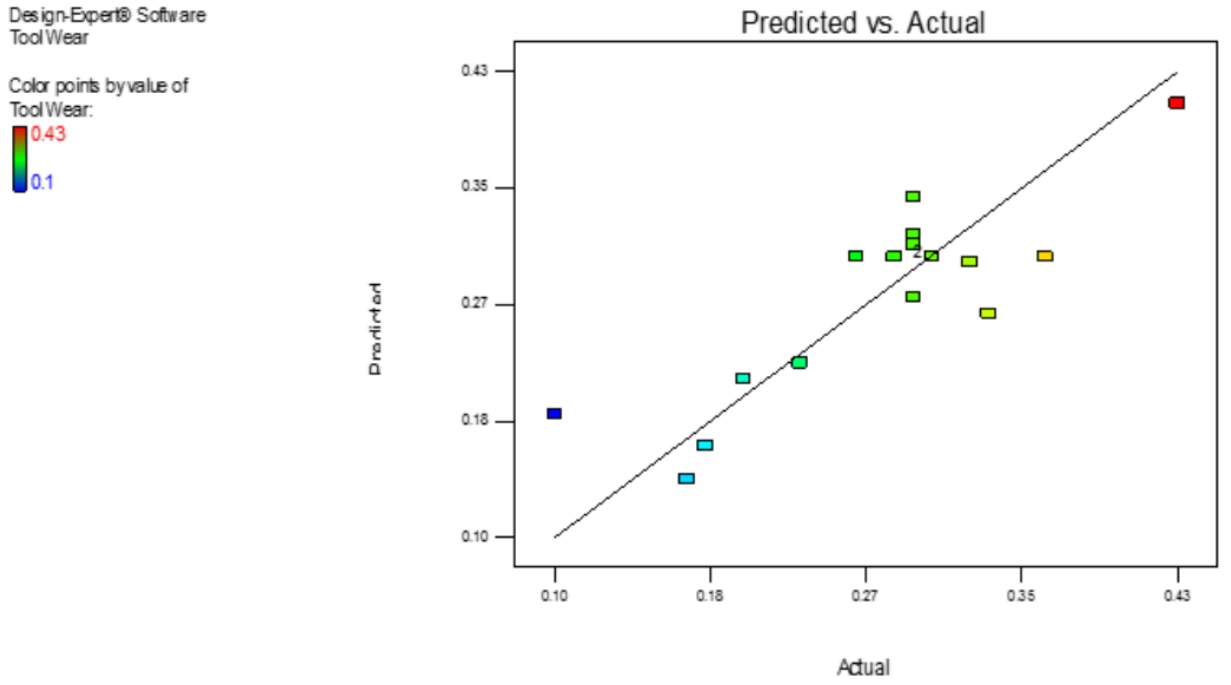

Figure 5-7: Predicted versus Actual

Figure 5-8 is the Box Cox Plot for Power Transforms. This plot provides a guideline for selecting the correct power law transformation if needed in desingning a model. From Figure 5-8, no recommended transformation was stated as can be seen, based on the best lambda value, which is 1 found at the minimum point of the curve generated by the natural log of the sum of squares of the residuals. Because the 95% confidence interval around this lambda includes 1 then the software does not recommend any transformation meaning our model does not require any transformation. The plot shows the minimum lambda values, as well as lambdas at the 95% confidence range low confidence interval as 0.16 and High confedence interval as 2.85. The plot also shows the current power transformation to be 1 so, the model fits.

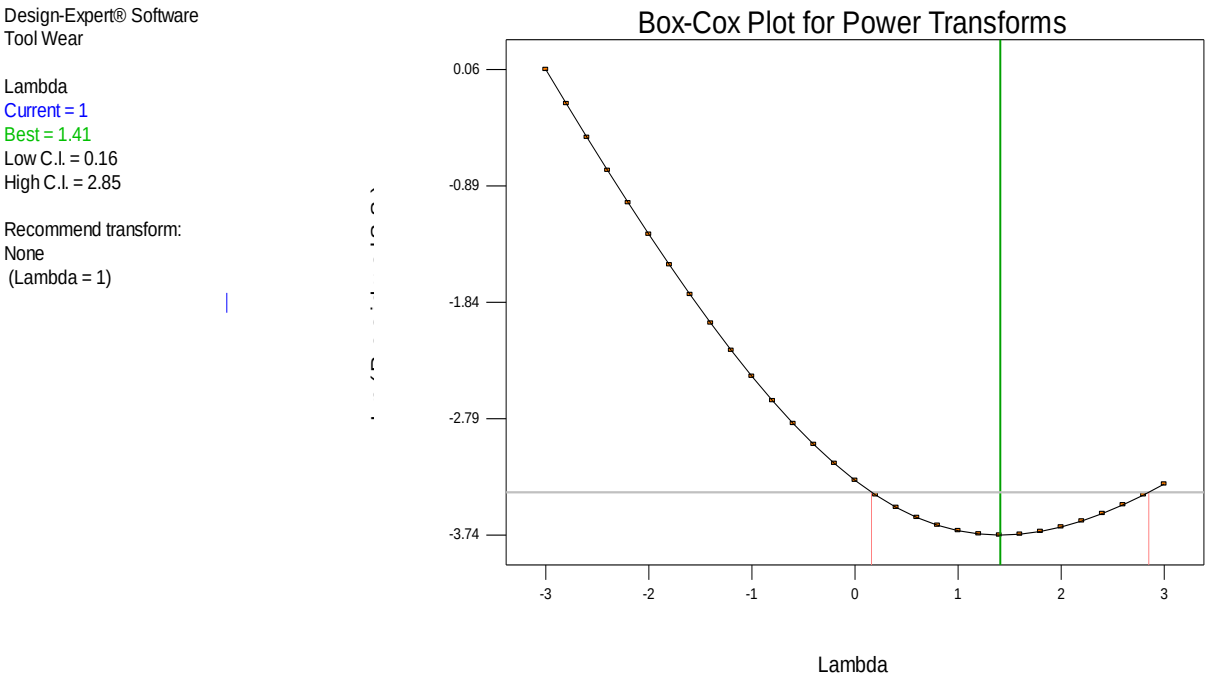

Figure 5-8: Box-cox plot

In the established model, above, there is little or no interaction between depth of cut and feed or speed but between feed and speed, therefore, the 3-D Contour plot of these two parameters are considered. In Figure 5-9, 3-D Contour plot of feed and speed practically explained what we have in Table 5-2. Looking at Figure 5-9, at a feed of 0.02mm/rev and a speed of 2900rpm a worst scenario was experienced in terms of Tool wear which is 0.43mm. this simply tells us that at the red portion of the plot that is at low speed and low feed, we may often experience constant tool

wear. But at the green to light blue part of the plot (top left corner) which represents low speed with high feed, our tool can be properly managed. However, a prediction was made at point 5 in the plot which says at about 4050rpm and about 0.06mm/rev, a maximum, optimal or allowable Tool wear of 0.298mm can be achieved. Generally, high feed with low speed will be good to work with in this regard. This explanation can also be seen in Figure 5-10, the 3-D Contour optimization plot.

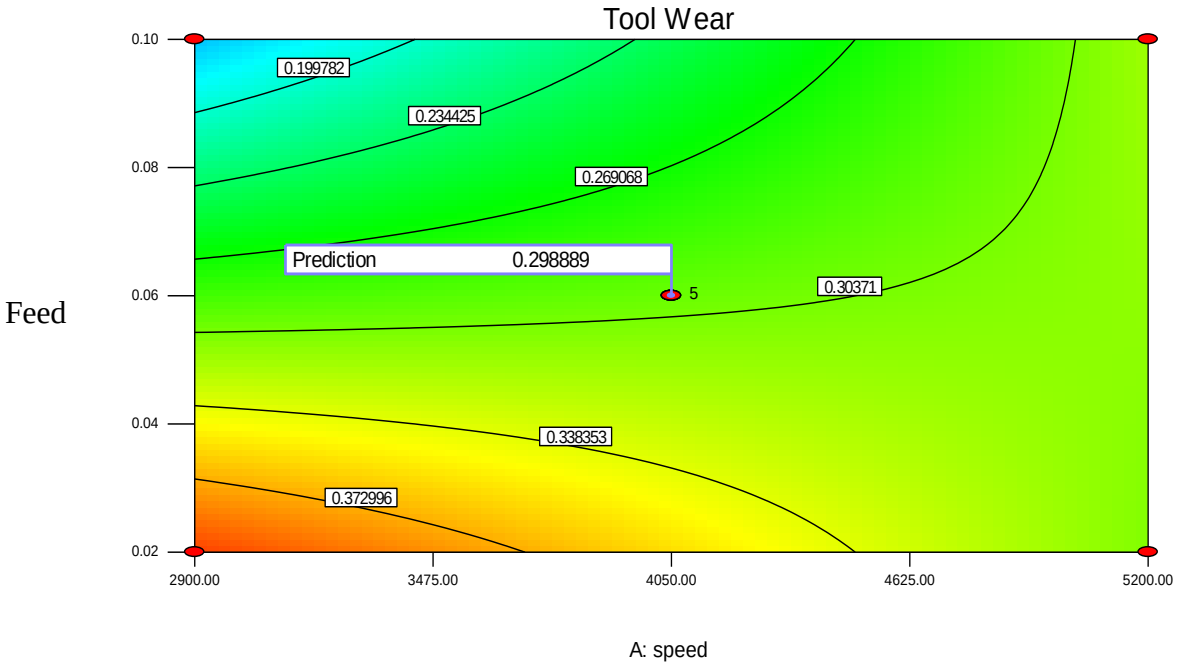

Figure 5-9: 3-D Contour Plot

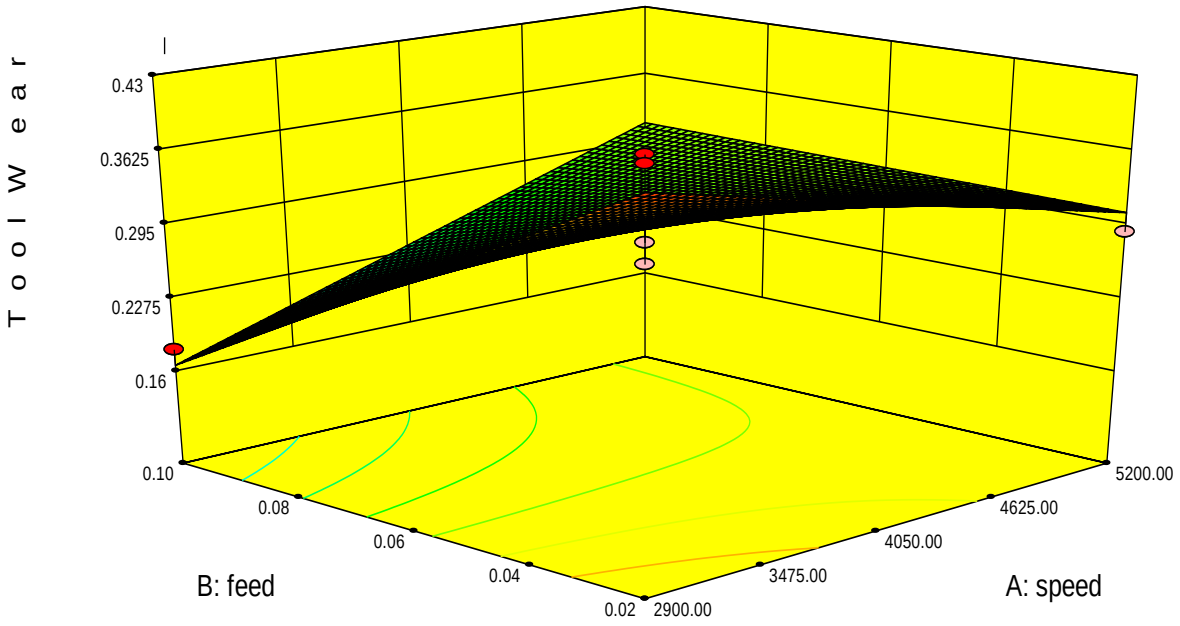

Figure 5-10: 3-D Optimization surface plot

ii. Model graphs

Perturbation plot in Figure 5- 11, shows how the response changes as each factor (speed, feed and depth of cut) moves from the chosen reference point, with all other factors held constant at the reference value. Perturbation plot helps us compare the effect of all the feed speed and depth of cut at a point in the design space. Feed, speed and depth of cut are plotted by changing only one factor over its range while holding of the other factors constant. A steep slope such as feed or curvature such as speed and depth of cut show that the Tool wear is sensitive to these factors. A relatively flat line shows insensitivity to change in that factor which we do not have in case of this experiment. The perturbation plot could be used to find those factors that most affect the Tool wear response. These influential factors are good choices for the axes on the contour plots.

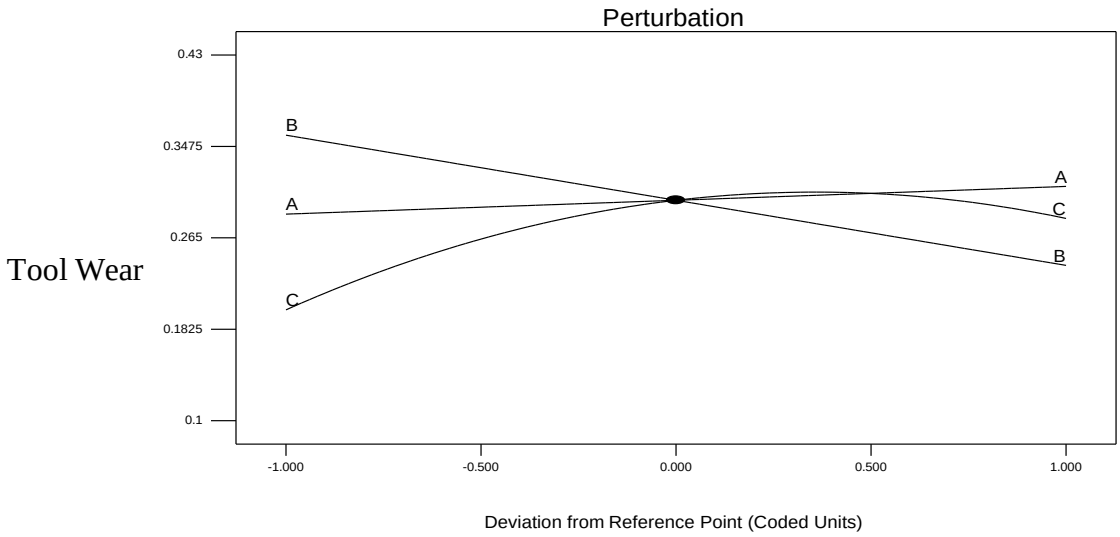

Figure 5-11*:* Perturbation *Plot (A= Speed, B = Feed and c = Depth)*

The plot of standard error in figure 5-12 of the mean shows how the error in the predicted Tool wear varies over the design space. It depends on the number and location of the design points as well as the standard error of the residuals from the ANOVA Table 5-8. Usually, to obtain the standard errors, we assume a sigma of one and the evaluation graph is based on this. When the estimate of sigma is obtained during the data analysis, it becomes a multiplier.

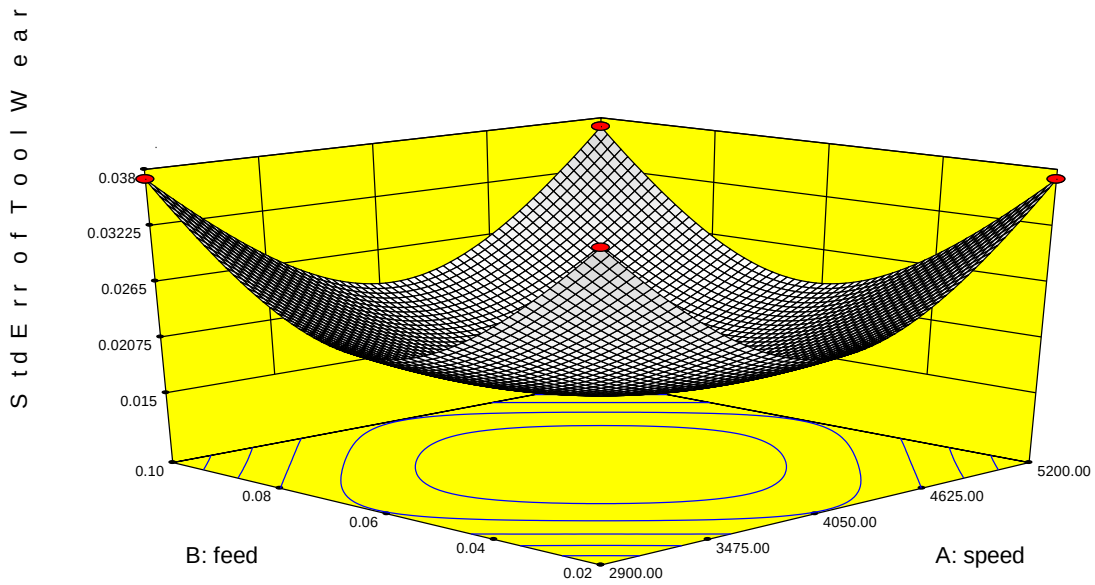

Figure 5-12: Standard error of tool wear for surface plot

Desirability plot (Figure 5-14) using Design experts is a convenient way of carrying out a powerful parameter combinations that are derived from model. Looking at the Figure 5-14, the red portion are good to go area for right combination for machining stainless steel 316 especially the predicted spot 1.00. see Table 5-11 and Table 5-12 for actual points in the graph.

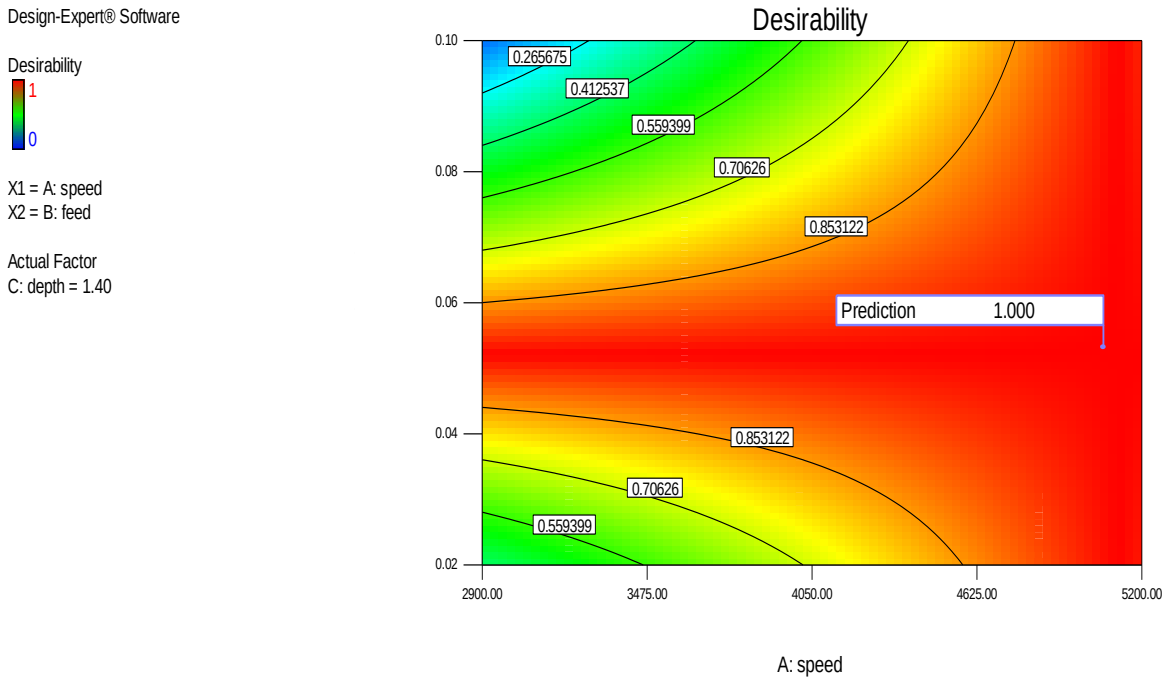

Figure 5-13: Desirability plot

Table 5-11*:* Constraint

Constraints

Name	Goal	Lower Limit	Upper Limit	Lower Weight	Upper Weight	Importance
speed	is in range	2900	5200	1	1	3
feed	is in range	0.025	0.1	1	1	3
depth	is in range	1	3	1	1	3
Tool Wear	is target = 0.2(	0.1	0.43	1	1	3

Solutions

Number	speed	feed	depth	Tool Wear	Desirability	
1	5066.32	0.06	1.40	0.265	1.000	Selected

Table 5-12: Point Prediction

Factor	Name	Level	Low Level	High Level	Std. Dev.	Coding
A	speed	4050.00	2900.00	5200.00	0.000	Actual
B	feed	0.063	0.025	0.100	0.000	Actual
C	depth	2.00	1.00	3.00	0.000	Actual

Response	Prediction	SE Mean	95% CI low	95% CI high	SE Pred	95% PI low	95% PI high
Tool Wear	0.298889	0.016	0.26	0.33	0.050	0.19	0.41

5.5 Optimization

Microsoft Excel was used to carry out profile plot for optimization as well. From Fig 5-15, the maximum depth of cut that is needed to have both maximum wear and minimum wear is about 2.3mm. The combined speed and feed for minimum wear is 2900rpm and 0.1mm/rev, the worst case for tool wear can be expected at speed of 5200rpm and feed of 0.1mm/rev.

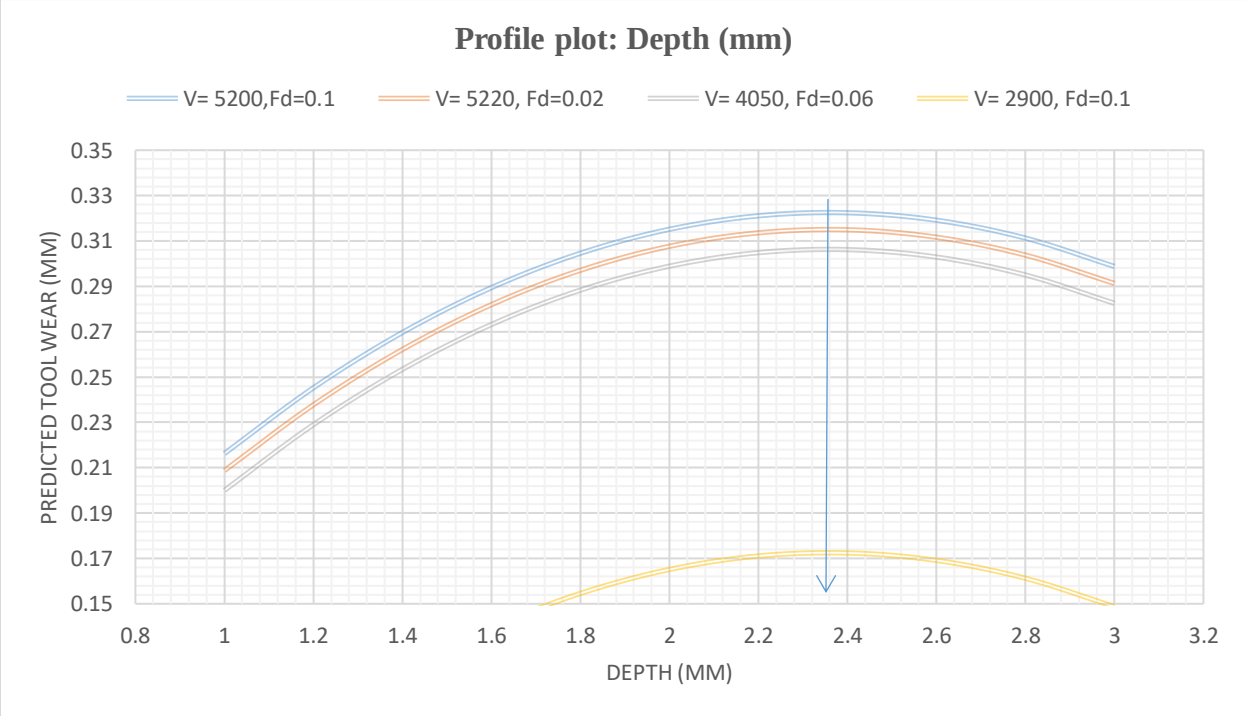

Figure 5-14: Profile plot for depth

5.6 Effect of Spindle speed on Flank wear:

The effects of spindle speed on the flank wear from Figure 5-16 to 5-18 have shown direct impact on the tool wear. In Figure 5-16, at constant feed of 0.02mm/rev regardless of the depth of cut between 1mm to 3mm, the higher the speed, the less Flank wear we experienced. However, opposite is the case when the feed rate is increased from 0.06 mm/rev to 0.1mm/rev. in the case, the higher the speed the faster we experience flank wear rate respectively.

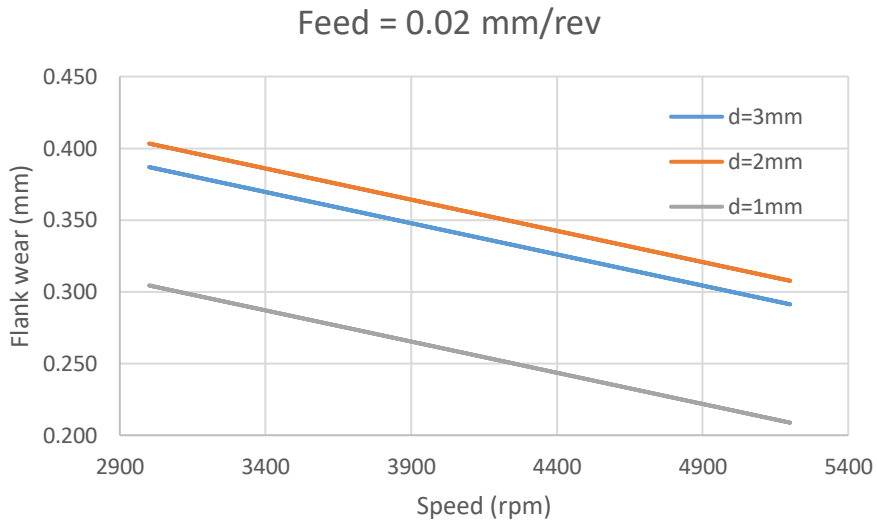

Figure 5-15: effect of spindle speed different depth of cut and flank wear at constant feed = 0.02mm/rev

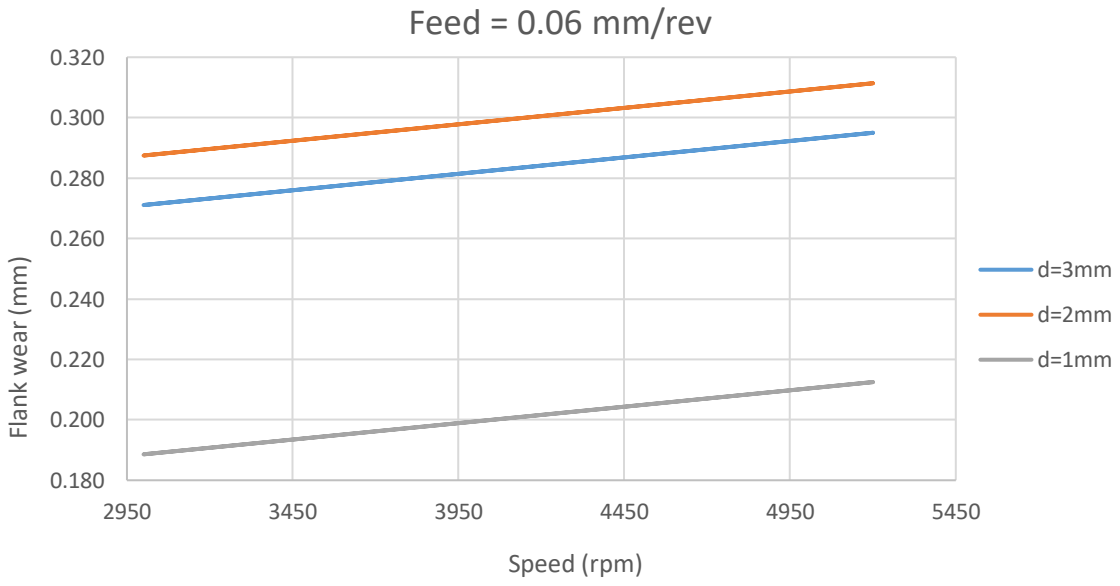

Figure 5-16: effect of spindle speed different depth of cut and flank wear at constant feed = 0.06mm/rev

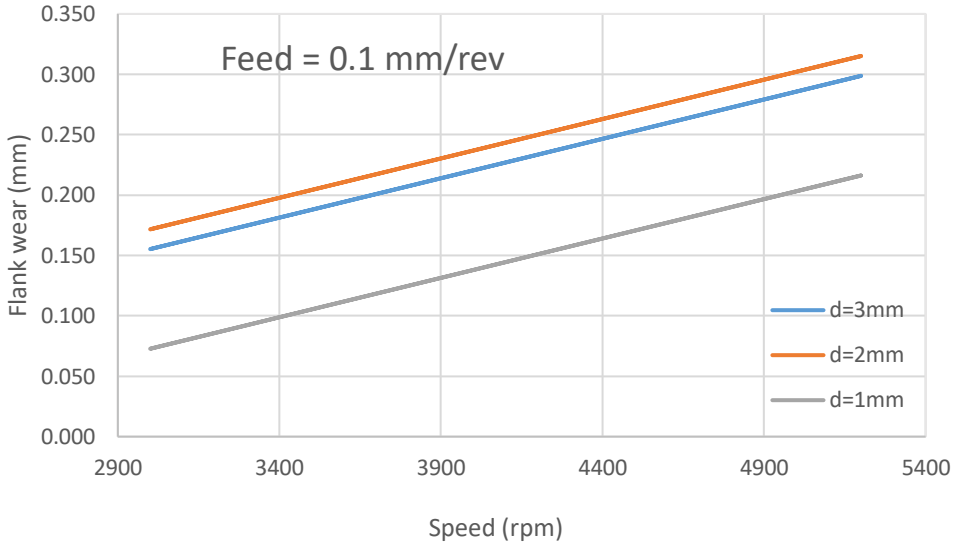

Figure 5-17: effect of spindle speed different depth of cut and flank wear at constant feed = 0.1mm/rev

5.7 Analysis of Tool wear progression

Fig 5-19, 5-20 and 5-21 show the relationships between cutting lengths and the flank wear at cutting speeds of 146, 261 and 204 m/min and feed of 0.02, 0.06 and 0.1 mm/rev respectively. The cutting experiment were stopped every 200mm and the flank wear Vb was measured using image analyzers (ZEISS and Olympus Microscopes). The tests were conducted until the tool were killed, Vb above 0.2 – 0.4. however, the ISO standard says once the flank wear exceeds 0.3, the tool is considered worn out.

Considering figures 5-19, 5-20 and 5-21, it can be noticed that, for most cutting experiments, the flank wear developed in three stages: rapid initial, gradual uniform and accelerating wear. Looking at figure 5-19, it can be seen that at feed 0.02mm/rev, for cutting speeds 146, 261 and 204 with depth of cuts 2 and 1 respectively all started their initial flank wear at 0.05mm but surprisingly, cutting speed with 204 m/min and dep of cut 3mm demonstrated a different and higher initial flank wear and very short cutting length. This indicates the effects of depth of cut on tools when machining this hard material of stainless steel. In all the three figures 5-19, 5-20 and 5-21, high depth of cut has shown its effects on cutting length of a tool. From figure 5-20, it appears that high

feed rate of 0.1mm/rev, low speed of 146m/min and a depth of cut 2mm can enhance cutting length.

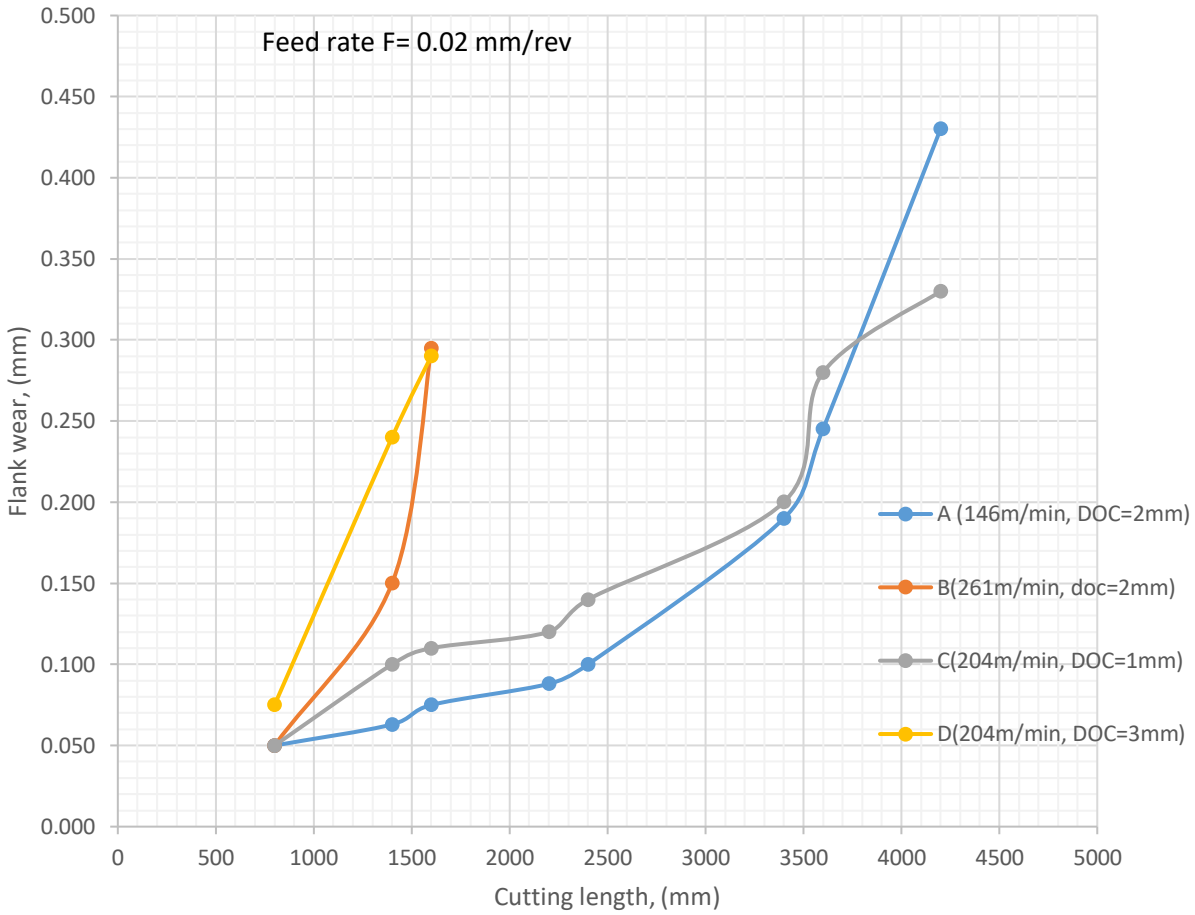

Figure 5-18: cutting length versus Flank wear at Feed = 0.02mm/rev

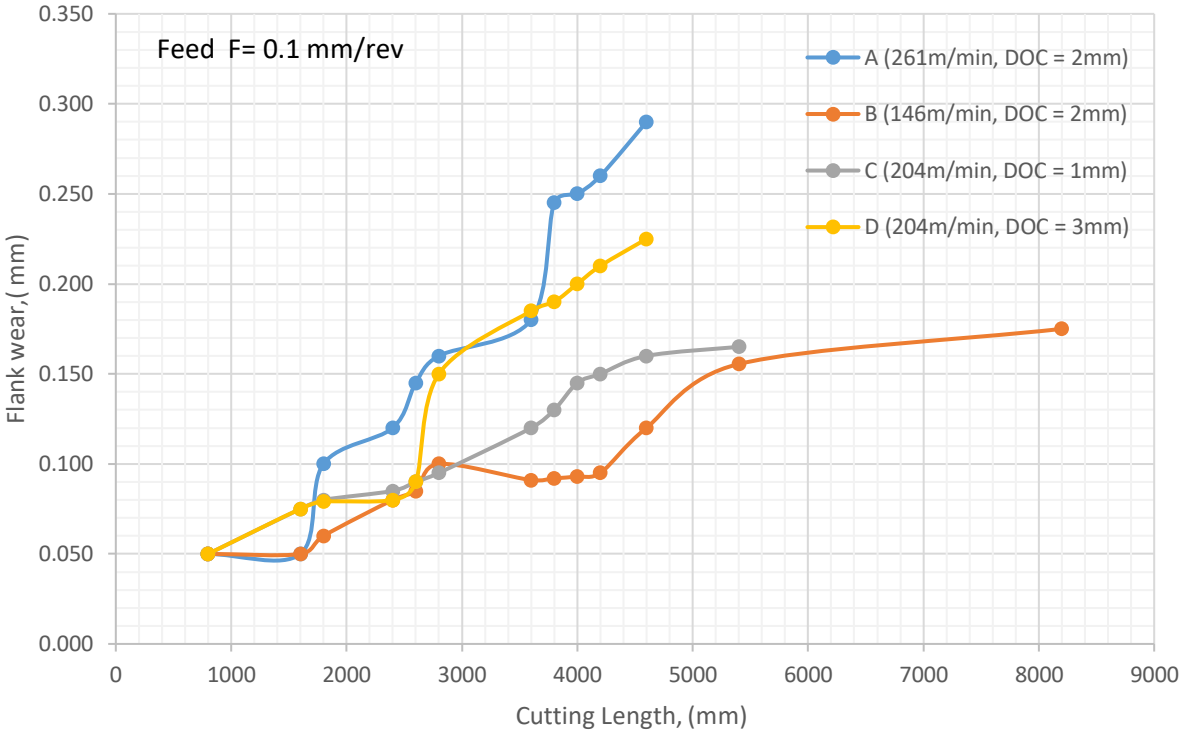

Figure 5-19: cutting length versus Flank wear at Feed = 0.1mm/rev

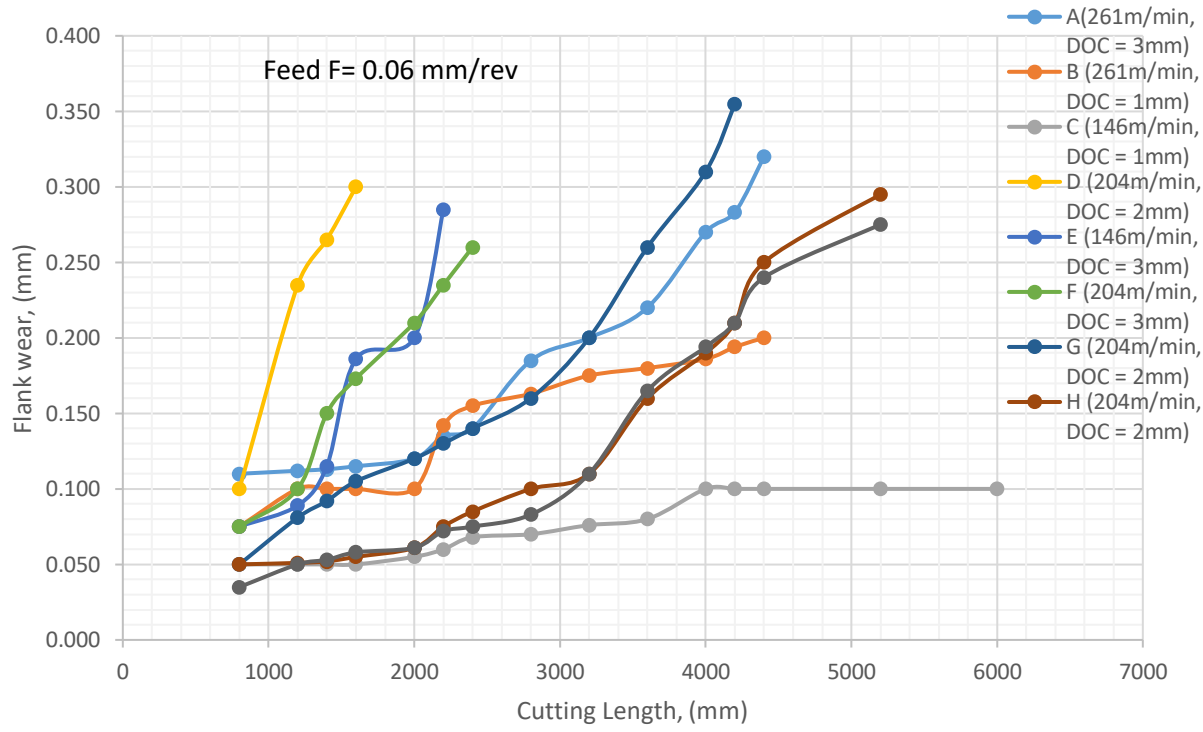

Figure 5-20: cutting length versus Flank wear at Feed = 0.06mm/rev

5.8 Effects of cutting Speed on Tool life

closely, looking at Figure 5-22, Figure 5-23 and Figure 5-24, an increase in cutting speed reduces the tool life. It is noticeable that when at constant feed a reduction in tool life is also experienced. At high speeds of 146, 204, 261m/min and variable feeds of 0.02, 0.06 and 0.1mm/rev, almost no effect was observed on the tool for the first 9 mins of their life. However, at low feed of 0.06mm/rev, the tool life almost double at high speed of 310mm/min. this could be due to chip load at this feed rate. To conclude on the effect of cutting speed on tool life, one can say high-speed end milling of AISI 316 should be carried out at low values of feed such as 0.02mm/rev (Figure 5-22).

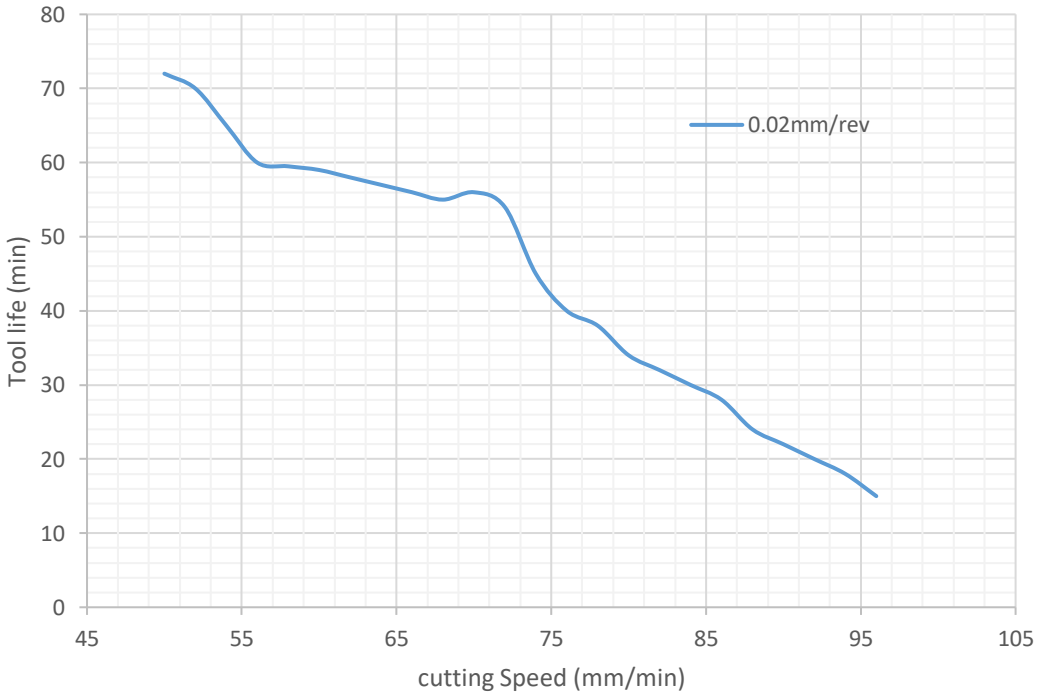

Figure 5-21: Cutting speed versus Tool life at feed = 0.02mm/rev

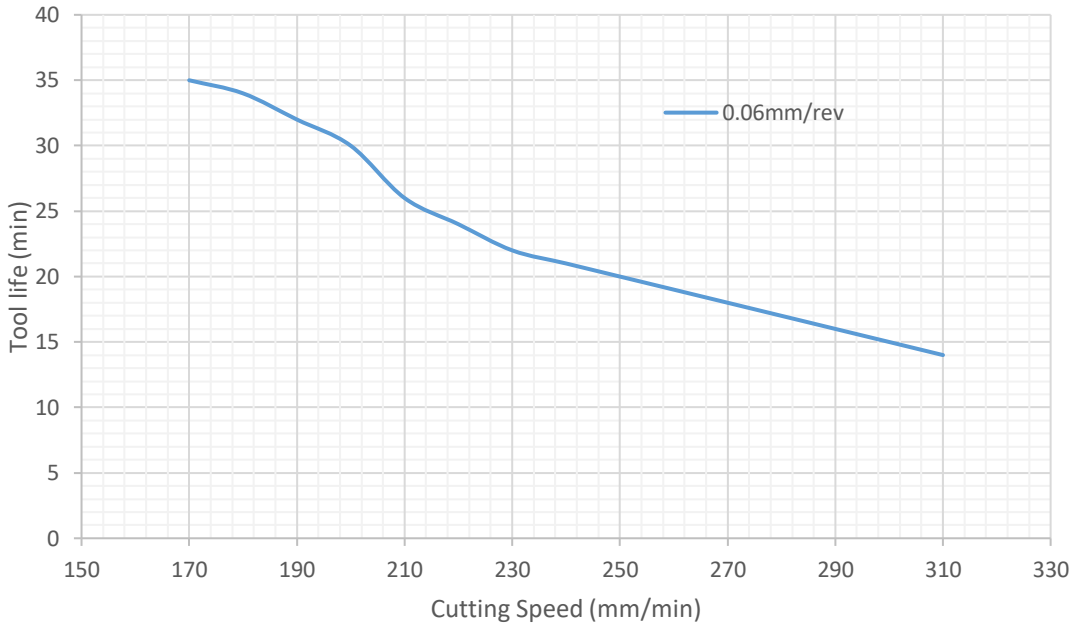

Figure 5-22: Cutting speed versus Tool life at feed = 0.06mm/rev

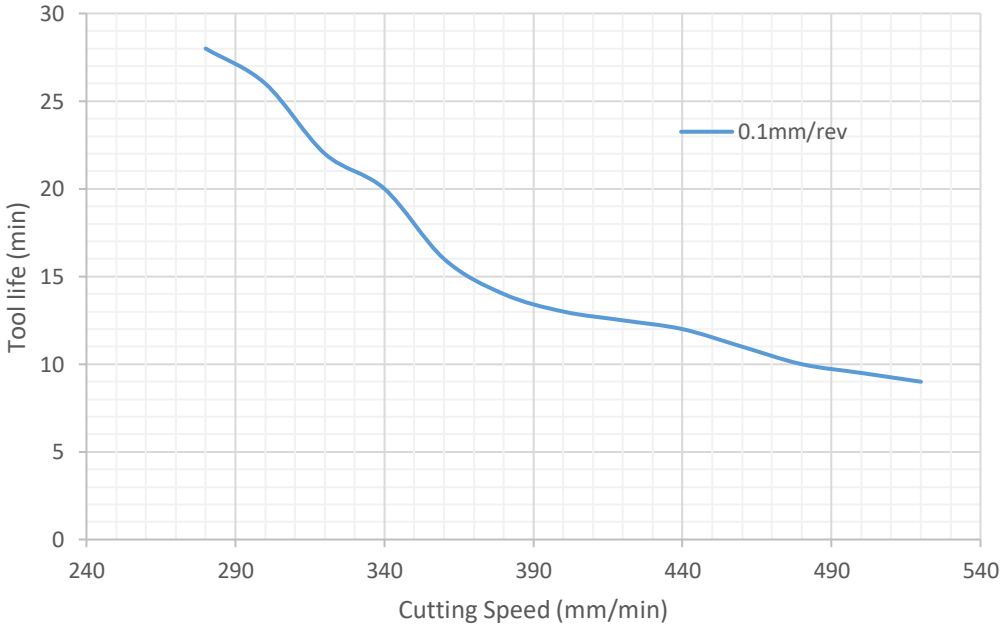

Figure 5-23: Cutting speed versus Tool life at feed = 0.1mm/rev

5.9 Productivity:

It is important to know that a very useful and remarkable pointer for performance of metal cutting operations is the volume of metal removed per unit time or popularly known as the productivity. In figure 5-25, 5-26 and 5-27, at constant feeds of 0.02, 0.06 and 0.1 mm/rev the relationships between Tool life and material removed shows the how the combinations of machine parameters can be maximized for productivity.

At feed 0.02mm/rev, speed 58mm/min and depth of 2mm, a tool life of 72 mins was achieved and 16200 mm^3 volume of material was successfully removed. Also, at feed 0.06mm/rev, speed 290mm/min and depth of 2mm, a tool life of 28mins was achieved and 33000 mm^3 volume of material removed. But when the feed was increased to a high feed rate at 0.1mm/rev, speed 174mm/min and depth of 1mm, a short tool life of 35mins and volume of 1200mm^3 was achieved.

From these observations, it seems that at low speed (58mm/min) and feed (0.02mm/rev), a lasting tool life can be achieved and at speed 290mm/min and feed 0.06mm/rev high volume of materials can be removed. Therefore, in conclusion, working on high-speed end milling of AISI 316, at elevated feed up to 0.06m/rev and high speed of 290mm/min, material removed can be maximized. Alternatively, at low feed of 0.02mm/rev and speed of 58mm/min, tool life can be optimized.

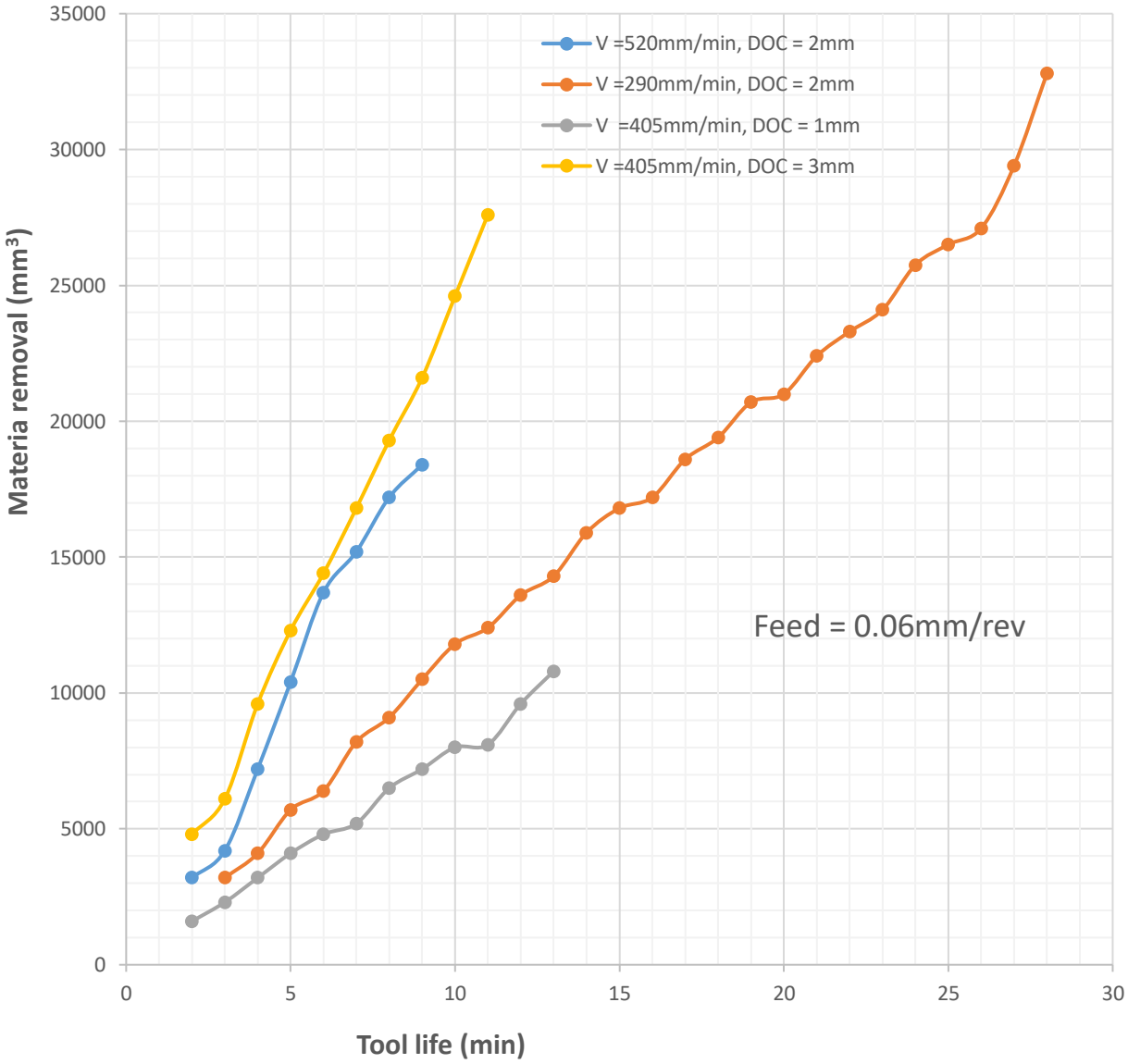

Figure 5-24: Tool life versus Material removal at feed 0.06mm/rev

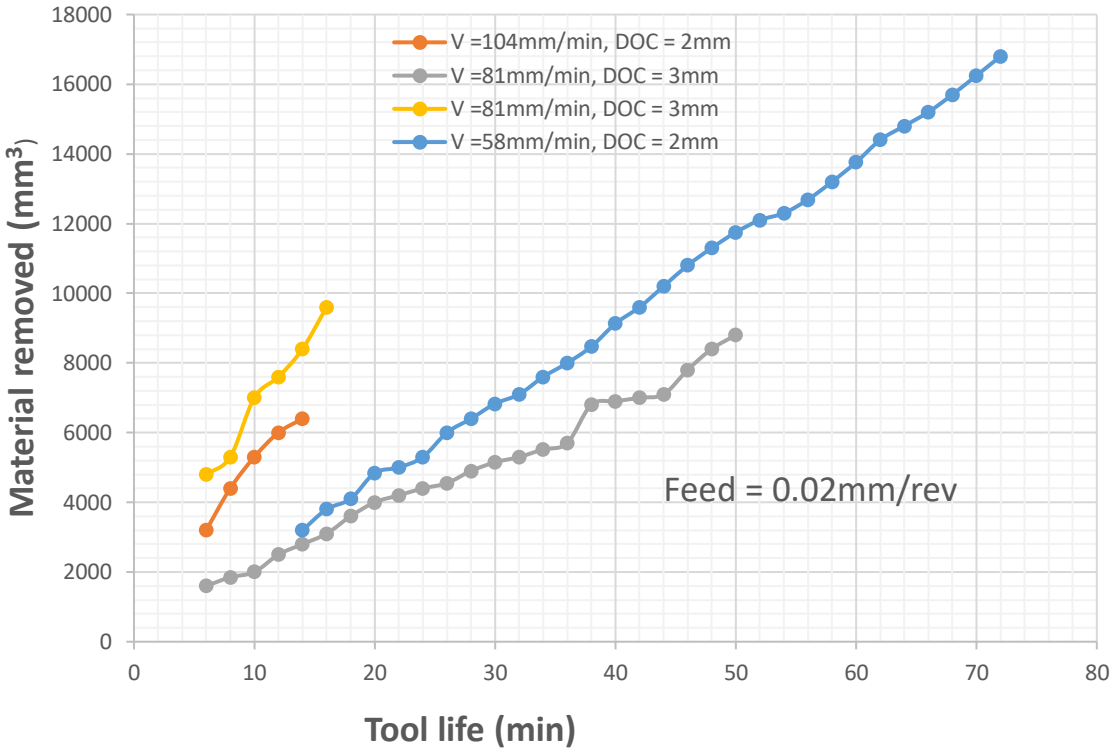

Figure 5-25: Tool life versus Material removal at feed 0.02mm/rev

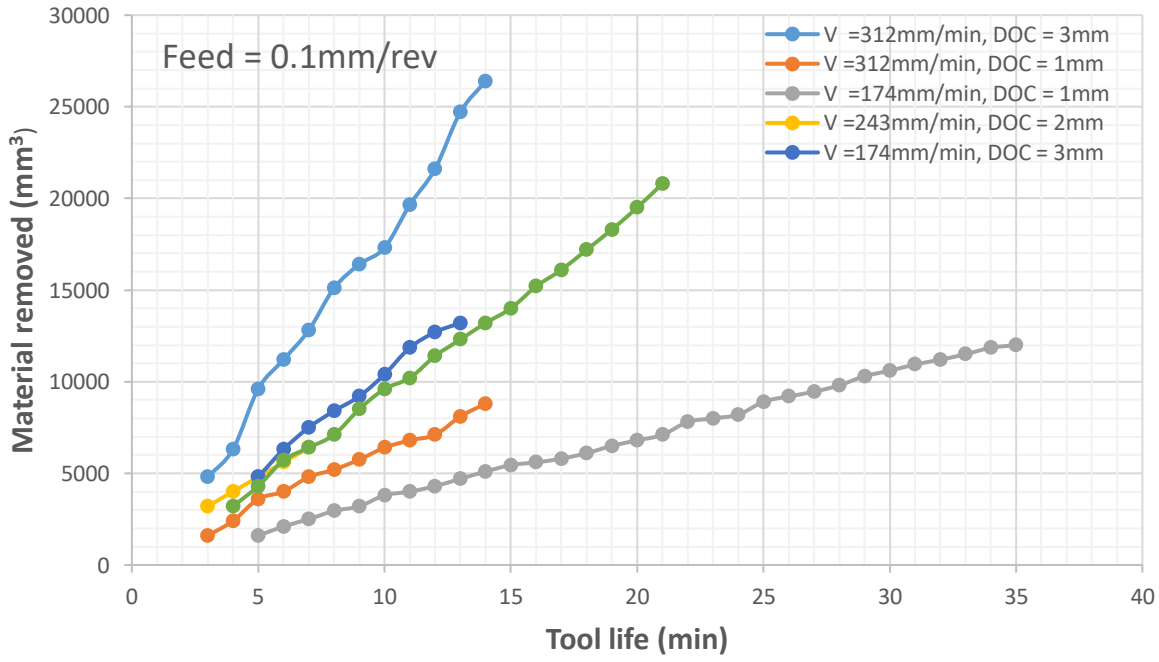

Figure 5-26: Tool life versus Material removal at feed 0.1mm/rev

5.10 Acoustic Emission, Signal Processing and Analysis

5.10.1 Introduction

Since monitoring the tool wear requires that process be classified into categories of three different levels. Based on the experimental runs and observed wear from the machining parameters selection which has a range from 0.01 to 0.3 mm was implemented. Although a maximum wear of 0.43 was reached in during the killing of the tools in the experiments, most tools were not machined to reach extreme levels in order to prevent a severe broken tool state for the purpose of modeling. A severely worn out tool was considered adequate for result processing. Table 5-13 indicates various wear classes.

Table 5-13: wear classes

Class	Flank Wear (V_b)	Tool State
0	**$v_b < 0.1$**	**New tool**
1	**$0.1 < v_b < 0.2$**	**Moderately worn**
2	**$0.2 < v_b < 0.4$**	**Worn out Tool**

Based on the cutting parameters shown in Table 4.6, the cutting tool performed several passes along the length of the workpiece. In this chapter, review of results and observations obtained during the research are discussed. Figure 5.28 gives a pictorial representation of the machining experiments and process definitions.

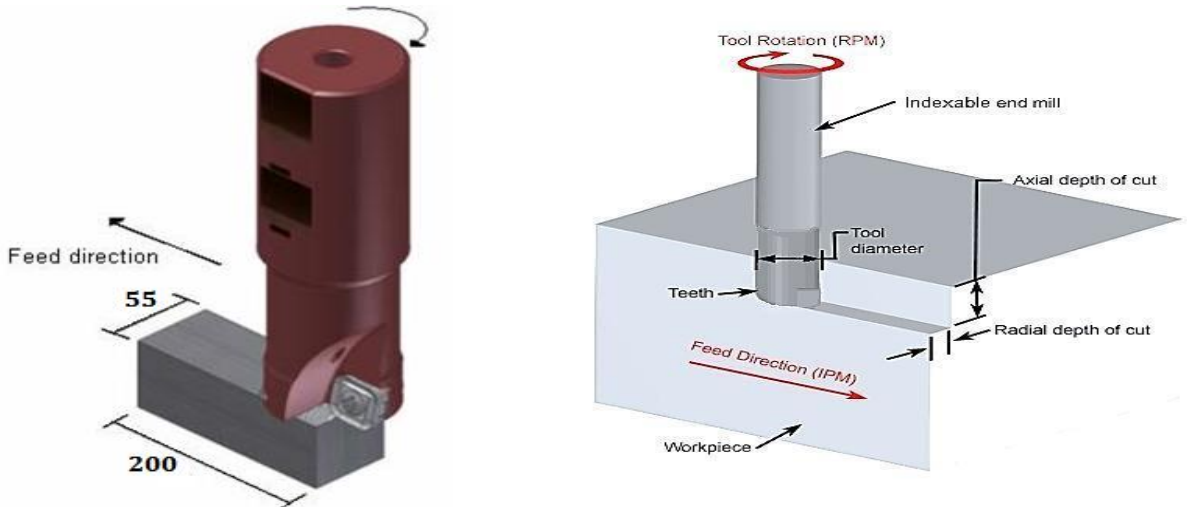

Figure 5-27: Scheme of Cutting process

5.10.2 Segmentation of data

The number of tool entry into the workpiece per second is an indication of the theoretical frequency of the machining process. This information helps in the selection of a time segment frame for signal processing. The theoretical cutting frequency of the milling operation was obtained from the equation below:

$$f = T \times \frac{n}{60} = \frac{T \times V_C \times 1000}{\pi \times D_c \times 60} \quad \textbf{(5-3)}$$

Where:

f = theoretical frequency

T = the number of the teeth on the tool

n = the number of rotational speed of the cutter in rpm

V_c = cutting speed in mm/min

D_c = cutting tool diameter in mm

For the purpose of this experiment, the theoretical cutting frequencies (Table 5-14) of the process were 99.45 Hz, 125.98 Hz and 172.39 Hz. Table 5-15 shows the segmentation of data values and the number of tool entry per segments.

Table 5-14: Theoretical cutting frequency

Vc (m/min)	Dc (mm)	T	Fc (Hz)
150	16	2	99.45
190	16	2	125.98
260	16	2	172.39

The PCI from National Instruments (PCI-6110E) used in the research work has further capabilities such as 4-Channel, Simultaneous-Sampling Multifunction DAQ with Extended Input Ranges up to ±42 V, 4 Simultaneously Sampled Analog Inputs, two 16-Bit Analog Outputs, 4 MS/s. Therefore, the author, by choice within the specification above used 1 MS/s of sampling rate, segmentation of the data for processing was implemented. The sampling occurred over a time frame of 35 seconds, yielding to an acquisition throughput of 35 million samples per pass.

Table 5-15: Segmentation of Data

Parameters	values		
Rotational speed (rpm)	2900	3800	5200
Sampling rate (S/s)		1,000,000	
Theoretical cutting frequency (Hz)	99.45	125.98	172.39
Acquisition time frame (s)		35	
Total acquired data		35,000,000	
Number of segments		4	
No. of segments selected for extraction		1	
Segment time frame (MS)		0.3	
Number of samples per segment		300,000	

5.10.3 Signal filtering

The most common frequency domain characteristic found in the literature is the spectral energy around the first natural frequency of the tool-workpiece system. It was established that the first natural frequency for this system lies at about 5 kHz. The spectral energy in the 5-kHz region was taken as a feature. However, some authors also found that useful information about the process can be found in the 'low' frequency domain. Investigations proved that the spectral energy between 100 - 1000 Hz also displays a significant trend towards tool wear. Therefore, this was also taken as a feature. SP Tool from Matlab was used to design and filter the raw data used for the analysis of Signal Processing. Figure 5-19 and Table 5-16 show filter design and the specifications for the filter designed.

5.10.4 Filter Design

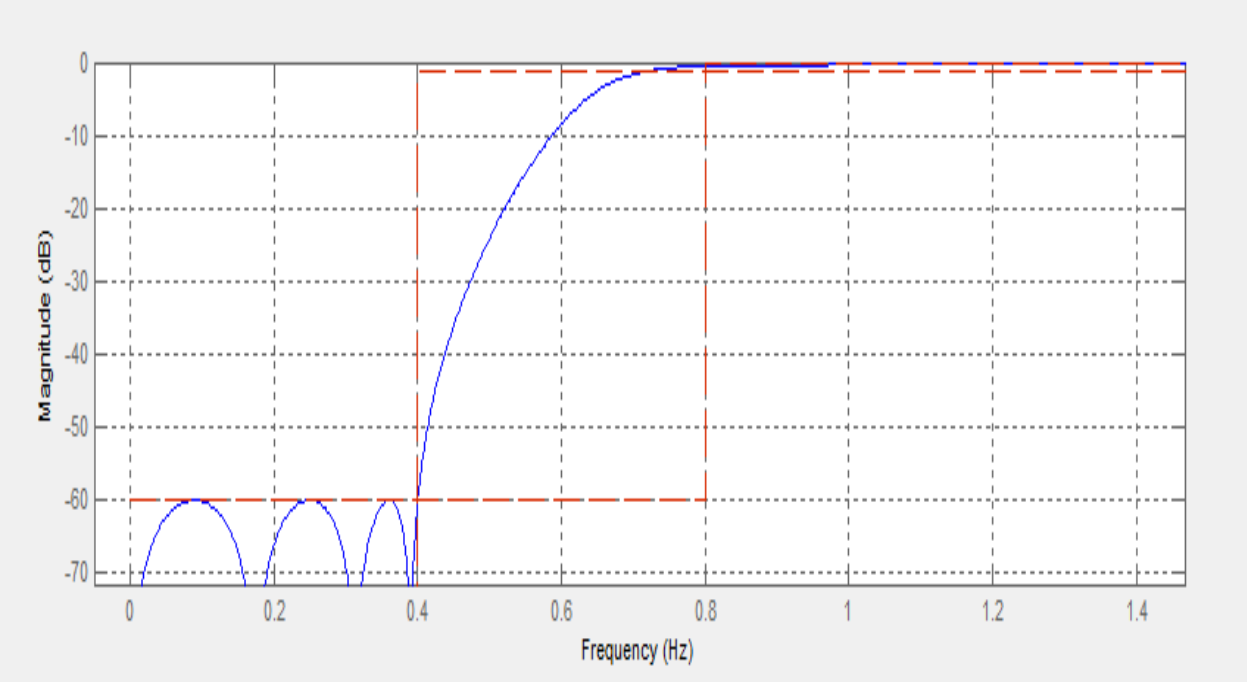

Figure 5-28: Filter

5.10.5 Filter specifications:

Table 5-16: Filter table

Response type	**High pass**
Design method	**Chebyshev type II**
Filter order	**Minimum order**
Match Exactly	**Stop band**
Frequency specification	**Fs = 50Hz, F stop = 0.4, F pass = 0.8**
Magnitude Specification (dB)	**A stop = 60, A pass = 1**
Structure	**Direct-form II second order section**
Order	**7**
Sections	**4**
Stable	**Yes**

5.11 Domains observations and feature extractions

Fundamentally, the purpose and the focus of the signal processing is to extract features from acquired and recorded signals, and automatically select the features that demonstrate a consistent trend towards tool wear. To achieve this and to increase the reliability of the tool wear monitoring system, a monitoring strategy was devised based on features extracted from the time and frequency domains, as well as features extracted from time series models and wavelet Transform analysis.

5.11.1 Time domain observation and feature extraction

Tool wear occurrence can be categorized in three stages viz new, moderate and worn. Therefore, data acquired are segmented and classified into these three categories Figures 5-30 and 5-31, represent new tool, Figures 5-32 and 5-33 represent moderately worn and Figures 5-34 to 5-37 represent worn out tool. Looking carefully at the figures we can see a trend in the amplitude of raw AE, it was observed that the higher the wear the bigger the uniform amplitude of the tool. In Figure 5-38 to 5-41, a clear worn out tool can be seen with built up edge BUE in Figure 5-39. Looking at Figure 5-5-40 and 5-41, a confirmation of both MATLAB, Design experts and Excel software modeling was also shown in the signal processing phase (Time-domain, Frequency-domain and Spectrum). This worn-out tool at 0.43mm Tool wear has a speed of 2900rpm, depth of cut of 2mm and feed of 58mm/min Therefore, it shows that when the tool is practically worn out, the sinusoidal waves of the signals during machining will eventually fade out and become uniform amplitude.

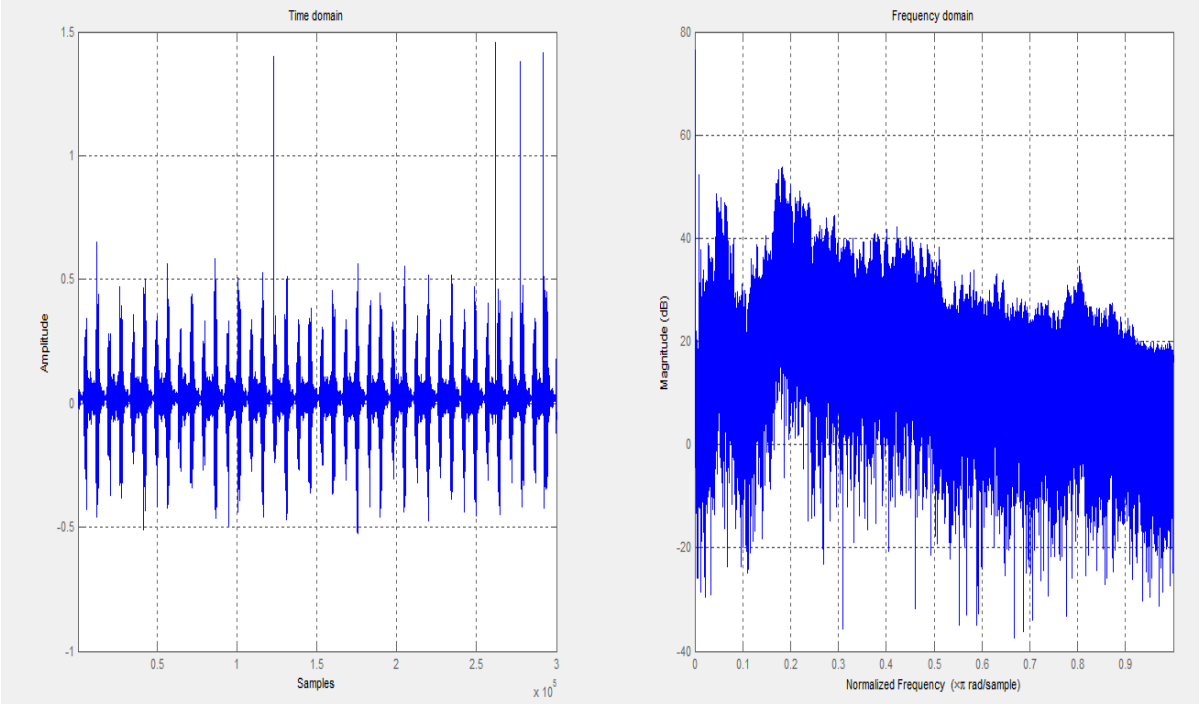

Figure 5-29: round 1 tool 16, AE signal in Time and Frequency domain at Speed=4050rpm, Feed = 243mm/min Depth= 2

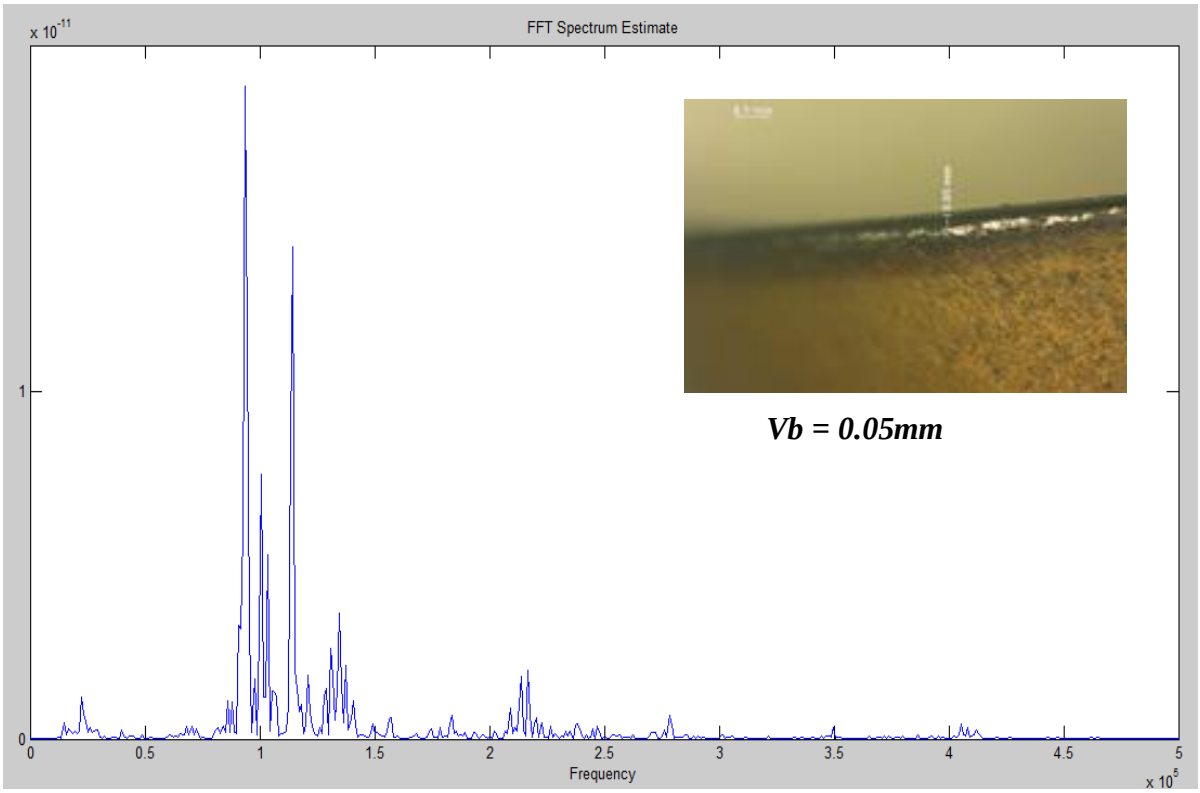

Figure 5-30: round 1 tool 16 AE burst (Spectrum)at Speed=4050rpm, Feed = 243mm/min,

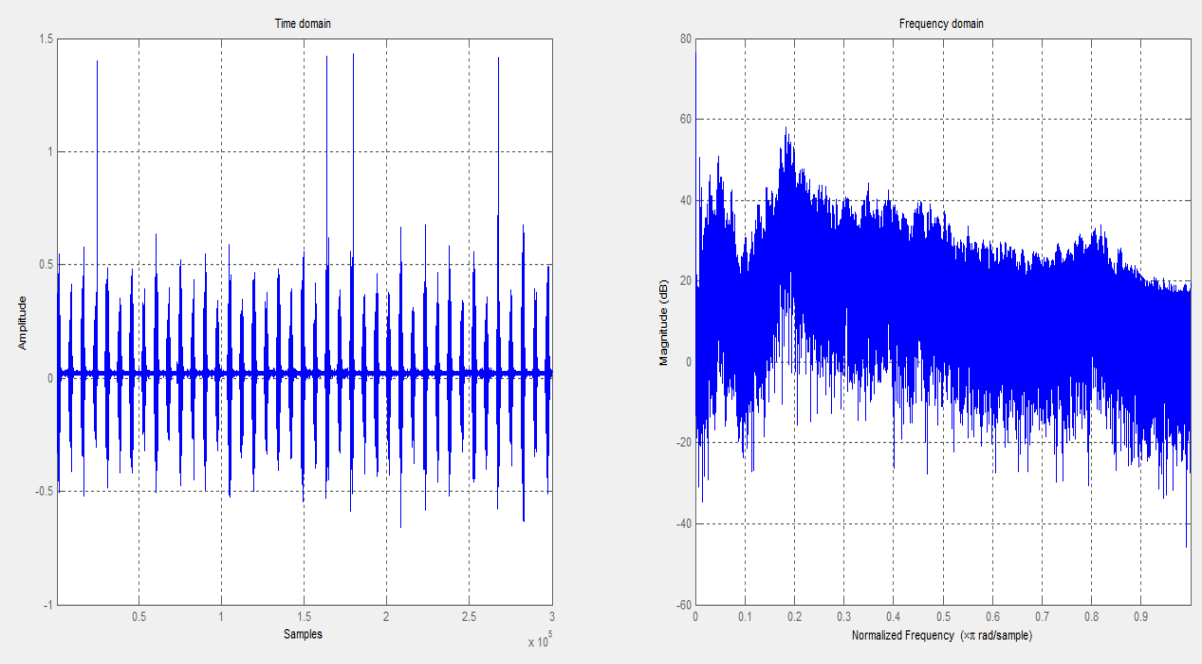

Figure 5-31: round 1 tool 17 showing AE signal in Time and Frequency domain at Speed=4050rpm, Feed = 243mm/min Depth= 2

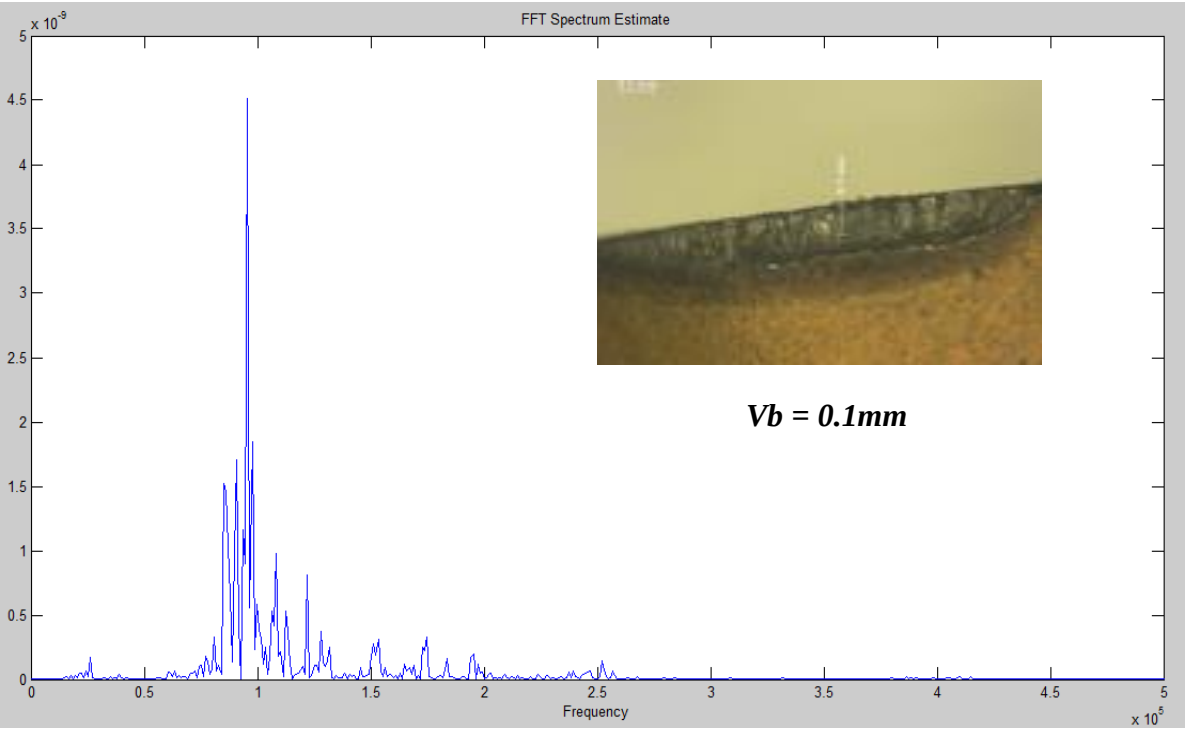

Figure 5-32: round 1 tool 17 AE burst (Spectrum)at Speed=4050rpm, Feed = 243mm/min,

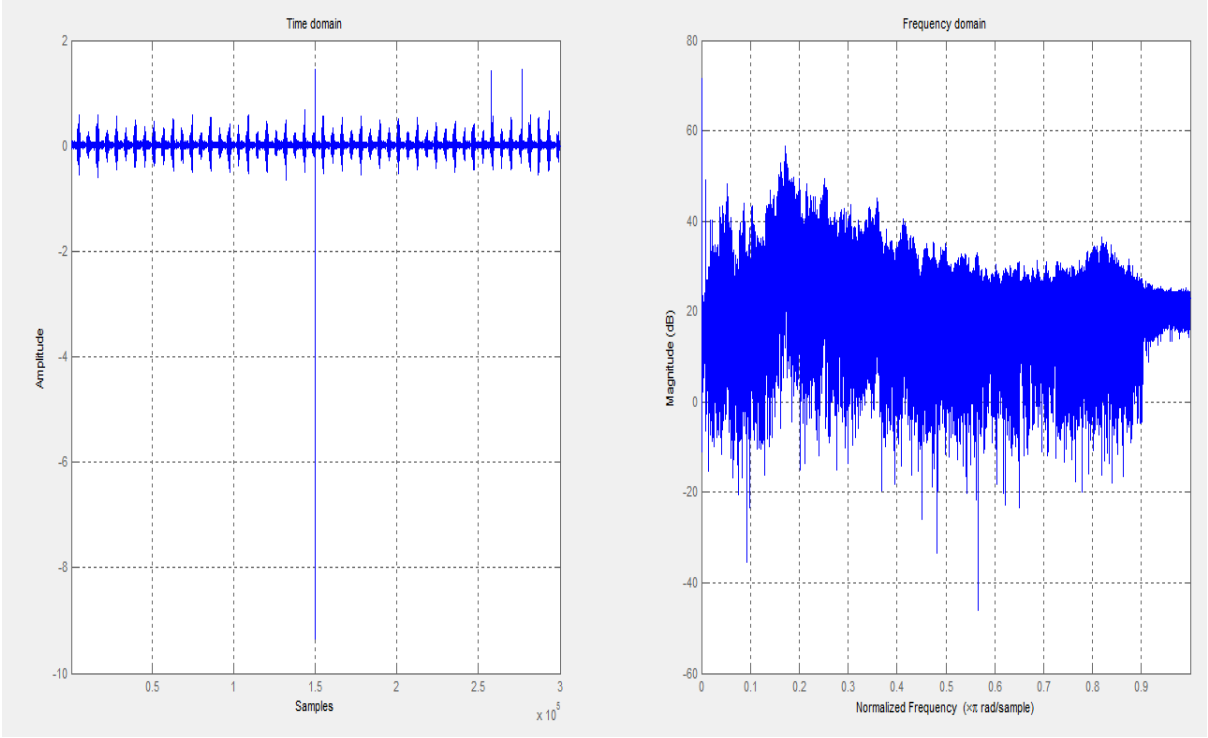

Figure 5-33: round 2 tool 5 showing AE signal in Time and Frequency domain at Speed=5200rpm, Feed = 104mm/min Depth= 2

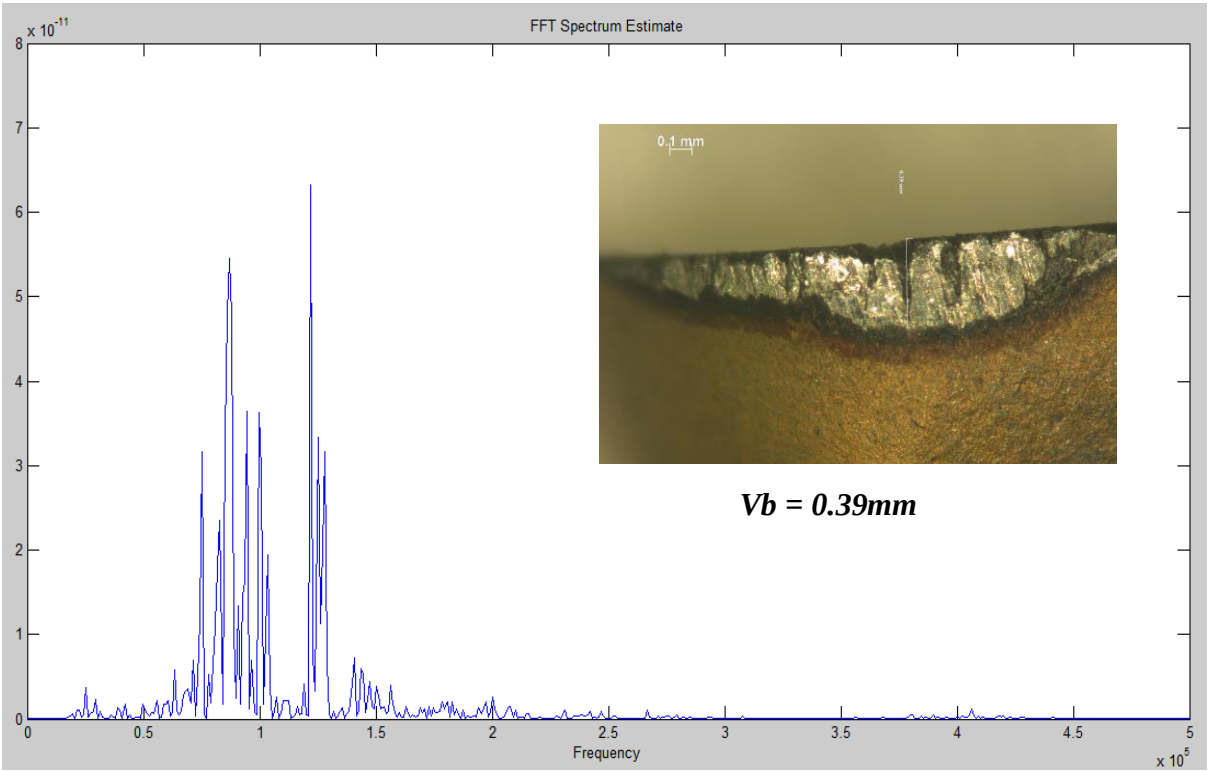

Figure 5-34: round 1 tool 1 AE burst (Spectrum)at Speed=5200rpm, Feed = 104mm/min, Depth=

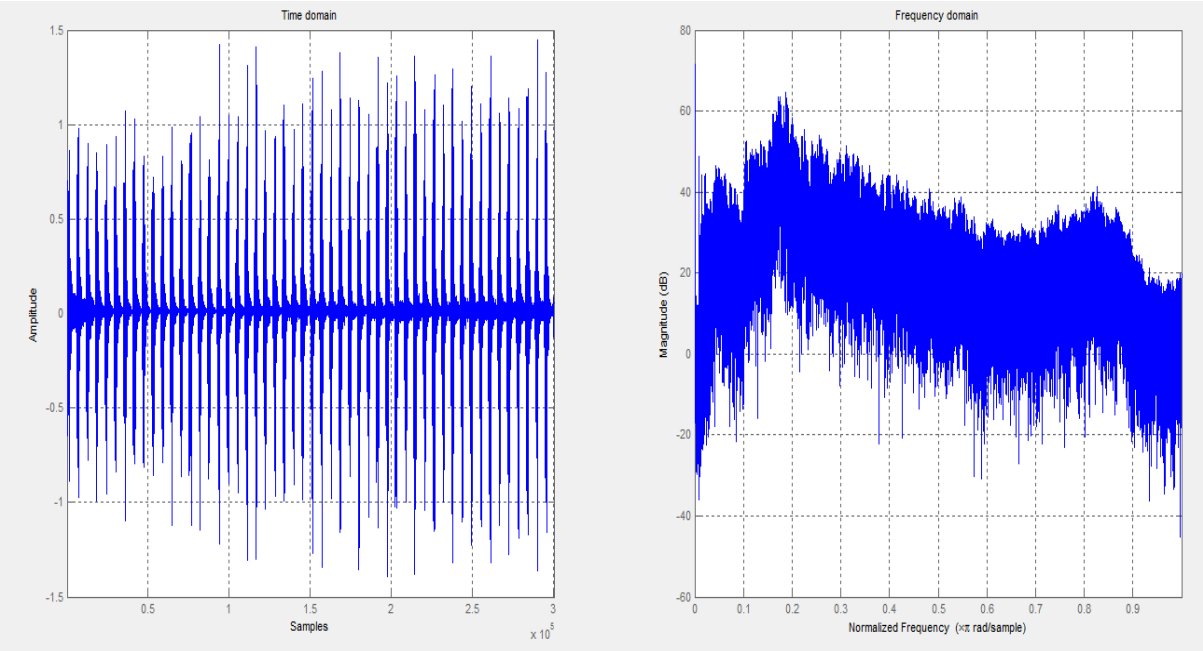

Figure 5-35: AE signal in Time and Frequency domain at Speed=5200rpm, Feed = 312mm/min Depth= 3mm

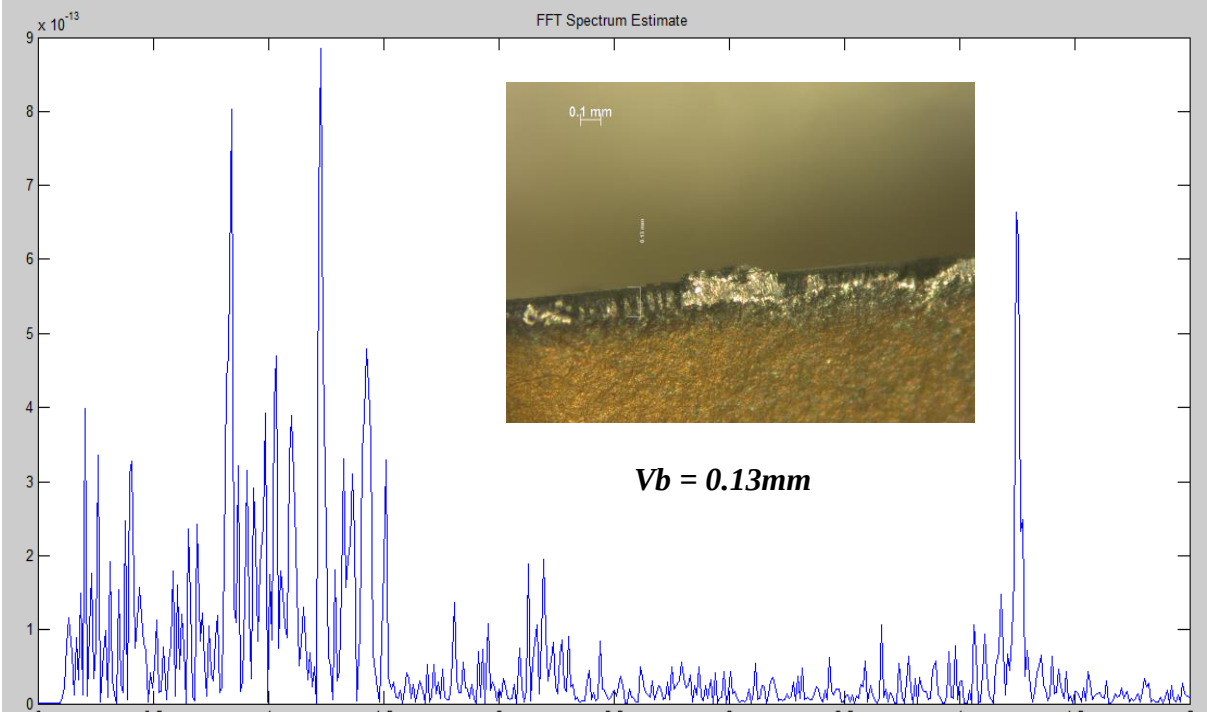

Figure 5-36: round 1 tool 16 AE burst (Spectrum)at Speed=5200rpm, Feed = 312mm/min, Depth= 3

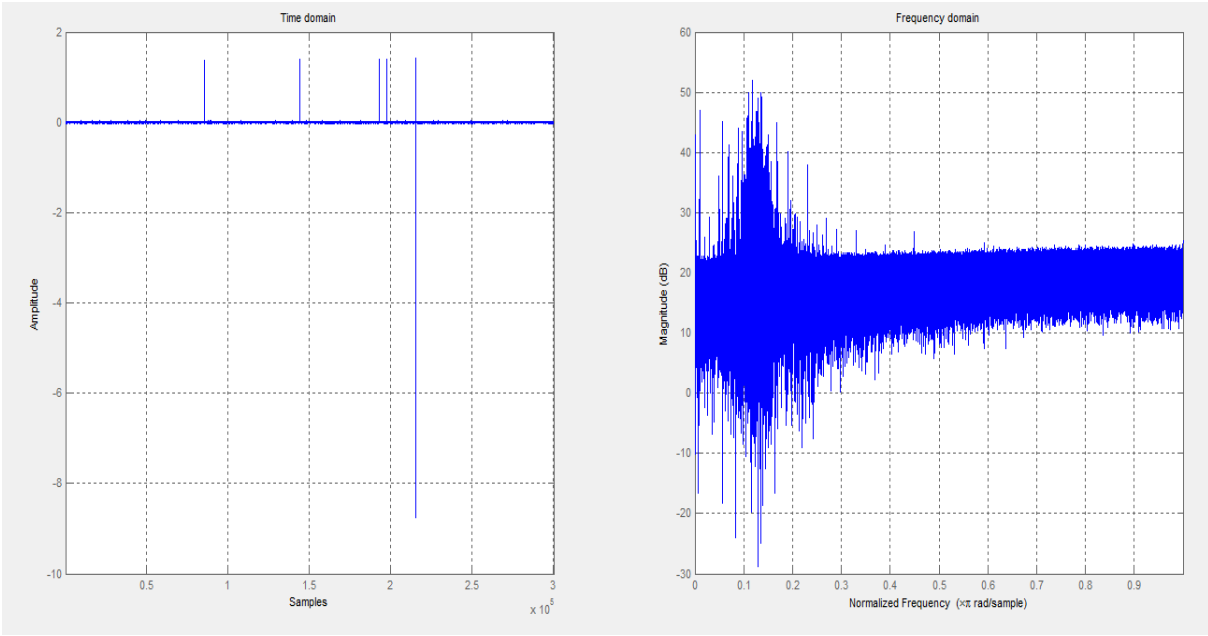

Figure 5-37: AE signal in Time and Frequency domain at Speed=4050rpm, Feed = 243mm/min Depth= 2mm

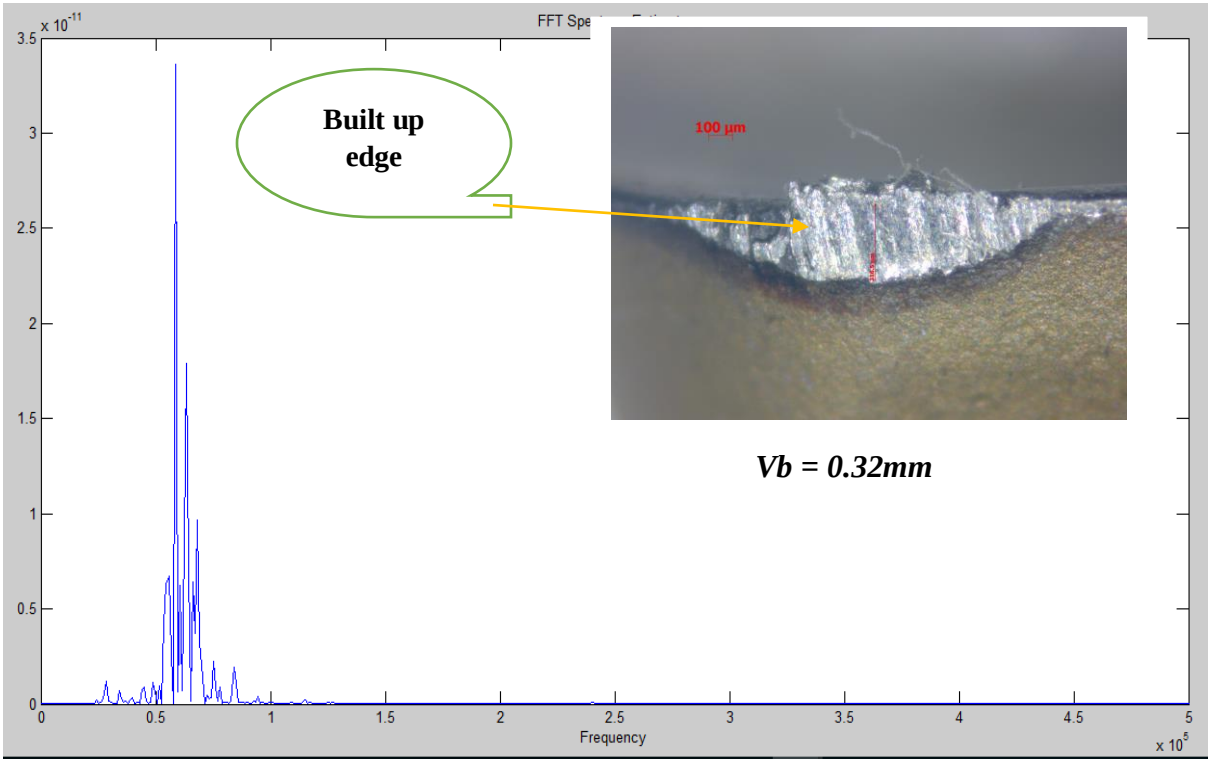

Figure 5-38: round 4 Tool 13: AE burst (Spectrum) at Speed=4050rpm, Feed = 243mm/min, Depth= 2mm

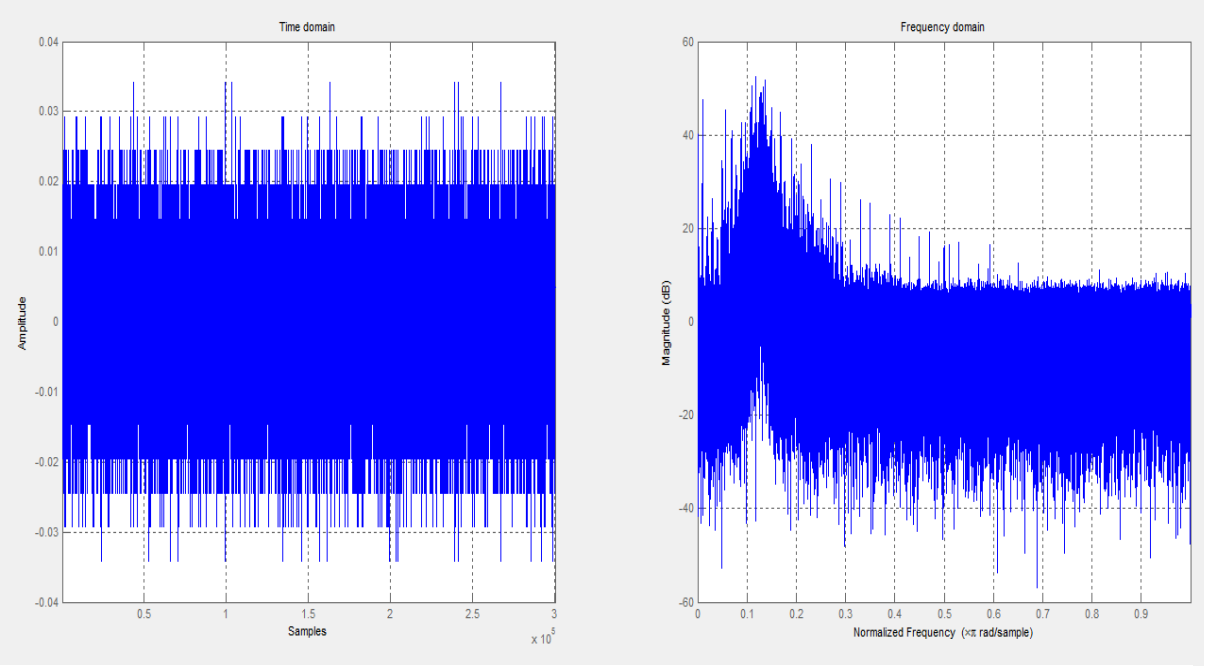

Figure 5-39: uniform AE signal in Time Domain and Frequency domain at Speed=2900rpm, Feed = 58mm/min Depth= 2mm

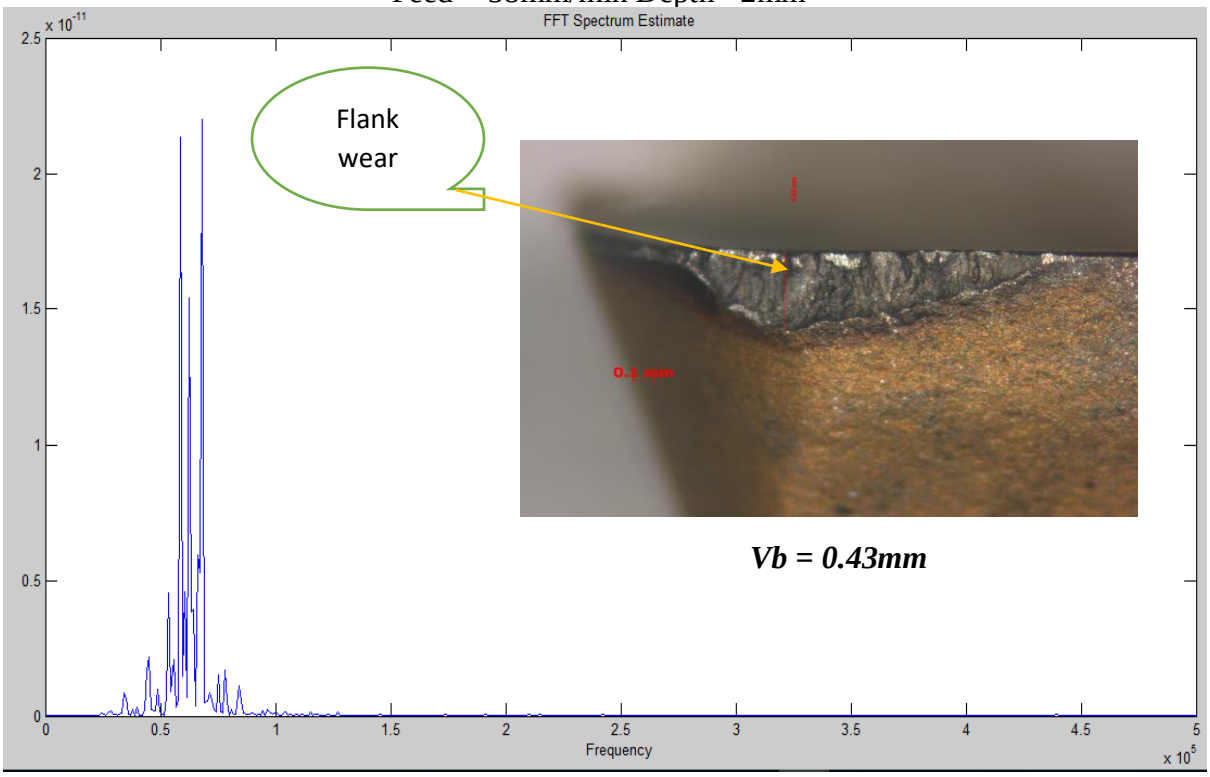

Figure 5-40: round 5 Tool 1 AE burst (Spectrum) at Speed=2900rpm, Feed = 58mm/min, Depth = 2mm

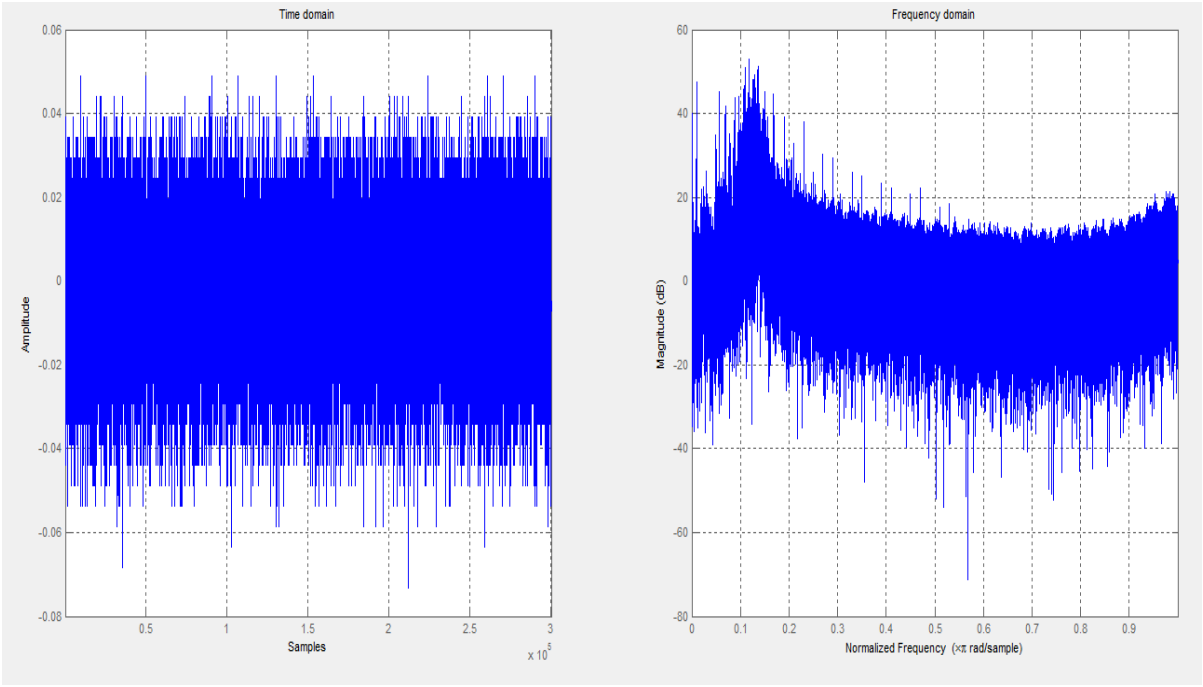

Figure 5-41: uniform AE signal in Time Domain and Frequency domain at Speed=4050rpm, Feed = 243mm/min Depth= 2mm

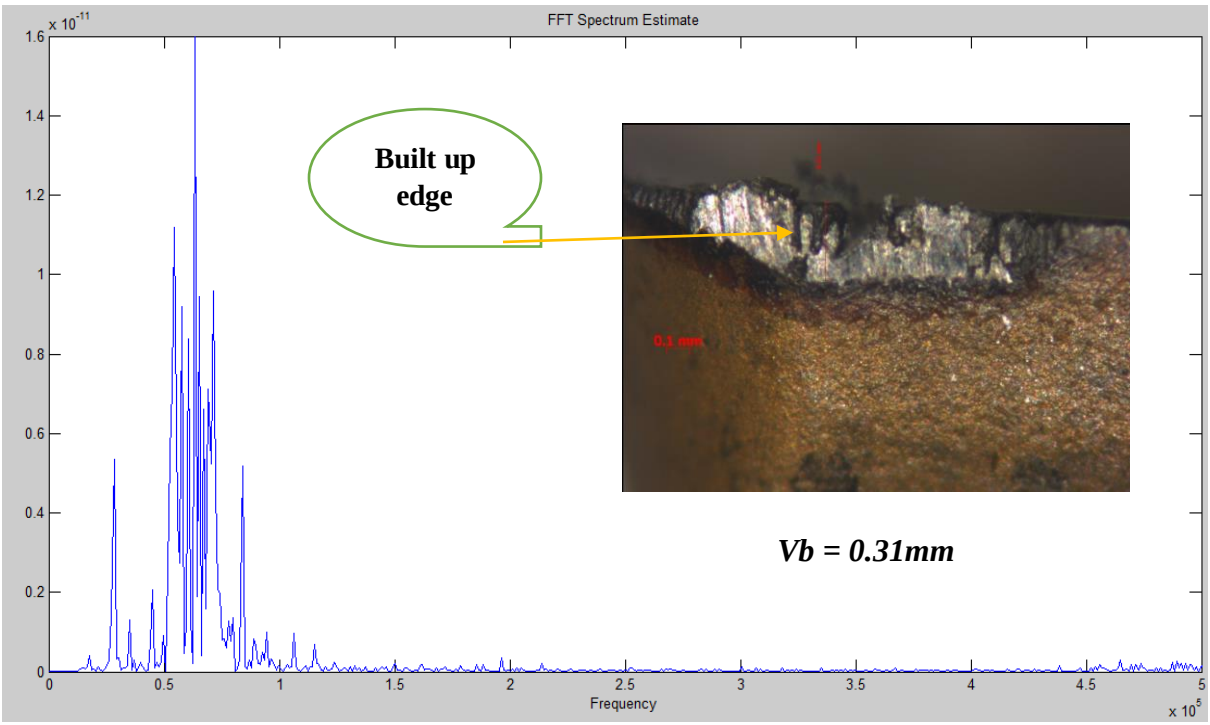

Figure 5-42: round 5 Tool 16: AE burst (Spectrum) at Speed=4050rpm, Feed = 405mm/min, Depth = 1mm

5.11.2 Frequency domain observations and features extraction.

The most common frequency domain characteristics found in the literature is the spectral energy around the first natural frequency of the tool-workpiece system. It was established that the first natural frequency for this system lies at about 5 kHz Figure 5-44. The spectral energy in the 5-kHz region was taken as a feature. However, some authors also found that useful information about the process can be found in the 'low' frequency domain. Investigations proved that the spectral energy between 100 - 1000 Hz also displays a significant trend towards tool wear. Therefore, this was also taken as a feature see Figure 5-45 to 5-46.

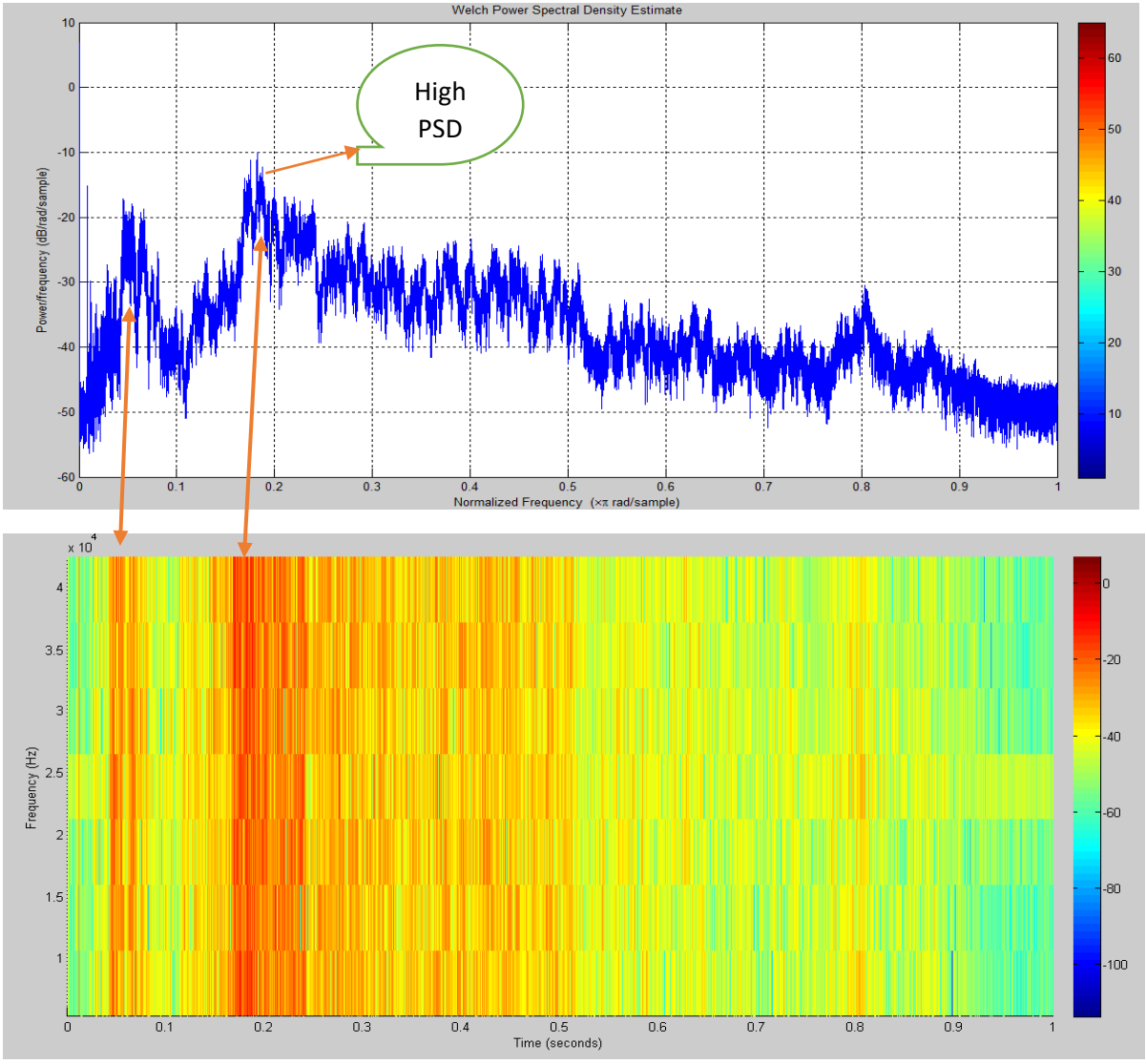

Figure 5-43: Experiment round 1 tool 16, AE welch PSD and its corresponding Spectrogram at Speed=4050rpm, Feed = 243mm/min Depth= 2

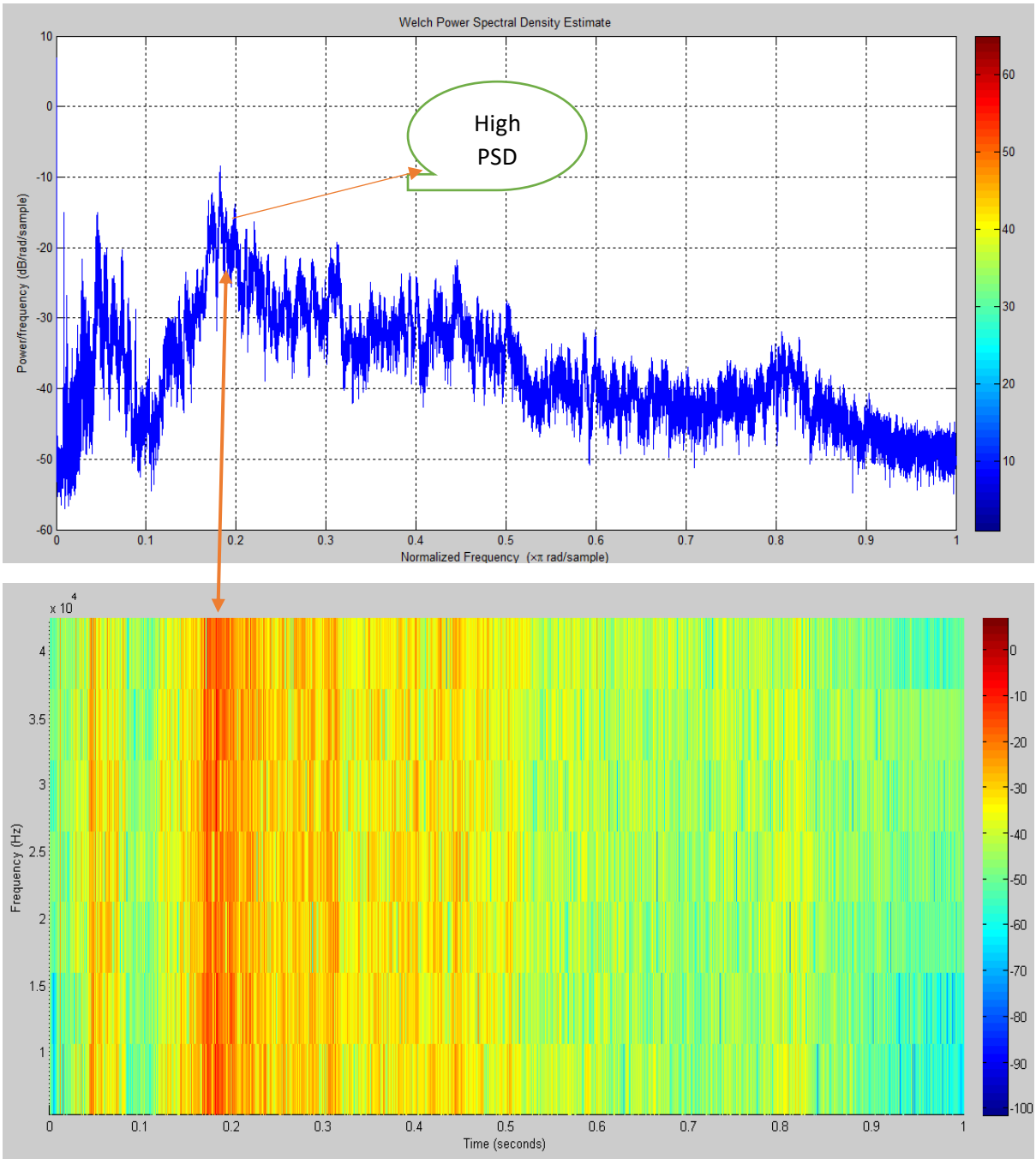

Figure 5-44: Experiment round 1 tool 17, AE welch PSD and its corresponding Spectrogram at Speed=4050rpm, Feed = 243mm/min Depth= 2

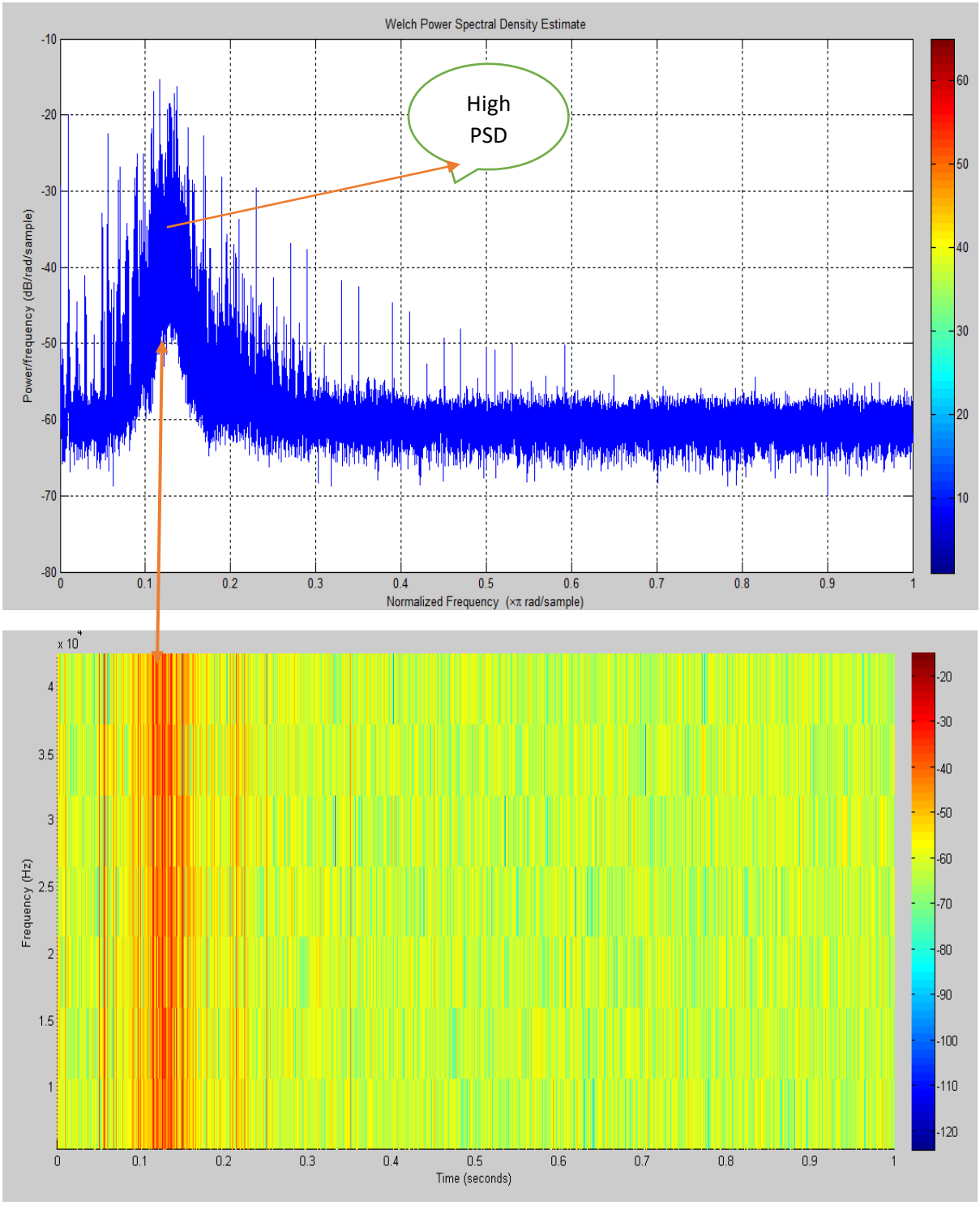

Figure 5-45: Experiment round 5 tool 1, AE welch PSD and its corresponding Spectrogram at Speed=290rpm, Feed = 58mm/min Depth= 2

In the course of this study, the following features were considered in the frequency domain. Frequency mean: which is the pitch measurement that accesses the center of power distribution across the frequencies. Spectral peaks: this signifies the maximum energy in the frequency spectrum. Frequency deviation: is the deviation of the frequency components from the mean frequency. Overall, the frequency components of the acoustic signal showed a better variation with the flank wear values compared to the amplitude levels of the raw AE signals. Otherwise, raw AE amplitudes may not be the best observation for monitoring the tool wear when machining stainless steel.

5.12 Wavelet domain, observations and feature extractions

Wavelet transform can be explained as a spectral estimation technique in which any general function can be expressed as an infinite series of wavelets. The basic knowledge underlying wavelet analysis comprises of expressing a signal as a linear combination of a particular set of functions (wavelet transform,), that is obtained by shifting and dilating one single function called a mother wavelet. The decomposition of the signal leads to a set of coefficients called wavelet coefficients.

Therefore, the signal can be reconstructed as a linear combination of the wavelet functions weighted by the wavelet coefficients. In order to obtain an exact reconstruction of the signal, adequate number of coefficients must be calculated. The key feature of wavelets is the time-frequency localization. This means that most of the energy of the wavelet is restricted to a finite time interval. Frequency localization means that the Fourier transform is band limited. When compared to STFT, the advantage of time-frequency localization is that wavelet analysis varies the time-frequency aspect ratio, producing good frequency localization at low frequencies (long time windows), and good time localization at high frequencies (short time windows). This produces a segmentation, or tiling of the time-frequency plane that is appropriate for most physical signals, especially those of a transient nature. The wavelet technique applied to the Tool wear monitoring signal will reveal features related to the transient nature of the signal which are not obvious by the Fourier transform.

It should be well noted that the selection of suitable wavelet and the number of decomposition levels is very important in analysis of signals using the DWT. The number of decomposition levels is chosen based on the dominant frequency components of the signal. The levels are chosen such

that those parts of the signal that correlate well with the frequencies necessary for classification of the signal are retained in the wavelet coefficients Figure 5-47. In the present study, since the AE signals do not have any useful frequency components above 60 Hz, the number of decomposition levels was chosen to be 7.

Thus, the AE signals were decomposed into details D1–D7 and one final approximation, A7. According to literatures, the lower order Daubechies wavelets are not differentiable every-where and it also consists of a sharp edge geometrical appearance, but the higher order Daubechies wavelets are relatively smooth in form. Normally, tests are performed with different types of wavelets and the one which gives maximum efficiency is selected for the application. The smoothing feature of the Daubechies wavelet of order 3 (db3) made it more appropriate to detect changes of AE signals. Hence, the wavelet coefficients were computed using the db3 in the present study Figure 5-47.

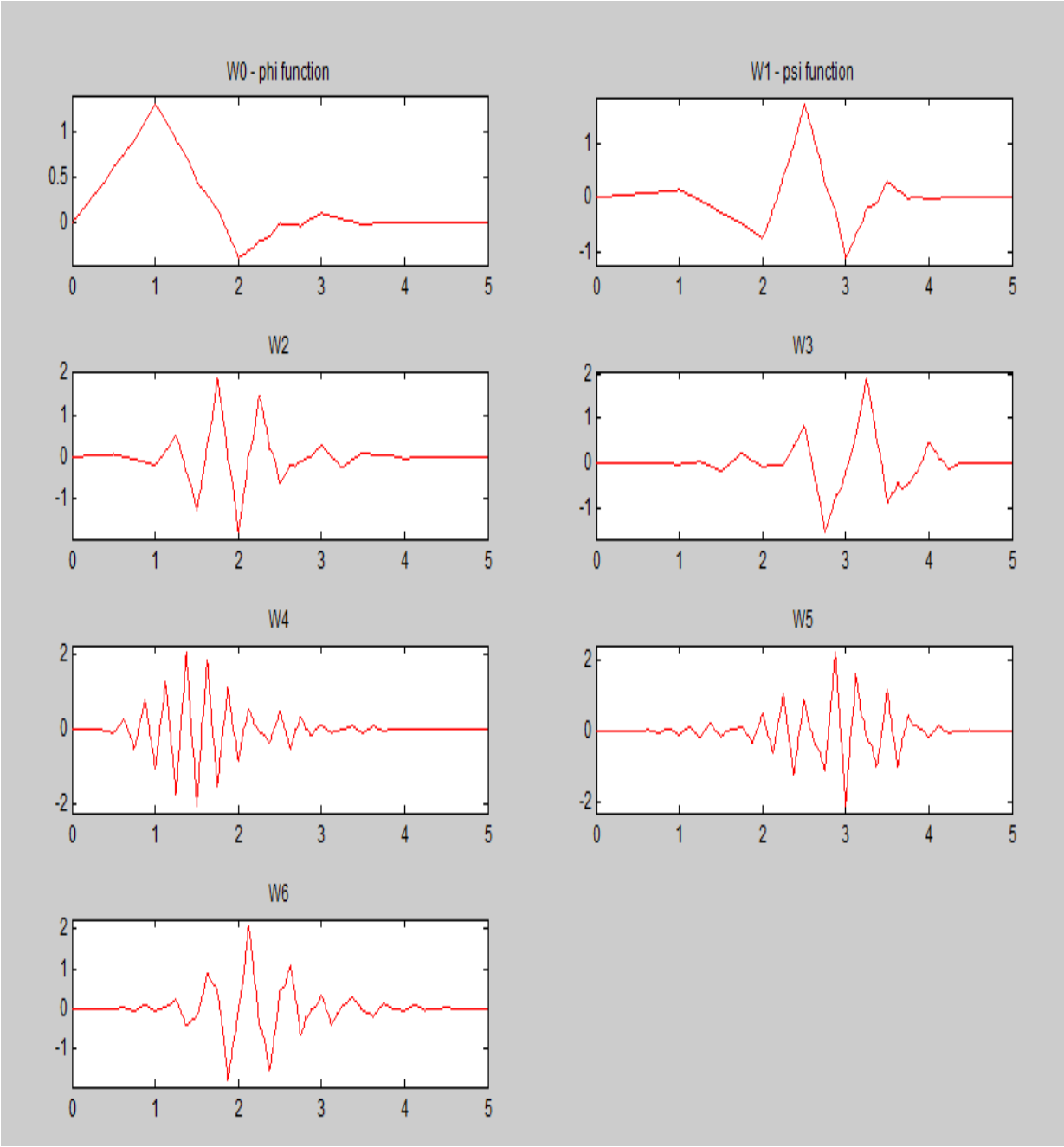

Figure 5-46: Daubechies wavelet waveform of the third order (db3) at Level 7.

5.13 Feature selections

Furthermore, the selection of appropriate wavelet and the number of decomposition levels are very important for the analysis of signals using DWT because one of the objects of wavelet analysis is to decompose signals into several frequency bands. The number of decomposition levels is chosen based on the dominant frequency components of the signal. The levels are chosen such that those parts of the signal that correlate well with the frequencies necessary for classification of the signal are retained in the wavelet coefficients. In this work, Daubechies 3 (db3) is selected because its smoothing feature was suitable for detecting changes of the AE signals. Daubechies wavelets are the most popular wavelets representing foundations of wavelet signal processing, and are used in numerous applications. [144, 145, 146].

The frequency band of each detail scale of the DWT is directly related to the sampling rate of the:

$$\left[\frac{f_m}{2}; f_m\right] \quad \textbf{(5-4)}$$

original signal, which is given by:

$$f_m = \left[\frac{f_s}{2^{l+1}}\right] \quad \textbf{(5-5)}$$

where fs is the sampling frequency, and l is the level of decomposition. In this study, the sampling frequency is 1Million (Hz) of the AE signal. The highest frequency that the signal could contain, from Nyquist' theorem, would be fs/2. Frequency bands corresponding to Seven decomposition levels for wavelet db3 with sampling frequency of 1Million (Hz) of AE signals were listed in Table 5-20. The signals were decomposed into details D1-D7 and one final approximation A7.

Table 5-20: Signal Decomposition level

Decomposition Signal	Frequency band (KHz)
D1	250 – 500
D2	125 – 250
D3	62.5 – 125
D4	31.25 – 62.5
D5	15.63 – 31.25
D6	7.813 – 15.63
D7	3.906 – 7.813
A7	0 – 3.906

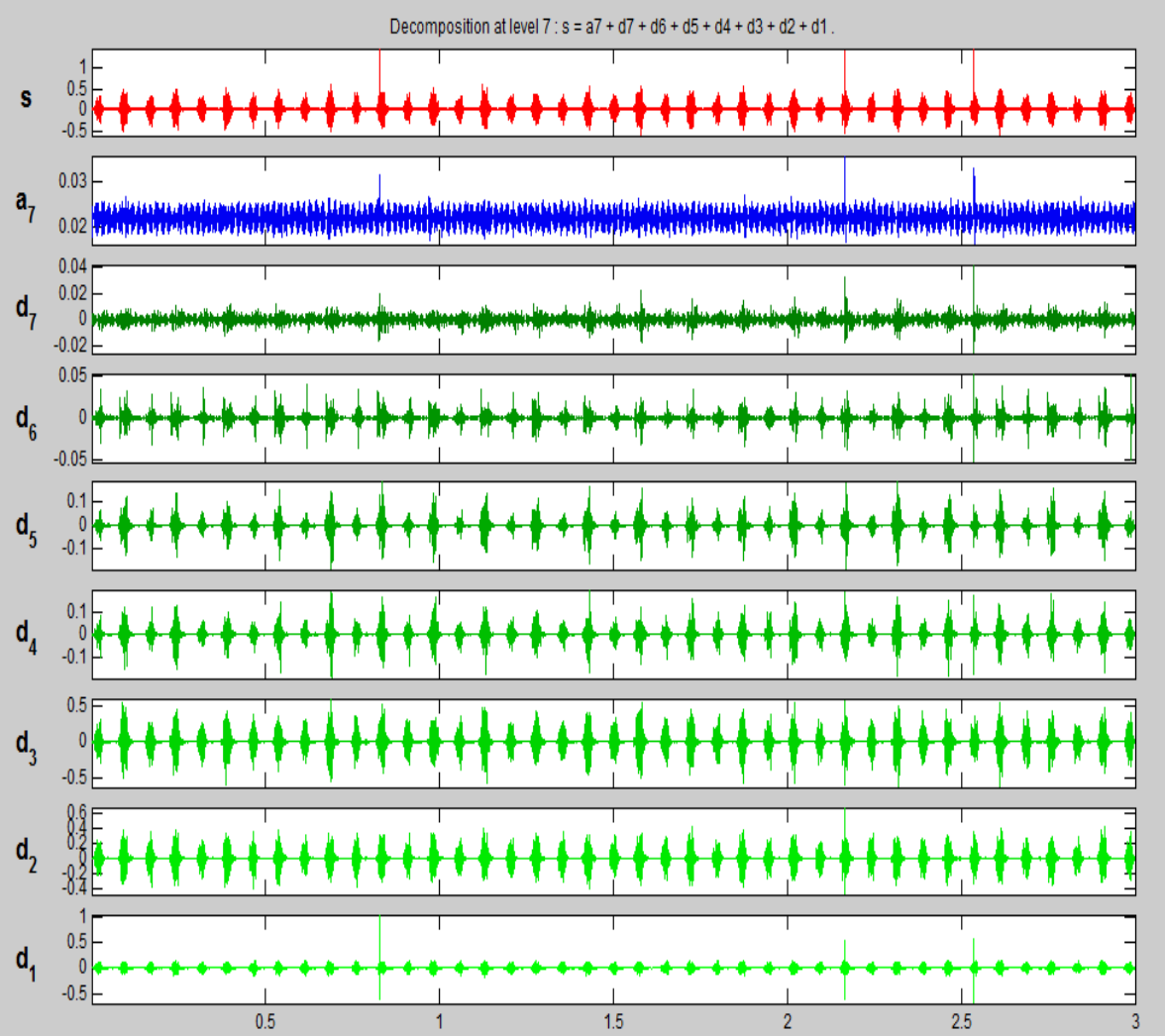

Figure 5-47: The decomposition Level of AE Signal using Wavelet analysis

A critical look at the Figure 5-48 above shows that the sub-band D2, D1, D3, D4 and D5 had the highest amplitude. This indicates that the majority of the AE spectral contents for the wavelets are centered within the frequency range of 125 kHz-250 kHz, 250kHz–500kHz, 62.5 kHz-125 kHz, 31.25kHz – 62.5kHz and 15.63kHz- 31.25kHz respectively (Table 5.20). Also, substantial correlations were also noticed with variations in sub-bands D2, D1, D3, D4, D5 and the Tool wear. Therefore, the following domain features were extracted from the wavelet decomposition Table 5-21 and Table 5-22.

Table 5-21: Time domain

Time domain	
Features	
Root mean square	**RMS**
Range	**range**
Standard Deviation of frequency	**St Dev**
Mean	**Mean**
Variance	**variance**
Maximum	**max**
Minimum	**min**
Kurtosis	**Kurtosis**
Skewness	**Skewness**
Peak -To - Peak	**P-T-P**

Table 5-22: Time -Frequency domain

Time - frequency domain	
Features	
Frequency distribution in sub-band 1	**d1**
Frequency distribution in sub-band 2.	**d2**
Frequency distribution in sub-band 3.	**d3**
Frequency distribution in sub-band 4.	**d4**
Frequency distribution in sub-band 5.	**d5**
Standard deviation in sub-band 1.	**St Dev D1**
Standard deviation in sub-band 2	**St Dev D2**
Standard deviation in sub-band 3	**St Dev D3**
Standard deviation in sub-band 4	**St Dev D4**
Standard deviation in sub-band 5.	**St Dev D5**
Absolute distribution in sub-band 1.	**Abs D1**
Absolute distribution in sub-band 2	**Abs D2**
Absolute distribution in sub-band 3	**Abs D3**
Absolute distribution in sub-band 4.	**Abs D4**
Absolute distribution in sub-band 5	**Abs D5**
Total Energy density of wavelet	**Energy**

5.14 Feature selection and evaluation

Altogether a total of 29 features were extracted and used. These are divided as follows (Table 5-23):

Table 5-23: Feature domain division

Feature domain	Numbers of features
Machine parameters	**3**
Time domain	**10**
Time-frequency domain (Wavelet)	**16**
Total	**29**

These 29 features were selected thus: first, the 3 machine parameters and the remaining 26 features were extracted from 16 different experimental runs which are classified as new tool, early wear, moderate wear and worn out tool Figure 5-23. In each category, the author used four experimental runs. Therefore, the total features data used in this research work is 464 data (29 times 16 matrix). The author has attached the normalized feature data at the appendix.

According to most recent and similar studies, authors have correlated the trend in the features with the measured tool wear in order to select the best features. In this case, it was not possible to disturb the production process for wear measurement. Although this is not a true representation of the tool wear, but it can give an indication of which features show consistent trend in time, and whether the trend is towards higher or lower values of the feature. Therefore, the quantity r, called the linear correlation coefficient (also known as Pearson product moment correlation coefficient in honor of its developer Karl Pearson), measures the strength and the direction of a linear relationship between two variables in our case its features and tool wear.

Mathematically computed as:

$$r = \frac{n\sum xy - (\sum x)(\sum y)}{\sqrt{n(\sum x^2) - (\sum x)^2}\sqrt{n(\sum y^2) - (\sum y)^2}} \qquad \textbf{(5-6)}$$

Where x and y are the variables (features and tool wear). Further exposition, for positive correlation, if x and y have a strong positive linear correlation, i.e. r is close to +1. An r value of exactly +1 indicates a perfect positive fit. This means that Positive values indicate a relationship between x and y variables such that as values for x increases, values for y also increase. On the other hand, for negative correlation, if x and y have a strong negative linear correlation, such that r is close to -1. An r value of exactly -1 indicates a perfect negative fit. Negative values indicate a relationship between x and y such that as values for x increase, values for y decrease. However, for no correlation, a situation where there is no linear correlation or a weak linear correlation, r is close to 0. A value near zero means that there is a random, nonlinear relationship between the two variable. Below in the table shows the correlation coefficients of the features extracted and the tool wear.

Table 5-24: feature correlation

No	features	corrcoeff	No Cont'd	features Cont'd	Corrcoeff Cont'd
1	feed	-0.37	16	d3	0.04
2	speed	0.12	17	d4	0.04
3	depth of cut	0.37	18	d5	0.56
4	RMS	-0.40	19	St Dev D1	-0.19
5	range	0.75	20	St Dev D2	-0.41
6	St Dev	-0.39	21	St Dev D3	-0.39
7	Mean	-0.29	22	St Dev D4	-0.31
8	variance	-0.25	23	St Dev D5	-0.58
9	max	0.58	24	Abs D1	-0.40
10	min	-0.50	25	Abs D2	-0.38
11	Kurtosis	0.43	26	Abs D3	-0.34
12	Skewness	-0.02	27	Abs D4	-0.22
13	P-T-P	0.29	28	Abs D5	-0.54
14	d1	0.78	29	Energy	0.45
15	d2	0.27			

5.15 Neural Networks

5.15.1 Artificial Neural network procedure, architecture and results

A comprehensive literature has been discussed in review part on ANN, therefore the process will be briefly explained here. A total of 29 feature sets were selected for building the neural network, based on correlation coefficients in the table above and literature, including the machining parameters, mean, root mean square and standard deviation, frequency content and deviations in sub-band D1, D2, D3, D4, D5 and the total energy of wavelets.

5.15.2 Normalization of data set

The selected feature dataset was transformed and normalized to values ranging between 0 and 1 using equation below where 0 and 1 value correspond to the lowest and highest feature value in the subset respectively (Table 5.24). The normalization was done to achieve standardization of the feature values and reduce redundancy before feeding them into the network for training.

$$\mathbf{t_n} = \frac{(\mathbf{f_o} - \mathbf{f_{min}})}{(\mathbf{f_{max}} - \mathbf{f_{min}})} \quad \textbf{(5-7)}$$

Where:

$\mathbf{t_n}$- Normalized value of $\mathbf{f_o}$, $\mathbf{f_o}$ - observed value (i.e. feature), $\mathbf{f_{max}}$ – maximum observed value in the subset and $\mathbf{f_{min}}$ – minimum observed value in the subset. See the appendix for normalized data.

5.15.3 Classification of Features

ANN is a powerful data-modelling tool that is able to capture and represent complex input-output relationships to classify wear output. It involves the usability of artificial intelligence as an adequate tool in machine tool monitoring. Data set with the selected key features were used to run a neural network. A feed forward and back propagation multilayer ANN was used for solving the problem, and the network training and testing were carried out using the MATLAB software package. In this research work, the author used hyperbolic tangent sigmoid transfer function (tansig) in the hidden layers and linear transfer function (purelin) in the output layer as the activation function were preferred, the resilient back propagation function (trainrp) was used as the training algorithm, and the gradient descent with momentum back propagation algorithm (traingdm) was used as the learning rule.

The data in the training and testing sets must be normalized as earlier carried out due to the use of the hyperbolic tangent sigmoid function in the model also in order to equalize the importance of variables. In Table 5-25, a learning rate of 0.3 on a gradient descent training function with a momentum of 0.7 was used. An adaptive learning rate method aided in quick generalization of the error and reduced training time. The weights of the network were selected at random from a range of -1 to 1. No optimization algorithms were implemented on the BPNN due to its reverse operation

mode which provides an adequate optimization structure for the system. The training was run for a thousand epochs with no validation queries.

Table 5-25: Network model and architecture

Parameters of multilayer neural network	Values
Epochs	1,000
Performance function	Mean square error
Number of layers	3
Transfer Function at layer 1	Log-sigmoid
Transfer Function at layer 2	Log-sigmoid
Transfer Function at layer 3	Log-sigmoid
Layer 1 size	29
Layer 2 size	58
Layer 3 size	3
Learning rate	0.3
Momentum	0.7
Bias	B [1]
Weights	Random from [-1 1]
Training Function	Gradient Descent with adaptive learning rate and momentum
Training method	Batch process

A three-layer feed forward BPNN with one hidden layer was adopted to train the network for the classification process. The network architecture Figure 5-49, comprises 29 input neurons which are: Feed, Speed, Depth of cut, RMS, Range, Standard deviation of frequency, Mean, Variance, Maximum, Minimum, Kurtosis, Skewness, Peak to Peak, Frequency distribution band (1-5), Standard deviation sub band (1-5), Absolute deviation sub band (1-5), 58 hidden layer neurons and three outputs as new, moderate wear and worn out. During the analysis of the neural network, Matlab was used to feed 29 inputs and automatically 58 neurons was generated. However, the

choice of different hidden layers from 1-3 that was used in this work was to see any effect the number of hidden layers could have on the training of data. Therefore, it is by choice to use any number of hidden layers. In fact, some literatures said that the more hidden layers we may have during training may impact our output results.

The Neural network was trained to identify each sample line from the input data and generate a binary number as output that corresponds to a target coded wear value. Table 5-26 shows the coded binary representation of wear values corresponding to target output for the neural network developed.

The training results presented in this work indicates that the neural network architecture composed of multiple hidden layers of 3 with 58 neurons can identify both perfect as well as noisy characters effectively with minimum error in last epoch as seen in Figure 5-52 and Figure 5-53. Increasing the number of neurons further only seems to increase the complexity of the network as well as the training time for the network, and is found to be unsuitable exhibited by visual findings. As per choice of hidden layers, single layer means a single non-linear function of linear combinations of inputs. Two layers means a non-linear function of a linear combination of non-linear functions of linear combinations of inputs. The second one is much richer than the first one. The same sequence goes to three hidden layers. Hence the difference in performance. Basically, more layers mean, more non-linearity applied to data and it also means more distangling of the data before the final classifier (last layer) decides what the given instance is.

Table 5-26: Coded representation of tool wear values

Wear ranges	**0.01<x<0.1**	**0.1<x<0.2**	**0.2<x<0.43**
Binary representation	**0 0 1**	**0 1 0**	**1 0 0**

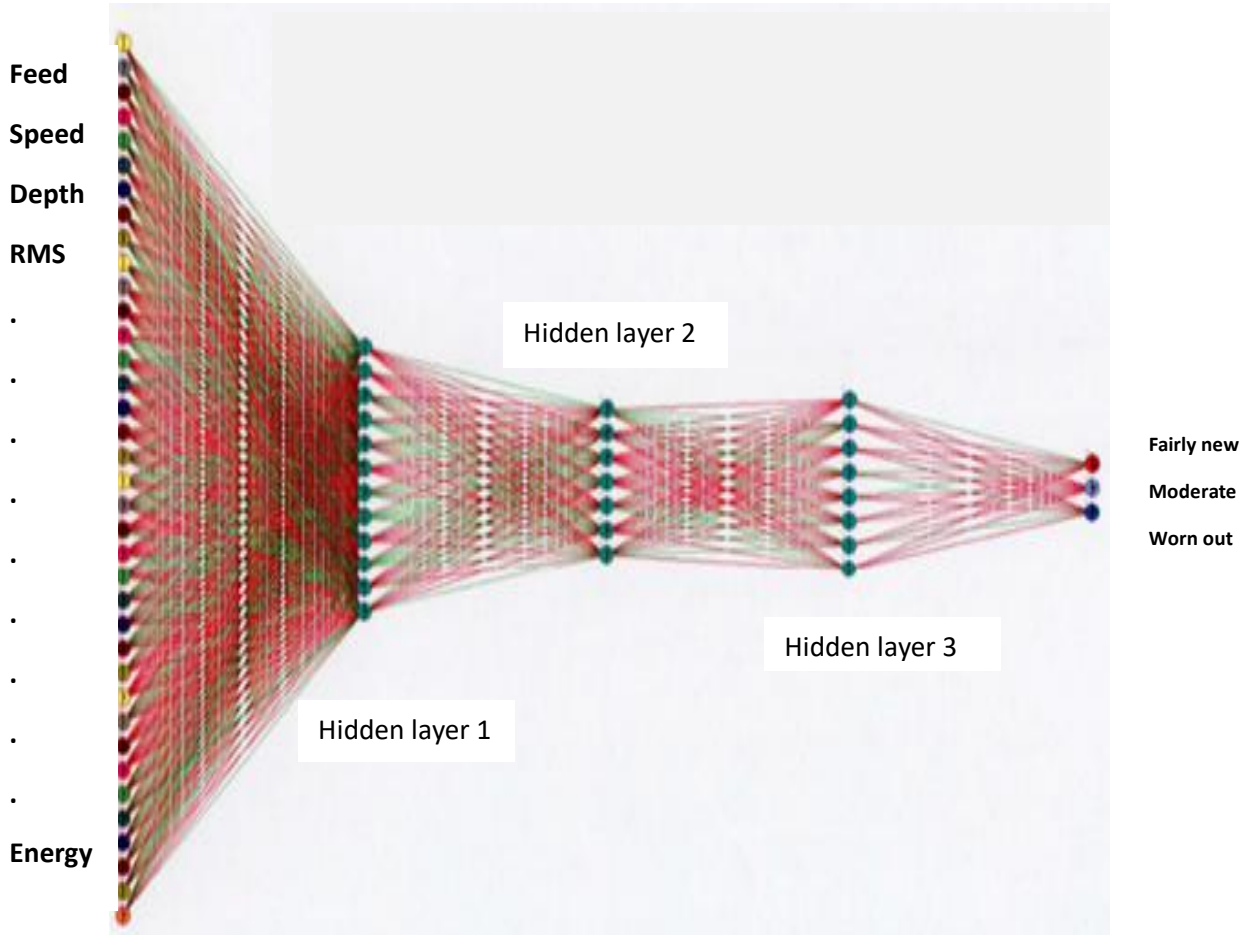

Figure 5-48: Typical Neural networks for the analysis ranging from 1-3 hidden layers 1-output with 3-neurons.

During training process, observations and evaluations were made on the regression plot Figure 5-50 and confusion plot Figure 5 -51.

5.15.4 Process evaluation and observations:

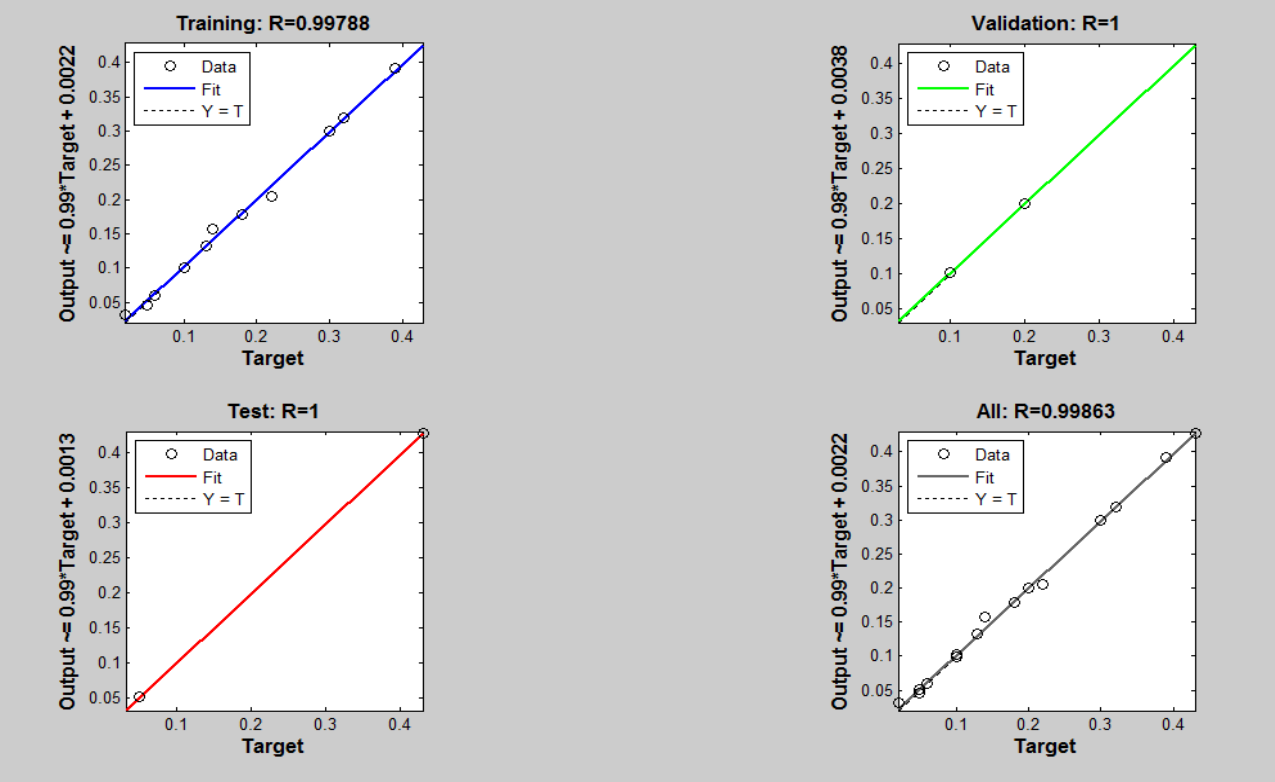

Figure 5-49: Regression Plot

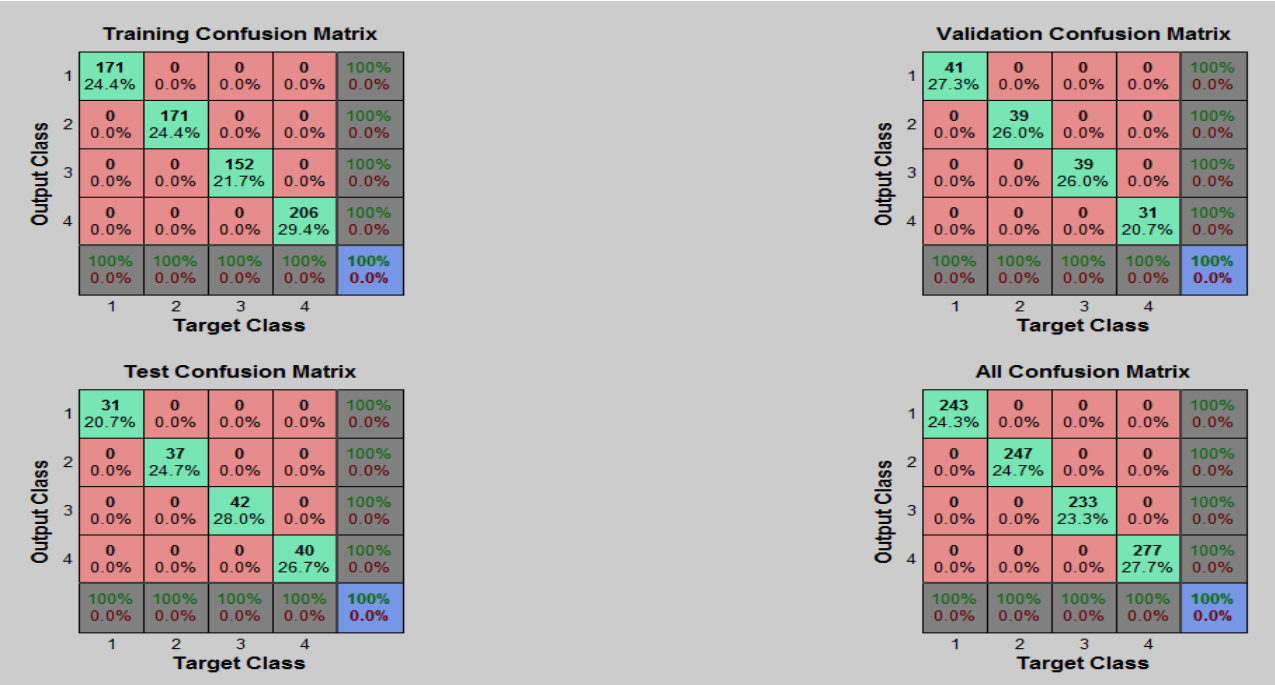

Figure 5-50: confusion Plots

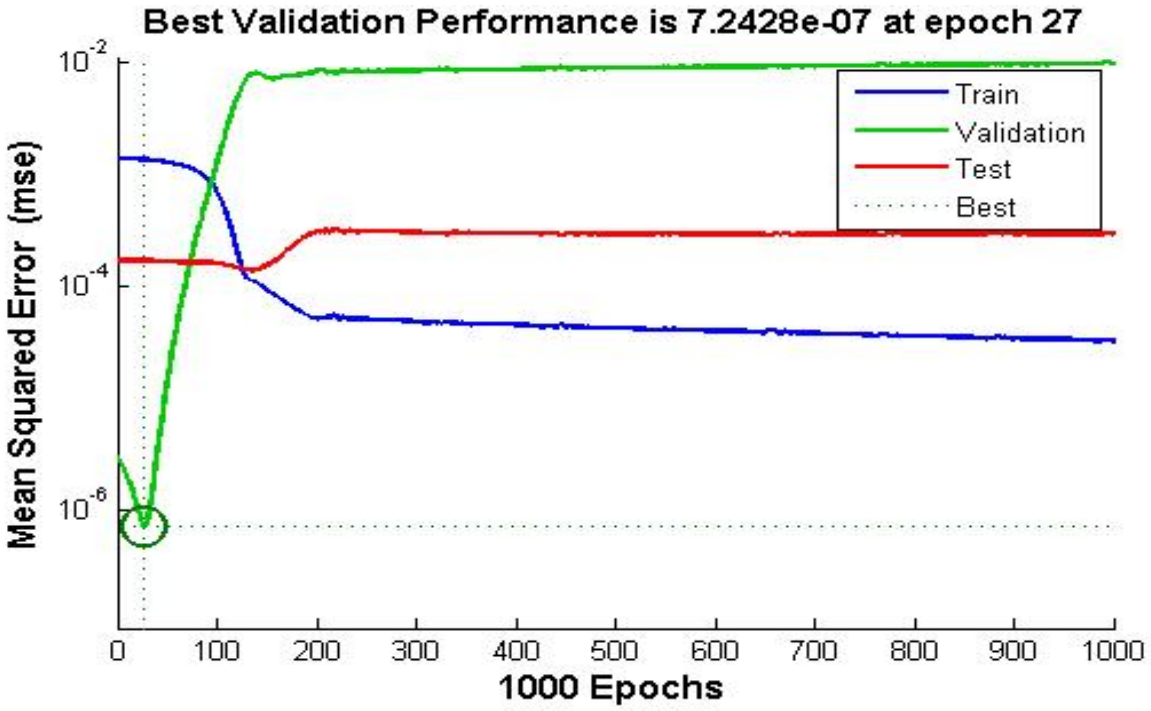

Figure 5-51: Performance Plot

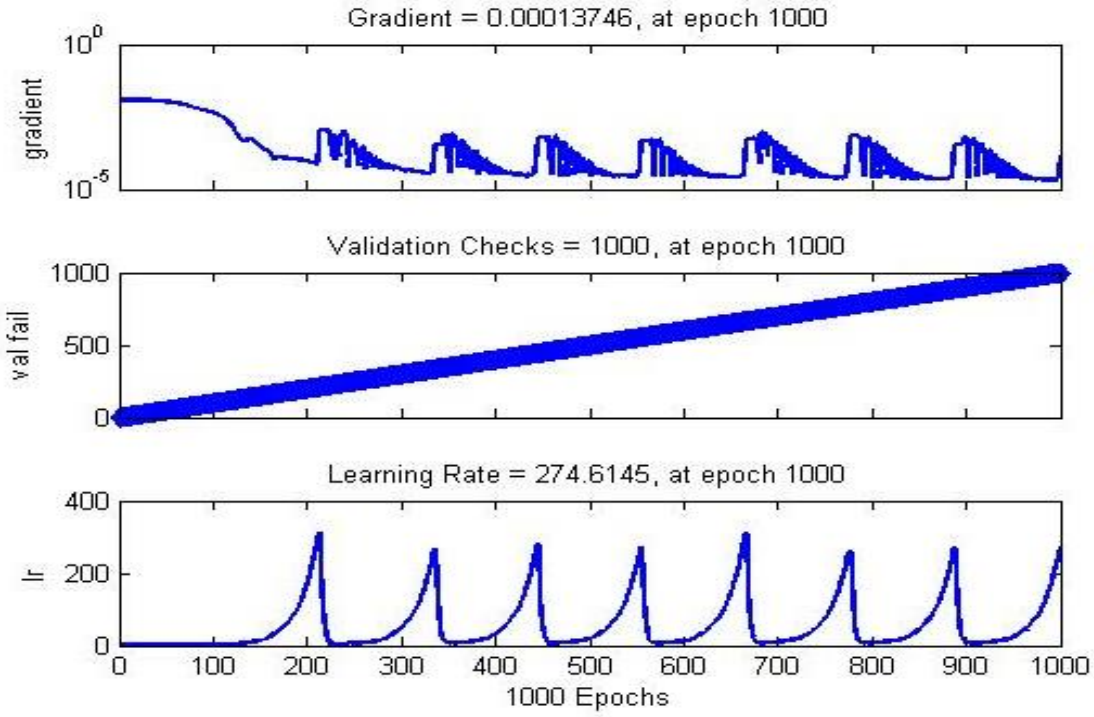

Figure 5-52: Validation Check, Gradient and Learning rate during Training

5.16 Network training

During training and testing of data, 15% of the features were selected from the new stage, moderate stage and worn out stage. The results predicted from the Neural networks were compared with the experimental wear. The table 5-27 shows the experimental flank wear compared with neural network for some selected experimental runs contain in the feature extracted. In table 5-27, it was observed that when fewer input neurons (10) were used in training the data, very close flank wears were obtained compare to Table 5-28 when 58 input neurons were used. Figure 5-54 and figure 5-55 also validates these results.

Table 5-27: Neural Networks architecture for 29 inputs features, 10 neurons, 1 hidden layer, 1 output layer with 3 Output Neurons

S/N	Exp round	Tool no	Pass no	Exp (mm)	NN (mm)	S (rpm)	F(mm/min)	D(mm)	%error	Accuracy
1	1	17	4th	0.02	0.03	4050	243	2	55	45
2	1	16	1st	0.05	0.05	4050	243	2	1	99
4	1	17	1st	0.05	0.06	4050	243	2	20	80
8	2	6	1st	0.13	0.13	5200	312	3	1	99
10	5	3	1st	0.18	0.18	2900	290	2	2	98
11	4	9	1st	0.20	0.20	4050	81	1	0	100
13	4	11	1st	0.30	0.30	4050	243	2	0	100
15	2	5	1st	0.39	0.39	5200	104	2	0	100
16	5	1	1st	0.43	0.43	2900	58	2	1	99

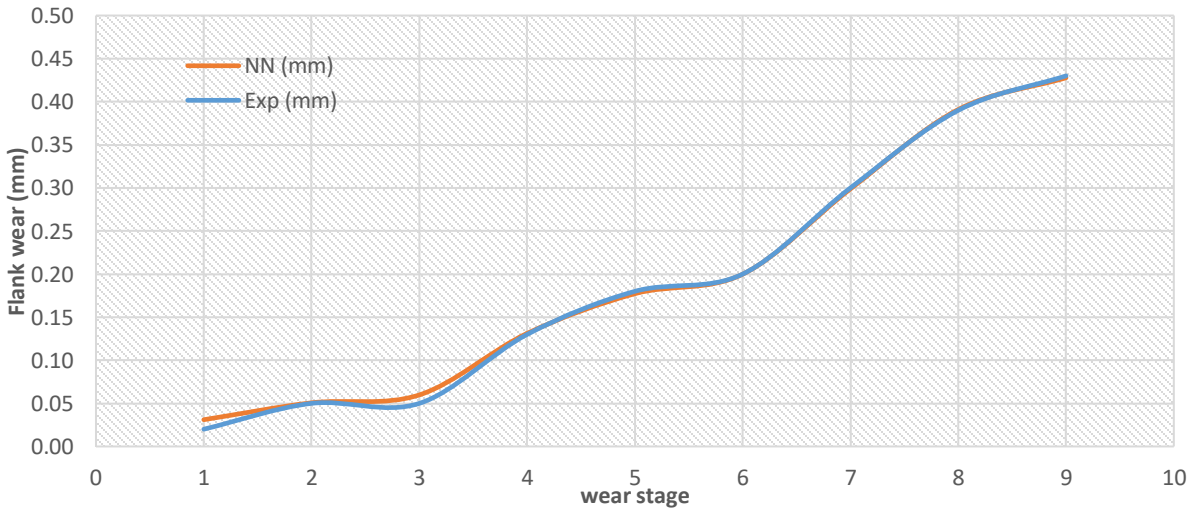

Figure 5-53: Graph of experimental Flank wear and Predicted Flank wear using 10 neurons

Table 5-28: Neural Networks architecture for 29 inputs features, 58 neurons, 1 hidden layer, 3 output Neurons

S/N	Exp round	Tool no	Pass no	Exp (mm)	NN (mm)	S (rpm)	F(mm/min)	D(mm)	%error	Accuracy
1	1	17	4th	0.02	0.04	4050	243	2	83	17
2	1	16	1st	0.05	0.03	4050	243	2	30	70
4	1	17	1st	0.05	0.06	4050	243	2	22	78
8	2	6	1st	0.13	0.04	5200	312	3	68	32
10	5	3	1st	0.18	0.18	2900	290	2	1	99
11	4	9	1st	0.2	0.19	4050	81	1	5	95
13	4	11	1st	0.3	0.30	4050	243	2	0	100
15	2	5	1st	0.39	0.39	5200	104	2	0	100
16	5	1	1st	0.43	0.41	2900	58	2	4	96

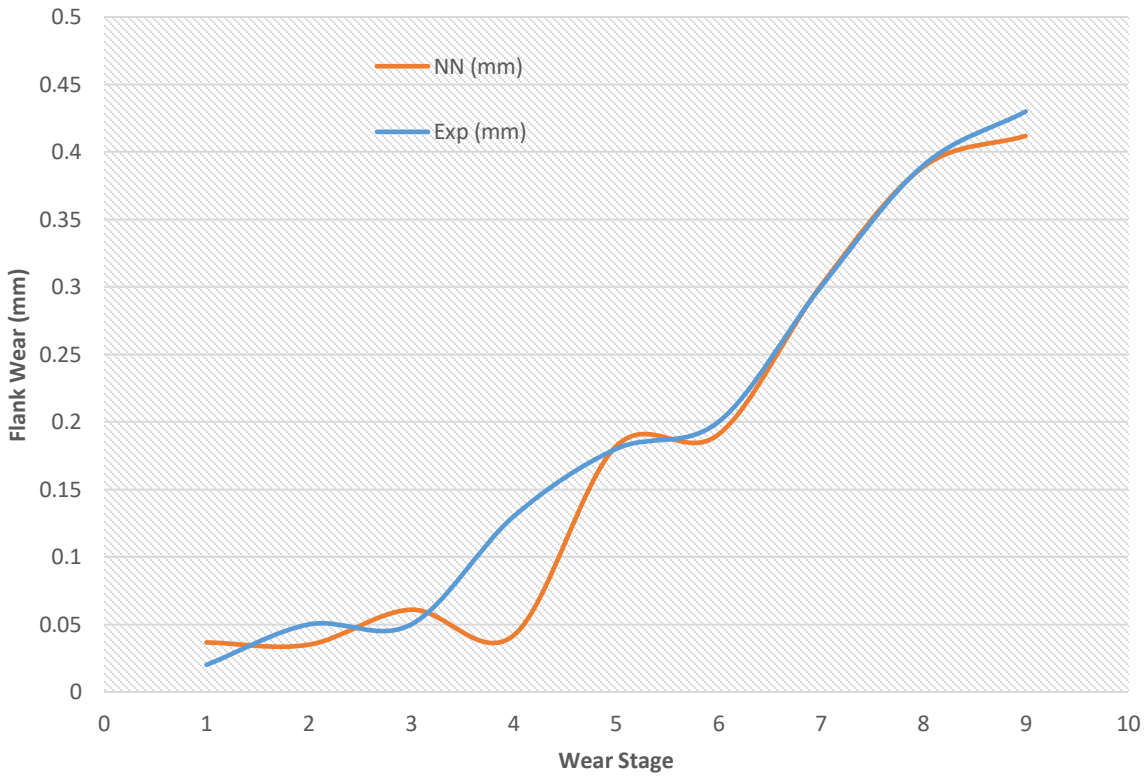

Figure 5-54: Graph of experimental Flank wear and Predicted Flank wear using 58 neuron

5.16.1 Network testing and Validation

Testing was also carried out for the two scenarios of numbers of neurons in hidden layers. The tables 5-29 and 5-30 below show the predicted flank wear during testing. During testing, features were randomly taken from fairly new data for testing and neural network showed a reasonable flank wears. Although it was a little bit higher than experimental and predicted values. But it was confirmed that the neural network is active. The testing was carried out using different numbers for inputs hidden neurons. Table 5-29 and 5-30 show the results of testing and the three graphs were plotted Fig 5-56 and 5- 57. The data used in Table 5-29 can be found in Appendix C.

Table 5-29: Neural Networks architecture 29 inputs, 10 neurons, 1 hidden layer, 3 Output Neurons

Exp Run	Exp Round	Tool no	Pass no	Exp (mm)	NN1 (mm)	NN2 Testing	state	S (rpm)	F(mm/min)
1	**1**	**17**	**4th**	**0.02**	**0.03**	**0.04**		**4050**	**243**
2	**1**	**16**	**1st**	**0.05**	**0.05**	**0.03**	**Fairly new**	**4050**	**243**
4	**1**	**17**	**1st**	**0.05**	**0.06**	**0.06**		**4050**	**243**
8	**2**	**6**	**1st**	**0.13**	**0.13**	**0.07**		**5200**	**312**
10	**5**	**3**	**1st**	**0.18**	**0.18**	**0.15**	**Moderately**	**2900**	**290**
11	**4**	**9**	**1st**	**0.2**	**0.20**	**0.23**	**worn**	**4050**	**81**
13	**4**	**11**	**1st**	**0.3**	**0.30**	**0.26**		**4050**	**243**
15	**2**	**5**	**1st**	**0.39**	**0.39**	**0.38**	**Worn out**	**5200**	**104**
16	**5**	**1**	**1st**	**0.43**	**0.43**	**0.41**		**2900**	**58**

Note: NN1 (Training) and NN2 (Prediction)

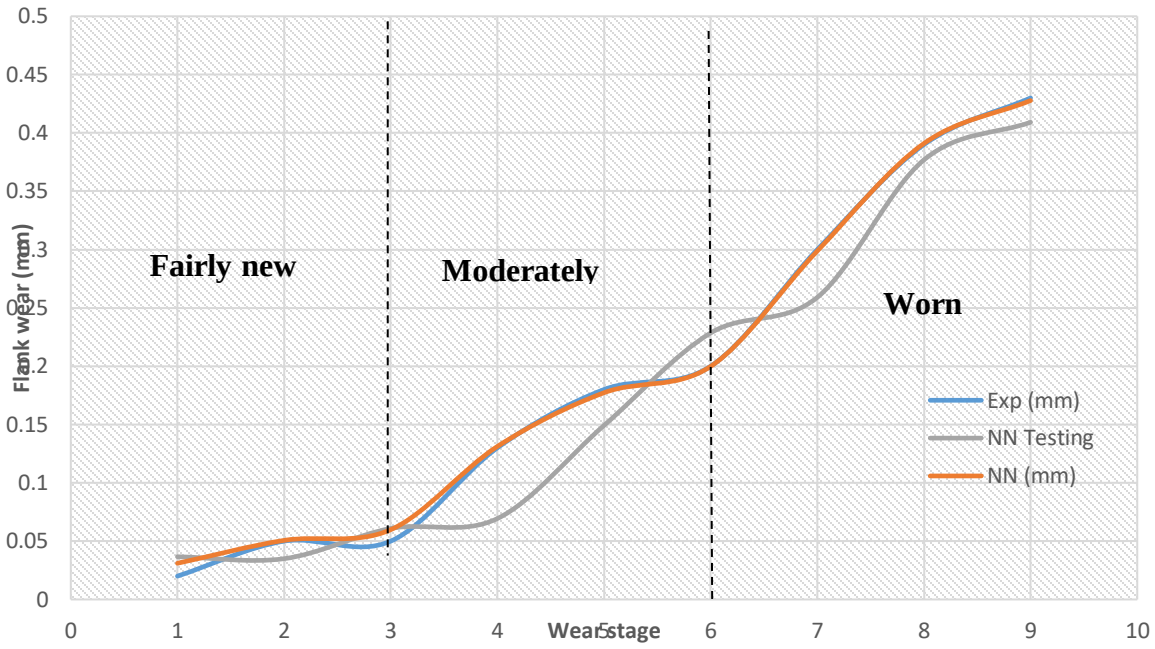

Figure 5-55: Graph showing the variation in Experimental, Training and Prediction Flank wears for 10 Neurons.

Table 5-30: Neural Networks architecture 29 inputs, 58 neurons, 1 hidden layer, 3 output Neurons

S/N	Exp round	Tool no	Pass no	Exp (mm)	NN (mm)	NN Testing	state	S (rpm)	F(mm/min)	D(mm)
1	1	17	4th	0.02	0.04	0.03		4050	243	2
2	1	16	1st	0.05	0.03	0.05	fairly new	4050	243	2
4	1	17	1st	0.05	0.06	0.06		4050	243	2
8	2	6	1st	0.13	0.04	0.19		5200	312	3
10	5	3	1st	0.18	0.18	0.21	moderately	2900	290	2
11	4	9	1st	0.2	0.19	0.11	worn	4050	81	1
13	4	11	1st	0.3	0.30	0.28		4050	243	2
15	2	5	1st	0.39	0.39	0.35	worn out	5200	104	2
16	5	1	1st	0.43	0.41	0.43		2900	58	2

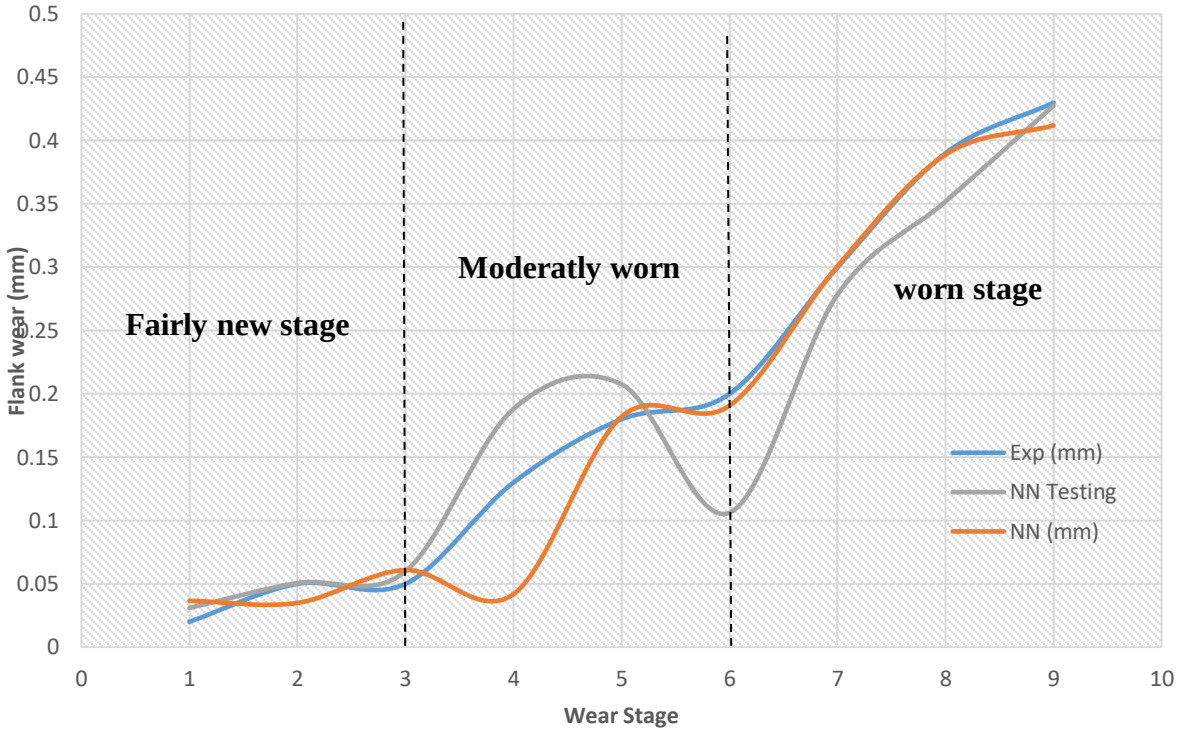

Figure 5-56: Graph showing the variation in Experimental, Training and Prediction Flank wear for 58 Neurons.

5.17 Conclusions and recommendations

5.17.1 Conclusions

Considering the growing market of the aerospace, marine and automobile industry that uses more stainless steels and the push for reduced assembly flow time, opportunities for the advancement of machining technology are prominent. This studies established progress over the performance reported in current literature.

Bearing in mind that the ultimate task in tool condition monitoring is the ability to establish an ideal model to investigate tool wear. To this effect, this research was aimed at modelling and analyzing machine parameters and validating the model using AE as a viable means for tool wear identification. The study was performed on Grade 316 stainless steel material being machined by end-milling process. To achieve this, a series of experimental runs and signal processing techniques were employed.

In the course of this research work, a comprehensive feasibility study of using the machine parameters, tool wear model and the principles of AE sensing technique for Tool condition monitoring was carried out. Productivity, optimization and a monitoring process framework was used to monitor the end milling operation at different machining parameters using one industrial Acoustic Emission sensor.

This research work has proposed a tool wear modelling scheme premised on design of experiment and signal processing framework to validate the model by identifying a feature selection, extraction and process conditioning followed by a comparison of the two approaches. Within the signal processing framework, the results certified and validated the importance of both time domain and frequency domain information in wear estimation. AE Sensing provided viable information on wear formation but not all features appropriately described machining state. A direct link was identified between some AE features and the rate of wear generated on the tool. A model using machine parameters and signal features are suitable enough to predict deplorable tool state wear. The model and signal features identified the high correlation and influence of the following under listed features:

a. The developed design of experiment model can predict 75% of the total variability in the tool wear.
b. The feed rate has the highest effect on the tool wear.
c. A minimum tool wear value of 0.174mm was achieved through optimization at low values of feed, speed and depth of cut. Hence, better surface finishes can be achieved by using lower machining parameters.
d. When working with stainless steel 316, a maximum Tool wear value of 0.296mm was achieved through optimization at low values of feed about 0.06mm/rev, speed of 4050mm/min and depth of cut about 2mm.
e. At high feed, low speed and cutting depth, Tool wear can be improved with an increased cutting length.
f. At low cutting speed and feed tool life can be improved
g. For productivity, it was proposed that low feed, speed and depth of cut can yield long lasting tool with volume of materials being removed. However, an elevated feed, depth of cut and speed will yield better volume removed but tool life will be half truncated.

h. The amplitudes of the raw AE voltage do follow a consistent increasing trend with the increase in tool wear values therefore, they may be suitable for online monitoring.
i. Time-frequency domain features (wavelets) show a better correlation with the Flank wear compared to time domain features and frequency domain features. Therefore, they serve as a better choice of input to the neural network scheme.
j. The overall extracted AE features show a unique pattern with the changes in Tool wear
k. The extracted wavelet features from sub-bands 1,2 3 and 4, range, Kurtosis, and Wavelet energy show the most significant correlation with flank wear compared to other sub-bands. Hence, they are more suitable features although all the feature extracted were used for predicting the Tool wear.
l. Artificial Neural Networks process are suitable for predicting and validating such ill-pattern variations derived from the research work by achieving a high percentage prediction accuracy for most of the flank wear value from the experimental.
m. Signal processing and Neural networks are good combination of tools to validate tool wear model from design of experiment. Hence, it can also be used to model and deployed for tool wear in industry.

5.17.2 Recommendations

The following observations were made during the research work which could be inform of recommendation for future work:

i. Apart from the three parameters used during machining in this research work, more tool parameters such as, rake angle, nose radius could be added to have more inputs parameters during modelling.
ii. Dry milling operations with the use of temperature sensor can be carried out on stainless steel.
iii. Using the same guide provided in this research work, different workpiece can be worked on.
iv. Different and multiple sensors can be deployed during data acquisition.
v. For signal processing, wavelet packet can be employed for Time frequency analysis.
vi. Other types of artificial Intelligent can be used to model and validate data.

PUBLICATIONS:

Poster Presentation:

1. **Odedeyi B. Peter,** Khaled Abou-El-Hossein, Tool wear monitoring in selected milling operation of stainless steel using Acoustic emission- UNESCO Africa Engineering week, NMMU Port Elizabeth, 28-19 September, 2016.

Conference Paper:

2. Muhammad M. Liman, Khaled Abou-El-Hossein, Odedeyi P. Babatunde and Abubakar I. Jumare "Ultra-High Precision Diamond Turning of Contact Lens Polymer", Proceedings of the 1st International Conference of Institute of Polymer Engineers, Abuja, Nigeria, 15th-17th December 2016. PP 8-10

References:

[1] Engineering Access. [Online]. Available: https://accessengineeringlibrary.com/browse/steel-metallurgy-properties-specifications-and-applications. [Accessed 03 March 2016].

[2] Mandal S K, Steel Metallurgy, McGraw-Hill Professional, 2015.

[3] Novak C J, Peckner D and Bernstein I M, "Handbook of stainless steel," New York., McGraw-Hill,, pp. 4-1-4-78.

[4] D. O'Sullivan and M. Cotterell, "Machinability of austenitic stainless steel SS303," *Journal of Materials Processing Technology ,* vol. 124, pp. 153-159, 2002.

[5] K. Abou-El-Hossein and Z. Yahya, "High-speed end-milling of AISI 304 stainless steels using new geometrically developed carbide inserts," *Journal of Materials Processing Technology,* Vols. 162-163, pp. 596-602, 2005.

[6] Imo T M R, Practical guideliness for the Fabrication of Duplex stainless steels, Pittsburg, PA, USA: IMO (UK LONDON, UK), 2014.

[7] Outokumpu A B, Handbook of stainless steels, Avestar, Sweden: Outokumpu Oyj, 2013.

[8] Specialty Steel Industy, Designer Handbook - stainless steel for machining, Washinton DC, 1997.

[9] Tsann-Shyi Chern , Tsai H S and Kuang-Hung Tseng, "Study of the characteristics of duplex stainless steel activated tungsten inert," *Materials and Design,* no. 32 (2011), p. 255–263, 2010.

[10] Specialty steel Industry of North America, Design Handbook- Design guidlines for the selection and use of stainless steel, Washinton DC: Specialty steel Industry of North America.

[11] Baddoo N R, "Stainless steel in construction: A review of research, applications, challenges," *Journal of Constructional Steel Research,* no. 64, p. 1199–1206, 2008.

[12] Engineering News , "Creamer Media Engineering News," 2015. [Online]. Available: http://www.engineeringnews.co.za/article/global-stainless-steel-production-up-83-in-2014-2015-04-28. [Accessed 28 04 2016].

[13] Nomani J, Pramanik A, Hilditch T and Littlef G, "Machinability studyof first generationduplex(2205),second generationduplex(2507)andaustenitestainlesssteelduring drilling process," *Wear,* no. 304, p. 20–28, 2013.

[14] H. Shao, L. Liu and H. Qu, "Machinability study on 3%Co–12%Cr stainless steel in milling," Wear, no. 263, p. 736–744, 2007..

[15] Cashell K A and Baddoo N R, "Ferriticstainless steels in structural applications," *Thin-WalledStructures,* no. 83, p. 169–181, 2014.

[16] MCI, [Online]. Available: http://www.steelonthenet.com/consumption.html. [Accessed 20 April 2016].

[17] T. R. Lin, "Cutting conditions using variable feeds and variable speed when drilling stainless steels with TiN Carbide Drills," *international journal of Advance Manufacturing Technology,* vol. 19, pp. 629-636, 2002.

[18] I. Korkut, M. Kasap, I. Ciftci and U. Seker, "Determination of optimum cutting parameters during machining of AISI 304 austenitic stainless steel," *Materials and Design* , vol. 25, pp. 303-305, 2004.

[19] [Online]. Available: http://www.buzzle.com/articles/physical-properties-of-stainless-steel.html. [Accessed 18 May 2016].

[20] H. Ernst and M.E. Merchant, Chip formation friction and high quality machined surfaces, in: Surface Treatment of Metals, New York: ASM, 1941.

[21] M. Merchant, "Basic mechanics of the metal cutting process," *J. Appl of Phys,* vol. 16, p. 318–324., 1945.

[22] S.-H. Rhim and S.-I. Oh, "Prediction of serrated chip formation in metal cutting process with new flow stress model for AISI 1045 steel," *Journal of Materials Processing Technology 2,* vol. 171, pp. 417-422, 2006.

[23] M. Shaw, Metal Removal, in CRC Handbook of Lubricants Theory and Practice of Tribology, Volume II: theory and design R.E. Booser,, CRC Press, 1988.

[24] Kurniawan Denni, Sharif Safian and Sultan A Z , "Chip Formation When Drilling AISI 316L Stainless Steel using Carbide Twist Drill," *Procedia Manufacturing,* vol. 2, p. 224 – 229, 2015.

[25] D. Biermanna and M. Steinera, "Analysis of Micro Burr Formation in Austenitic Stainless Steel X5CrNi18-10," *Procedia CIRP* , no. 3, pp. 97-102, 2012.

[26] H. K. Toenshoff and B. Denkena, "Basics of Cutting and Abrasive Processes, Lecture Notes in Production Engineering," in *chip formation*, Berlin Heidelberg, Springer-Verlag, 2013, pp. 21-25.

[27] [Online]. Available: http://www.slideshare.net/nakulrtm/machining-45898299. [Accessed 24 May 2016].

[28] P. M. [Online]. Available: http://www.slideshare.net/palanivendhan/metal-cutting-38254541. [Accessed 24 May 2016].

[29] P. Li, X. Qiu, L. Zhang and S. Tang, "Study on serrated chip formation and tool wear of cermet tools for milling stainless steel 3Cr13Cu," *Int J Adv Manuf Technol* , no. 77, pp. 461-467, 2015.

[30] A. Y, Manufacturing Automation: Metal cutting mechanics, Machine tool vibrations, and CNC design, Cambridge University Press, 2000.

[31] G. Oosthuizen, "MSc Thesis-Innovative cutting materials for finish shoulder milling Ti-6Al-4V Aero-engine alloy," Stellenbosch University, Cape town, March 2009.

[32] G. Byrne, D. Dornfeld and B. Denkena, "Advancing cutting technology, Keynote Papers STC "C"," *Annals of CIRP,* vol. 2, no. 52, pp. 483-508, 2003.

[33] Sandvik Group , "Titanium Machining Application Guide," Sandvik Coromant, sweeden, 2004.

[34] P. Muñoz-Escalona, "Surface Roughness Prediction when," University of Bath, Department of Mechanical Engineering, Bath, April 2010.

[35] K. Abou-El-Hossein, "Cutting fluid efficiency in end milling of AISI 304 stainless steel," *Industrial Lubrication and Tribology,,* vol. 60, no. 3, http://dx.doi.org/10.1108/00368790810871039, pp. 115 - 120, 2008.

[36] M. Dhananchezian, M. P. Kumar and a. T. Sornakumar, "Cryogenic Turning of AISI 304 Stainless Steel with Modified Tungsten Carbide Tool Inserts," *Materials and Manufacturing Processes,* no. 26, p. 781–785, 2011.

[37] Venugopal K A, Paul S and Chattopadhyay A B, "Growth of tool wear in turning of Ti-6Al-4V.," *Wear,* no. 262, p. 1071 –1078., 2007.

[38] D. Umbrello, "Analysis of the white layers formed during machining of hardened AISI 52100 steel under dry and cryogenic cooling conditions," *Int J Adv Manuf Technol* , no. 64, p. 633–642, 2013.

[39] D. N. R and K. M, "Cutting temperature, tool wear, surface roughness and dimensional deviation in turning AISI-4037 steel under cryogenic condition," *International Journal of Machine Tools & Manufacture,* no. 47, p. 754 –759, 2007.

[40] T. Childs, C. Evans, E. Browy, J. Troutman and E. Paul, "Tool temperatures and wear in micro-machining Cu-Ni alloys with diamond tools: models, simulations and experiments," *Procedia CIRP* , no. 31 , p. 270 – 275, 2015.

[41] Mohanty Siba brata, Ajit Kumar and Senapati, "A Review on the Effect of Process Parameters on Different Output Parameters During Machining of Several Materials," *International Journal of Engineering Sciences & Research Technology,* vol. 3(3), pp. 1499-1508, March, 2014.

[42] J. Thakkar and M. I. Patel, "A Review on Optimization of Process Parameters for Surface Roughness and Material Removal Rate for SS 410 Material During Turning Operation,"

Int. Journal of Engineering Research and Applications, vol. 4, no. 2, pp. 235-242, February 2014.

[43] P. Dearnley and A. Grearson, "Evaluation of principal wear mechanisms of cemented carbides and ceramics used for machining Titanium alloy IMI 318," *Materials Science and Technology,* vol. 2, no. 1, pp. 47-58, 1986.

[44] Ghose Joyjeet. [Online]. Available: http://www.slideshare.net/gauravgunjan24/theory-ofmetalcutting. [Accessed 6th June 2016].

[45] IEEE Global spec. [Online]. Available: http://www.globalspec.com/learnmore/manufacturing_process_equipment/cutting_tools/tool_inserts. [Accessed 6th June 2016].

[46] [Online]. Available: (Cutting Tool Materials: Fundamental Manufacturing Processes Video Series Study Guide) www.sme.org. [Accessed 11th May 2016].

[47] Mitsubishi. [Online]. Available: http://www.mitsubishicarbide.net/contents/mmus/enus/html/product/technical_information/information/sessaku.html. [Accessed 8th June 2016].

[48] Dr David J Grieve, "Manufacturing Processes - 2.7 Materials for cutting tools," 23rd March 2009.. [Online]. Available: http://www.tech.plym.ac.uk/sme/mfmt201/cuttingtoolmats.htm. [Accessed 8th June 2016].

[49] V. Marinov, Manufacturing Process Design, Kendall Hunt Publishing Company, 2012.

[50] B. P. Hede, Condition monitoring of tools in CNC turning, Loughborough: Loughborough University's Institutional Repository, January 2008.

[51] E. Trent and P. Wright, Metal cutting., Boston, USA: 3rd Edition, Butterworth Heinemann, 2000.

[52] D. J. Grieve, "Manufacturing Processes - 2.6 Cutting Tools," 17th March 2009. [Online]. Available: http://www.tech.plym.ac.uk/sme/mfrg315/cuttool1.htm. [Accessed 08 June 2016].

[53] Groover M P, Fundamentals of Modern Manufacturing., Second Edition John Wiley & sons, Inc., 2002.

[54] O. Olufayo, K. Abou-El-Hossein and T. v. Niekerk, "Online Tool Wear Monitoring," *Robotics and Mechatronics Conference of South Africa ROBMECH ,* 2011.

[55] Krar S F , Gill A R and Smid P, Techonology of Machine Tools, New York: MC: 6th ed Graw Hill, 2005.

[56] L. P.M., "On-line metal cutting tool condition monitoring. I: force and vibration analyses," *International Journal of Machine Tools & Manufacture,* vol. 40, pp. 739-768, 2000.

[57] Shao Chenhui, Guo Weihong, Kim Tae H, Jin Jionghua, Spicer J Patrick, Abell A Jeffrey and Hu S Jack, "Characterization and monitoring of tool wear in ultrasonic metal welding," HONOLULU, U.S.A., OCTOBER 5-8, 2014.

[58] Shao H, Wang H L and Zhao X M, "A cutting power model for tool wear monitoring in milling," *International Journal of Machine Tools and Manufacture,* vol. 44, no. 14, pp. 1503-1509, 2004.

[59] M. A. Elforjani, "PhD Thesis: Condition Monitoring of Slow Speed Rotating Machinery Using Acoustic Emission Technology," School of Engineering Cranfield University, Cranfield Uk, June 2010.

[60] W. P. Dong and W. Y. Wang, "Condition Monitoring and Diagnostic Management," in *The Second International Congress on Procedings ofCOMADEM.*, Beijing Institute of Technology China, Chapman and Hall, 1999.

[61] L. Dan and J. Mathew, "Tool wear and failure monitoring techniques for turning- A review.," *International Journal of Machine Tools and Manufacture,* vol. 30, no. 4, pp. 579-598., 1990.

[62] Scheffer Cornelius, "Masters Thesis:Monitoring of tool wear in turning operations using vibration measurements," Department of Mechanical and Aeronautical Engineering, University of Pretoria, Pretoria, 1999.

[63] B. L. I, "Experimental Comparison of sensors for tool-wear monitoring on milling," *Sensors and Actuators,* Vols. 37-38, pp. 589-595, 1993.

[64] T. Szecsi, "Automatic cutting-tool condition monitoring on CNC lathes," *Journal of Materials Processing Technology,* vol. 77, pp. 64-69, 1998.

[65] S. K. Sikdar and M. Chen, "Relationship between tool flank wear area and component forces in single point turning," *Journal of Materials Processing Technology,* vol. 128, no. 1-3, pp. 210-215, 2002.

[66] Cakir M C and Isik Y, "Detecting tool breakage in turning aisi 1050 steel using coated and uncoated cutting tools," *Journal of Materials Processing Technology,* vol. 159, no. 2, pp. 191-198, 2005.

[67] Guo Y B and Ammula S C, "Real-time acoustic emission monitoring for surface damage in hard machining," *International Journal of Machine Tools & Manufacture,* vol. 45, pp. 1622 -1627, March 2005.

[68] Li X A, "Brief review: acoustic emission method for tool wear monitoring during turning.," *International Journal of Machine Tools & Manufacture,* vol. 42, p. 157–165, 2002.

[69] Kannatey-Asibu J E and Dornfeld D A, "A study of tool wear using statistical analysis of metal-cutting acoustic emission," *Wear,* vol. 76, no. 2, pp. 247-261, 1982.

[70] Dimla E Dimla, "Sensor signals for tool-wear monitoring in metal cutting operations—a review of methods," *International Journal of Machine Tools & Manufacture,* vol. 40, pp. 1073-1098, 2000.

[71] Liang S Y and Dornfeld D A, "Tool Wear Detection Using Time Series Analysis of Acoustic Emission," *ASME Journal of Engineering for Industry,* vol. 111(3), pp. 199-205, 1989.

[72] Dornfeld D A, Lee Y and Chang A, "Monitoring of Ultraprecision Machining Processes," *International Journal of Advanced Manufacturing Technology,* vol. 21, pp. 571 - 578, 2003.

[73] Dornfeld D A and Diei E N, "Acoustic Emission Sensing ofTool Wear in Face Milling," *Journal of Engineering for Industry,* vol. 109, pp. 234 - 240, 1987.

[74] D. V. Hutton and F. Hu, "Acoustic Emission Monitoring of Tool Wear in End Milling Using Time-Domain Averaging," *Journal of Manufacturing Science and Engineering,* vol. 121, pp. 8-13, 1999.

[75] Puhar J, "Manufacturing Technologies," in *1st Seminar on Manufacturing Technologies*, University of Ljubljana, Slovenia.

[76] Bould Fathi Mohamed, "PhD Thesis: An Investigation of the relationship between temperature, forces and tool wear in turning and drilling," Aston University, 1998.

[77] Oluwole Olufayo Ayodeji, "MEng Thesis: Tool Wear Monitoring in end milling of mould Steel using acoustic emission," Nelson Mandela University, Port Elizabeth, 2011.

[78] Krar S F, Gill A R and Smid P, Techonology of Machine Tools, New york: 6th ed Mc Graw Hill, 2005.

[79] A. Zmitrowicz, "Wear patterns and laws of Wear- Review," *Journal of theoretical and applied mechanics,* vol. 44, no. 2, pp. 219-253, Warsaw 2006.

[80] Silva R G, "PhD Thesis: Cutting tool condition monitoring of the turning process using Artificial Intelligence," The University of Glamorgan, Glamorgan, 1997.

[81] Hoglund U, "Cutting edge wear in microscale physical conditions," *Wear processing CIRP*, vol. 25, no. 1, pp. 99-103, 1976.

[82] Hastings W F and Oxley P L B, "Predicting tool life from fundamental work material properties and cutting conditions," *CIRP*, pp. 33 - 38, 1976.

[83] Loladze T N, "Tribology of metal cutting and creation of new materials," *CIRP,* vol. 25, no. 1, pp. 83 - 88, 1976.

[84] M. A. Elbestawi and M. Dumitrescu, "Tool Condition Monitoring in Machining - Neural Networks," *IFIP International Federation for Information Processing Information Information Technology for Balanced Manufacturing Systems, ed. Shen, W., (Boston: Springer),,* vol. 220, pp. 5-16, 2006.

[85] R. Teti, K. Jemielniak, G. O'Donnell and D. Dornfeld, "Advanced monitoring of machining operations," *CIRP Annals - Manufacturing Technology,* vol. 59, p. 717–739, 2010.

[86] B. Sick, "On-Line and Indirect Tool wear Monitoring in Turning with Artificial Neural Networks: A review of more than a decade of research," *Mechanical Systems and Signal Processing,* vol. 16, no. 4, pp. 487-546, 2002.

[87] P. Prickett and C. Johns, "An overview of approaches to end milling tool monitoring," *International Journal of Machine Tools and Manufacture,* vol. 39, no. 1, pp. 105-122, 1999.

[88] T. Blum and I. Inasaki, "A study on acoustic emission from the orthogonal cutting process," *ASME Trans. Journal of Engineering for Industry,* vol. 112, no. 3, pp. 203-211, 1990.

[89] D. Choi, W. Kwon and C. Chu, "Real-time monitoring of tool fracture in turning using sensor fusion," *International Journal of Advanced Manufacturing Technology,* vol. 15, no. 5, pp. 305-310, 1999.

[90] K. Jemielniak and O. Otman, "Tool failure detection based on analysis of accoustic emission signals," *Journal of Material Processing Technology,* vol. 76, pp. 192-197, 1998.

[91] Lee Gun, "PhD Thesis: Real-Time adaptive cutting tool Flank Wear Predition," University of Florida, Florida, 2010.

[92] S. Kakade, L. Vijayaraghavan and R. Krishnamurthy, "In-process tool wear and chip-form monitoring in face milling operation using acoustic emission," *Journal of Material Processing Technology,* vol. 44, pp. 207-214, 1994.

[93] Hartmut V, "AE Testing Fundamentals, Equipment Applications," *The e-Journal of Nondestructive Testing,* p. 7, 2002.

[94] McIntire P, Nondestructive Testing Handbook Second Edition Volume 5 Acoustic Emission Testing, American Society for Nondestructive Testing., 1987.

[95] J. Kim and P. K. Liaw, "The Nondestructive Evaluation of Advanced Ceramics and Ceramic-Matrix Composites," *JOM*

(http://www.tms.org/pubs/journals/JOM/9811/Kim/Kim-9811.html), vol. 50, no. 11, November 1998.

[96] A. Prateepasen, "PhD Thesis: Tool Wear Monitoring in Turning Using Fused Data Sets of Calibrated Acoustic Emission and Vibration," Brunel Centre of Manufacturing Metrology Brunel University, Cleveland Road, Uxbridge, Middlesex, January 2001.

[97] Jamaludin N, Mba D and Bannister R H, "Condition monitoring of slow-speed rolling element bearings using stress waves," *Proceedings of the Institution of Mechanical Engineers Part E-Journal of Process Mechanical Engineering,* vol. 215, pp. 245-271, 2001.

[98] Mba D and Rao R B K N , "Development of Acoustic Emission Technology for Condition Monitoring and Diagnosis of Rotating Machines: Bearings, Pumps, Gearboxes, Engines, and Rotating Structures," *The Shock and Vibration Digest,* vol. 38, no. 1, pp. 3-16, 2006.

[99] Endean and Edwards, "Materials in Action," *Manufacturing with Materials The Open University. UK,* pp. 233-272, 1990.

[100] S. Kalpakjian, "Manufacturing Processes for Engineering Materials and Technology," 2003, pp. 543-552.

[101] G. Boothroyd, "Fundamentos del Corte de Metales y de las Máquinas Herramientas," Latinoamericana. Mexico, McGraw-Hill. , 1989, pp. 127-142.

[102] M. Shaw, Metal Cutting Principles, Oxford Series of Advanced Manufacturing 3, 1991.

[103] R. Lindberg, "Processes and Materials of Manufacture," Prentice Hall. 4th Edition, 1983, pp. 42-48; 305-326.

[104] Barton C, Jones J D, Reuben R L and Wilknson P, "Surface finish parameters as diagnostics of tool wear in face milling," *wear,* vol. 205, pp. 47-54, 1997.

[105] Matsumura T, Obikawa T, Shirakashi T and Usui E, "Autonomous turning operations planning with adaptive prediction of tool wear and surface roughness,," *Journal of manufacturing systems,* vol. 12, no. 3, pp. 253-262, 1993.

[106] Goller J A and Barrow G, "The prediction of surface finish in turning operations," *Matador Conference, Manchester,* pp. 229-237, 20th-21st April, 1995.

[107] Komaraiah M and Narasimha Reddy P, "Relative performance of tool materials in ultrasonic machining," *wear,* vol. 161, pp. 1-10, 1993.

[108] Wada R, Kodama H and Nakamura K, "Wear characteristics of single crystal diamond tool," *CIRP,* vol. 29, no. 1, pp. 47-52, 1980.

[109] Yang K and Jeang A, "Statistical surface roughness checking procedure based on a cutting tool wear model," *Journal of Manufacturing Systems,* vol. 13, no. 1, pp. 1-8, 1994.

[110] K. Lee, M. Kang, Y. Jeong, D. Lee and J.S. Kim, "Simulation of the surface roughness and profile in high speed end milling," *Journal of Materials Processing Technology,* vol. 113, pp. 410-415, 2001.

[111] K. Ehmann and M.S. Hong, "A generalized model of the surface generation process in metal cutting,," *CIRP Annals,* vol. 43, pp. 483-486, 1994.

[112] L. Tan, Digital Signal Processing: Fundermental and Applications, San Diego Califonia USA: Elsevier, 2008.

[113] P. E. Mix, Introduction to Nondestructive Testing: A training Guide, New Jersey: John Wiley and sons Inc, 2005.

[114] R. Teti, K. Jemielniak, G. O'Donnell and D. Dornfeld, "Advanced monitoring of machining operations," *CIRP Annals - Manufacturing Technology,* vol. 59, pp. 717-739, 2010.

[115] P. Fragkiskos P, "PhD Thesis: Digital signal Processing for structral Health Monitoring of Building," Brunel University, London, 2014.

[116] L. Samantaray, M. Dash and R. Panda, "A review on Time-frequency, Time-scale and Scale-frequency domain signal analysis," *IETE Journal of Research,* vol. 51, pp. 287-293, 2005.

[117] D. Stranneby and W. Walker, Digital Signal Processing and Applications (Second Edition), Oxford: Newness, 2004.

[118] J. K. Abbas, "Investigation into the effect of fixturing systems on the design of condition monitoring for machine operations," Nottingham Trent University , Nottingham, UK, June 2013.

[119] Al-Habaibeh A, Powell N P and Gindy N N Z, "Comprehensive Process and Machine Condition Monitoring Strategy for the Variax Hexacenter," *Computational intelligence for modelling, control and automation:Neural networks & advanced control strategies, Vienna,* pp. 249-254, 1999.

[120] A. A. Jaber and R. Bicker, "A simulation of Non-stationary Analysis using Wavelet Transform Based on LabVIEW and Matlab," *UKSim- AMSS Modelling Symposium (EMS) (IEEE),* pp. 138-144, 2014.

[121] Bishop C M, Neural Networks for Pattern Recognition, Oxford, UK: Claredon Press, 1995.

[122] M. Misiti, Y. Misiti, G. Oppenheim and J.P. Poggi, Wavelet Toolbox for use with MATLAB user's guide Available from Mathworks at http://www.mathworks.com., Natick, MA: MathWorks, Inc., 2016a..

[123] S. Debdas, M.F.Quereshi, A.Reddy, D.Chandrakar and D.Pansari, "A Wavelet based multiresolution analysis for real time condition monitoring of AC machine using vibration analysis," *International Journal of Scientific and Engineering Research,* vol. 2, 2011.

[124] Z.-R. Feng, Q.Zhou, J.Zhang, P.Jiang and X.-W.Yang, "A target guided subband filter for acoustic event detection in noisy environments using wavelet packets," *Audio Speech Lang Process IEEE/ACM Trans,* vol. 23, pp. 361-372, 2015.

[125] V. Kumar and S. Minz, "Feature Selection: A literature Review," *Smart Computing Review,* vol. 4, no. 3, pp. 211-229, 2014.

[126] K. Goebel and W. Yan, "Feature Selection for Tool wear diagonise using soft computing Technique," *Proceedings of the ASME, Manufacturing in Engineering Division,* vol. 11, pp. 157-163, 2000.

[127] T. Chan, "A Fast Metric Approach to Feature Subset Selection," *Proceedings of 24th EUROMIRO Conference,* vol. 2, pp. 733-736, 1998.

[128] R. Duda and P. Hart, Pattern Classification and Scene Analysis, New York: Wiley, 1973.

[129] M. Ben-Bassat, Pattern Recognition and Reduction of dimensionality", Handbook of Statistics (P. Krishnaiah and L. Kanal, eds.), North Holland, 1982.

[130] A. Blum and P. Lanfley, "Selection of Relevant Features and Examples in Machine Learning," *Artificial Intelligence 97,* vol. 97, pp. 245-271, 1997.

[131] R. J. Schalkoff, Pattern recognition: Statistical, Structural and neural approaches, Canada: John Wiley & sons, Inc., 1992.

[132] E. Emel and E. K.-A. Jr., "Tool Failure onitoring in Turning by Pattern Recognition of AE Signals," *Journal of Engineering for Industry,* vol. 110, pp. 137-145, 1988.

[133] S. H. Chen, A. J. Jakeman and J. P. Norton, "Artificial Intelligence techniques: An introduction to their use for modelling environmental systems," *Mathematics and Computers in Simulation,* vol. 78, p. 379–400, 2008.

[134] Introduction to Neural Network Theory. [Online]. Available: http://neuromastersoftware.com/neural-network-theory-introduction/. [Accessed 1st July 2016].

[135] M. Caudill, Neural Networks Primer, Miller: Special Issue of A1 EXPERT, Freeman Publications, 1989.

[136] R. P. Lippmann, "Pattern Classification Using Neural Networks," *IEEE Connnunication Magazine,* pp. 47-64, Nov 1989.

[137] R. Arnab, P. Sushanta, M. Shamsuzzaman and R. Ishfaqur, "Design of an optimum antenna system for maximum power transfer using statistical design of experiment approach," in *PIERS Proceedings, pg 23-27*, Beijing, China, 2009.

[138] H. Mettas, "Design of Experiments and Data Analysis," in *Annual RELIABILITY and MAINTAINABILITY Symposium ,pages 1-27,* San Jose, CA, USA, January 25-28, 2010.

[139] A. Dean and D. Voss, "Design and Analysis of Experiments,," *G. Casella, S. Fienberg, and a.I. Olkin, Editors.Springer-Verlag Inc.: New York,* pp. 576-579, 1999.

[140] Stat-Ease Inc, "Copyright ©2007 v7.1.3 CD-07282007".

[141] DMG MORI, "DMU monoBLOCK® series – Universal Milling Machines," 12 June 2016. [Online]. Available: http://en.dmgmori.com/products/milling-machines/universal-milling-machines-for-5-sided-5-axis-machining/dmu-monoblock. [Accessed 12 June 2016].

[142] C. Franci and U. Zuper, "Approach to optimization of cutting condition by using artificial neural l network," *Journal of Materials Processing Technology,,* vol. 3, pp. 281-290, 2006.

[143] Arnab R, Sushanta P , Shamsuzzaman M and Ishfaqur R , "Design of an optimum antenna system for maximum power transfer using statistical design of experiment approach," in *PIERS Proceedings, pp. 23-27.*, Beijing, China, 2009.

[144] Patnaik L M and Manyam O K , "Epileptic EEG detection using neural networks and post-classification," *Comput Methods Programs Biomed,* vol. 2, no. 91, pp. 100 - 109, August, 2008.

[145] Adeli H, Zhou Z and Dadmehr N, "Analysis of EEG records in an epileptic patient using wavelet transform," *Journal of Neurosci Methods,* vol. 123, no. 1, pp. 69-87., 15 February, 2003.

[146] Omerhodzic I, Avdakovic S, Nuhanovic A and Dizdarevic K, "Energy Distribution of EEG Signals: EEG Signal Wavelet-Neural Network Classifier," *International Journal of Biological and life Sciences.,* vol. 6, no. 4, pp. 566- 571, 2010.

APPENDIX A: LabVIEW Code for Data Acquisition

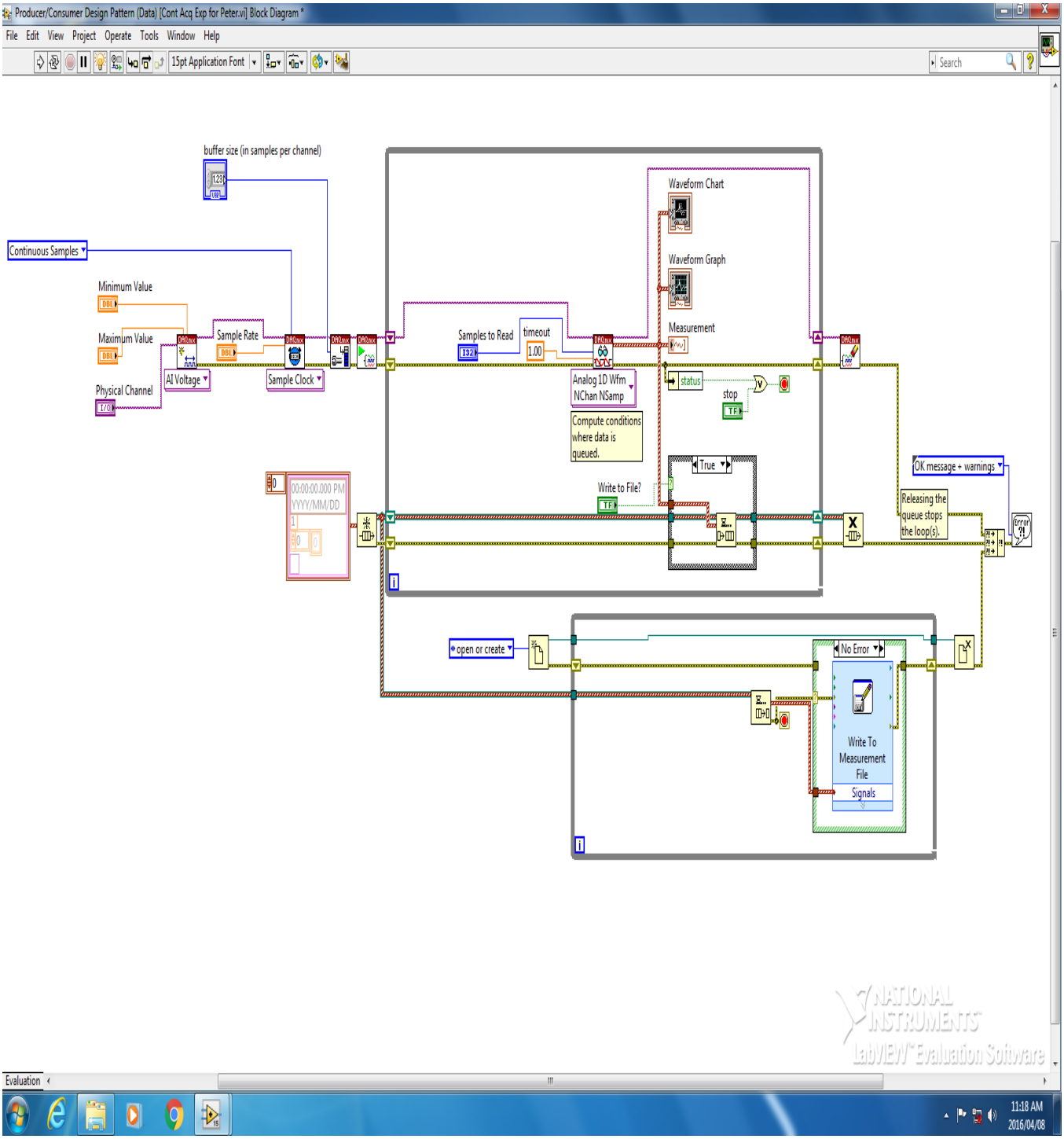

LabVIEW Code for Data Acquisition

APPENDIX B: Live Data Acquisition

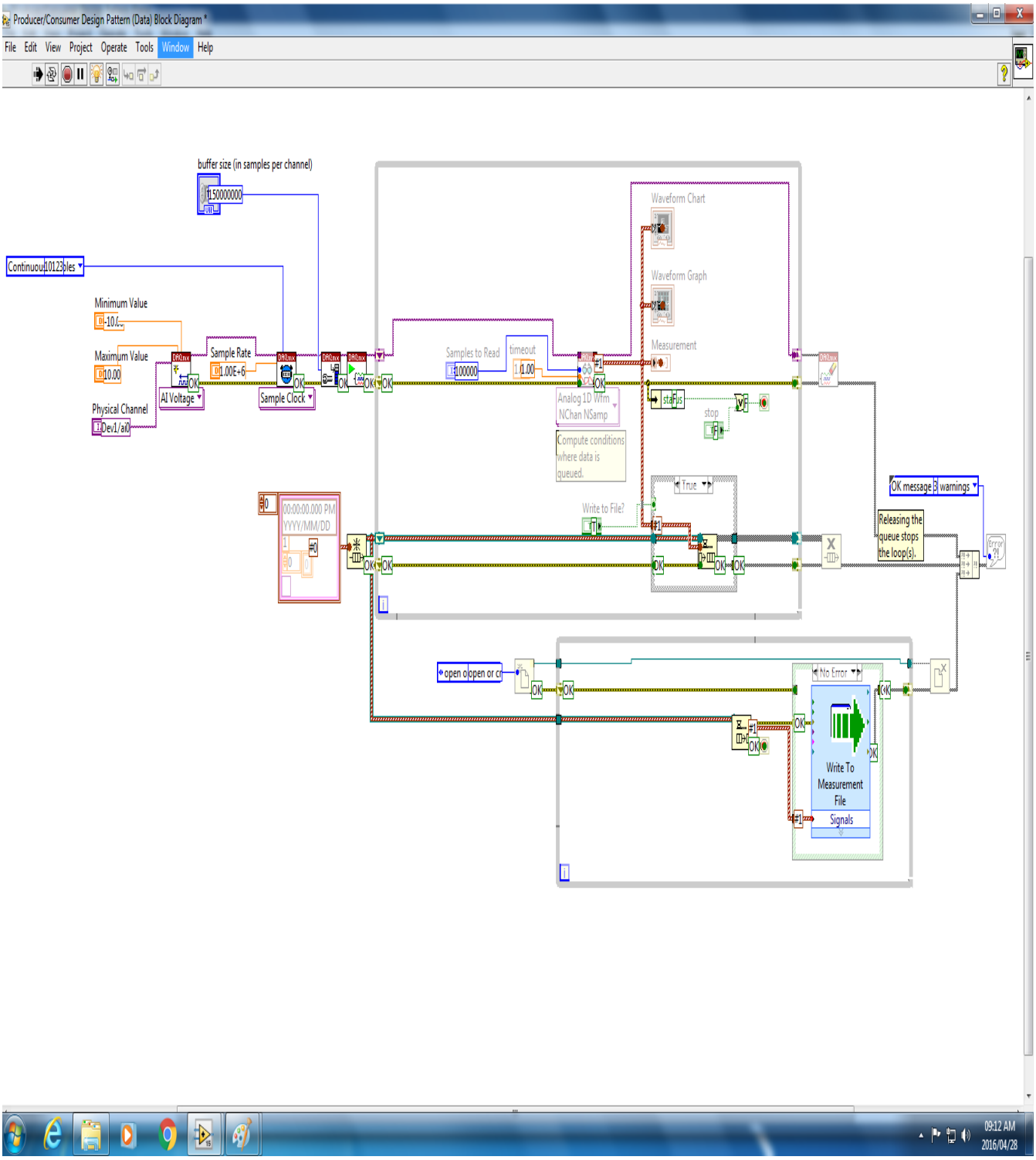

APPENDIX C: Experimental data Table development

Run	Tool (inserts)	Speed (rpm)	Feed (mm/rev)	feed(mm/min)	Doc (mm)	initial passes	Round 1 (mm)	MRR1	accm passes	Round 2 (mm)	MRR2	accm passes	Round 3 (mm)	MRR3	No of new passes	accm passes	Round 4	MRR4
1	1	2900	0.02	58	2	4	0.05	3200	8	0.10	6400.00	12	0.10	9600.00	6	18	0.27	14400.00
1	2	2900	0.02	58	2	4	0.05	3200	8	0.05	6400.00	12	0.10	9600.00	6	18	0.22	14400.00
2	3	5200	0.10	520	2	4	0.02	3200	9	0.10	7200.00	13	0.13	10400.00	6	19	0.24	15200.00
2	4	5200	0.10	520	2	4	0.05	3200	9	0.10	7200.00	13	0.16	10400.00	6	19	0.25	15200.00
3	5	2900	0.10	290	2	4	0.05	3200	8	0.05	6400.00	14	0.10	11200.00	7	21	0.09	16800.00
3	6	2900	0.10	290	2	4	0.05	3200	8	0.05	6400.00	14	0.10	11200.00	7	21	0.10	16800.00
4	7	4050	0.10	405	1	4	0.05	1600	8	0.05	3200.00	12	0.07	4800.00	8	20	0.14	8000.00
4	8	4050	0.10	405	1	4	0.05	1600	8	0.10	3200.00	12	0.10	4800.00	8	20	0.15	8000.00
5	9	5200	0.02	104	2	4	0.05	3200	8	0.20	6400.00	8	0.29	6400.00	0	8	0.29	6400.00
5	10	5200	0.02	104	2	4	0.05	3200	8	0.39	6400.00	8	0.29	6400.00	0	8	0.29	6400.00
6	11	5200	0.06	312	3	4	0.06	4800	8	0.10	9600.00	12	0.10	14400.00	6	18	0.19	21600.00
6	12	5200	0.06	312	3	4	0.05	4800	8	0.13	9600.00	12	0.18	14400.00	6	18	0.25	21600.00
7	13	5200	0.06	312	1	4	0.09	1600	6	0.10	2400.00	10	0.10	4000.00	6	16	0.20	6400.00
7	14	5200	0.06	312	1	4	0.06	1600	6	0.10	2400.00	10	0.10	4000.00	6	16	0.15	6400.00
8	15	2900	0.06	174	1	4	0.05	1600	8	0.05	3200.00	14	0.07	5600.00	6	20	0.10	8000.00
8	16	2900	0.06	174	1	4	0.05	1600	8	0.05	3200.00	14	0.07	5600.00	6	20	0.10	8000.00
9	17	4050	0.02	81	1	4	0.05	1600	7	0.10	2800.00	11	0.14	4400.00	6	17	0.21	6800.00
9	18	4050	0.02	81	1	4	0.05	1600	7	0.10	2800.00	11	0.10	4400.00	6	17	0.17	6800.00
10	19	4050	0.10	405	3	4	0.05	4800	8	0.10	9600.00	12	0.10	14400.00	6	18	0.20	21600.00
10	20	4050	0.10	405	3	4	0.05	4800	8	0.05	9600.00	12	0.06	14400.00	6	18	0.17	21600.00
11	21	4050	0.06	243	2	4	0.10	3200	6	0.20	4800.00	7	0.26	5600.00	1	8	0.31	6400.00
11	22	4050	0.06	243	2	4	0.10	3200	6	0.27	4800.00	7	0.27	5600.00	1	8	0.29	6400.00
12	23	2900	0.06	174	3	4	0.05	4800	7	0.13	8400.00	11	0.29	13200.00	0	11	0.29	13200.00
12	24	2900	0.06	174	3	4	0.10	4800	7	0.10	8400.00	11	0.28	13200.00	0	11	0.28	13200.00
13	25	4050	0.06	243	2	4	0.05	3200	7	0.20	5600.00	11	0.27	8800.00	1	12	0.32	9600.00
13	26	4050	0.06	243	2	4	0.10	3200	7	0.10	5600.00	11	0.20	8800.00	1	12	0.20	9600.00
14	27	4050	0.02	81	3	4	0.05	4800	7	0.29	8400.00	8	0.32	9600.00	0	8	0.32	9600.00
14	28	4050	0.02	81	3	4	0.10	4800	7	0.20	8400.00	8	0.26	9600.00	0	8	0.26	9600.00
15	29	4050	0.06	243	2	4	0.05	3200	8	0.11	6400.00	12	0.17	9600.00	6	18	0.30	14400.00
15	30	4050	0.06	243	2	4	0.05	3200	8	0.10	6400.00	12	0.11	9600.00	6	18	0.22	14400.00
16	31	4050	0.06	243	2	4	0.05	3200	8	0.06	6400.00	12	0.10	9600.00	6	18	0.16	14400.00
16	32	4050	0.06	243	2	4	0.05	3200	8	0.05	6400.00	12	0.07	9600.00	6	18	0.16	14400.00
17	33	4050	0.06	243	2	4	0.05	3200	6	0.05	4800.00	12	0.10	9600.00	6	18	0.20	14400.00
17	34	4050	0.06	243	2	4	0.02	3200	6	0.05	4800.00	12	0.05	9600.00	6	18	0.13	14400.00

APPENDIX D: Normalized Feature extracted

	EXP1T17/4	EXP1T16/4	EXP1T16	EXP1T17	EXP2T16	EXP2T9	EXP4T8	EXP2T6	EXP5T4	EXP5T3	EXP4T9	EXP5T7	EXP4T11	EXP4T13	EXP2T5	EXP5T1
	1	2	3	4	5	6	7	8	9	10	11	12	13	14	15	16
speed	0.50	0.50	0.50	0.50	0.50	0.50	0.00	1.00	0.50	0.00	0.50	1.00	0.50	0.50	1.00	0.00
feed	0.53	0.53	0.53	0.53	0.53	0.07	0.33	0.73	1.00	0.67	0.07	0.73	0.53	0.53	0.13	0.00
DoC	0.50	0.50	0.50	0.50	0.50	0.00	0.00	1.00	0.00	0.50	0.00	0.00	0.50	0.50	0.50	0.50
mean 2	0.02	0.02	0.02	0.02	0.01	0.01	0.00	0.11	0.00	0.00	0.00	0.00	0.00	0.00	0.01	0.00
range	0.06	0.05	0.06	0.08	0.06	0.08	0.04	0.08	0.00	0.04	0.05	0.00	0.29	0.29	0.31	1.00
RMS	0.41	0.37	0.37	0.36	0.50	0.21	0.02	1.00	0.02	0.02	0.03	0.02	0.08	0.07	0.37	0.00
St Dev	0.07	0.06	0.06	0.06	0.08	0.04	0.01	0.16	0.01	0.01	0.01	0.01	0.02	0.02	0.06	0.00
Variance	0.00	0.00	0.00	0.00	0.01	0.00	0.00	0.03	0.00	0.00	0.00	0.00	0.00	0.00	0.00	0.00
max	0.04	0.04	0.04	0.06	0.04	0.07	0.04	0.04	0.00	0.04	0.04	0.00	0.29	0.04	0.04	1.00
min	0.93	0.95	0.94	0.93	0.92	0.95	1.00	0.85	1.00	1.00	0.95	1.00	1.00	0.07	0.00	1.00
Kurtosis	0.00	0.00	0.00	0.00	0.00	0.00	0.02	0.00	0.00	0.03	0.03	0.00	1.00	0.96	0.01	0.00
Skewness	0.47	0.47	0.47	0.47	0.47	0.48	0.51	0.47	0.47	0.54	0.55	0.47	1.00	0.00	0.46	0.47
P-T-P	0.01	0.00	0.00	0.01	0.01	0.01	0.00	0.01	1.00	0.00	0.00	1.00	0.07	0.07	0.08	0.55
d1	0.06	0.01	0.08	0.16	0.08	0.06	0.01	0.03	0.00	0.08	0.01	0.00	1.00	0.33	0.67	0.83
d2	0.30	0.03	0.30	0.25	0.25	0.25	0.10	0.50	0.01	0.20	0.25	0.01	1.00	0.50	0.50	0.00
d3	0.48	0.48	0.48	0.48	0.48	1.00	0.17	1.00	0.01	0.38	1.00	0.01	1.00	0.48	1.00	0.00
d4	0.02	0.02	0.04	0.04	0.08	0.02	0.02	0.10	1.00	0.02	0.02	1.00	0.10	0.10	0.04	0.00
d5	0.02	0.02	0.04	0.04	0.02	0.02	0.02	0.04	0.00	0.02	0.02	0.00	0.08	0.04	0.04	1.00
St Dev D1	0.02	0.02	0.02	0.02	0.02	0.01	0.00	0.03	0.00	0.01	0.01	0.00	0.01	0.01	0.02	0.00
St Dev D2	0.03	0.03	0.03	0.03	0.04	0.02	0.00	0.08	0.00	0.00	0.02	0.00	0.01	0.01	0.03	0.00
St Dev D3	0.05	0.05	0.05	0.05	0.07	0.03	0.01	0.13	0.01	0.01	0.03	0.01	0.01	0.01	0.05	0.01
St Dev D4	0.01	0.01	0.01	0.01	0.03	0.01	0.01	0.04	0.01	0.01	0.01	0.01	0.01	0.01	0.02	0.01
St Dev D5	0.01	0.01	0.01	0.01	0.01	0.01	0.00	0.02	0.00	0.00	0.01	0.00	0.00	0.00	0.01	0.00
Abs D1	0.01	0.01	0.01	0.01	0.01	0.00	0.00	0.02	0.00	0.00	0.00	0.00	0.00	0.00	0.01	0.00
Abs D2	0.01	0.01	0.02	0.01	0.02	0.01	0.00	0.04	0.00	0.00	0.01	0.00	0.00	0.00	0.02	0.00
Abs D3	0.02	0.02	0.02	0.02	0.03	0.01	0.00	0.06	0.01	0.00	0.01	0.01	0.00	0.00	0.02	0.00
Abs D4	0.01	0.01	0.01	0.00	0.01	0.01	0.00	0.02	0.00	0.00	0.01	0.01	0.00	0.00	0.01	0.00
Abs D5	0.01	0.01	0.01	0.01	0.01	0.00	0.00	0.01	0.00	0.00	0.00	0.00	0.00	0.00	0.00	0.00
Energy	0.07	0.03	0.02	0.04	0.04	0.03	0.03	0.01	0.49	0.03	0.03	0.37	0.01	0.02	0.00	1.00
Flk Wear	0.02	0.05	0.05	0.05	0.06	0.10	0.10	0.13	0.14	0.18	0.20	0.22	0.30	0.32	0.39	0.43
	EXP1T17/4	EXP1T16/4	EXP1T16	EXP1T17	EXP2T16	EXP2T9	EXP4T8	EXP2T6	EXP5T4	EXP5T3	EXP4T9	EXP5T7	EXP4T11	EXP4T13	EXP2T5	EXP5T1

APPENDIX E: Some Flank wears

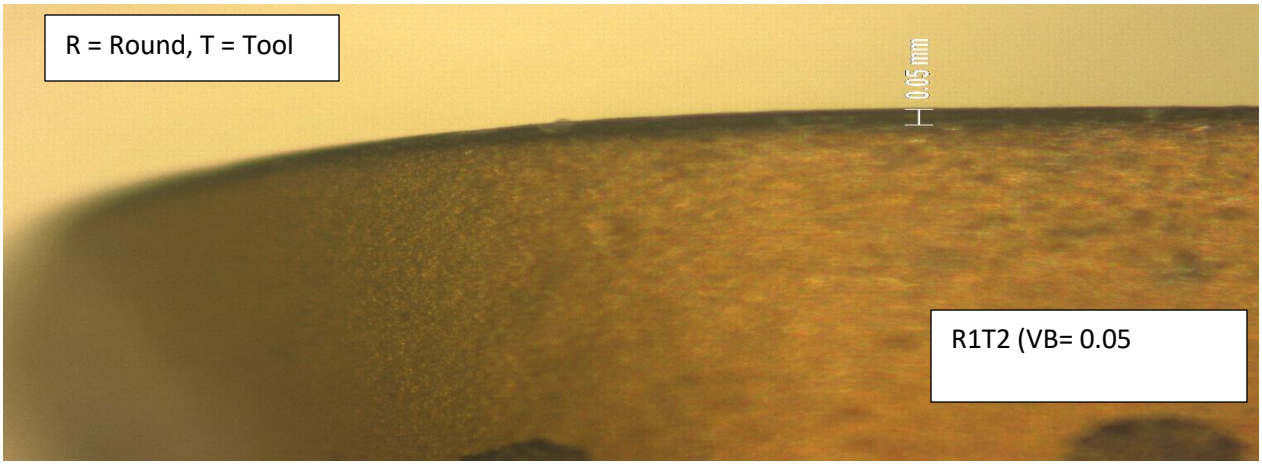

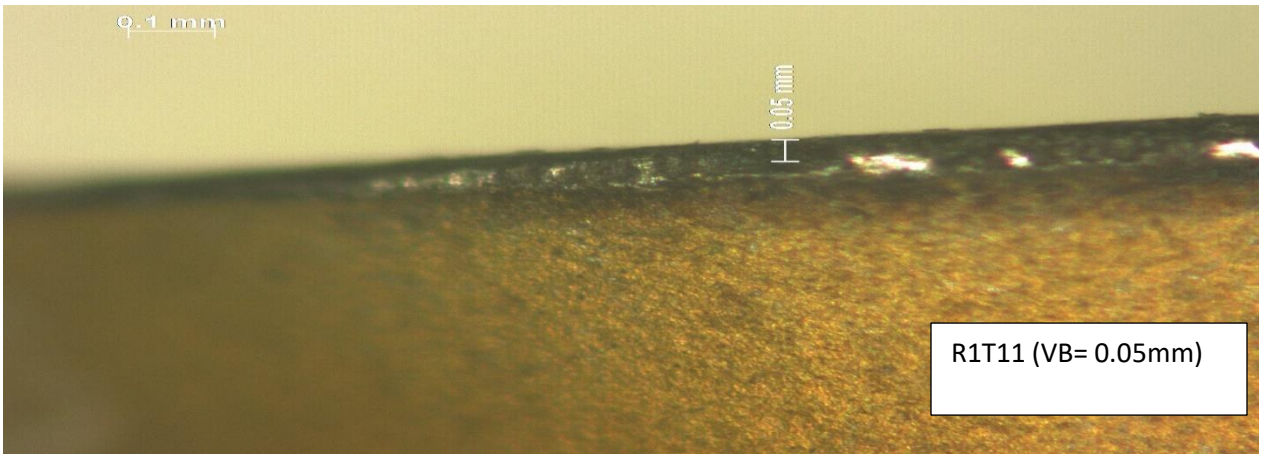

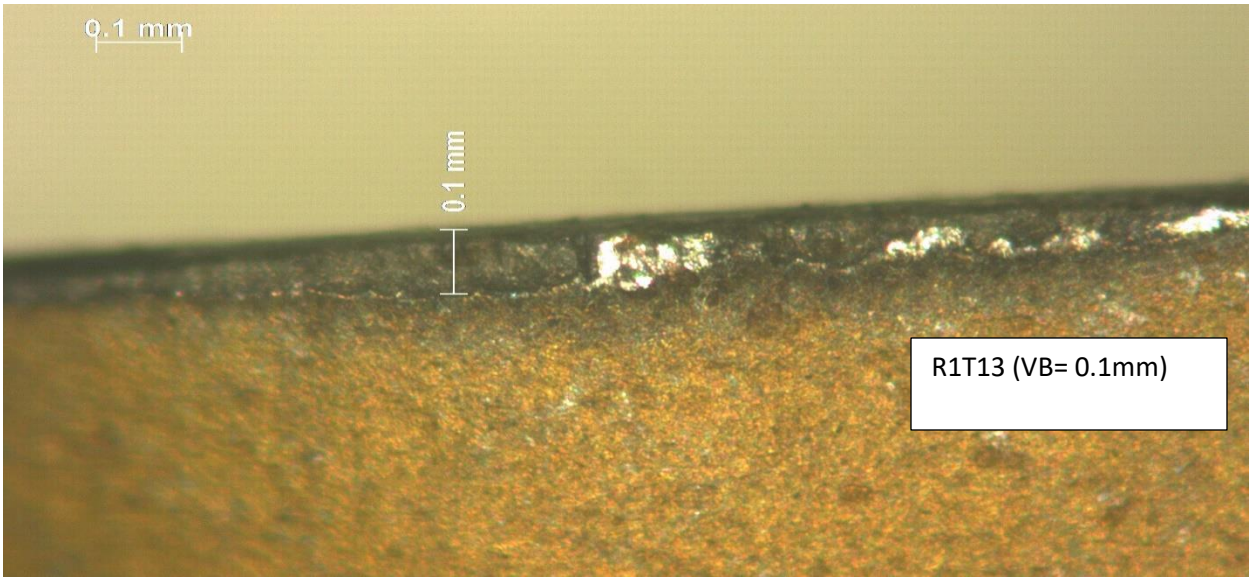

R = Round, T = Tool

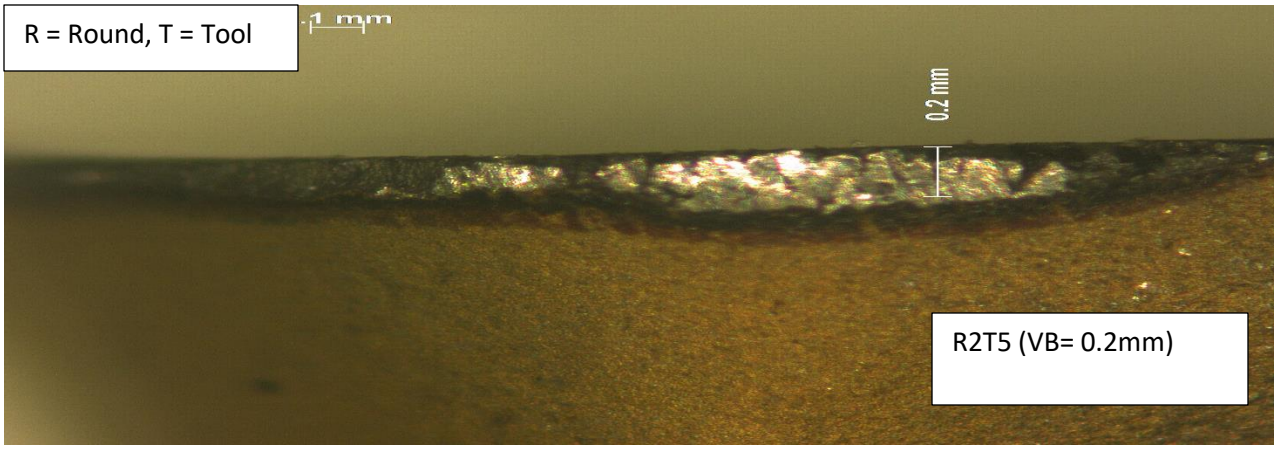

R2T5 (VB= 0.2mm)

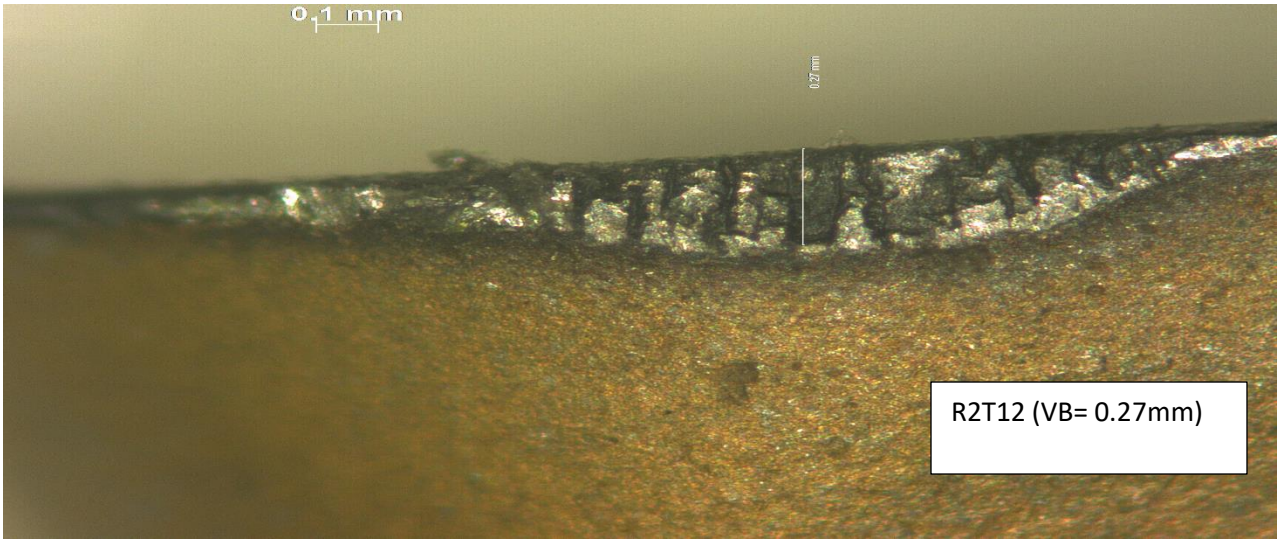

R2T12 (VB= 0.27mm)

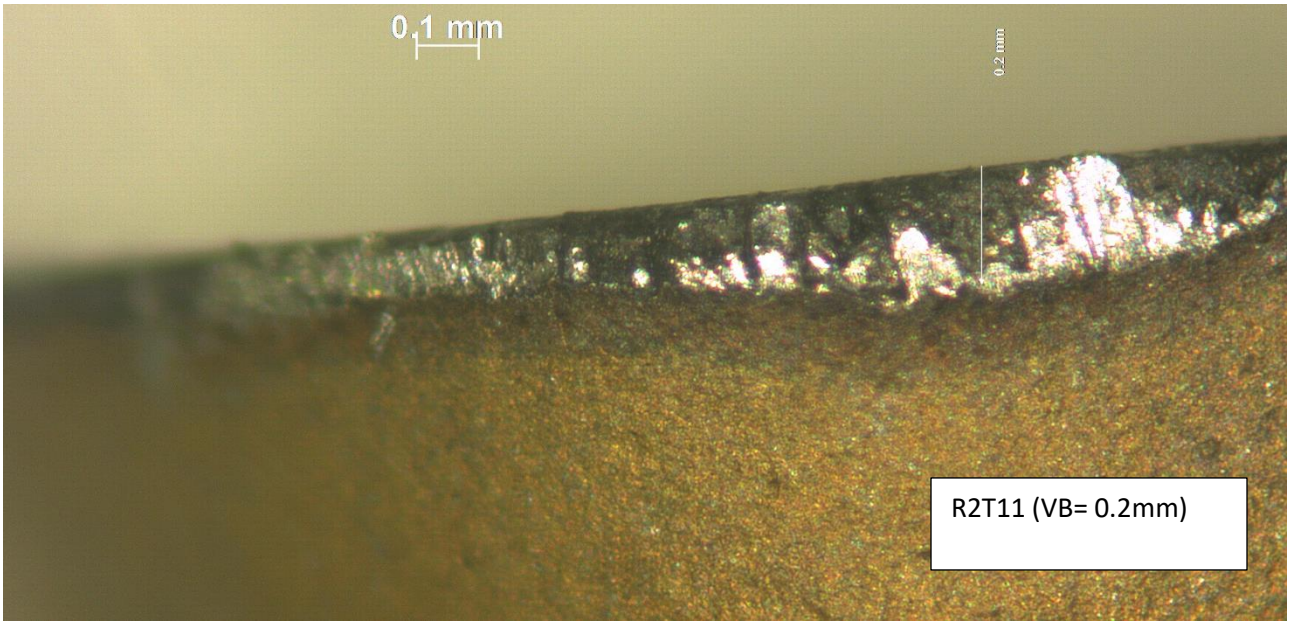

R2T11 (VB= 0.2mm)

R = Round, T = Tool

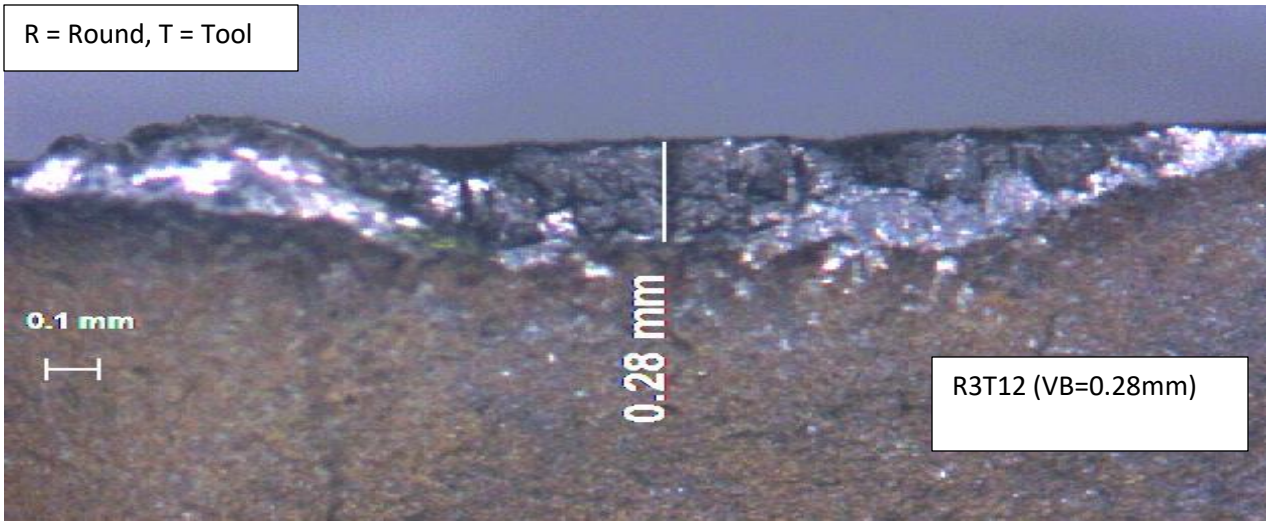

R3T12 (VB=0.28mm)

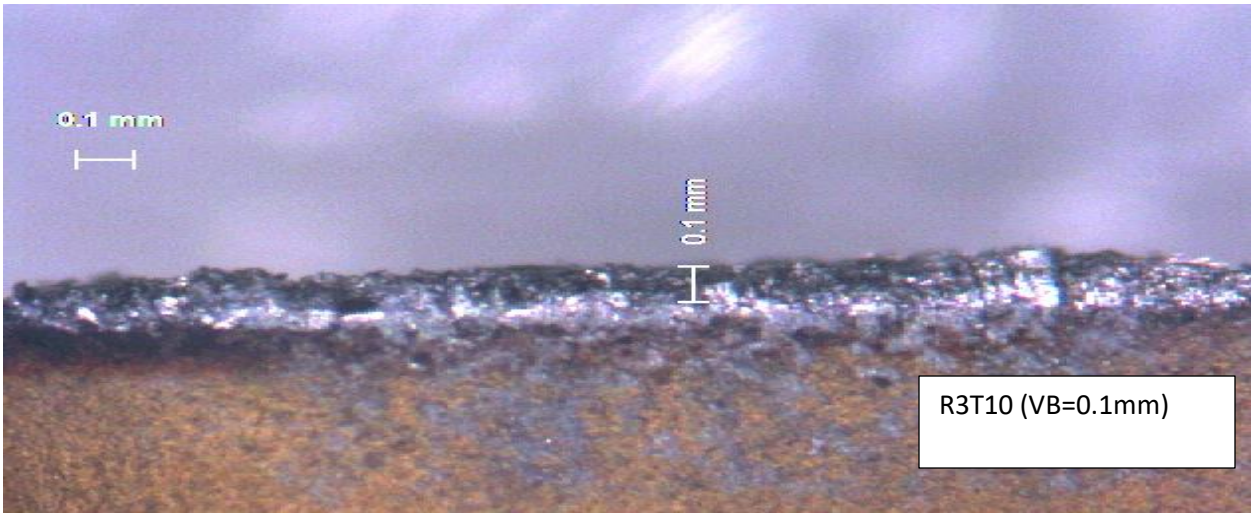

R3T10 (VB=0.1mm)

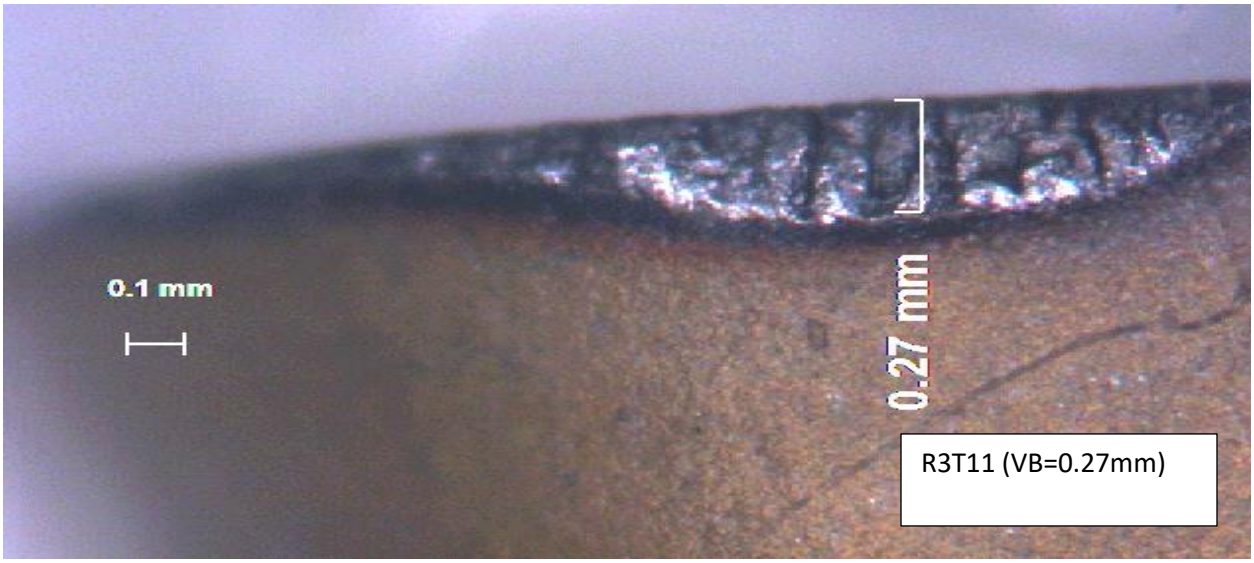

R3T11 (VB=0.27mm)

R = Round, T = Tool

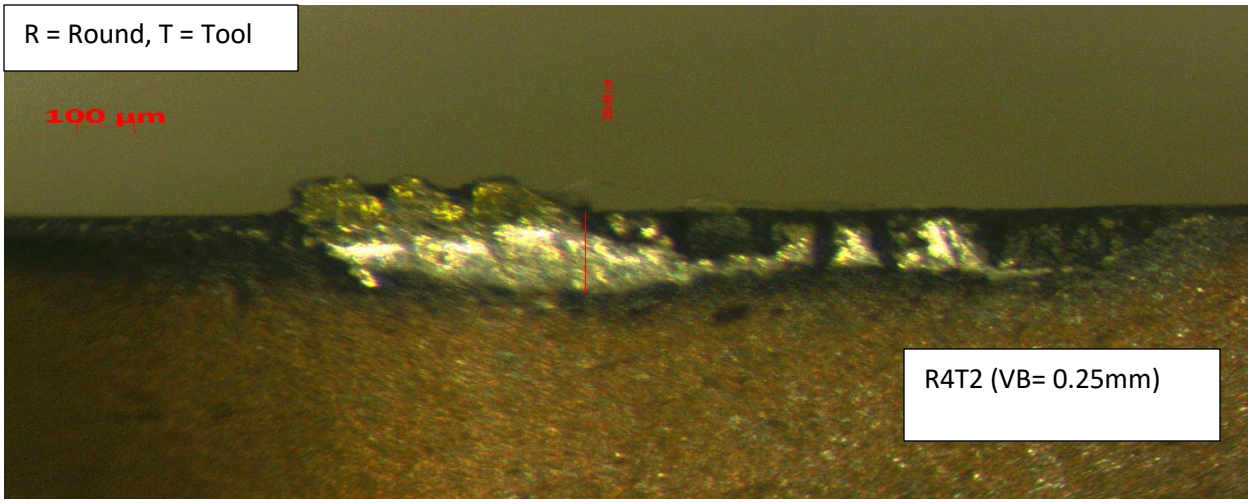

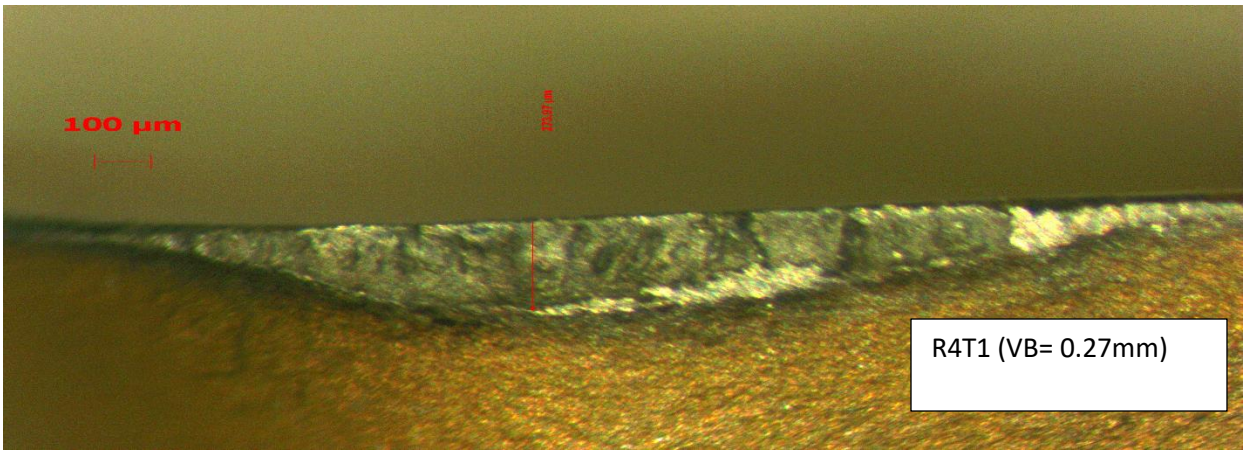

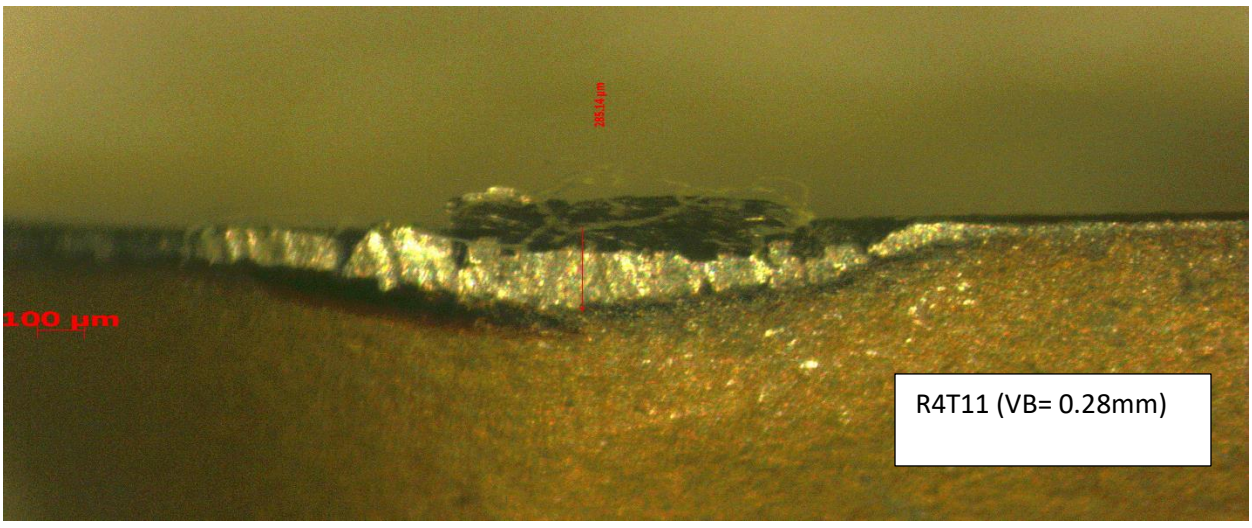

R = Round, T = Tool

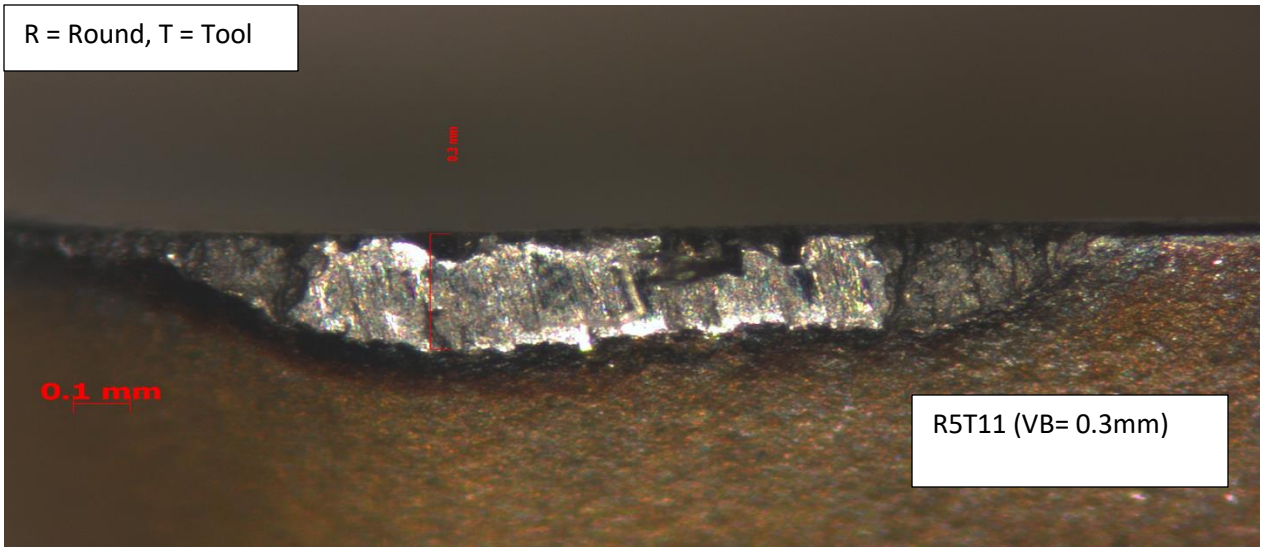

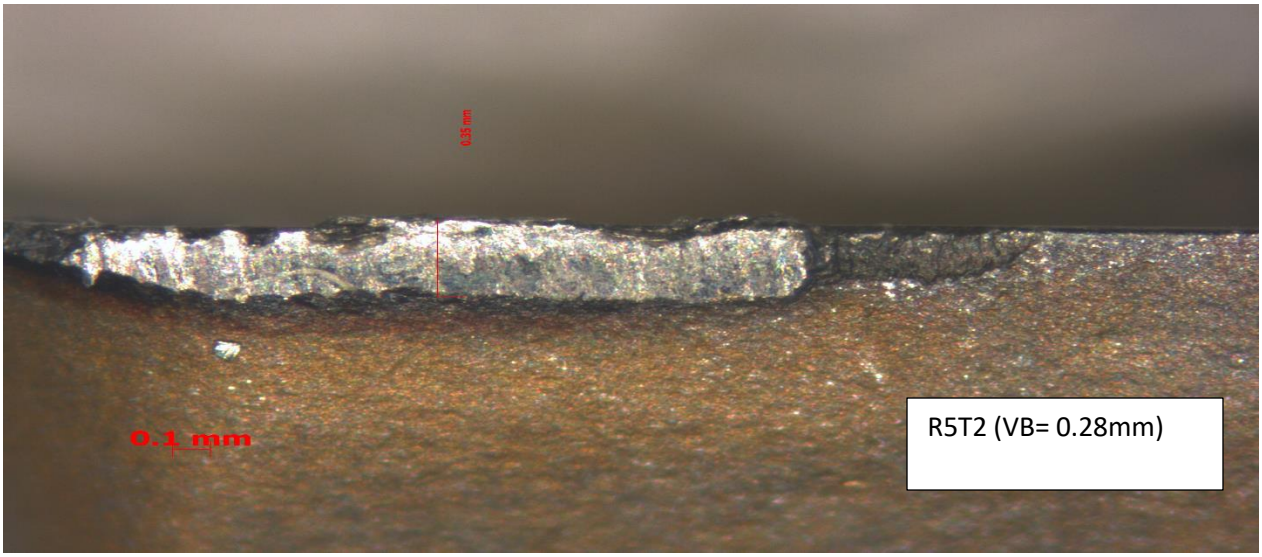

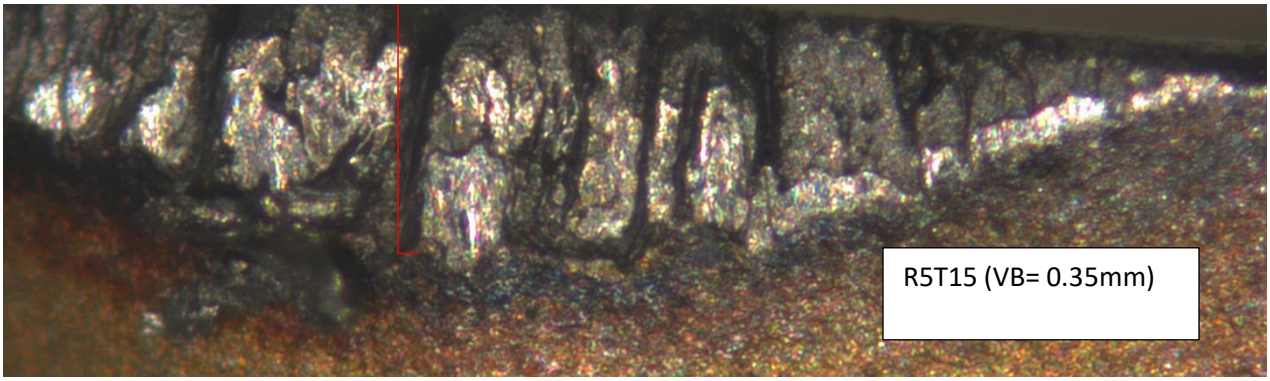

APPENDIX E: Some Matlab codes

```
function Hd = filter
%FILTER Returns a discrete-time filter System object.

% MATLAB Code
% Generated by MATLAB(R) 8.1 and the Signal Processing Toolbox 6.19.
% Generated on: 14-Sep-2016 11:18:48

Fstop = 0.4;  % Stopband Frequency
Fpass = 0.8;  % Passband Frequency
Astop = 60;   % Stopband Attenuation (dB)
Apass = 1;    % Passband Ripple (dB)
Fs    = 50;   % Sampling Frequency

h = fdesign.highpass('fst,fp,ast,ap', Fstop, Fpass, Astop, Apass, Fs);

Hd = design(h, 'cheby2', ...
    'MatchExactly', 'stopband', ...
    'SystemObject', true);

function createfigure(X1, YMatrix1, X2, Y1, X3, Y2, X4, Y3)
%CREATEFIGURE(X1, YMATRIX1, X2, Y1, X3, Y2, X4, Y3)
%  X1:  vector of x data
%  YMATRIX1:  matrix of y data
%  X2:  vector of x data
%  Y1:  vector of y data
%  X3:  vector of x data
%  Y2:  vector of y data
%  X4:  vector of x data
%  Y3:  vector of y data

%  Auto-generated by MATLAB on 31-Aug-2016 15:15:08

% Create figure
figure1 = figure('Tag','TRAINING_PLOTPERFORM','NumberTitle','off',...
    'Name','Neural Network Training Performance (plotperform), Epoch 1000,
Maximum epoch reached.');

% Create axes
axes1 = axes('Parent',figure1,'YScale','log','YMinorTick','on');
%% Uncomment the following line to preserve the X-limits of the axes
% xlim(axes1,[0 1000]);
%% Uncomment the following line to preserve the Y-limits of the axes
% ylim(axes1,[9e-08 0.11]);
hold(axes1,'all');

% Create multiple lines using matrix input to semilogy
semilogy1 = semilogy(X1,YMatrix1,'Parent',axes1,'LineWidth',2);
set(semilogy1(1),'Color',[0 0 1],'DisplayName','Train');
set(semilogy1(2),'Color',[0 0.8 0],'DisplayName','Validation');
set(semilogy1(3),'Color',[1 0 0],'DisplayName','Test');

% Create semilogy
semilogy(X2,Y1,'Parent',axes1,'LineStyle',':','Color',[0 0.48 0],...
```

```
    'DisplayName','Best');

% Create semilogy
semilogy(X3,Y2,'Parent',axes1,'MarkerSize',16,'Marker','o','LineWidth',1.5,..
.
    'LineStyle','none',...
    'Color',[0 0.48 0]);

% Create semilogy
semilogy(X4,Y3,'Parent',axes1,'LineStyle',':','Color',[0 0 0]);

% Create title
title('Best Validation Performance is 8.6353e-07 at epoch 0',...
    'FontWeight','bold',...
    'FontSize',12);

% Create ylabel
ylabel('Mean Squared Error  (mse)','FontWeight','bold','FontSize',12);

% Create xlabel
xlabel('1000 Epochs','FontWeight','bold','FontSize',12);
% Create legend
legend(axes1,'show');

function createfigure(X1, YMatrix1, X2, Y1, X3, YMatrix2, X4, YMatrix3, X5,
YMatrix4, X6)
%CREATEFIGURE(X1, YMATRIX1, X2, Y1, X3, YMATRIX2, X4, YMATRIX3, X5, YMATRIX4,
X6)
% X1:  vector of x data
%  YMATRIX1:  matrix of y data
%  X2:  vector of x data
%  Y1:  vector of y data
%  X3:  vector of x data
%  YMATRIX2:  matrix of y data
%  X4:  vector of x data
%  YMATRIX3:  matrix of y data
%  X5:  vector of x data
%  YMATRIX4:  matrix of y data
%  X6:  vector of x data
%  Auto-generated by MATLAB on 31-Aug-2016 15:12:24
% Create figure
figure1 = figure('Tag','TRAINING_PLOTREGRESSION','NumberTitle','off',...
    'Name','Neural Network Training Regression (plotregression), Epoch 1000,
Maximum epoch reached.');

% uicontrol currently does not support code generation, enter 'doc uicontrol'
for correct input syntax
% In order to generate code for uicontrol, you may use GUIDE. Enter 'doc
guide' for more information

% uicontrol(...);

% Create axes
axes1 = axes('Parent',figure1,...
```

```
    'Position',[0.13 0.593876272242609 0.304276096520464
0.331123727757391],...
    'PlotBoxAspectRatio',[1 1 1]);
%% Uncomment the following line to preserve the X-limits of the axes
% xlim(axes1,[0.02 0.43]);
%% Uncomment the following line to preserve the Y-limits of the axes
% ylim(axes1,[0.02 0.43]);
box(axes1,'on');
hold(axes1,'all');

% Create xlabel
xlabel('Target','FontWeight','bold','FontSize',12);

% Create ylabel
ylabel('Output ~= 0.99*Target + -0.00039','FontWeight','bold','FontSize',12);

% Create title
title('Training: R=0.98665','FontWeight','bold','FontSize',12);

% Create multiple lines using matrix input to plot
plot1 = plot(X1,YMatrix1,'Parent',axes1);
set(plot1(1),'LineStyle',':','DisplayName','Y = T','Color',[0 0 0]);
set(plot1(2),'LineWidth',2,'DisplayName','Fit');

% Create plot
plot(X2,Y1,'Parent',axes1,'Marker','o','LineStyle','none',...
    'DisplayName','Data',...
    'Color',[0 0 0]);

% Create legend
legend1 = legend(axes1,'show');
set(legend1,'Location','NorthWest');

% Create axes
axes2 = axes('Parent',figure1,...
    'Position',[0.587518430936152 0.593876272242609 0.317481569063848
0.331123727757391],...
    'PlotBoxAspectRatio',[1 1 1]);
%% Uncomment the following line to preserve the X-limits of the axes
% xlim(axes2,[0.038837655771357 0.427043907570427]);
%% Uncomment the following line to preserve the Y-limits of the axes
% ylim(axes2,[0.038837655771357 0.427043907570427]);
box(axes2,'on');
hold(axes2,'all');

% Create xlabel
xlabel('Target','FontWeight','bold','FontSize',12);

% Create ylabel
ylabel('Output ~= 1*Target + -0.0012','FontWeight','bold','FontSize',12);

% Create title
title('Validation: R=1','FontWeight','bold','FontSize',12);

% Create multiple lines using matrix input to plot
```

```
plot2 = plot(X3,YMatrix2,'Parent',axes2);
set(plot2(1),'LineStyle',':','DisplayName','Y = T','Color',[0 0 0]);
set(plot2(2),'LineWidth',2,'Color',[0 1 0],'DisplayName','Fit');

% Create plot
plot(X4,Y1,'Parent',axes2,'Marker','o','LineStyle','none',...
    'DisplayName','Data',...
    'Color',[0 0 0]);

% Create legend
legend2 = legend(axes2,'show');
set(legend2,'Location','NorthWest');

% Create axes
axes3 = axes('Parent',figure1,...
    'Position',[0.13 0.11 0.304276096520464 0.329981370316705],...
    'PlotBoxAspectRatio',[1 1 1]);
%% Uncomment the following line to preserve the X-limits of the axes
% xlim(axes3,[0.038837655771357 0.427043907570427]);
%% Uncomment the following line to preserve the Y-limits of the axes
% ylim(axes3,[0.038837655771357 0.427043907570427]);
box(axes3,'on');
hold(axes3,'all');

% Create xlabel
xlabel('Target','FontWeight','bold','FontSize',12);

% Create ylabel
ylabel('Output ~= 1*Target + -0.0097','FontWeight','bold','FontSize',12);

% Create title
title('Test: R=1','FontWeight','bold','FontSize',12);

% Create multiple lines using matrix input to plot
plot3 = plot(X3,YMatrix3,'Parent',axes3);
set(plot3(1),'LineStyle',':','DisplayName','Y = T','Color',[0 0 0]);
set(plot3(2),'LineWidth',2,'Color',[1 0 0],'DisplayName','Fit');

% Create plot
plot(X5,Y1,'Parent',axes3,'Marker','o','LineStyle','none',...
    'DisplayName','Data',...
    'Color',[0 0 0]);

% Create legend
legend3 = legend(axes3,'show');
set(legend3,'Location','NorthWest');

% Create axes
axes4 = axes('Parent',figure1,...
    'Position',[0.587518430936152 0.11 0.317481569063848
0.329981370316705],...
    'PlotBoxAspectRatio',[1 1 1]);
%% Uncomment the following line to preserve the X-limits of the axes
% xlim(axes4,[0.02 0.43]);
%% Uncomment the following line to preserve the Y-limits of the axes
```

```
% ylim(axes4,[0.02 0.43]);
box(axes4,'on');
hold(axes4,'all');

% Create xlabel
xlabel('Target','FontWeight','bold','FontSize',12);

% Create ylabel
ylabel('Output ~= 0.99*Target + -0.00015','FontWeight','bold','FontSize',12);

% Create title
title('All: R=0.98786','FontWeight','bold','FontSize',12);

% Create multiple lines using matrix input to plot
plot4 = plot(X1,YMatrix4,'Parent',axes4);
set(plot4(1),'LineStyle',':','DisplayName','Y = T','Color',[0 0 0]);
set(plot4(2),'LineWidth',2,'Color',[0.4 0.4 0.4],'DisplayName','Fit');

% Create plot
plot(X6,Y1,'Parent',axes4,'Marker','o','LineStyle','none',...
    'DisplayName','Data',...
    'Color',[0 0 0]);

% Create legend
legend4 = legend(axes4,'show');
set(legend4,'Location','NorthWest');


function createfigure(X1, Y1, Y2)
%CREATEFIGURE(X1, Y1, Y2)
%  X1:  vector of x data
%  Y1:  vector of y data
%  Y2:  vector of y data

%  Auto-generated by MATLAB on 31-Aug-2016 15:10:30

% Create figure
figure1 = figure('Tag','TRAINING_PLOTTRAINSTATE','NumberTitle','off',...
    'Name','Neural Network Training Training State (plottrainstate), Epoch
1000, Maximum epoch reached.');
```

Moderate

```
% uicontrol currently does not support code generation, enter 'doc uicontrol'
for correct input syntax
% In order to generate code for uicontrol, you may use GUIDE. Enter 'doc
guide' for more information

% uicontrol(...);
```

Worn out

```
% Create axes
axes1 = axes('Parent',figure1,'YScale','log','YMinorTick','on',...
    'XTickLabel','',...
    'Position',[0.13 0.709264705882353 0.775 0.190936624649861]);
%% Uncomment the following line to preserve the X-limits of the axes
% xlim(axes1,[0 1000]);
box(axes1,'on');
```

```
hold(axes1,'all');

% Create semilogy
semilogy(X1,Y1,'Parent',axes1,'MarkerFaceColor',[1 0 0],'LineWidth',2);

% Create ylabel
ylabel('gradient');

% Create title
title('Gradient = 0.00013746, at epoch 1000');

% Create axes
axes2 = axes('Parent',figure1,'XTickLabel','',...
    'Position',[0.13 0.409632352941176 0.775 0.190936624649861);
%% Uncomment the following line to preserve the X-limits of the axes
% xlim(axes2,[0 1000]);
box(axes2,'on');
hold(axes2,'all');

% Create plot
plot(X1,X1,'Parent',axes2,'MarkerFaceColor',[1 0 0],'Marker','diamond',...
    'LineWidth',1,...
    'LineStyle','none');

% Create ylabel
ylabel('val fail');

% Create title
title('Validation Checks = 1000, at epoch 1000');

% Create axes
axes3 = axes('Parent',figure1,'Position',[0.13 0.11 0.775 0.190936624649861]);
%% Uncomment the following line to preserve the X-limits of the axes
% xlim(axes3,[0 1000]);
box(axes3,'on');
hold(axes3,'all');

% Create plot
plot(X1,Y2,'Parent',axes3,'MarkerFaceColor',[1 0 0],'LineWidth',2);

% Create ylabel
ylabel('lr');

% Create xlabel
xlabel('1000 Epochs');

% Create title
title('Learning Rate = 274.6145, at epoch 1000');
```